

# Fault transient analysis and simulation of series compensated e.h.v. transmission lines and associated protective gear.

Kalam, Akhtar

*Award date:*
1981

*Awarding institution:*
University of Bath

# FAULT TRANSIENT ANALYSIS AND SIMULATION OF SERIES COMPENSATED E.H.V. TRANSMISSION LINES AND ASSOCIATED PROTECTIVE GEAR

by

AKHTAR KALAM

B.Sc., B.Sc.(Engg.), M.S.

Thesis submitted for the degree of Doctor of Philosophy

of

The University of Bath

1981



Akhtar Kalam

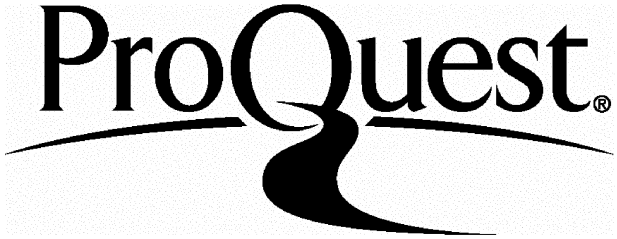

TO

MY PARENTS

MY WIFE AND TWO DAUGHTERS

SYNOPSIS

The advantages of series capacitor compensated lines in long distance transmission are well known. There are, however, problems encountered in the protection of such lines and these basically arise because, under faulted conditions, the primary system parameters are often subjected to rapid changes due largely to capacitor protective gap operation.

The successful longer term development of new transmission line protection techniques is heavily dependent upon a detailed knowledge of the behaviour of practical compensated e.h.v. feeder configurations. In this thesis methods have been developed for accurately simulating the responses of series compensated system using digital simulation techniques based on frequency domain methods.

The digital simulation of practical series compensated systems with shunt reactors has hitherto presented a particularly difficult problem. This thesis highlights these problems and outlines the basis of the techniques which have been developed to overcome them. In particular, the basis of some of the novel techniques developed for simulating the essentially random nature of series capacitor spark gap operation together with the non-linearities

associated with single pole autoreclosure techniques has been explained. Interesting results relating to the responses of a practical 500 kV long distance transmission interconnection and its effect on the performance of modern distance protection has been presented. By examining the performance of the present day distance protection as applied to series compensated lines with spark gap operations, this work has contributed to the solution of a major problem associated with such lines.

ACKNOWLEDGEMENTS

The work presented in this thesis was carried out under the supervision of Dr R K Aggarwal, B.Eng, Ph.D, C.Eng, MIEE, of the School of Electrical Engineering, University of Bath, whose assistance, encouragement and constant guidance are gratefully acknowledged. Appreciation is also extended to Dr A T Johns who has given invaluable advice and helpful comments at various times during the course of this work. The author wishes to express his thanks to Professor J F Eastham, staff members of this School and certain postgraduate students for their encouragement. Thanks are also due to the University of Bath and Rutherford and Appleton Laboratories Computer Department for their co-operation. The author is indebted to Mr P Dyke, Assistant Librarian of this University, for doing literature searches.

Gratitude is also expressed to the University of Bath for the provision of a Research Studentship.

Last, but not least, the author wishes to thank Diane Milton for typing the manuscript.

LIST OF CONTENTS

List of Principal Symbols

| | | |
|---|---|---|
| $P$ | = | power transfer capability |
| $E_S, E_R$ | = | sending and receiving end voltages |
| $\Theta$ | = | vector angle by which $E_S$ leads/lags $E_R$ |
| $X_L$ | = | line inductive reactance |
| $x$ | = | distance to fault |
| $Z, Y$ | = | series impedance and shunt admittance matrix per unit length |
| $\Psi$ | = | $Q\ \gamma\ Q^{-1}$ |
| $\overline{V}_i, \overline{V}_r$ | = | incident and reflected voltage transforms |
| $Q$ | = | voltage eigenvector matrix |
| $\gamma$ | = | modal propagation constant matrix |
| $Z_0, Y_0$ | = | polyphase surge impedance and admittance matrix |
| $S_{cap}$ | = | amount or degree of series compensation |
| p.p.s. | = | positive phase sequence |
| z.p.s. | = | zero phase sequence |
| $L_1$ | = | per unit p.p.s. line inductance |
| $C$ | = | capacitance of series capacitor bank |
| $\ell$ | = | any line length $\ell_1$, $\ell_2$, etc |
| $X_{cap}$ | = | series capacitor reactance |
| $\omega_0$ | = | nominal system angular frequency |
| $\omega$ | = | angular frequency |
| $U$ | = | unit matrix |
| $Z_{cap}$ | = | impedance of the capacitor bank |
| $0$ | = | null matrix |
| $\overline{V}_S, \overline{V}_R$ | = | sending and receiving end prefault voltage transform |

$\bar{I}_S, \bar{I}_R$ = sending and receiving end prefault current transforms

$\bar{E}_{FS}, \bar{E}_{FR}$ = transform of voltages at point of fault

$\bar{I}_{FS}, \bar{I}_{FR}$ = transform of currents at point of fault

$\ell_{cap}$ = length at which the capacitor is located from either end

$L$ = length of the faulted line section

$\bar{V}_{FS}$ = prefault voltage transform at the point of fault

$\bar{V}_{Ss}, \bar{I}_{Ss}$ = prefault voltage and current transforms at sending end of the line

$\bar{V}_{Rs}, \bar{I}_{Rs}$ = prefault voltage and current transforms at receiving end of the line

$\bar{I}_{FSs}, \bar{I}_{FRs}$ = prefault current transforms at the point of fault

$\bar{E}_{Ssc}, \bar{V}_{Scs}$ = prefault voltage transforms before and after capacitor (when located at the sending end)

$\bar{V}_{Rcs}, \bar{E}_{Rsc}$ = prefault voltage transforms before and after capacitor (when located at the receiving end)

$\bar{E}_{Scs}, \bar{E}_{Rcs}$ = superimposed voltage transforms across sending and receiving end capacitors

$\bar{I}_{Scs}, \bar{I}_{Rcs}$ = prefault current transforms through the capacitor for the sending and the receiving end

$c_1, c_0$ = p.p.s. and z.p.s. shunt capacitance per unit length of assumed ideally transposed line

$h_1, h_0$ = degree of p.p.s. and z.p.s. shunt compensation

$L_{1R}, L_{0R}$ = p.p.s. and z.p.s. inductance per reactor

$Z_p, Z_n$ = phase and neutral impedances of shunt reactor bank

$Y_{SR}, Z_{SR}$ = admittance and impedance matrices of the reactor bank

$T$ = transposition matrix

$t$ = transpose of a matrix

$Z_{SR}, Z_{RT}$ = sending and receiving end total composite impedance matrices

$t$ = time

$e, v, i$ = instantaneous (time) variation of voltages and currents

$\alpha$ = frequency-shift constant

$\Omega$ = truncation frequency

$\sigma$ = sigma factor

$\bar{E}, \bar{V}, \bar{I}$ = frequency transform of voltages and current

$\bar{V}_{BSk}, \bar{V}_{BASk}$ = kth superimposed voltage transforms before and after sending end capacitors

$Z_S, Z_R$ = sending and receiving end main source impedance matrices

$\bar{I}_{BSk}, \bar{I}_{BRk}$ = kth superimposed current transforms through the sending and receiving end breakers

$\bar{E}_{SSk}, \bar{V}_{Sk}$ = kth superimposed voltage transforms before and after sending end capacitors

$\bar{I}_{Sk}, \bar{I}_{Rk}$ = kth superimposed currents through sending and receiving end capacitors

$\bar{I}_{SSk}, \bar{I}_{RRk}$ = kth superimposed current transforms through the sending and receiving end bypass switches

$\bar{I}_{cSk} = \bar{I}_{Sk} - \bar{I}_{SSk}$

$\bar{I}_{cRk} = \bar{I}_{Rk} - \bar{I}_{RRk}$

$\overline{E}_{Sk}, \overline{E}_{Rk}$ = kth superimposed voltage transforms across sending and receiving end capacitors

$\overline{V}_{FFk}, \overline{E}_{FFk}$ = kth superimposed voltages at fault point

$\overline{I}_{FSRk} = \overline{I}_{FSk} - \overline{I}_{FRk}$ = kth superimposed current transforms at the fault point

$\overline{E}_{BSk}, \overline{E}_{BRk}$ = kth superimposed voltage transforms across the sending and receiving end breakers

TOB = the observation time

$\overline{V}_{Rk}, \overline{E}_{RRk}$ = kth superimposed voltage transforms before and after receiving end capacitor

$\overline{V}_{BRk}, \overline{V}_{BARk}$ = kth superimposed voltages before and after receiving end capacitors

$\overline{I}_{capk}$ = kth superimposed current transforms through the sending and receiving end bypass switches

FFT = Fast Fourier Transform

p.u. = per unit

$X_1$ = neutral reactance of the main reactors

$X_n$ = neutral reactance of the four reactor bank

$B_1, B_0$ = magnitude of p.p.s. and z.p.s. capacitive susceptance of any line section at nominal system frequency

$B'_1, B'_0$ = magnitude of p.p.s. and z.p.s. capacitive susceptance of any line section at nominal system frequency

$Z_{S0}, Z_{S1}$ = zero and positive phase sequence source impedance

$Z_{L0}, Z_{L1}$ = z.p.s. and p.p.s. impedances of line under consideration

$Z_r$ = replica impedance

$Z_r'$ = replica impedance referred to the secondary

$n_c, n_v$ = turns ratio of the c.t. and v.t.

c.t., v.t. = current and voltage transformers

$\phi_T$ = mho characteristic argument

$R_b$ = burden resistance

$K$ = residual compensating factor $\frac{1}{3}\left[\left|\frac{Z_{L0}}{Z_{L1}}\right| - 1\right]$

$f_c$ = cut-off frequency

$n_t$ = ratio of secondary to primary turns on transformer-reactor

$v_o(t), v_i(t)$ = time variation of output and input voltages

$\Delta T$ = time interval between samples of voltage or current

$k_p = |K_p| \angle 90°$ = sound phase polarising voltage constant

$k_s$ = synchronous polarising voltage constant

$R_p, C_p$ = component values for polarising phase shift circuit

$H(j\omega)$ = amplitude response

$S_1, S_2$ = general form of relaying signals

VCVS = voltage controlled voltage source

$\mu$ = gain of the VCVS

$n$ = order of the filter

$I, V$ = relaying current and voltage at c.t. and v.t. secondaries respectively

$I_{res}$ = residual current at c.t. secondaries

$V_p$ = sound phase polarising voltage

S.E., R.E. = sending and receiving ends

cap = capacitor

F/O = flashover

S/C = sequence comparator

B/A = block average

Subscripts

a,b,c = phases a, b and c

S,R = sending and receiving ends

F = fault point

# CHAPTER 1 INTRODUCTION

## 1.1 Literature Survey

A transmission system comprising of short lines, especially that encountered in the UK, is fairly stiff at the generator ends (busbars) because there are a number of infeeding lines from other sources connected to the busbar. As the line is short, both the line reactance and line capacitance are relatively small, and in fact the latter can be neglected. This means that a generator can operate at a reasonably low load angle in order to transmit an appreciable amount of power over the line, so that the problem of generator instability due to disturbances is reduced. Because of the stiffness of busbars and the interconnection of the system even when a line does go out due to a fault, the majority of faults being transitory in nature anyway, a 3-phase autoreclosure scheme is successfully employed without loss of stability or any serious disruption. Moreover, the presence of a second circuit helps to maintain stability during the autoreclosure sequences of the faulted circuit.

On long lines, however, where the source of generation is often remote from the load points, especially in countries which employ hydro-power schemes, the system at the generator end is very weak. In fact, in the majority

of cases, there are just one or two machines connected to a busbar and the feeder is more of a radial type, ie the line is single-end fed with a large load at the other end. In such cases, the problem of maintaining stability becomes that much greater. Double circuit lines are very uneconomical to use because of the very long distances involved. Thus, as there is only one single circuit line, 3-phase autoreclosure schemes in which all the three phase conductors are isolated for any type of fault, are not very practical, because in the majority of cases the closing of the breakers is not fast enough to maintain stability. A single pole auto-reclosure techniques can be used to advantage in such cases[52].

Because the line is long, both the line inductance and line capacitance are large. The increase in line inductance has the following effects:

(1) The power transfer capability of the line is reduced.

(2) Both the transient and steady-state stability margins of the system for a given power transfer are lowered.

(3) The voltage drop becomes excessive.

The power transfer capability (P) of a transmission line is approximately given by equation 1.1[2,3].

$$P = \frac{E_S E_R}{X_L} \sin\theta \qquad \ldots (1.1)$$

$E_S$, $E_R$ are the sending and the receiving end voltages respectively, $X_L$ is the inductive reactance of the transmission circuit between the terminals, and $\theta$ is the vector angle by which $E_S$ leads or lags $E_R$. The power transfer capability can be increased by either increasing $E_S$, $E_R$ or $\theta$, or by decreasing $X_L$. The maximum values by which $E_S$ and $E_R$ can be increased to are normally fixed by the steady-state and transient insulation limitations of the transmission system itself. This includes the line and terminal equipment. The value of $X_L$ is determined by the transmission line and terminal equipment (transformers, generators, etc) reactances, the minimum value of which is limited by the physical size of equipment and economic considerations.

Because of the increase in line capacitance, the

line charging current becomes quite significant, especially under lightly loaded conditions or sudden loss of load. This excessive reactive power can cause large voltage rises on the system. The adoption of shunt reactors to compensate a portion of line charging VAR is an indispensable method for excessive voltage and reactive power control[34].

The majority of faults on an e.h.v. a.c. transmission line are single-line-to-earth faults, mainly due to lightning strikes and are transitory in nature. From a viewpoint of minimising the disturbances, especially loss of synchronism caused by such faults, it is desirable to clear them by opening the circuit-breaker poles on the faulted phase only and then reclosing them rapidly[81]. However, opening the terminal breakers at the ends of the faulted line conductor does not ensure fault clearance, mainly because the isolated conductor is both capacitively and inductively coupled to the other healthy conductors which are still energised at normal system voltage and carrying a load current. This coupling has two main effects:

(1) Before fault arc extinction, it feeds current to the fault and maintains the arc.

(2) After the arc current becomes zero (as it does twice per cycle) the coupling causes a recovery voltage across the arc path.

Of the two types of coupling, the capacitive coupling is usually the more important. Its importance increases with the increase of the circuit voltage, line length, etc[52].

Extinction of the secondary arc depends on the magnitude of the secondary arc current and the magnitude of, and therefore the rate of rise of steady-state recovery voltage. Secondary arc phenomena is an inherently unstable one. However, it is generally accepted that the criteria for satisfactory extinction of the secondary arc in about 20-30 cycles (which is the limit of stability) is such that the magnitude of the residual arc current should be $\leq$ 20A r.m.s. and that the recovery voltage should be $\leq$ 47kV r.m.s. Whilst in the case of short lines ($\leq$ 80km) this is easily met[80], in the case of long lines however, because of higher system voltages and increased capacitive coupling, both the secondary arc current and the recovery voltage are that much higher, so that some method of neutralising the capacitive coupling has to be used. One way of doing this is by using a form of shunt compensation employing a four-reactor bank[52] in which a fourth reactor is connected to the neutral. Economically the scheme is justified, as e.h.v. reactors are used for

reactive power control anyway and the cost of additional neutral reactor required for secondary arc suppression is a small fraction of the total cost of the main reactors.

As mentioned previously, the power transfer capability of a long line is reduced due to an increase in the series line inductance, and some form of reducing this line inductance has to be employed. There are several methods of doing so, as suggested by Elliot and Cuttino[3], Starr and Evans[12], Johnson et al[25], which are:

(1) Multiple circuit operation.

(2) Direct current transmission.

(3) Line reactance compensation.

The use of two or more transmission circuits decreases the reactance and as a result increases the power transfer capability. Considerable improvement in operating characteristics and transient stability limits can be obtained when multiple circuits are sectionalised at one or more points. Individual line sections can be isolated on the occurrence of fault. However, such sectionalised lines are very uneconomical to use, especially where long distances are involved.

Direct current transmission has received considerable attention in recent years. It is basically an extension of reduced frequency, because if the frequency is reduced to zero, direct current at high voltage can be employed. Power delivered is increased two-fold as the effective voltage is increased by 41%. The major problem is the converter and inverter terminal equipment. Moreover, d.c. transmission is not suited for supplying power to the intervening area, as there is no equivalent yet for the a.c. transformer.

One of the most effective and economical means of compensating large inductive reactances of the e.h.v. transmission lines is by incorporating a series capacitor in the line, the use of which has been reported in the past by many authors[7-29]. It has been found that the series capacitors, by artificially reducing the line inductance, offer an effective and economical means of improving stability limits and thus permit the lines to carry more

power. The pioneer work in this field has been carried out in the USA[19] and Sweden[21]. Recently, the performance of series compensated lines has been studied by various authors[4-6]. These studies show the advantages of compensating the inductive reactance of transmission lines by the use of capacitors in series with the line. Also, these studies describe schemes for protecting the capacitors against overvoltages, without any reference to the performance of line protection.

Some of the reasons attributed to possible applications of series capacitors are[30,40]:

(a) Improvements in the performance and stability of the transmission lines.

(b) The possibility of attaining more favourable load distributions between different lines functioning in parallel.

(c) The scope for regulating the line voltage as well as reducing the voltage drop along the line.

(d) Providing cheaper substitute[31,32] as an alternative to construction of new lines.

Having established the usefulness of series capacitors, there arises a fundamental question of the location of the capacitors in the system. Series capacitors can

be placed either in the line or at intermediate sub-stations. The advantages attributed to the location along the line are easier protection[32]. However, location along the line means higher installation and operating costs because special intermediate capacitor stations have to be built at a distance from the switching and transformer stations and these require the services and facilities of any normal station.

Opinions differ on the optimum amount of compensation and position for the capacitor installation on the line. In practice, the amount of compensation and the location depends on various factors, including economy, easier protection, power transfer capability, etc[32]. The most common location for any capacitor bank is either in the vicinity of the line end for a 70% compensation (usually split up into two halves) or the line mid-point for a compensation of about 50%. In this respect, the European manufacturers and utilities show a preference for location along the line[4], whereas the majority of American utilities locate their capacitors at the line terminals[92].

In general, when a capacitor is subjected to disturbances, abnormal changes take place in the dielectric which result in breakdown or at least produce fatigue phenomena which cause ageing and shorten its useful life.

To protect the capacitors from overloads, use must be made of by-passes, connected in parallel with the capacitor unit and the gaps are set to breakdown and short circuit the capacitor unit when the capacitor voltage exceeds a pre-determined safe threshold value[93]. It is desirable to have the capacitor reinserted back into the circuit immediately after the capacitor voltage has reduced below the critical value in order to improve the transient stability of the line. The two types of spark gaps normally used are the self-clearing and the non-self-clearing type.

Series compensation introduces numerous problems not ordinarily encountered in the normal transmission system design, one of which is the maloperation of the various types of protective relaying scheme. The protection of series compensated transmission line is complicated[36] by the fact that the circuit impedance is changed abruptly if the capacitor is short circuited by its own protective equipment (which is there to protect it from overvoltages) upon the occurrence of a fault. Hence the distance measuring devices are the most adversely affected. Although, phase comparison techniques

are also employed, which are completely dependent on reliable communication links between the line ends.

Little work[69,70] has been reported on the effect of travelling waves on distance relay performance, as applied to series compensated lines. Moreover, there is practically no work reported on the fault-transient phenomena associated with combined series-shunt compensated e.h.v. long distance transmission lines, in which such effects as the frequency variance of the transmission line parameters, discrete transposition of the line and capacitor by-passing have been considered. Johns and Aggarwal[37], in their study of short lines, have shown that if the frequency variance of the transmission line parameters are neglected, the resulting waveforms contain considerably more distortion than is the case in practice and hence have suggested that to obtain a more realistic indication of the performance of distance protection it is necessary to take into account frequency variation of the line parameters.

One present-day practice[82,83] is to use a distance relay in which the setting is determined assuming that the capacitor is always in the circuit under fault conditions. This method is, however, unreliable, due to random nature in which a capacitor flashes over under various fault conditions, resulting in the possible maloperation of the

protective relay. The other method is to set the relay assuming that the capacitors have flashed over. Again, because of the aforementioned reason, there would be a tendency for the relay to overreach if the capacitor does not subsequently flash over under certain fault conditions. Also, in some cases[36,38] it is common to use a conventional distance relay to cater for line faults occurring between relay location and capacitor position only, especially when the capacitor is located at the line mid-point. The local relays operate and initiate carrier signal transmission to the remote end whose circuit breaker trips sequentially. This method, besides being costly due to the cost of carrier equipment and transmission channel, is undesirable if high speed autoreclosing is required, the non-simultaneous opening of the circuit breakers at both ends of the faulted sections results in no 'dead time' during the autoreclosure cycle for the secondary arc to be extinguished and for ionised gases to clear, which can result in a permanent lockout of the circuit breakers at each end of the line section for a transient fault.

Careful planning and considerations have to be given, before any of the above methods is utilised. Moreover, it has to be realised wherever the system security is hindered, that this method should not be considered. Harder et al[39] have in the past tried to analyse the

effects of capacitor compensated line on distance protection using constant line and source parameters, which is only true under steady-state conditions. In the transient state the line and source impedances are no longer constant and they have a significant amount of high frequency components. However, they have presented useful analogue studies and analysed the voltages and currents due to various types of fault at different locations, associated with distance and phase comparison protection. Recently, various authors have highlighted the problems associated with protecting the series compensated long distance lines. Elketeb and Cheetham[82] have considered the effect of distance relay responding to the possibility of voltage and/or current inversion on a series compensated double circuit line for a three-phase fault. They have also described a new technique utilising the superimposed voltages and currents due to faults, which might overcome the problems of unwanted blockings of distance relays due to operation of directional voltage relays or the apparent capacitive source impedance, utilising the fully cross-polarised mho relay. Mathews and Wilkinson[83] have described two measuring relays to determine direction for all fault types on a series compensated single circuit line. The first being a positive-sequence distance relay with a mho characteristic, which provides protection for three-phase faults. The second being a negative-sequence directional relay which provides

protection for all unbalanced faults. Both the aforementioned studies do not include the flashover effect of the capacitor unit spark gaps. Whereas, Tureli et al[91] have investigated the performance of various types of distance, ground overcurrent, directional and phase comparison (carrier) relays on a series compensated double circuit line. They have also considered the flashover effect of the capacitor unit spark gaps. But their operation of various relays is based on steady-state quantities.

When an e.h.v. long line is subjected to a fault or switching operation, abnormal voltages and currents are produced, which have a wide range of frequency components. It is not possible to prevent the occurrence of these disturbances, but their subsequent effects can be limited with proper system design and protective devices. Hence a realistic and accurate knowledge of the transient behaviour of the system under such conditions is essential.

Faults on modern e.h.v. transmission systems have to be cleared as soon as possible to avoid excessive damage. Furthermore, fast fault clearance is essential to maintain system stability, to prevent any possible danger to people, and to prevent the escalation of single-line-to-earth fault to multi-phase-to-earth faults. For these reasons many studies currently focus on very high speed distance

protection utilising mini-computers or microprocessor based systems. Extensive work in this field, however, does not give a clear indication of the true viability of many digital protective schemes from a practical point of view[37]. From a measurement point of view, the nature of the problem is completely different when making the transition from the conventional protective schemes to those in which measurements are to be made from signals derived from a power system during a relatively short period of time following fault inception. With many conventional relays, the very noisy period following a fault is effectively ignored, and measurements commence after a delay without any loss of accuracy[34,37]. Here it is unnecessary to have a very precise knowledge of the response derived from faulted systems during this initial period. However, the same is not true when very high speed measurements are considered,

because the waveforms from which measurements must be made can include very significant travelling wave components in both faulted and healthy phases. In order to design, test and develop any new high speed protective schemes an accurate knowledge of the fault transient response is essential.

The advantages of computer simulation techniques, particularly in respect of the improved accuracy and realism with which they enable transmission systems to be modelled, are particularly well known[68]. The computational techniques used may be broadly classified into the following:

(1) Frequency domain methods based on the Fourier transform using the theory of natural modes[42].

(2) Time domain methods employed by Dommel[43] using a travelling-wave approach.

(3) The reflection lattice technique originally described by Bewley[44] and later used by others in the earlier work for computer simulation of travelling waves in power systems.

In all these cases a considerable amount of effort has been devoted to validating the results obtained. The use of such methods has tended to concentrate on the calculation of voltage transients, mainly because of their importance in circuit breaker designing and in the determination of line-energisation overvoltages for the purposes of attaining economical system insulation levels[35,70]. Recent years have seen a strong desire on the part of power-system engineers to achieve rapid fault-clearance times which in turn necessitate faster response times from the protective gear[86,87]. As a consequence, the travelling wave components in the fault current have become of importance, both in the manner in which they affect relay performance, and as a possible means of very rapid fault detection. The methods of Dommel and Bewley, however, assume lossless or distortionless propagation, and also in the latter method the line

parameters are calculated at a single frequency. Most power lines have small losses, and for transmission involving only the lines themselves, the line distributed parameters can be considered nearly constant over a wide range of frequency. However, for transmission involving the earth, line resistance and inductance vary significantly with frequency. Therefore, it follows that a lossless or distortionless model as devised by Dommel and Bewley is not a satisfactory representation of the line model, if extreme accuracy is required.

The occurrence of a fault on a line causes disturbances to be propagated away from the fault towards each source. As a result, this constitutes the formation of the travelling waves, which are ultimately damped by the system losses. Such phenomena represent a wide frequency variation and it is therefore necessary to evaluate the system response over the entire frequency spectrum. In this respect frequency domain methods based on the theory of natural modes as developed by Wedepohl[42] can be used to advantage. The accuracy of such methods for predicting the precise nature of the fault transient waveforms is now well established[34,37]. At this point it must be emphasised that a very realistic knowledge of the power system transients not only serves the purpose of examining effects of such transients on the protective equipments, but also their importance in predicting any

system overvoltages, according to which, suitable and economical insulation levels can be determined.

It is important to note that, quite apart from any effect the capacitor locations and amount of compensation may have on relay performance, the source side network transmission system comprising of a number of infeeding lines itself can significantly affect distance relay performance[69]. In particular, the lower apparent frequencies of the travelling wave induced components which arise in long line application are generally more troublesome because they can fall within the bandwidth of the signal transducers and protective relays and thereby more significantly affect relay performance[34]. Here, irrespective of the precise nature of the protective relays used, the variation of distance protection performance with system configuration is likely to be very marked in long distance series compensated lines.

## 1.2 Aims of the Thesis

This thesis describes in detail the development of frequency domain methods of fault transient analysis as applied to capacitor compensated lines, both for a single and multi-section feeder. The methods developed are suitable for studying a series compensated line both with and without shunt compensation; the latter being either

in the form of a 3-reactor or a 4-reactor bank.

The main objectives are:

(1) To develop mathematical and digital techniques to simulate practical series compensated systems.

(2) To develop techniques to accommodate for the random behaviour in which a capacitor (or capacitors) sparks over, under various fault conditions. Here it must be stressed that this non-linearity makes a series compensated line one of the most difficult to protect.

(3) To develop techniques for studying the fault transient phenomena associated with single-pole autoreclosure of combined series-shunt compensated lines.

The techniques developed are hence used to study the effects of series compensated lines on the primary system waveforms, both for the purposes of studying protection performance and the overvoltage phenomena. The methods developed have been designed to be sufficiently flexible so as to enable a variety of system configuration (including complex source side network) to be studied under various fault conditions. The two possible capacitor

locations studied are at the protected line ends and the mid-point. In the former case, the amount of compensation used is 70%, whereas for the latter 50% and 30% respectively. Moreover, both 3-reactor and 4-reactor schemes at each end of the protected line with practical levels of both p.p.s. and z.p.s. shunt compensation are used.

It is also the objective of this thesis to report the salient features of an extensive off-line study of the performance of typical cross polarised mho relays utilising the block average principle[69] and sequence comparator[84], the latter offering faster operating times, when applied to a typical 500kV horizontal constructed line. The effect of the location of capacitor, amount of compensation and feeder configurations on both speed and accuracy of the relay is established. It is intended to reach conclusions regarding the most efficient and reliable method of applying the spark gap techniques to distance protection and thus contributing to the solution of a major problem associated with series compensated e.h.v. transmission lines.

The methods developed to incorporate series capacitors either at line ends or at mid-point of a single section feeder along with a brief review of series compensation are presented in Chapter 2. It also deals with the simulation techniques for determining the shunt

reactor bank and the analysis of transposition, combined series and shunt compensation, and multi-section feeder system primarily for the purpose of a more realistic representation of source side models.

In Chapter 3, different spark gap schemes are described followed by the application of single pole autoreclosure techniques to combined series and shunt compensated system. The techniques developed to simulate arrangements for by-passing the capacitor are also presented.

The circuit configuration is shown in Chapter 4. Besides the basic parameters, the series capacitor parameters, including the threshold voltage for various capacitor location and shunt reactor parameters, are presented. The parameters for the various protective schemes used are also included in this Chapter.

Chapters 5-8 cover the digital computer results of the various fault studies. Chapter 5 shows the effect of capacitor location, degree of series compensation, combined series and shunt compensation, etc, on both single and multi-section feeders. In Chapter 6 the effects of system overvoltages due to capacitors sparking over are presented. Chapter 7 deals with the complete simulation of the combined series and shunt compensation

with special reference to single pole autoreclosure techniques. Chapter 8 shows a detailed study of the performance of the cross polarised mho relay as applied to the well-known block average relay and the sequence comparator relay on both single and multi-section feeders.

General conclusions and suggestions for future work are presented in Chapter 9.

# CHAPTER 2 STEADY STATE ANALYSIS OF A SERIES COMPENSATED FEEDER

## 2.1 Introduction

The usefulness of series capacitors to compensate for the increase in line inductance of long lines, and thus improve their power transfer capabilities, is well known[4,5].

Furthermore, in such lines, the use of shunt compensation to compensate the line charging current under normal healthy conditions and the suppression of ground-fault arcs especially in single-circuit lines employing single pole autoreclosure techniques, is a well established technique[34]. Hence, widespread use is made of combined series and shunt compensation in such systems.

Also, in long distance transmission, it is normal practice to transpose the line at regular intervals, usually at one-third of the total distance.

This Chapter is primarily concerned with outlining a detailed steady state analysis of a combined series-shunt compensated line, for both a simple source model and a more practical source model. Furthermore, in order to have a more accurate evaluation of the transient

behaviour of such lines, it is necessary to consider more realistic source-side models which can comprise not only of the main source, but also a number of infeeding lines each with its own local generation (hence the multi-section feeder) as opposed to a line terminating at the busbar in a source model comprising only of series lumped parameters.

A brief review of the existing series compensated schemes is presented in Section 2.2, which includes a brief discussion on the amount of compensation used in practice (also the various problems encountered, specially when the line is overcompensated) and the location of capacitors.

In Section 2.3 the theory of matrix function as applied to a transmission line is briefly reviewed.

The simulation of series capacitor bank is presented in Section 2.4, followed by the transfer matrix function up to and beyond the points of fault which is described in Section 2.5.

Section 2.6 considers the mathematical model of the system and this leads to the steady state analysis used for calculating the steady state voltages and currents at the relaying points, the prefault steady

state voltage at the point of fault followed by the steady state calculation of the voltage across capacitor and the current through it, a knowledge of all this being essential in simulating different aspects such as fault inception, single pole autoreclosure and spark gap operation.

Section 2.7 presents a brief description of the digital simulation of shunt reactor bank, followed by the simulation of the transposition scheme in Section 2.8.

Section 2.9 deals with the simulation of combined series and shunt compensation systems, and fundamentally the simulation of a multi-section feeder, primarily for a more realistic source representation, is detailed in Section 2.10.

## 2.2 Basic Review of Series Compensation

### 2.2.1 Amount of Compensation

The amount of compensation used in long lines is referred to as the degree of compensation, and this is defined as the ratio of capacitive reactance of the series capacitor to that of total series line inductive reactance[71,72].

There are no general recommendations stating to

what extent the inductive reactance should be compensated. However, only the minimum capacitive reactance necessary to reduce the voltage drop to the desired level should be attempted. The effect of overcompensation must be approached with caution, as this would only add to the problems of protecting such lines as already mentioned in Chapter 1. Here it is worth mentioning that whilst from a normal steady state point of view overcompensation is desirable, as this would be an automatic boost to compensate for almost all of the reactive drop and part or all of the resistive drop, in practice, however, the amount of compensation is never increased to more than 70%[73-75], primarily because of the protection problem. The other problems that can be encountered with a series compensated line are[22,27,94]:

(1) Sub-synchronous resonance (SSR) during motor starting.

(2) Ferro-resonance in transformers.

(3) Hunting of synchronous motors during normal operation.

2.2.1.1 Sub-synchronous resonance

As the starting currents of large induction or synchronous motors contain substantial sub-harmonic components, resonance can be set up between series capacitive reactance and the inductive reactance of the

circuit and motor. This occurs at a frequency below the nominal power frequency and the result is that the motor accelerates from rest up to sub-synchronous speed corresponding to the resonant frequency and continues to rotate at this reduced speed[1]. This may result in excessive vibration and large current pulsation which may damage the machine. The problem can be overcome by damping out the resonance using a resistor of at least 10 to 20 times the capacitive reactance in parallel with series capacitor or short circuiting the capacitor during sub-harmonic disturbances. SSR is most likely to occur if the system contains a motor having a rating larger than about 10% of the circuit full loading.

2.2.1.2 Ferro-resonance

This problem is associated with the shape of the magnetisation characteristic of the transformer. If the magnetising reactance is considerably reduced it may resonate with the series capacitor reactance.

It occurs when the transformer is energised with no load on the secondary, or when the primary voltage is substantially increased. If the load is suddenly removed, the capacitor discharge current causes saturation and resonance. High voltages may appear across the capacitor and during ferro-resonance may make the capacitor protective gap to flashover, and this condition may continue

until the circuit is de-energised. The remedy to this problem is to put parallel damping resistor across the capacitors so as to retain a minimum amount of voltage on the transformer side of the capacitor during energisation or by siting the capacitor remote from the transformer.

2.2.1.3 Hunting

Synchronous motor connected to transmission lines may 'hunt' when subjected to sudden load variation. Hunting tends to increase in a circuit which has a low X:R ratio. However, in practice no such problem has been known to occur in series compensated lines.

2.2.2 Location of Capacitor

At present, two well-known solutions are in use as regards the possible location of the capacitor[13,16,32,72]. These are:

(i) Location along the lines, i.e. a single capacitor bank is placed at the mid-point if the desired compensation level is less than 50%, one or two banks are placed one-third or two-thirds of the way along the line from about 30% up to 70% compensation.

(ii) Location at one or both line terminals in the substations.

The location along the lines is advantageous as line protection is simplified and short circuit currents in the capacitor and allied protective equipment are reduced. However, the operating cost increases considerably and maintenance becomes an additional problem. The location at line terminals in the substations, besides being economical (as there is no need to build separate capacitor protection station) is of special interest when a large amount of series compensation is required, because in this case smaller capacitor units are used at each end of the line.

The question of the best capacitor location is still very debatable. The Europeans prefer to locate them along the lines, whilst capacitor location at one or both terminals is preferred by the Americans. In any case, series capacitors can be placed at any convenient location on a feeder, provided the following requirements are met:

(a) Voltage level at the output terminals of the bank should be well below the line insulation and lightning arrestor breakdown levels.

(b) In the case of long transmission lines, where stray capacitance is significant, series capacitor location is normally related to both the technical and economical problems of series capacitor installations. This would involve the study of the behaviour of transmission lines as to where the capacitors should be inserted, ie (i) at the centre of the line, (ii) at the sending end, (iii) at the receiving end, and (iv) at each end of the transmission lines.

The overall parameters of the transmission system are affected by the above-mentioned locations of the series capacitors. The situation which offers the most economical evaluation should be chosen.

It must be remembered that when the capacitor is placed at the sending end, leading sending and receiving end power factor results[25]. Leading power factors at the sending and

receiving ends are undesirable, because they reduce the efficiency and steady state stability of synchronous generators. Hence this situation should be avoided.

The best possible location of the capacitor, if the power transfer is unidirectional, is at the receiving end. But, if the system is a double-end fed, then the series capacitor should be placed either in the middle or one at each end, the latter being for a higher degree of compensation.

(c) Line protection should be adequately dealt with.

(d) Effective insulation of available MVAR capacity has to be considered.

(e) Economics and feasibility of the configuration should be considered covering availability of auxiliary supply for protection.

Therefore, it is evident that the best possible location cannot be dealt with off-hand, but has to be carefully considered, taking into consideration all the various possibilities and economical aspects.

## 2.3 Matrix function for line modelling

In this Section, methods suitable for representing a distributive line model under steady state conditions are considered. The basic methods used in the calculation of the series impedance and shunt admittance matrices are those developed by Galloway et al[41], which takes into account conductor geometry, the parameters due to the conductor itself and the effect of the earth return.

The theory of natural modes developed by Wedepohl[33] enables a solution to the system voltage steady state equations given by equation 2.1 to be transferred into a series of independent differential equations of the form of equation 2.2.

$$\frac{d^2 \bar{V}}{dx^2} = Z\,Y\,\bar{V} \qquad \ldots (2.1)$$

Therefore $\bar{V} = \exp(-\Psi x)\,\bar{V}_i + \exp(\Psi x)\,\bar{V}_r \qquad \ldots (2.2)$

where $\Psi = Q\,\gamma\,Q^{-1}$

The techniques used in calculating the propagation constant, characteristic impedance and characteristic admittance of a single equivalent conductor of a transmission line cannot be employed when a matrix analysis of a multiconductor line is being made. This problem is resolved by evaluating the eigenvalues and eigenvectors of the matrix for which the function is desired. The

theory of matrix function permits the evaluation of the hyperbolic functions, the polyphase surge impedance and surge admittance necessary for the solution of the problem.

For example, the polyphase surge impedance matrix is given by equations 2.3 and 2.4:

$$Z_0 = Q\,\gamma^{-1}\,Q^{-1}\,Z \qquad \ldots (2.3)$$

and $$\cosh(\Psi x) = Q \cosh(\gamma x)\, Q^{-1} \qquad \ldots (2.4)$$

At power frequency, line parameters are calculated by considering each mode of propagation, the multi-port equations representing each element in the system are formulated and voltages and currents at the relaying points evaluated.

## 2.4 Simulation of Series Capacitor Bank

Figure 2.1 shows the circuit of the capacitor arrangement considered. The degree of compensation ($S_{cap}$) in terms of the positive phase sequence (p.p.s.) line inductance ($L_1$) for a series capacitor bank of

capacitance (C) compensating a line section of length ($\ell$) is given by equation 2.5.

$$S_{cap} = \frac{X_{cap}}{X_L} = \frac{1}{\omega_0^2 L_1 C \ell} \quad \ldots (2.5)$$

where $X_{cap}$ and $X_L$ are the series capacitive and line reactance respectively.

The degree of compensation ($S_{cap}$), adopted in major transmission systems, is generally within the range of 20% to 80%[5].

It follows from equation 2.5 that the capacitive reactance is given by:

$$X_{cap} = \frac{1}{j\omega C} = -\frac{j}{\omega(S_{cap}\,\omega_0^2 L_1 \ell)}$$

for a capacitor located at the middle.

Or: $$X_{cap} = -\frac{2j}{\omega(S_{cap}\,\omega_0^2 L_1 \ell)} \quad \ldots (2.6)$$

for a capacitor at each end of the line.

The cannonical form of the two port or transfer matrix function defining arrangement of Figure 2.1 is given in equation 2.7.

$$\begin{bmatrix} \bar{V}_1 \\ \bar{I}_1 \end{bmatrix} = \begin{bmatrix} U & Z_{cap} \\ 0 & U \end{bmatrix} \begin{bmatrix} \bar{V}_2 \\ \bar{I}_2 \end{bmatrix} \quad \ldots (2.7)$$

where $\left[Z_{cap}\right] = \begin{bmatrix} X_{cap} & 0 & 0 \\ 0 & X_{cap} & 0 \\ 0 & 0 & X_{cap} \end{bmatrix}$

## 2.5 Transfer Matrix Function

A faulted transmission system with a series capacitor at each end is given in Figure 2.2. It should be mentioned here that although in most practical systems employing two capacitors per phase, the location of the capacitors is close to the busbars, there however are systems when the capacitors are located along the line, away from the terminating busbars. For this reason, the system and the analysis, both steady state and transient (Chapter 3) presented here, considers a general case whereby the two capacitors can be located anywhere along the line.

The transfer matrix function representing the line section up to the point of fault is given by equation 2.8.

$$\begin{bmatrix} \bar{V}_S \\ \bar{I}_S \end{bmatrix} = \begin{bmatrix} A_1 & B_1 \\ C_1 & D_1 \end{bmatrix} \begin{bmatrix} U & Z_{cap} \\ 0 & U \end{bmatrix} \begin{bmatrix} A_2 & B_2 \\ C_2 & D_2 \end{bmatrix} \begin{bmatrix} \bar{E}_{FS} \\ \bar{I}_{FS} \end{bmatrix} \quad \ldots (2.8)$$

where: $A_1 = \cosh(\Psi \ell_{cap})$, $B_1 = \sinh(\Psi \ell_{cap}) Z_0$,

$C_1 = Y_0 \sinh(\Psi \ell_{cap})$, $D_1 = Y_0 \cosh(\Psi \ell_{cap}) Z_0$ ,

U is a unit vector matrix, $\ell_{cap}$ is the distance of capacitor location from either end.

The submatrices defining the transfer matrix representing the line section beyond capacitor location and up to the fault point are found by substituting the length by $(x - \ell_{cap})$.

Equation 2.8 can be used in combination with the corresponding matrices between the point of discontinuity and the receiving end busbars, to yield a relationship between voltages and currents at either end of the line as given[37,46-48] in equation 2.9, which shows the multiplication process involved.

$$\begin{bmatrix} \bar{V}_S \\ \bar{I}_S \end{bmatrix} = \begin{bmatrix} A_1 & B_1 \\ C_1 & D_1 \end{bmatrix}\begin{bmatrix} U & Z_{cap} \\ 0 & U \end{bmatrix}\begin{bmatrix} A_2 & B_2 \\ C_2 & D_2 \end{bmatrix}\begin{bmatrix} A_F & B_F \\ C_F & D_F \end{bmatrix} \quad X$$

$$\begin{bmatrix} A_3 & B_3 \\ C_3 & D_3 \end{bmatrix}\begin{bmatrix} U & Z_{cap} \\ 0 & U \end{bmatrix}\begin{bmatrix} A_4 & B_4 \\ C_4 & D_4 \end{bmatrix}\begin{bmatrix} \bar{V}_R \\ \bar{I}_R \end{bmatrix} \quad \ldots (2.9)$$

In the above equation the submatrices representing the line section beyond the fault and capacitor location and also between the capacitor location and the receiving end are found by substituting the lengths by

$(L - x - \ell_{cap})$ and $\ell_{cap}$ respectively. The matrix defining the fault discontinuity is formulated according to the type of fault simulated.

## 2.6 Mathematical Model of the System

With reference to Figure 2.3, $\overline{V}_{Fs}$ is sinusoidal and equal to the steady state voltage at the point of fault before the disturbance. A suddenly applied voltage, which when added to $\overline{V}_{Fs}$, represents the post-fault voltage. A solution may thus be obtained by performing two separate calculations in which the desired voltages and currents are evaluated when $\overline{V}_{Fs}$ is applied to the energised system, and the superimposed suddenly applied voltage applied to the de-energised system. The latter is primarily a transient part, the analysis of which is dealt with in detail in Chapter 3.

### 2.6.1 Steady State Calculation of Voltage Vector $\overline{V}_{Fs}$

As mentioned previously, a knowledge of the steady state voltage vector $\overline{V}_{Fs}$ is not only required as a pre-requisite to the transient part of the analysis, but is also necessary when studying single pole autoreclosure techniques (Chapter 3). The vector $\overline{V}_{Fs}$ is evaluated from a knowledge of the pre-fault voltages at the terminating busbars. It should be noted that before

the fault, the sending and receiving end current and voltage transforms are related by equation 2.10.

$$\begin{bmatrix} \bar{V}_{Ss} \\ \bar{I}_{Ss} \end{bmatrix} = \begin{bmatrix} A_L & B_L \\ C_L & D_L \end{bmatrix} \begin{bmatrix} A_R & B_R \\ C_R & D_R \end{bmatrix} \begin{bmatrix} \bar{V}_{Rs} \\ \bar{I}_{Rs} \end{bmatrix}$$

$$= \begin{bmatrix} A_E & B_E \\ C_E & D_E \end{bmatrix} \begin{bmatrix} \bar{V}_{Rs} \\ \bar{I}_{Rs} \end{bmatrix} \quad \ldots (2.10)$$

where $$\begin{bmatrix} A_L & B_L \\ C_L & D_L \end{bmatrix} = \begin{bmatrix} A_1 & B_1 \\ C_1 & D_1 \end{bmatrix} \begin{bmatrix} U & Z_{cap} \\ 0 & U \end{bmatrix} \begin{bmatrix} A_2 & B_2 \\ C_2 & D_2 \end{bmatrix}$$

and $$\begin{bmatrix} A_R & B_R \\ C_R & D_R \end{bmatrix} = \begin{bmatrix} A_3 & B_3 \\ C_3 & D_3 \end{bmatrix} \begin{bmatrix} U & Z_{cap} \\ 0 & U \end{bmatrix} \begin{bmatrix} A_4 & B_4 \\ C_4 & D_4 \end{bmatrix}$$

The sending and receiving end current before the fault is then given by equations 2.11 and 2.12.

$$\bar{I}_{Ss} = (C_E - D_E B_E^{-1} A_E)\, \bar{V}_{Rs} + D_E B_E^{-1}\, \bar{V}_{Ss} \quad \ldots (2.11)$$

and $$\bar{I}_{Rs} = B_E^{-1}\, (\bar{V}_{Ss} - A_E \bar{V}_{Rs}) \quad \ldots (2.12)$$

Also,

$$\begin{bmatrix} \bar{V}_{Fs} \\ \bar{I}_{FRs} \end{bmatrix} = \begin{bmatrix} A_R & B_R \\ C_R & D_R \end{bmatrix} \begin{bmatrix} \bar{V}_{Rs} \\ \bar{I}_{Rs} \end{bmatrix} \quad \ldots (2.13)$$

Therefore, $$\bar{V}_{Fs} = (A_R - B_R B_E^{-1} A_E)\, \bar{V}_{Rs} + B_R B_E^{-1} V_{Ss} \quad \ldots (2.14)$$

Each of the equations 2.11, 2.12 and 2.14 is evaluated at power frequency because the prefault condition is essentially a steady state one.

### 2.6.2 Analysis for Determining Currents Through and Voltages across Capacitor

A knowledge of the prefault steady state voltages across the series capacitor and the currents through them is essential when simulating the capacitor spark gap techniques (Chapter 3).

With reference to Figure 2.4(a), which is concerned with the sending end, matrix relations as shown in equations 2.15 and 2.16 are obtained.

$$\begin{bmatrix} \bar{E}_{Ssc} \\ -\bar{I}_{Scs} \end{bmatrix} = \begin{bmatrix} A_1 & B_1 \\ C_1 & D_1 \end{bmatrix} \begin{bmatrix} \bar{V}_{Ss} \\ -\bar{I}_{Ss} \end{bmatrix} \quad \ldots (2.15)$$

and

$$\begin{bmatrix} \bar{V}_{Scs} \\ -\bar{I}_{Scs} \end{bmatrix} = \begin{bmatrix} U & Z_{cap} \\ 0 & U \end{bmatrix} \begin{bmatrix} \bar{E}_{Ssc} \\ -\bar{I}_{Scs} \end{bmatrix} \quad \ldots (2.16)$$

$$\bar{E}_{Scs} = \bar{E}_{Ssc} - \bar{V}_{Scs} \quad \ldots (2.17)$$

Using equations 2.15 and 2.17 it can be easily shown that the current through and voltage across the sending end capacitor are as given in equations 2.18 and 2.19.

$$\bar{E}_{Scs} = Z_{cap} D_1 \bar{I}_{Ss} - Z_{cap} C_1 \bar{V}_{Ss} \quad \ldots (2.18)$$

and

$$\bar{I}_{Scs} = D_1 \bar{I}_{Ss} - C_1 \bar{V}_{Ss} \quad \ldots (2.19)$$

Likewise from Figure 2.4(b) it can be similarly shown that the current and voltage across the

receiving end capacitor are as given in equations 2.20 and 2.21.

$$\bar{I}_{Rcs} = C_4 \bar{V}_{Rs} + D_4 \bar{I}_{Rs} \quad \ldots (2.20)$$

and $$\bar{E}_{Rcs} = Z_{cap} C_4 \bar{V}_{Rs} + Z_{cap} D_4 \bar{I}_{Rs} \quad \ldots (2.21)$$

## 2.7 Simulation of Shunt Reactor Bank

Shunt compensation of long line serves two purposes[50,51].

1. Limitations of power frequency overvoltage.
2. Neutralisation of shunt capacitive coupling between phases.

There are various reactor configurations in use[52-54], but the most common are the three-phase reactor or the four reactor scheme, as illustrated in Figures 2.5(a) and 2.5(b). In terms of the p.p.s. and z.p.s. values of the shunt capacitance of the line ($C_1$, $C_0$) the parameters of any shunt reactor bank compensating one-half of any line section of length ($\ell$) are given by equation 2.22[49].

$$h_1 = 2 / (\omega_0^2 L_{1R} C_1 \ell)$$

and $$h_0 = 2 / (\omega_0^2 L_{0R} C_0 \ell) \quad \ldots (2.22)$$

The reactor impedances as given in equation 2.23 are essentially those determined by Johns et al[34].

$$Z_p = R_p + j\omega \frac{2}{\omega_0^2 h_1 C_1 \ell}$$

$$\text{and} \quad Z_n = R_n + j\omega \frac{2}{3\omega_0^2 h_0 h_1 C_0 C_1 \ell} (h_1 C_1 - h_0 C_0) \qquad \ldots (2.23)$$

Using these impedances, the matrix representation of a three reactor bank or a four reactor bank is given by equations 2.24 and 2.25 respectively. This part is again dealt with in some detail in Reference 34.

$$\left[ Z_{SR} \right] = \begin{bmatrix} Z_p & 0 & 0 \\ 0 & Z_p & 0 \\ 0 & 0 & Z_p \end{bmatrix} \qquad \ldots (2.24)$$

$$\text{and} \quad \left[ Z_{SR} \right] = \begin{bmatrix} Z_p+Z_n & Z_n & Z_n \\ Z_n & Z_p+Z_n & Z_n \\ Z_n & Z_n & Z_p+Z_n \end{bmatrix} \qquad \ldots (2.25)$$

It is convenient ultimately to combine the shunt reactor arrangements with the line sections involved, and for this purpose the canonical form of the two port or transfer matrix function defining the arrangement of Figures 2.5(a) and 2.5(b) by equation 2.25 is particularly useful.

$$\begin{bmatrix} \bar{V}_1 \\ \bar{I}_1 \end{bmatrix} = \begin{bmatrix} U & 0 \\ Y_{SR} & U \end{bmatrix} \begin{bmatrix} \bar{V}_2 \\ \bar{I}_2 \end{bmatrix} \quad \ldots (2.26)$$

where $\left[Y_{SR}\right]$ is the reactor admittance matrix and is equal to $\left[Z_{SR}\right]^{-1}$ .

In this thesis 3-reactor banks, when studying the performance of the protective gear and 4-reactor banks, when studies related to single pole autoreclosure as applied to series compensated lines are used.

## 2.8 Simulation of Transposed Line Section

When a communication circuit runs in parallel with a high voltage overhead transmission lines, large voltages may be induced in the former resulting in acoustic shocks and waves, thus causing not only interference in the communication circuit but also posing a hazard. The induced voltages are due to electrostatic and electro-magnetic induction, and are reduced considerably by transposing (ie artificially balancing) the power line[55]. Transposition which is effectively exchanging the positions of the conductors at regular intervals along the line so that each conductor occupies the original position of every other conductor over an equal distance. The effect of transposition is to provide an equilateral spacing, so as to balance first the

capacitances of the lines, which means that the electrostatically induced voltages balance out over the length of a complete set of transpositions, and secondly to reduce the electromagnetically induced emfs in the conductors. A complete transposition cycle is shown in Figure 2.6, where a, b, and c are the phase conductors. Transposition results in each conductor having the same average inductances and capacitances over the whole cycle.

In modern power lines, it is not common practice to build overhead lines with transposition towers, for economic reasons[34]. However, an interchange of the conductor position is made at switching stations. Hence discrete transposition is often performed at the termination of each section or at intermediate points thereon. Since transposition represents an abrupt point of discontinuity from which incident wave components are partially reflected, it is important to simulate their effect when studying the transient behaviour of lines. It is convenient initially to compute the matrices describing each homogenous line section and with reference to Figure 2.6 the transfer matrices for a first section fault between the fault point F and the receiving end R are given by equations 2.27, 2.28 and 2.29.

$$\begin{bmatrix} \bar{V}_{FR} \\ \bar{I}_{FR} \end{bmatrix} = \begin{bmatrix} A_{2F} & B_{2F} \\ C_{2F} & D_{2F} \end{bmatrix} \begin{bmatrix} \bar{V}_{R5} \\ \bar{I}_{R5} \end{bmatrix} \qquad \ldots (2.27)$$

$$\begin{bmatrix} \bar{V}_{R4} \\ \bar{I}_{R4} \end{bmatrix} = \begin{bmatrix} A & B \\ C & D \end{bmatrix} \begin{bmatrix} \bar{V}_{R3} \\ \bar{I}_{R3} \end{bmatrix} \quad \ldots (2.28)$$

$$\begin{bmatrix} \bar{V}_{R2} \\ \bar{I}_{R2} \end{bmatrix} = \begin{bmatrix} A & B \\ C & D \end{bmatrix} \begin{bmatrix} \bar{V}_{R1} \\ \bar{I}_{R1} \end{bmatrix} \quad \ldots (2.29)$$

where $A_{2F} = \cosh\{\Psi(\ell/3 - x)\}$, $B_{2F} = \sinh\{\Psi(\ell/3 - x)\}Z_0$

$C_{2F} = Y_0\sinh\{\Psi(\ell/3 - x)\}$, $D_{2F} = Y_0\cosh\{\Psi(\ell/3 - x)\}Z_0$

and $A = \cosh(\Psi\ell/3)$, $B = \sinh(\Psi\ell/3)Z_0$, $C = Y_0\sinh(\Psi\ell/3)$,

$D = Y_0\cosh(\Psi\ell/3)Z_0$

A transposition matrix $[T]$ can be introduced to effect the necessary transposition by relating $\left[\bar{V}_{R5}, \bar{I}_{R5}\right]^t$, $\left[\bar{V}_{R4}, \bar{I}_{R4}\right]^t$, $\left[\bar{V}_{R3}, \bar{I}_{R3}\right]^t$ and $\left[\bar{V}_{R2}, \bar{I}_{R2}\right]^t$. Therefore the order in which equations 2.27 to 2.29 has been mentioned is as follows.

$$\begin{bmatrix} \bar{V}_{R5} \\ \bar{I}_{R5} \end{bmatrix} = \left[\bar{V}_{R5a}\ \bar{V}_{R5b}\ \bar{V}_{R5c}\ \bar{I}_{R5a}\ \bar{I}_{R5b}\ \bar{I}_{R5c}\right]^t \quad \ldots (2.30)$$

$$\begin{bmatrix} \bar{V}_{R4} \\ \bar{I}_{R4} \end{bmatrix} = \left[\bar{V}_{R4c}\ \bar{V}_{R4a}\ \bar{V}_{R4b}\ \bar{I}_{R4c}\ \bar{I}_{R4a}\ \bar{I}_{R4b}\right]^t \quad \ldots (2.31)$$

$$\begin{bmatrix} \bar{V}_{R3} \\ \bar{I}_{R3} \end{bmatrix} = \begin{bmatrix} \bar{V}_{R3c} & \bar{V}_{R3a} & \bar{V}_{R3b} & \bar{I}_{R3c} & \bar{I}_{R3a} & \bar{I}_{R3b} \end{bmatrix}^t \quad \ldots (2.32)$$

$$\begin{bmatrix} \bar{V}_{R2} \\ \bar{I}_{R2} \end{bmatrix} = \begin{bmatrix} \bar{V}_{R2b} & \bar{V}_{R2c} & \bar{V}_{R2a} & \bar{I}_{R2b} & \bar{I}_{R2c} & \bar{I}_{R2a} \end{bmatrix}^t \quad \ldots (2.33)$$

Matrix T is therefore as given in equation 2.34 and the overall line transfer matrix between fault points F and R is given by equation 2.35.

$$\begin{bmatrix} \bar{V}_{R3} \\ \bar{I}_{R3} \end{bmatrix} = [T] \begin{bmatrix} \bar{V}_{R2} \\ \bar{I}_{R2} \end{bmatrix} \quad \ldots (2.34)$$

$$\begin{bmatrix} \bar{V}_{FR} \\ \bar{I}_{FR} \end{bmatrix} = \begin{bmatrix} A_{2F} & B_{2F} \\ C_{2F} & D_{2F} \end{bmatrix} [T] \begin{bmatrix} A & B \\ C & D \end{bmatrix} [T] \begin{bmatrix} A & B \\ C & D \end{bmatrix} [T] \begin{bmatrix} \bar{V}_R \\ \bar{I}_R \end{bmatrix}$$

$$= \begin{bmatrix} A'_{LR} & B'_{LR} \\ C'_{LR} & D'_{LR} \end{bmatrix} \begin{bmatrix} \bar{V}_R \\ \bar{I}_R \end{bmatrix} \quad \ldots (2.35)$$

where $\begin{bmatrix} A'_{LR} & B'_{LR} \\ C'_{LR} & D'_{LR} \end{bmatrix} = \begin{bmatrix} A_{2F} & B_{2F} \\ C_{2F} & D_{2F} \end{bmatrix} [T] \begin{bmatrix} A & B \\ C & D \end{bmatrix} [T] \begin{bmatrix} A & B \\ C & D \end{bmatrix} [T]$,

$[T] = \begin{bmatrix} T' & 0 \\ 0 & T' \end{bmatrix}$ and $[T'] = \begin{bmatrix} 0 & 1 & 0 \\ 0 & 0 & 1 \\ 1 & 0 & 0 \end{bmatrix}$

By a similar approach the line transfer matrix between points F and S is obtained as shown in equation 2.36.

$$\begin{bmatrix} \bar{V}_{FS} \\ -\bar{I}_{FS} \end{bmatrix} = \begin{bmatrix} A_{1F} & B_{1F} \\ C_{1F} & D_{1F} \end{bmatrix} \begin{bmatrix} \bar{V}_S \\ -\bar{I}_S \end{bmatrix} \quad \ldots (2.36)$$

where $A_{1F} = \cosh(\Psi x)$, $B_{1F} = \sinh(\Psi x) Z_0$,

$C_{1F} = Y_0 \sinh(\Psi x)$, $D_{1F} = Y_0 \cosh(\Psi x) Z_0$

It should be noted that the overall line transfer matrix of an unfaulted line section of any length, $\ell$, will be given as by equation 2.37.

$$\begin{bmatrix} \bar{V}_S \\ \bar{I}_S \end{bmatrix} = \left[ \begin{bmatrix} A_L & B_L \\ C_L & D_L \end{bmatrix} \quad [T] \right]^3 \begin{bmatrix} \bar{V}_R \\ \bar{I}_R \end{bmatrix} \quad \ldots (2.37)$$

where $A_L = \cosh(\Psi \ell/3)$, $B_L = \sinh(\Psi \ell/3) Z_0$,

$C_L = Y_0 \sinh(\Psi \ell/3)$, $D_L = Y_0 \sinh(\Psi \ell/3) Z_0$

## 2.9 Simulation of the Combined Series and Shunt Compensation

It is a well established fact that a long distance e.h.v. a.c. transmission system requires the use of series capacitors and shunt reactors. This is done so as to reduce series reactance and shunt susceptance of the lines, which in turn improves system stability and voltage control, increases the efficiency of power transmission, facilitates line energisation and reduces temporary and transient overvoltages[57].

There can be numerous different locations as to where the series capacitors and shunt reactors can be located[56,58]. The majority of the work presented in this thesis has been carried for the shunt reactors placed at the busbars and for two positions of the series capacitors, (i) a capacitor bank located at each end of the line, and (ii) a single capacitor bank at the mid-point of the line.

From a steady state point of view it is convenient computationally to combine the reactor-capacitor bank and the transposed line section for the case where a capacitor is located at each end.

With reference to Fig 2.7(a), the relationship between the fault point voltage and current and the receiving end quantities is as shown in equation 2.38.

$$\begin{bmatrix} \bar{V}_F \\ \bar{I}_{FR} \end{bmatrix} = \begin{bmatrix} A_{LR} & B_{LR} \\ C_{LR} & D_{LR} \end{bmatrix} \begin{bmatrix} U & Z_{cap} \\ 0 & U \end{bmatrix} \begin{bmatrix} A_2 & B_2 \\ C_2 & D_2 \end{bmatrix} \begin{bmatrix} U & 0 \\ Y_{SR} & U \end{bmatrix} \begin{bmatrix} \bar{V}_R \\ \bar{I}_R \end{bmatrix}$$

$$= \begin{bmatrix} A_{CR} & B_{CR} \\ C_{CR} & D_{CR} \end{bmatrix} \begin{bmatrix} \bar{V}_R \\ \bar{I}_R \end{bmatrix} \qquad \ldots (2.38)$$

where

$$\begin{bmatrix} A_{CR} & B_{CR} \\ C_{CR} & D_{CR} \end{bmatrix} = \begin{bmatrix} A_{LR} & B_{LR} \\ C_{LR} & D_{LR} \end{bmatrix} \begin{bmatrix} U & Z_{cap} \\ 0 & U \end{bmatrix} \begin{bmatrix} A_2 & B_2 \\ C_2 & D_2 \end{bmatrix} \begin{bmatrix} U & 0 \\ Y_{SR} & U \end{bmatrix}$$

Similarly, the transfer matrix linking points F and S is described by equation 2.39.

$$\begin{bmatrix} \bar{V}_F \\ -\bar{I}_{FS} \end{bmatrix} = \begin{bmatrix} A_{1F} & B_{1F} \\ C_{1F} & D_{1F} \end{bmatrix} \begin{bmatrix} U & Z_{cap} \\ 0 & U \end{bmatrix} \begin{bmatrix} A_1 & B_1 \\ C_1 & D_1 \end{bmatrix} \begin{bmatrix} U & 0 \\ Y_{SR} & U \end{bmatrix} \begin{bmatrix} \bar{V}_S \\ -\bar{I}_S \end{bmatrix}$$

$$= \begin{bmatrix} A_{CL} & B_{CL} \\ C_{CL} & D_{CL} \end{bmatrix} \begin{bmatrix} \bar{V}_S \\ -\bar{I}_S \end{bmatrix} \qquad \ldots (2.39)$$

where

$$\begin{bmatrix} A_{CL} & B_{CL} \\ C_{CL} & D_{CL} \end{bmatrix} = \begin{bmatrix} A_{1F} & B_{1F} \\ C_{1F} & D_{1F} \end{bmatrix} \begin{bmatrix} U & Z_{cap} \\ 0 & U \end{bmatrix} \begin{bmatrix} A_1 & B_1 \\ C_1 & D_1 \end{bmatrix} \begin{bmatrix} U & 0 \\ Y_{SR} & U \end{bmatrix}$$

## 2.10 Simulation of Composite Source Impedances (particularly with reference to a multi-section feeder)

In power system analysis, although it is common practice to assume that the line under consideration is energised either from infinite busbars or lumped parameter sources, however, for an accurate and realistic evaluation of system transients for the purpose of examining protection equipment performance, etc, it is often necessary to have a more realistic source-side representation.

Source side networks rarely comprise of only localised generation and in general the busbar at either end of the line often terminates other lines, which in turn are remotely terminated in equally complex source networks. As the analysis is arranged to consider simply sources as impedance matrices ($Z_{ST}$ and $Z_{RT}$), any arbitrary source configurations can be incorporated into the analysis by pre-computing the source impedance matrices at all frequencies of interest[34]. A change in source side network is thus readily effected without any fundamental change to the simulation software. Hence a change in the source represents only a change in the program data. This flexibility is fundamental to all frequency domain methods and is particularly useful in practice, in that one basic simulation package then effectively satisfies the requirements of any arbitrary sources (and for that matter any line configuration).

In practice, a line may have several infeeds terminating at a switching station busbar. There are a number of possibilities as regards practical source side networks[34] and one such system considered in the present study is as shown in Figure 2.8.

On the source side, the equivalent impedance matrix can be made up of impedances of various infeeds and their local generations (together with the impedance of the main generation) terminating in busbar under consideration.

The system considered here consists of the main generator on each side of the line, together with one infeed on the sending end busbar side with its local generation, and two infeeds (with local generation) on the receiving end busbar side. The line under consideration has both series and shunt compensation. A series capacitor and a shunt reactor are located at each end of the faulted line as shown in Figure 2.8.

To understand the modelling of this complex source representation, it is best to start with a model as shown in Figure 2.9(a), which represents a typical practical system). The transfer matrix equation 2.40 defines the response of the first section.

$$\begin{bmatrix} \bar{V}_R \\ \bar{I}_{R3} \end{bmatrix} = \begin{bmatrix} A_{\ell 3} & B_{\ell 3} \\ C_{\ell 3} & D_{\ell 3} \end{bmatrix} \begin{bmatrix} \bar{V}_{R5} \\ \bar{I}_{R4} \end{bmatrix} \quad \ldots (2.40)$$

where $A_{\ell 3} = \cosh(\Psi \ell_3)$, $B_{\ell 3} = \sinh(\Psi \ell_3) Z_0$,

$C_{\ell 3} = Y_0 \sinh(\Psi \ell_3)$, $D_{\ell 3} = Y_0 \cosh(\Psi \ell_3) Z_0$

The total current entering the first section at, say, the receiving end is given by

$$\bar{I}_R = \left[ Z_{R1} \right]^{-1} \bar{V}_R + \bar{I}_{R3}$$

and it follows that the overall transfer matrix of the first section, including the local infeeding source of impedance $\left[ Z_{R1} \right]$ is given by equation 2.41.

$$\begin{bmatrix} \bar{V}_R \\ \bar{I}_R \end{bmatrix} = \begin{bmatrix} A_{\ell 3} & B_{\ell 3} \\ C_{\ell 3} + \left[ Z_{R1} \right]^{-1} A_{\ell 3} & D_{\ell 3} + \left[ Z_{R1} \right]^{-1} B_{\ell 3} \end{bmatrix} \begin{bmatrix} \bar{V}_{R5} \\ \bar{I}_{R4} \end{bmatrix} \quad \ldots (2.41)$$

Similarly, equation 2.42 defines the canonical relationship of the second section.

$$\begin{bmatrix} \bar{V}_{R5} \\ \bar{I}_{R5} \end{bmatrix} = \begin{bmatrix} A_{\ell 4} & B_{\ell 4} \\ C_{\ell 4} & D_{\ell 4} \end{bmatrix} \begin{bmatrix} \bar{V}_{R6} \\ \bar{I}_{R6} \end{bmatrix} \quad \ldots (2.42)$$

where $A_{\ell 4} = \cosh(\Psi \ell_4)$, $B_{\ell 4} = \sinh(\Psi \ell_4) Z_0$,

$C_{\ell 4} = Y_0 \sinh(\Psi \ell_4)$, $D_{\ell 4} = Y_0 \cosh(\Psi \ell_4) Z_0$

Again taking the local infeed and main source impedance as $[Z_{R2}]$ and $[Z_R]$ respectively, a relationship of the form of equation 2.43 develops.

$$\begin{bmatrix} \bar{V}_{R5} \\ \bar{I}_{R4} \end{bmatrix} = \begin{bmatrix} A_{\ell 4} & B_{\ell 4} \\ C_{\ell 4} + [Z_{R2}]^{-1} A_{\ell 4} & D_{\ell 4} + [Z_{R2}]^{-1} B_{\ell 4} \end{bmatrix} \begin{bmatrix} \bar{V}_{R6} \\ \bar{I}_{R6} \end{bmatrix}$$

Therefore:

$$\begin{bmatrix} \bar{V}_R \\ \bar{I}_R \end{bmatrix} = \begin{bmatrix} A_{\ell 3} & B_{\ell 3} \\ C_{\ell 3} + [Z_{R1}]^{-1} A_{\ell 3} & D_{\ell 3} + [Z_{R1}]^{-1} B_{\ell 3} \end{bmatrix} *$$

$$\begin{bmatrix} A_{\ell 4} & B_{\ell 4} \\ C_{\ell 4} + [Z_{R2}]^{-1} A_{\ell 4} & D_{\ell 4} + [Z_{R2}]^{-1} B_{\ell 4} \end{bmatrix} \begin{bmatrix} U & Z_R \\ 0 & U \end{bmatrix} \begin{bmatrix} 0 \\ I_{R6} \end{bmatrix}$$

$$= \begin{bmatrix} A_{RE} & B_{RE} \\ C_{RE} & D_{RE} \end{bmatrix} \begin{bmatrix} 0 \\ \bar{I}_{R6} \end{bmatrix} \qquad \ldots (2.43)$$

where:

$$\begin{bmatrix} A_{RE} & B_{RE} \\ C_{RE} & D_{RE} \end{bmatrix} = \begin{bmatrix} A_{\ell 3} & B_{\ell 3} \\ C_{\ell 3} + [Z_{R1}]^{-1} A_{\ell 3} & D_{\ell 3} + [Z_{R1}]^{-1} B_{\ell 3} \end{bmatrix} *$$

$$\begin{bmatrix} A_{\ell 4} & B_{\ell 4} \\ C_{\ell 4} + [Z_{R2}]^{-1} A_{\ell 4} & D_{\ell 4} + [Z_{R2}]^{-1} B_{\ell 4} \end{bmatrix} \begin{bmatrix} U & Z_R \\ 0 & U \end{bmatrix}$$

From equation 2.43 it can be shown that

$$\bar{V}_R = B_{RE} D_{RE}^{-1} \bar{I}_R \qquad \ldots (2.44)$$

Now, for the sending end side, say (Figure 2.9(b)) the transfer matrix is given by equation 2.45.

$$\begin{bmatrix} \bar{V}_S \\ -\bar{I}_{S1} \end{bmatrix} = \begin{bmatrix} A_{\ell 1} & B_{\ell 1} \\ C_{\ell 1} & D_{\ell 1} \end{bmatrix} \begin{bmatrix} \bar{V}_{S2} \\ -\bar{I}_{S2} \end{bmatrix} \quad \ldots (2.45)$$

where $A_{\ell 1} = \cosh(\Psi \ell_1)$, $B_{\ell 1} = \sinh(\Psi \ell_1) Z_0$,

$C_{\ell 1} = Y_0 \sinh(\Psi \ell_1)$, $D_{\ell 1} = Y_0 \cosh(\Psi \ell_1) Z_0$

Taking local infeed and main source impedance as $[Z_{S1}]$ and $[Z_S]$ respectively the relationship as given in equation 2.46 is obtained.

$$\begin{bmatrix} \bar{V}_S \\ -\bar{I}_S \end{bmatrix} = \begin{bmatrix} A_{\ell 1} & B_{\ell 1} \\ C_{\ell 1} + [Z_{S1}]^{-1} A_{\ell 1} & D_{\ell 1} + [Z_{S1}]^{-1} B_{\ell 1} \end{bmatrix} \begin{bmatrix} \bar{V}_{S2} \\ -\bar{I}_{S2} \end{bmatrix}$$

$$= \begin{bmatrix} A_{\ell 1} & B_{\ell 1} \\ C_{\ell 1} + [Z_{S1}]^{-1} A_{\ell 1} & D_{\ell 1} + [Z_{S1}]^{-1} B_{\ell 1} \end{bmatrix} \begin{bmatrix} U & Z_S \\ 0 & U \end{bmatrix} \begin{bmatrix} 0 \\ -\bar{I}_{S2} \end{bmatrix}$$

$$= \begin{bmatrix} A_{SE} & B_{SE} \\ C_{SE} & D_{SE} \end{bmatrix} \begin{bmatrix} 0 \\ -\bar{I}_{S2} \end{bmatrix} \quad \ldots (2.46)$$

$$\begin{bmatrix} A_{SE} & B_{SE} \\ C_{SE} & D_{SE} \end{bmatrix} = \begin{bmatrix} A_{\ell 1} & B_{\ell 1} \\ C_{\ell 1} + [Z_{S1}]^{-1} A_{\ell 1} & D_{\ell 1} + [Z_{S1}]^{-1} B_{\ell 1} \end{bmatrix} \begin{bmatrix} U & Z_S \\ 0 & U \end{bmatrix}$$

From equation 2.46, it can be easily shown that

$$\bar{V}_S = - B_{SE} D_{SE}^{-1} \bar{I}_S \quad \ldots (2.47)$$

Hence the total composite source impedance matrix at the receiving and sending end is given by equation 2.48 which is obtained from equations 2.44 and 2.47.

$$Z_{RT} = B_{RE} \; D_{RE}^{-1}$$

$$\text{and} \quad Z_{ST} = B_{SE} \; D_{SE}^{-1} \qquad \ldots \; (2.48)$$

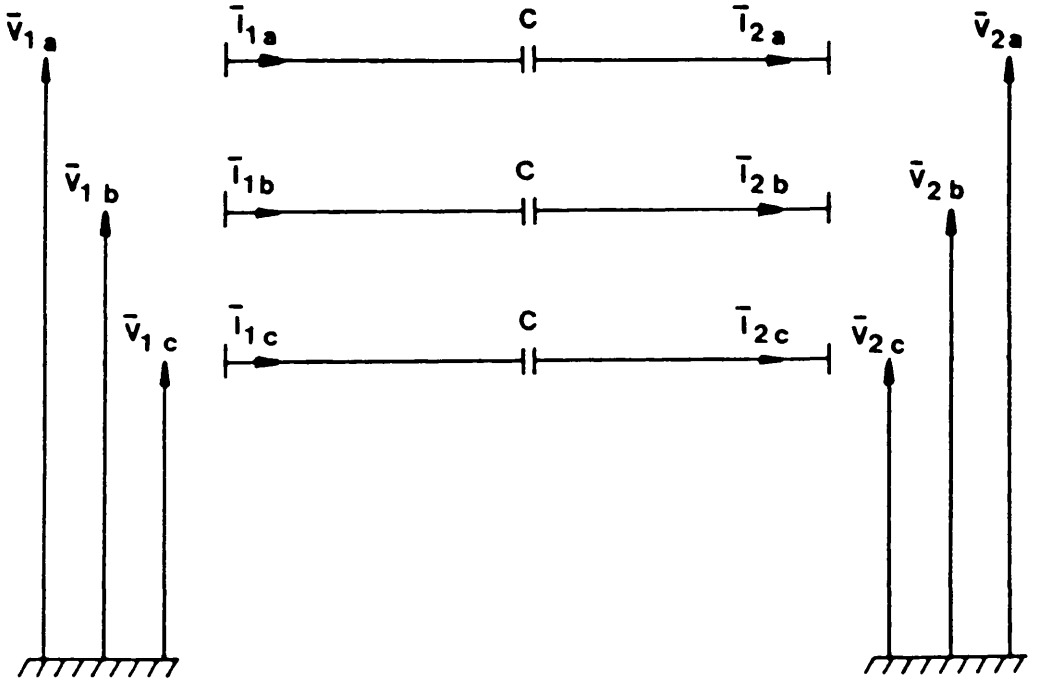


Figure 2.1 Capacitor bank arrangement

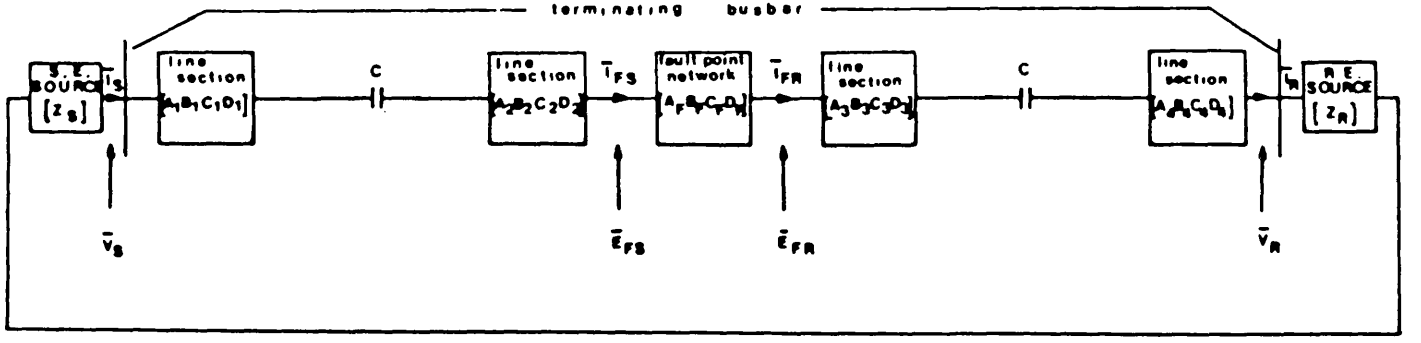


Figure 2.2 Basic system model

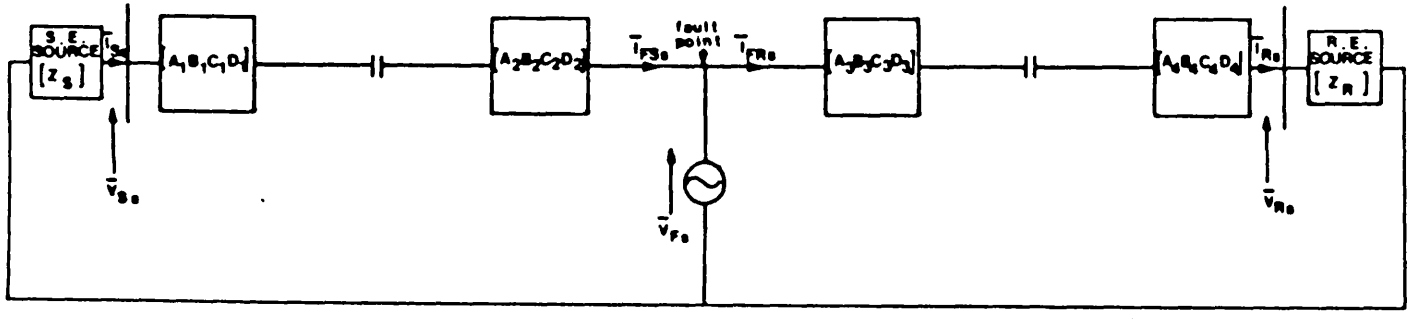


Figure 2.3 Steady state or prefault model

(a) (b)

Figure 2.4 Voltage across capacitor

(a) sending end
(b) receiving end

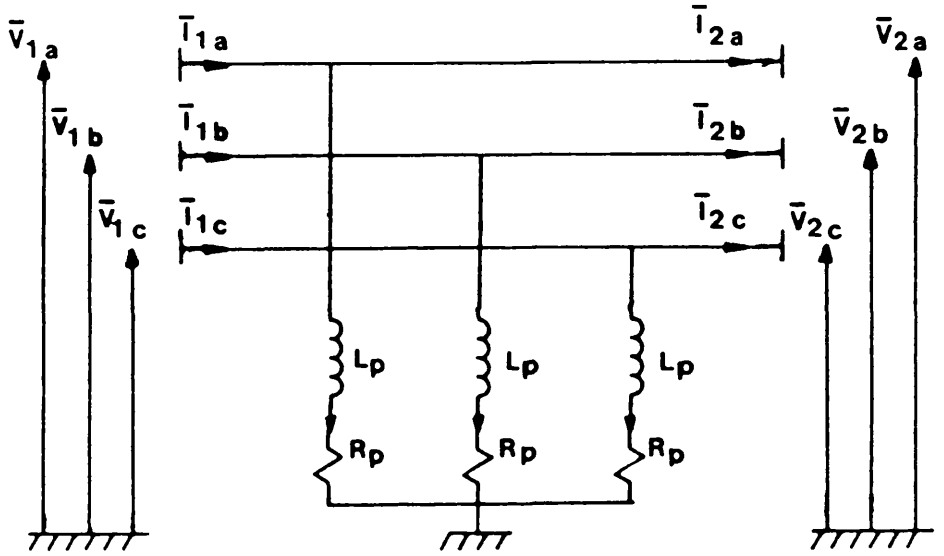


(a)

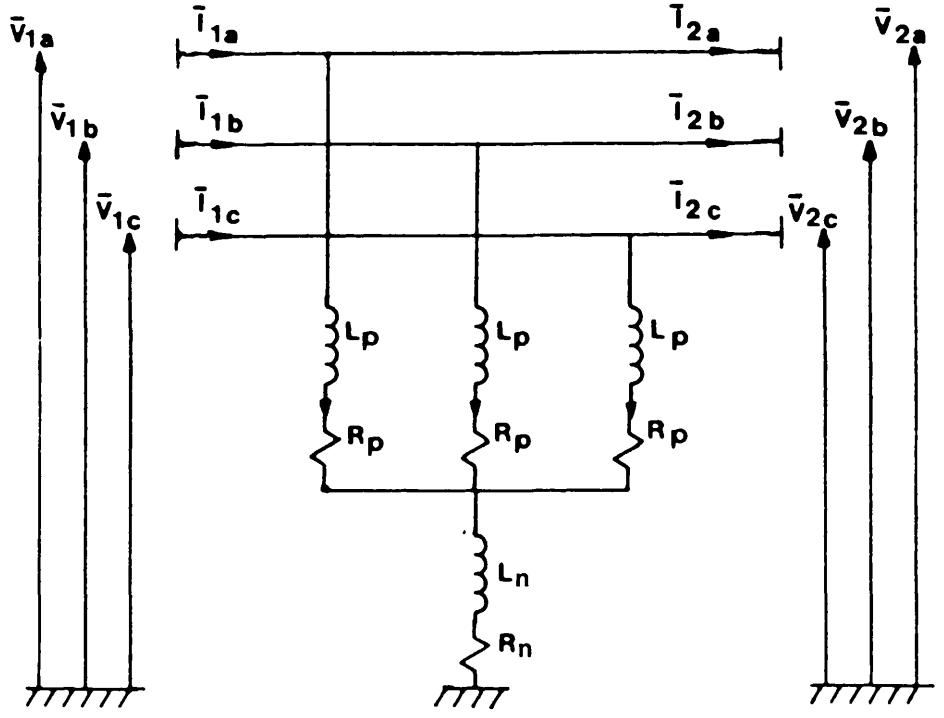


(b)

Figure 2.5 Shunt reactor arrangement

(a) Three phase reactor
(b) Four reactor bank

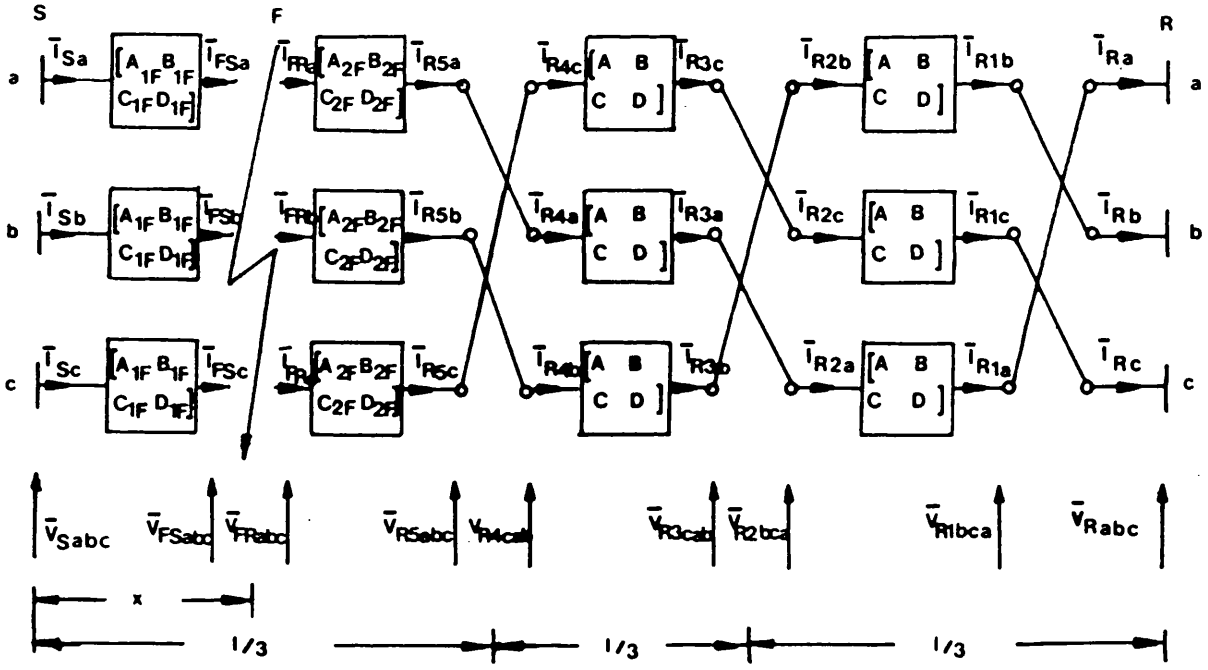


Figure 2.6 Discretely transposed line model

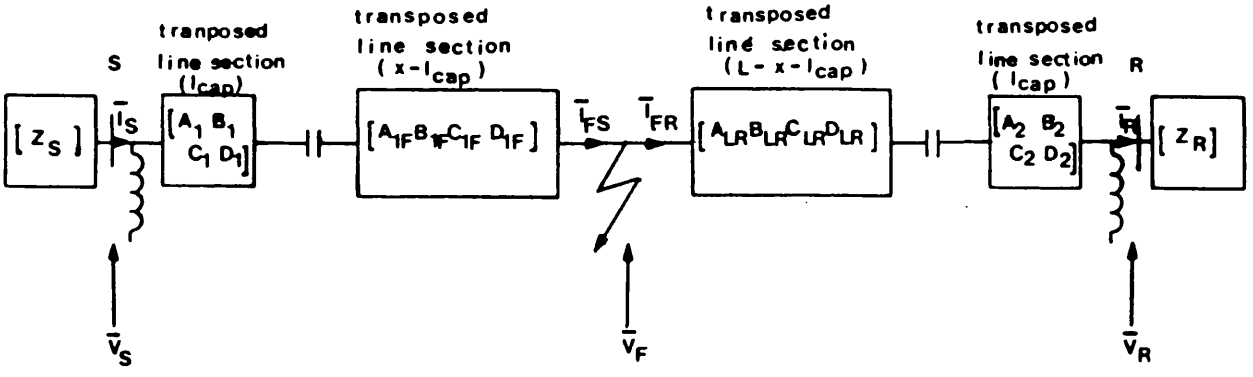


(a)

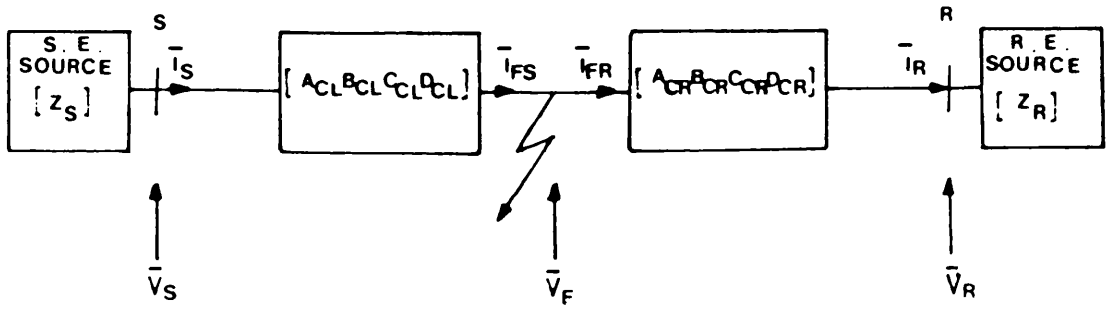


(b)

Figure 2.7 Combination of capacitor-reactor-line section

(a) actual arrangement
(b) equivalent arrangement

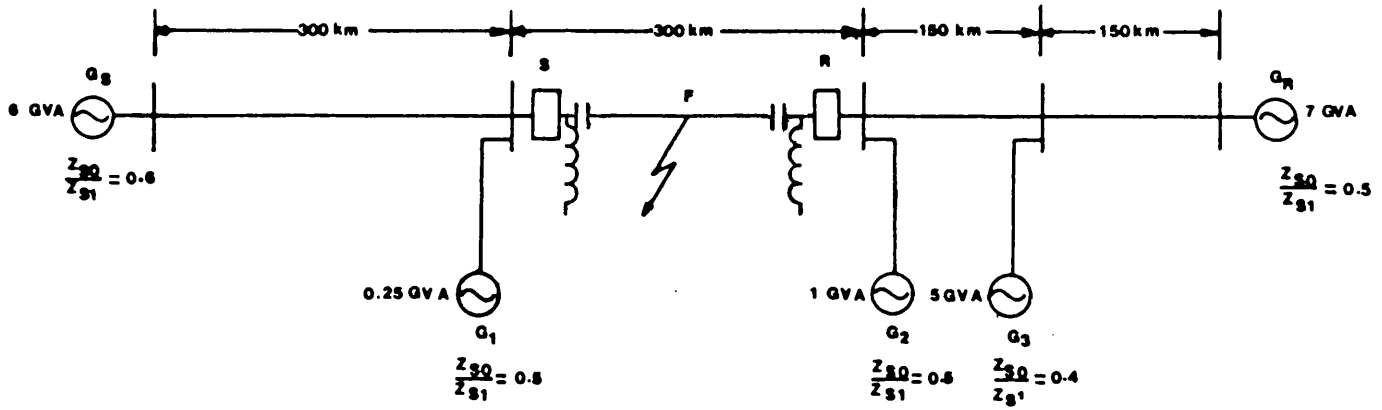


Figure 2.8 Typical system configuration ($h_1$ = 0.75 and $S_{cap}$ = 0.70)

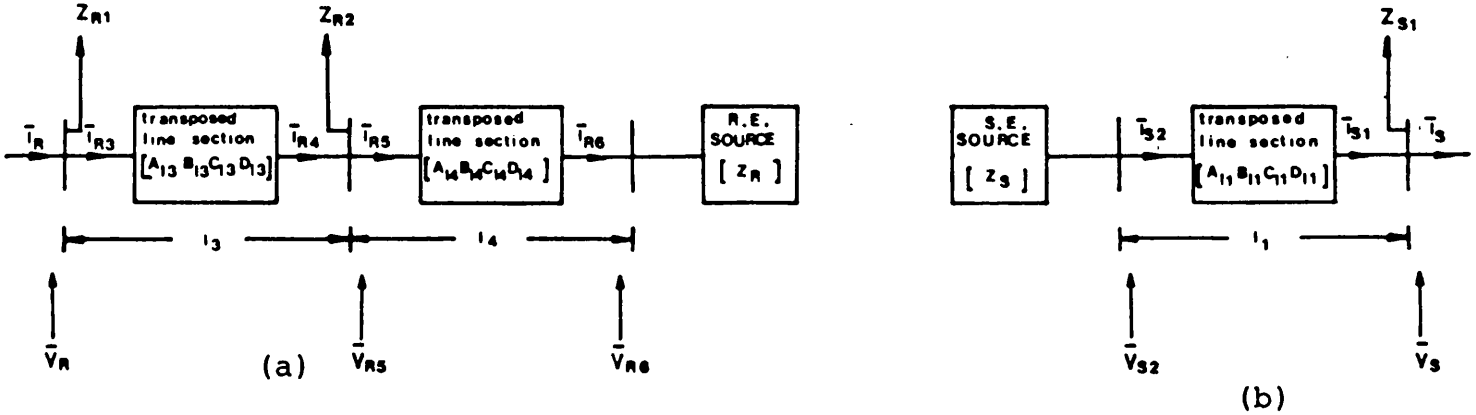


Figure 2.9 Composite source equivalent

(a) receiving end
(b) sending end

# CHAPTER 3 TRANSIENT-FAULT ANALYSIS OF A COMBINED SERIES-SHUNT COMPENSATED SYSTEM WITH SPECIAL REFERENCE TO SINGLE POLE AUTO-RECLOSURE

## 3.1 Introduction

The demand for an accurate and realistic model representation to predict the fault transient behaviour of e.h.v. transmission systems is increasing. Digital based methods of simulation provide a means of realistically simulating the very complex transients which can affect the operation of the protection schemes and also predict any system overvoltages, according to which suitable and economical insulation levels can be determined.

The techniques for simulating the fault transient phenomena for an uncompensated and shunt compensated system are well established[34,37]. However, in the case of series compensated lines, the problem becomes more complex due to the additional non-linearities introduced by the spark gap operations under fault conditions.

Before going to the detail of the mathematical analysis, a brief review of the various protection schemes in use for protecting the series capacitor against excessive overvoltages is presented in Section 3.2.

As mentioned previously, single pole autoreclosure techniques can be used to advantage in long distance transmission lines. Such techniques when applied to a series compensated line can add to already existing problem of protecting it. This is so because of the abrupt changes in the circuit impedances (due to capacitor flashovers) during the fault period. The problem being further accentuated by the sequence of events during the fault clearance and breaker closures, which can have a profound effect on the protective gear. It was in the light of this that it was decided to do some studies relating to single pole autoreclosure techniques as applied to series compensated lines, the basic arrangement and complete frequency domain solution of which is detailed in Sections 3.3 and 3.4.

## 3.2 Spark Gap Classification[59-62]

When high currents due to fault initiation are flowing through the capacitors continuously, a dangerously high voltage is developed across it. Hence the capacitor/capacitors need to be protected against these undesirable overvoltages. All capacitor protective schemes on e.h.v. system use spark gaps connected across it[88,89]. These spark gaps are set in such a manner that when the voltage across it reaches a certain predetermined threshold value, that particular capacitor is

removed from the system. Spark gaps can be classified into the following two broad based lines:

(a) Self-clearing type;

(b) Non-self-clearing type.

### 3.2.1 Self-clearing type

This is a high speed type of protection and very commonly used in the USA. It consists of complicated gaps as shown in Figure 3.1, utilising air blast to suppress the arc. Under fault conditions, the capacitor is usually short circuited in the first 5-20 ms at spark over voltages of about 2.5 to 3.5 p.u. In the absence of protection, overvoltages as high as 5-6 times the normal voltage can be reached[78].

The air blast is not without its own problems and requires correct functioning, and is dependent on the following:

(i) air pressure failure:

(ii) high/low pressure on control air;

(iii) mechanical/valve/regulator/switch failure.

Hence the valves have to be protected separately and this involves extra financial resources, along with added risk. Also the repetitive arc tries to reinsert

the capacitor at overload conditions and this may cause extra stresses on capacitor discharge.

Because of the negative attitude to air blast Ahlgren and Grundmark[11] developed magnetic quenching gap equipment. However, this gap is of limited size and must be made to match the power system. It, too, may extinguish at instants of clearing and reflash every half cycle causing extra stresses on the capacitor dielectric.

### 3.2.2 Non-self-clearing Gaps

The spark gap is the most vital protective item of a series capacitor and hence it must be robust and safe from any failure. Because of the limited size of self-clearing gaps (although to reduce the switching transients to a minimum the gap must be large) and the extra stresses on capacitors exposed to repetitive arcs and consecutive discharge, the European manufacturers prefer the open ventilated non-self-clearing gaps with large carbon electrodes and rotating spark without the need for valve controls. The triggering system is also robust and safe; that is the reason it is mounted outside the power gap cubicles. The scheme is simple and initiates an instantaneous voltage rise and sparkover in the power gap without waiting for charging of auxiliary capacitors and additional voltage swings in oscillatory circuits[4,7].

The various alternative schemes are described below.

3.2.2.1 Single gap scheme

The advantage of this scheme is its simplicity and safety, as illustrated in Figure 3.2(a). The open ventilated, heavy duty spark gap with triggering device has been described by Ahlgren et al[67] as the most reliable coupling device in power system.

The spark gap can be exposed to a short circuit current of 10kA r.m.s. maximum for 3 to 5 cycles and it allows for a moderate speed reinsertion along the dead interval of the line reclosure. This is accepted in many places, particularly as most faults are single-phase-to ground type in which single phase capacitor/capacitors reinsertion may be utilised.

In this thesis the action of single gap schemes is particularly considered.

3.2.2.2 Dual gap or 'Flip-Flop' scheme

The greatest advantage of this scheme is that it provides the necessary high speed capacitor reinsertion by using the same simple and heavy duty equipment as in the basic single gap scheme. In other words, this too does not have any complicated or expensive items.

Figure 3.2(b) illustrates such a scheme.

High speed reinsertion is obtained by adding a parallel branch consisting of a spark gap with a lower setting in series with a breaker. The breaker is opened immediately after the line fault has cleared.

3.2.2.3 Dual gap or 'Stability Booster' scheme

This scheme, as shown in Figure 3.2(c) is particularly suited in those systems exposed to the following:

(a) Extreme voltage transients;

(b) High short circuit loads;

(c) SSR disturbances.

In this case, the extra branch consists of a spark gap in series with a non-linear resistor and a breaker. The non-linear resistor automatically reinserts the capacitor into the transmission system as soon as the fault current through the stability booster drops, on fault clearing. Another advantage of the stability booster is that it is connected into the circuit and supports the stability during the fault time.

## 3.3 Basic Arrangement of the Complete System for the Transient Solution

Figure 3.3 shows a single line diagram of the basic arrangement considered. As mentioned previously, the shunt reactors at each end are combined with the line section between the busbar and the capacitor location. In this context it is quite obvious that for the case where the capacitor location is close to the busbars, the combined shunt reactor-line section simply reduces to a matrix representing the shunt reactors only. Using this model, an earth fault (or a phase-phase fault) can be easily simulated by closing the appropriate switches at the fault point. Fault break-off is likewise simulated by opening the appropriate fault point switches in series with the fault path resistors. The capacitor sparkover simulation and the subsequent reinsertion, together with the opening and reclosure of the circuit breakers (the latter being associated with single pole autoreclosure techniques) is simulated in a similar fashion. In this respect, it must be mentioned that the operation of the various switches is assumed to be ideal, a commonly made assumption, the simulation of the non-linear behaviour of the arcing phenomena, especially across the fault path, being beyond the scope of this work.

In series compensated lines, the protective gaps across the capacitors are arranged to sparkover whenever

the voltage across a capacitor reaches a certain predetermined threshold value, this being in the region of about 2.75 p.u. for most practical systems. The operation of the spark gaps, especially under fault conditions, is essentially of a random nature, ie it is impossible to predefine in advance firstly as to how many capacitors would flashover during the fault period, and secondly the precise sequence in which the spark gaps would operate, both the aforementioned being dependent on the type of fault study carried out. This therefore introduces a large number of network time non-linearities, the number varying according to whether a system has just one single capacitor in each phase or two capacitor banks per phase. Furthermore, the complexity of the whole simulation procedure is accentuated when single pole autoreclosure sequences have also to be implemented. In fact, the scale of the problem becomes so great that it makes it very impractical to develop discrete mathematical methods for simulating each possible sequence. Furthermore, there are limitations posed by the digital computer storage requirements for implementing such large numbers of discrete programs. It was in the light of this that an extensive study was carried out, resulting in the development of mathematical modelling techniques for solving the foregoing problems.

## 3.4 The Mathematical Techniques

The principles underlying the mathematical techniques developed for studying the transient behaviour of a series compensated line under fault conditions are essentially an extension of those developed by Johns and Aggarwal[68] for an uncompensated system and can best be explained by considering a system going through the various aforementioned time variant sequences.

It can be clearly seen from what has been said so far that essentially there are two different problems: (i) the time variant manner in which the various sequences of events take place, and (ii) the wide range of the frequency contents of the transient responses. This means that the principle of superposition has to be applied in two different contexts to deal with the two mentioned problems.

### 3.4.1 Simulation of the Time Variant Non-linearities

As regards the first problem, the time non-linearities generated by the various sequences such as fault inception, capacitor bypass switch operations and the circuit breaker operations can be simulated indirectly by replacing each switch in Figure 3.3 by a set of parallel current generators, the number of these being dependent on the number of circuit states 'n'. This is shown in Figure 3.4, which shows a single line

diagram of the system considered. For the system simulated, it can be seen that during a complete cycle, the number of possible circuit states are:

(i) the normal prefault steady state for all time;

(ii) fault inception at time $t_1$;

(iii) capacitor flashover at time $t_2$;

(iv) breaker pole opening at time $t_3$;

(v) fault break-off at time $t_4$;

(vi) capacitor reinsertion at time $t_5$;

(vii) breaker reclosure at time $t_6$.

Thus, there are seven possible circuit states associated with this practical study and this means that there have to be seven parallel current generators associated with each switch in Figure 3.3. So that in Figure 3.4, the total current, say, through the capacitor bypass switch is given by equation 3.1.

$$i_{SS} = \sum_{k=1}^{7} i_{SSk} \qquad \ldots (3.1)$$

The individual components of the current are arranged so that for any period of time for which the switch is open, the total current $i_{SS} = 0$. Likewise, during any time the switch is closed, $e_S$ the voltage across the capacitor is zero.

Applying the principle of superposition to the circuit of Figure 3.4, the circuit can now be de-coupled into seven separate circuits as shown in Figures 3.5 (a-g). It can be clearly seen that there are an infinite number of combinations of currents and voltages within the super-imposed circuits of Figure 3.5. However, the computational process is greatly simplified by making use of the fact that the voltages and currents associated with each switch do not always have finite values during one complete cycle of events. As, for example, considering the current components through the capacitor bypass switch $i_{SS1} = 0$ for all time, $i_{SS2} = 0$ for $t < t_1$, $i_{SS3} = 0$ for $t < t_2$, . . . , $i_{SS7} = 0$ for $t < t_6$. Likewise, for other currents and voltages. In the case of the total current $i_{SS}$ through the capacitor bypass switch it should be noted that $i_{SS} = 0$ for $t_5 < t < t_2$. Thus, by constraining the various current and voltage components to zero during the various sequences, the whole computational process is greatly simplified.

The subsequent parts of the response are then determined by a series of voltage and current injection at appropriate points in the circuit coupled with the principle of superposition; this is shown in Figures 3.5(a-g). With reference to Figure 3.5 Figure (a) shows the steady state response of the system, ie response for all time. This part is solved with the sinusoidal

source voltage as the forcing function, as shown in Chapter 2. The remaining superimposed circuits (Figures 3.5(b-g)) are then solved by setting all the source voltages to zero.

The steady state value $e_{FF1}$ (as discussed in Chapter 2) thus obtained from Figure 3.5(a) is used to calculate the suddenly applied voltage $e_{FF2} = - e_{FF1}\, h(t - t_1)$ driving the first superimposed circuit of Figure 3.5(b). The resulting solutions to the circuits of Figures 3.5(a,b) then enable the driving voltage for the second superimposed circuit of Figure 3.5(c), $[e_{s3} = - (e_{s1} + e_{s2})\, h(t - t_2)]$ to be determined as a pre-requisite to its solution. Similarly, other dependent solutions on the remaining circuits of Figures 3.5(d-g) are likewise performed by applying the current and voltage.

$$[i_{BS4} = -(i_{BS1} + i_{BS2} + i_{BS3})h(t-t_3)]$$

$$[i_{FF5} = -(i_{FF1} + i_{FF2} + i_{FF3} + i_{FF4})h(t-t_4)]$$

$$[i_{SS6} = -(i_{SS1} + i_{SS2} + i_{SS3} + i_{SS4} + i_{SS5})h(t-t_5)]$$

and

$$[e_{BS7} = -(e_{BS1} + e_{BS2} + e_{BS3} + e_{BS4} + e_{BS5} + e_{BS6})h(t-t_6)]$$

The above simplified example clearly shows that this technique can be readily applied to any arbitrary configuration. Once the steady state response is known, a

series of de-energised circuit models with current generators connected at the various points where the changes occur are solved, the injection being made at such points.

### 3.4.2 Frequency Domain Analysis

The steady state response is obtained from a solution of the basic equations obtained in Chapter 2. However, when a transmission system is undergoing the various aforementioned circuit changes, it is subjected to a wide range of frequency variations and in order to take into account these variations the simulation technique as discussed in Section 3.4.1 should be implemented in frequency domain.

The basic Fourier integral in its continuous form is given by equation 3.2.

$$f(t) = \frac{1}{2\pi} \int_{-\infty}^{\infty} f(\omega) \exp(j\omega t) d\omega \qquad \ldots (3.2)$$

In practice the frequency components are truncated, giving rise to considerable inaccuracies in the time domain. As a result, the modified Fourier integral[45] of the form as shown in equation 3.3 is used in this work for obtaining the time domain response.

$$f(t) = \mathrm{Re} \frac{\exp(\alpha t)}{\pi} \int_{0}^{\Omega} \sigma f(\omega - j\alpha) \exp(j\omega t) d\omega \qquad \ldots (3.3)$$

A frequency shift constant, $\alpha$, is introduced to ensure numerical stability, when the integral is evaluated digitally.

The finite range of integration gives rise to Gibbs oscillations and this is overcome by the introduction of the sigma factor, as given in equation 3.4.

$$\sigma = \frac{\sin(\pi\omega/\Omega)}{\pi\omega/\Omega} \qquad \ldots (3.4)$$

It should be noted that for the purposes of simulating the aforementioned time-variant non-linearities, a modified Fourier integral of the form of equation 3.5 has also to be evaluated

$$\bar{I}_k = \int_{-\infty}^{\infty} i_k \exp(-j(\omega - j\alpha))t \, dt \qquad \ldots (3.5)$$

computationally in order to obtain the frequency spectra of the suddenly applied quantities (such as $i_k$, etc, which are in the time domain) at the point of change.

The frequency domain solution can be best explained with reference to Figure 3.6, which shows a single-line superimposed model of the full system. From the previous Section, it is obvious that in order to obtain a complete solution to the full sequence of events, six such circuits have to be solved. In this analysis, in order

to make the explanation simpler, the suffix k (= 2,3,4,5, 6,7) is used to relate to the $k^{th}$ superimposed circuit. Representing the various line section by the two port network as shown in Chapter 2 and from Figure 3.6 the following matrix relationships are obtained for the quantities on the sending-end side of the fault.

$$\bar{V}_{BSk} = -Z_S \bar{I}_{BSk} = \bar{V}_{BASk} - \bar{E}_{BSk} \quad \ldots (3.5)$$

$$\begin{bmatrix} \bar{V}_{BASk} \\ \bar{I}_{BSk} \end{bmatrix} = \begin{bmatrix} A_1 & B_1 \\ C_1 & D_1 \end{bmatrix} \begin{bmatrix} \bar{E}_{SSk} \\ \bar{I}_{Sk} \end{bmatrix} \quad \ldots (3.6)$$

$$\bar{I}_{SSk} = \bar{I}_{Sk} - \bar{I}_{cSk}, \quad \bar{E}_{Sk} = \bar{V}_{Sk} - \bar{E}_{SSk} \quad \ldots (3.7)$$

$$\begin{bmatrix} \bar{V}_{Sk} \\ \bar{I}_{Sk} \end{bmatrix} = \begin{bmatrix} A_2 & B_2 \\ C_2 & D_2 \end{bmatrix} \begin{bmatrix} A_3 & B_3 \\ C_3 & D_3 \end{bmatrix} \begin{bmatrix} \bar{V}_{FFk} \\ \bar{I}_{FSk} \end{bmatrix} \quad \ldots (3.8)$$

$$\bar{V}_{FFk} = \bar{E}_{FFk} + R_F \bar{I}_{FSRk} \quad \ldots (3.9)$$

Likewise for the relationships on the receiving end of the fault.

Using these various equations, a matrix relationship between the $k^{th}$ superimposed transform currents at the points of change such as the fault path current $\bar{I}_{FSRk}$, the currents $\bar{I}_{SSk}$ and $\bar{I}_{RRk}$ through the two

capacitor bypass siwthces and the breaker point currents $\overline{I}_{BSk}$ and $\overline{I}_{BRk}$, and the associated transform voltages across each current generator, these being $\overline{E}_{FFk}$, $\overline{E}_{Sk}$, $\overline{E}_{Rk}$, $\overline{E}_{BSk}$ and $\overline{E}_{BRk}$ respectively, as shown in equation A1.34, is obtained. The actual derivation of this matrix relationship is shown in detail in Appendix (A1.1).

The (15 x 15) admittance matrix relationship of equation A1.34 is essentially a universal relationship, (for all faults involving earth), ie for a particular fault study, remains unchanged irrespective of the circuit (as there is a possible number of six of these) under consideration. For this reason this matrix is computed only once and then stored at the beginning of each study, thus cutting down on the computational process considerably. The matrix relationship shown in equation A1.34 has been derived for a system subjected to a single-phase-to-earth fault. When dealing with a phase-to-phase fault (Figure 3.7) simulation the various currents and voltages are obviously related via a totally different matrix. Appendix (A1.2) shows the derivation of such a matrix relationship for a phase-to-phase fault and it can be seen that the form of the final matrix derivation is similar to the one devised for a single-phase-to-earth fault.

Studies have also been carried out with a single

capacitor located at the mid-point. In such a case, a completely different matrix of the order (12 x 12) is obtained. With reference to Figure 3.8 (single-phase-to-earth fault), a relationship between the fault path current $\overline{I}_{FSRk}$, the current $\overline{I}_{capk}$ through the capacitor bypass switch and the breaker point currents $\overline{I}_{BSk}$ and $\overline{I}_{BRk}$ and the associated voltages across each current generator $\overline{E}_{FFk}$, $\overline{E}_{capk}$, $\overline{E}_{BSk}$ and $\overline{E}_{BRk}$ can be similarly obtained.

### 3.4.3 Superimposed circuit solution

With reference to the matrix relationship of equation A1.34 it can be seen that there are a vast number of combinations of the fifteen known transforms which can arise, and it is very impractical to compute all the matrix operations necessary to provide a solution for each possible superimposed circuit. However, this problem is partly overcome by making use of the fact that there are always fourteen known zero valued transforms (combinations of currents and voltages) associated with any superimposed circuit. The fifteenth value is the known frequency transfer of the voltage or current which energises the superimposed circuit at the point at which the circuit change represented occurs.

The simplest way of illustrating the computational procedures involved is by considering the full system

model of Figure 3.6, going through the various aforementioned circuit changes. Analysis for two different types of fault, ie single-phase-to-earth and a pure phase-to-phase, would be shown. In the first part it would be assumed that the system is subjected to a single-phase-to-earth fault on the 'a' phase, followed by the 'a' phase receiving end capacitor flashover, the opening of the 'a' phase breaker poles, fault break off, capacitor reinsertion and finally the breaker reclosure. In the second part, the analysis for a system subjected to a 'b'-'c' phase fault followed by the spark gap operation across the sending end 'c' phase capacitor would be chosen. In this respect, it should be mentioned that it is normal practice to utilise 3-phase autoreclosure schemes for all faults other than single-phase-to-earth. Simulation of such a scheme for the second part where a phase-to-phase fault is involved is beyond the scope of this work.

### 3.4.3.1 Single-phase-to-earth fault

#### 3.4.3.1.1 Fault inception simulation

With reference to equation A1.35 the zero valued transforms are $\overline{E}_{BSka,b,c}$, $\overline{E}_{BRka,b,c}$, $\overline{I}_{FSRkb,c}$, $\overline{I}_{SSka,b,c}$ and $\overline{I}_{RRka,b,c}$. The above mentioned transforms are placed in their appropriate current and voltage vectors of the universal impedance matrix, which when written in extended form is as given in equation 3.10.

$$
\begin{bmatrix}
\bar{E}_{FFka} \\ \bar{E}_{FFkb} \\ \bar{E}_{FFkc} \\ \bar{E}_{Ska} \\ \bar{E}_{Skb} \\ \bar{E}_{Skc} \\ \bar{E}_{Rka} \\ \bar{E}_{Rkb} \\ \bar{E}_{Rkc} \\ 0 \\ 0 \\ 0 \\ 0 \\ 0 \\ 0 \\ 0
\end{bmatrix}
=
\begin{bmatrix}
a_{1,1} & a_{1,2} & a_{1,3} & a_{1,4} & a_{1,5} & a_{1,6} & a_{1,7} & a_{1,8} & a_{1,9} & a_{1,10} & a_{1,11} & a_{1,12} & a_{1,13} & a_{1,14} & a_{1,15} \\
a_{2,1} & a_{2,2} & a_{2,3} & a_{2,4} & a_{2,5} & a_{2,6} & a_{2,7} & a_{2,8} & a_{2,9} & a_{2,10} & a_{2,11} & a_{2,12} & a_{2,13} & a_{2,14} & a_{2,15} \\
a_{3,1} & a_{3,2} & a_{3,3} & a_{3,4} & a_{3,5} & a_{3,6} & a_{3,7} & a_{3,8} & a_{3,9} & a_{3,10} & a_{3,11} & a_{3,12} & a_{3,13} & a_{3,14} & a_{3,15} \\
a_{4,1} & a_{4,2} & a_{4,3} & a_{4,4} & a_{4,5} & a_{4,6} & a_{4,7} & a_{4,8} & a_{4,9} & a_{4,10} & a_{4,11} & a_{4,12} & a_{4,13} & a_{4,14} & a_{4,15} \\
a_{5,1} & a_{5,2} & a_{5,3} & a_{5,4} & a_{5,5} & a_{5,6} & a_{5,7} & a_{5,8} & a_{5,9} & a_{5,10} & a_{5,11} & a_{5,12} & a_{5,13} & a_{5,14} & a_{5,15} \\
a_{6,1} & a_{6,2} & a_{6,3} & a_{6,4} & a_{6,5} & a_{6,6} & a_{6,7} & a_{6,8} & a_{6,9} & a_{6,10} & a_{6,11} & a_{6,12} & a_{6,13} & a_{6,14} & a_{6,15} \\
a_{7,1} & a_{7,2} & a_{7,3} & a_{7,4} & a_{7,5} & a_{7,6} & a_{7,7} & a_{7,8} & a_{7,9} & a_{7,10} & a_{7,11} & a_{7,12} & a_{7,13} & a_{7,14} & a_{7,15} \\
a_{8,1} & a_{8,2} & a_{8,3} & a_{8,4} & a_{8,5} & a_{8,6} & a_{8,7} & a_{8,8} & a_{8,9} & a_{8,10} & a_{8,11} & a_{8,12} & a_{8,13} & a_{8,14} & a_{8,15} \\
a_{9,1} & a_{9,2} & a_{9,3} & a_{9,4} & a_{9,5} & a_{9,6} & a_{9,7} & a_{9,8} & a_{9,9} & a_{9,10} & a_{9,11} & a_{9,12} & a_{9,13} & a_{9,14} & a_{9,15} \\
a_{10,1} & a_{10,2} & a_{10,3} & a_{10,4} & a_{10,5} & a_{10,6} & a_{10,7} & a_{10,8} & a_{10,9} & a_{10,10} & a_{10,11} & a_{10,12} & a_{10,13} & a_{10,14} & a_{10,15} \\
a_{11,1} & a_{11,2} & a_{11,3} & a_{11,4} & a_{11,5} & a_{11,6} & a_{11,7} & a_{11,8} & a_{11,9} & a_{11,10} & a_{11,11} & a_{11,12} & a_{11,13} & a_{11,14} & a_{11,15} \\
a_{12,1} & a_{12,2} & a_{12,3} & a_{12,4} & a_{12,5} & a_{12,6} & a_{12,7} & a_{12,8} & a_{12,9} & a_{12,10} & a_{12,11} & a_{12,12} & a_{12,13} & a_{12,14} & a_{12,15} \\
a_{13,1} & a_{13,2} & a_{13,3} & a_{13,4} & a_{13,5} & a_{13,6} & a_{13,7} & a_{13,8} & a_{13,9} & a_{13,10} & a_{13,11} & a_{13,12} & a_{13,13} & a_{13,14} & a_{13,15} \\
a_{14,1} & a_{14,2} & a_{14,3} & a_{14,4} & a_{14,5} & a_{14,6} & a_{14,7} & a_{14,8} & a_{14,9} & a_{14,10} & a_{14,11} & a_{14,12} & a_{14,13} & a_{14,14} & a_{14,15} \\
a_{15,1} & a_{15,2} & a_{15,3} & a_{15,4} & a_{15,5} & a_{15,6} & a_{15,7} & a_{15,8} & a_{15,9} & a_{15,10} & a_{15,11} & a_{15,12} & a_{15,13} & a_{15,14} & a_{15,15}
\end{bmatrix}
\begin{bmatrix}
\bar{I}_{FSRka} \\ 0 \\ 0 \\ 0 \\ 0 \\ 0 \\ 0 \\ 0 \\ 0 \\ \bar{I}_{BSka} \\ \bar{I}_{BSkb} \\ \bar{I}_{BSkc} \\ \bar{I}_{BRka} \\ \bar{I}_{BRkb} \\ \bar{I}_{BRkc}
\end{bmatrix}
$$

where 'a' is the inverse of 'A' matrix, order(15 x 15) and is the universal impedance matrix . . . (3.10)

With reference to equation 3.10 all the rows and columns corresponding to zero valued transforms in the current vector can be removed, which produces a reduced matrix relationship of equation 3.11 which in turn is inverted to produce 3.12.

$$\begin{bmatrix} \bar{E}_{FFka} \\ 0 \\ 0 \\ 0 \\ 0 \\ 0 \\ 0 \end{bmatrix} = \begin{bmatrix} a_{1,1} & a_{1,10} & a_{1,11} & a_{1,12} & a_{1,13} & a_{1,14} & a_{1,15} \\ a_{10,1} & a_{10,10} & a_{10,11} & a_{10,12} & a_{10,13} & a_{10,14} & a_{10,15} \\ a_{11,1} & a_{11,10} & a_{11,11} & a_{11,12} & a_{11,13} & a_{11,14} & a_{11,15} \\ a_{12,1} & a_{12,10} & a_{12,11} & a_{12,12} & a_{12,13} & a_{12,14} & a_{12,15} \\ a_{13,1} & a_{13,10} & a_{13,11} & a_{13,12} & a_{13,13} & a_{13,14} & a_{13,15} \\ a_{14,1} & a_{14,10} & a_{14,11} & a_{14,12} & a_{14,13} & a_{14,14} & a_{14,15} \\ a_{15,1} & a_{15,10} & a_{15,11} & a_{15,12} & a_{15,13} & a_{15,14} & a_{15,15} \end{bmatrix} \begin{bmatrix} \bar{I}_{FSRka} \\ \bar{I}_{BSka} \\ \bar{I}_{BSkb} \\ \bar{I}_{BSkc} \\ \bar{I}_{BRka} \\ \bar{I}_{BRkb} \\ \bar{I}_{BRkc} \end{bmatrix} \quad \ldots (3.11)$$

$$\begin{bmatrix} \bar{I}_{FSRka} \\ \bar{I}_{BSka} \\ \bar{I}_{BSkb} \\ \bar{I}_{BSkc} \\ \bar{I}_{BRka} \\ \bar{I}_{BRkb} \\ \bar{I}_{BRkc} \end{bmatrix} = \begin{bmatrix} b_{1,1} \\ b_{2,1} \\ b_{3,1} \\ b_{4,1} \\ b_{5,1} \\ b_{6,1} \\ b_{7,1} \end{bmatrix} \begin{bmatrix} \bar{E}_{FFka} \end{bmatrix} \quad \ldots (3.12)$$

Now $\bar{E}_{FFka}$ is the fifteenth known transform which is the suddenly applied voltage of the form $\int_{t_1}^{TOB} e_{FF1a} e^{-j\omega t}\, dt$;

where $e_{FF1a}$ is the time domain variation of prefault steady state component and TOB the observation time. Further substitution of the resulting known current vector of equation 3.12 into the full impedance matrix of equation 3.10 enables the remaining voltage transforms to be obtained. The transforms of the quantities of interest are then converted into the time domain using the FFT routine, and these when added to the time variation of the steady state component give the total solution at this stage. For example, the total time domain response of, say, the receiving end 'a' phase capacitor voltage at this stage would be:

$$e_{RTa}(t) = e_{R1a}(t) + e_{R2a}(t - t_1)$$

3.4.3.1.2 Capacitor flashover simulation

The procedure adopted for simulating the capacitor flashover is, on fault inception, to scan all the voltages across the six capacitors in the time domain and whichever of these voltages reaches the pre-defined threshold value first, that constitutes the first capacitor flashover and therefore a circuit change. A solution to the superimposed circuit associated with this circuit change is then obtained (as would be shown later on) resulting in the time domain variation (after transfer from frequency to time domain) of a new component, which when added to all the previous components gives the total time domain response at this

stage. The process is then repeated for the remaining five capacitors. At this point, it must be mentioned that the capacitors, which do flashover mostly do so within a cycle from fault inception.

In this particular example if, say, the 'a' phase receiving end capacitor flashover first, then with reference to equation A1.35 the zero valued transforms are $\bar{E}_{FFka}$ , $\bar{E}_{BSka,b,c}$ , $\bar{E}_{BRka,b,c}$ , $\bar{I}_{FSRkb,c}$ , $\bar{I}_{SSka,b,c}$ and $\bar{I}_{RRkb,c}$ . Again, by adopting the foregoing procedure, the matrix relationship as shown in equation 3.13 is obtained, which in turn is inverted to produce equation 3.14.

$$\begin{bmatrix} 0 \\ \bar{E}_{Rka} \\ 0 \\ 0 \\ 0 \\ 0 \\ 0 \\ 0 \end{bmatrix} = \begin{bmatrix} a_{1,1} & a_{1,7} & a_{1,10} & a_{1,11} & a_{1,12} & a_{1,13} & a_{1,14} & a_{1,15} \\ a_{7,1} & a_{7,7} & a_{7,10} & a_{7,11} & a_{7,12} & a_{7,13} & a_{7,14} & a_{7,15} \\ a_{10,1} & a_{10,7} & a_{10,10} & a_{10,11} & a_{10,12} & a_{10,13} & a_{10,14} & a_{10,15} \\ a_{11,1} & a_{11,7} & a_{11,10} & a_{11,11} & a_{11,12} & a_{11,13} & a_{11,14} & a_{11,15} \\ a_{12,1} & a_{12,7} & a_{12,10} & a_{12,11} & a_{12,12} & a_{12,13} & a_{12,14} & a_{12,15} \\ a_{13,1} & a_{13,7} & a_{13,10} & a_{13,11} & a_{13,12} & a_{13,13} & a_{13,14} & a_{13,15} \\ a_{14,1} & a_{14,7} & a_{14,10} & a_{14,11} & a_{14,12} & a_{14,13} & a_{14,14} & a_{14,15} \\ a_{15,1} & a_{15,7} & a_{15,10} & a_{15,11} & a_{15,12} & a_{15,13} & a_{15,14} & a_{15,15} \end{bmatrix} \begin{bmatrix} \bar{I}_{FSRka} \\ \bar{I}_{RRka} \\ \bar{I}_{BSka} \\ \bar{I}_{BSkb} \\ \bar{I}_{BSkc} \\ \bar{I}_{BRka} \\ \bar{I}_{BRkb} \\ \bar{I}_{BRkc} \end{bmatrix}$$

. . . (3.13)

$$\begin{bmatrix} \bar{I}_{FSRka} \\ \bar{I}_{RRka} \\ \bar{I}_{BSka} \\ \bar{I}_{BSkb} \\ \bar{I}_{BSkc} \\ \bar{I}_{BRka} \\ \bar{I}_{BRkb} \\ \bar{I}_{BRkc} \end{bmatrix} = \begin{bmatrix} b_{1,2} \\ b_{2,2} \\ b_{3,2} \\ b_{4,2} \\ b_{5,2} \\ b_{6,2} \\ b_{7,2} \\ b_{8,2} \end{bmatrix} \begin{bmatrix} \bar{E}_{Rka} \end{bmatrix} \quad \ldots (3.14)$$

$\bar{E}_{Rka}$ is the known transform and is given by

$$\bar{E}_{Rka} = \int_{t_2}^{TOB} (e_{R1a} + e_{R2a})\, e^{-j\omega t}\, dt ,$$

where $e_{R1a}$ = time domain variation of prefault steady state component, and $e_{R2a}$ = component due to fault inception.

As mentioned before, the quantities are converted to the time domain using the FFT and the necessary addition done to give the total solution at this stage. For example, the total time domain solution of, say, the 'a' phase sending and receiving end breaker current would be:

$$i_{BSTa}(t) = i_{BS1a}(t) + i_{BS2a}(t-t_1) + i_{BS3a}(t-t_2)$$

and $i_{BRTa}(t) = i_{BR1a}(t) + i_{BR2a}(t-t_1) + i_{BR3a}(t-t_2)$.

As mentioned earlier in this Section, the process is repeated for the remaining five capacitors.

3.4.3.1.3 Breaker current interruption simulation

For this study purpose, it will be assumed that both the sending end and the receiving end poles are opened simultaneously, although the program can quite easily deal with the non-simultaneousity of this process. The criteria used are with reference to equation A1.34; the known zero valued transforms are $\bar{I}_{FSRkb,c}$ , $\bar{I}_{SSka,b,c}$ , $\bar{I}_{RRkb,c}$ , $\bar{E}_{FFka}$ , $\bar{E}_{RKa}$ , $\bar{E}_{BSkbc}$ , $\bar{E}_{BRkb,c}$ . Again, by adopting the foregoing procedure the matrix relationship of equation 3.15 is obtained which in turn is inverted to produce equation 3.16. Here it should be noted that because the known transforms are current, the admittance matrix is made use of rather than the impedance matrix of the previous two processes.

$$\begin{bmatrix} 0 \\ 0 \\ 0 \\ 0 \\ 0 \\ 0 \\ 0 \\ \bar{I}_{BSka} \\ \bar{I}_{BRka} \end{bmatrix} = \begin{bmatrix} A_{2,2} & A_{2,3} & A_{2,4} & A_{2,5} & A_{2,6} & A_{2,8} & A_{2,9} & A_{2,10} & A_{2,13} \\ A_{3,2} & A_{3,3} & A_{3,4} & A_{3,5} & A_{3,6} & A_{3,8} & A_{3,9} & A_{3,10} & A_{3,13} \\ A_{4,2} & A_{4,3} & A_{4,4} & A_{4,5} & A_{4,6} & A_{4,8} & A_{4,9} & A_{4,10} & A_{4,13} \\ A_{5,2} & A_{5,3} & A_{5,4} & A_{5,5} & A_{5,6} & A_{5,8} & A_{5,9} & A_{5,10} & A_{5,13} \\ A_{6,2} & A_{6,3} & A_{6,4} & A_{6,5} & A_{6,6} & A_{6,8} & A_{6,9} & A_{6,10} & A_{6,13} \\ A_{8,2} & A_{8,3} & A_{8,4} & A_{8,5} & A_{8,6} & A_{8,8} & A_{8,9} & A_{8,10} & A_{8,13} \\ A_{9,2} & A_{9,3} & A_{9,4} & A_{9,5} & A_{9,6} & A_{9,8} & A_{9,9} & A_{9,10} & A_{9,13} \\ A_{10,2} & A_{10,3} & A_{10,4} & A_{10,5} & A_{10,6} & A_{10,8} & A_{10,9} & A_{10,10} & A_{10,13} \\ A_{13,2} & A_{13,3} & A_{13,4} & A_{13,5} & A_{13,6} & A_{13,8} & A_{13,9} & A_{13,10} & A_{13,13} \end{bmatrix} \begin{bmatrix} \bar{E}_{FFkb} \\ \bar{E}_{FFkc} \\ \bar{E}_{Ska} \\ \bar{E}_{Skb} \\ \bar{E}_{Skc} \\ \bar{E}_{Rkb} \\ \bar{E}_{Rkc} \\ \bar{E}_{BSka} \\ \bar{E}_{BRka} \end{bmatrix}$$

. . . (3.15)

$$\begin{bmatrix} \bar{E}_{FFkb} \\ \bar{E}_{FFkc} \\ \bar{E}_{Ska} \\ \bar{E}_{Skb} \\ \bar{E}_{Skc} \\ \bar{E}_{Rkb} \\ \bar{E}_{Rkc} \\ \bar{E}_{BSka} \\ \bar{E}_{BRka} \end{bmatrix} = \begin{bmatrix} B_{1,8} & B_{1,9} \\ B_{2,8} & B_{2,9} \\ B_{3,8} & B_{3,9} \\ B_{4,8} & B_{4,9} \\ B_{5,8} & B_{5,9} \\ B_{6,8} & B_{6,9} \\ B_{7,8} & B_{7,9} \\ B_{8,8} & B_{8,9} \\ B_{9,8} & B_{9,9} \end{bmatrix} \begin{bmatrix} \bar{I}_{BSka} \\ \bar{I}_{BRka} \end{bmatrix} \quad \ldots (3.16)$$

$\bar{I}_{BSka}$ and $\bar{I}_{BRka}$ are the known transforms and are given by:

$$\bar{I}_{BSka} = \int_{t_3}^{TOB} (i_{BS1a} + i_{BS2a} + i_{BS3a})\, e^{-j\omega t}\, dt$$

and $$\bar{I}_{BRka} = \int_{t_3}^{TOB} (i_{BR1a} + i_{BR2a} + i_{BR3a})\, e^{-j\omega t}\, dt$$

where $i_{BS1a}$ , $i_{BR1a}$ = time domain variation of prefault steady state component.

$i_{BS2a}$ , $i_{BR2a}$ = component due to fault inception.

$i_{BS3a}$ , $i_{BR3a}$ = component due to capacitor flashover.

At this stage, the total time domain fault point variation would be:

$$i_{FSRTa}(t) = i_{FSR2a}(t-t_1) + i_{FSR3a}(t-t_2) + i_{FSR4a}(t-t_3)$$

$i_{FSR1a}(t)$, the steady state part component is zero.

3.4.3.1.4 Fault break off simulation

After the breaker current interruption, the fault is broken off at the first zero crossing after the magnitude of the secondary arc current reaches 28A peak. Again the admittance /matrix is made use of and with reference to equation A1.34 the known zero valued transforms are $\overline{I}_{FSRkb,c}$ , $\overline{I}_{SSka,b,c}$ , $\overline{I}_{RRkb,c}$ , $\overline{I}_{BSka}$ , $\overline{I}_{BRka}$ , $\overline{E}_{Rka}$ , $\overline{E}_{BSkb,c}$ , $\overline{E}_{BRkb,c}$ and the resulting matrix relationship is given in equation 3.17, which in turn is inverted to yield equation 3.18.

$$\begin{bmatrix} \overline{I}_{FSRka} \\ 0 \\ 0 \\ 0 \\ 0 \\ 0 \\ 0 \\ 0 \\ 0 \\ 0 \end{bmatrix} = \begin{bmatrix} A_{1,1} & A_{1,2} & A_{1,3} & A_{1,4} & A_{1,5} & A_{1,6} & A_{1,8} & A_{1,9} & A_{1,10} & A_{1,13} \\ A_{2,1} & A_{2,2} & A_{2,3} & A_{2,4} & A_{2,5} & A_{2,6} & A_{2,8} & A_{2,9} & A_{2,10} & A_{2,13} \\ A_{3,1} & A_{3,2} & A_{3,3} & A_{3,4} & A_{3,5} & A_{3,6} & A_{3,8} & A_{3,9} & A_{3,10} & A_{3,13} \\ A_{4,1} & A_{4,2} & A_{4,3} & A_{4,4} & A_{4,5} & A_{4,6} & A_{4,8} & A_{4,9} & A_{4,10} & A_{4,13} \\ A_{5,1} & A_{5,2} & A_{5,3} & A_{5,4} & A_{5,5} & A_{5,6} & A_{5,8} & A_{5,9} & A_{5,10} & A_{5,13} \\ A_{6,1} & A_{6,2} & A_{6,3} & A_{6,4} & A_{6,5} & A_{6,6} & A_{6,8} & A_{6,9} & A_{6,10} & A_{6,13} \\ A_{8,1} & A_{8,2} & A_{8,3} & A_{8,4} & A_{8,5} & A_{8,6} & A_{8,8} & A_{8,9} & A_{8,10} & A_{8,13} \\ A_{9,1} & A_{9,2} & A_{9,3} & A_{9,4} & A_{9,5} & A_{9,6} & A_{9,8} & A_{9,9} & A_{9,10} & A_{9,13} \\ A_{10,1} & A_{10,2} & A_{10,3} & A_{10,4} & A_{10,5} & A_{10,6} & A_{10,8} & A_{10,9} & A_{10,10} & A_{10,13} \\ A_{13,1} & A_{13,2} & A_{13,3} & A_{13,4} & A_{13,5} & A_{13,6} & A_{13,8} & A_{13,9} & A_{13,10} & A_{13,13} \end{bmatrix} \begin{bmatrix} \overline{E}_{FFka} \\ \overline{E}_{FFkb} \\ \overline{E}_{FFkc} \\ \overline{E}_{Ska} \\ \overline{E}_{Skb} \\ \overline{E}_{Skc} \\ \overline{E}_{Rkb} \\ \overline{E}_{Rkc} \\ \overline{E}_{BSka} \\ \overline{E}_{BRka} \end{bmatrix} \quad \ldots (3.17)$$

$$\begin{bmatrix} \bar{E}_{FFka} \\ \bar{E}_{FFkb} \\ \bar{E}_{FFkc} \\ \bar{E}_{Ska} \\ \bar{E}_{Skb} \\ \bar{E}_{Skc} \\ \bar{E}_{Rkb} \\ \bar{E}_{Rkc} \\ \bar{E}_{BSka} \\ \bar{E}_{BRka} \end{bmatrix} = \begin{bmatrix} B_{1,1} \\ B_{2,1} \\ B_{3,1} \\ B_{4,1} \\ B_{5,1} \\ B_{6,1} \\ B_{7,1} \\ B_{8,1} \\ B_{9,1} \\ B_{10,1} \end{bmatrix} \begin{bmatrix} \bar{I}_{FSRka} \end{bmatrix} \quad \ldots \quad (3.18)$$

$\bar{I}_{FSRka}$ is the known transform and is given by

$$\bar{I}_{FSRka} = \int_{t_4}^{TOB} (i_{FSR2a} + i_{FSR3a} + i_{FSR4a})\, e^{-j\omega t}\, dt.$$

$i_{FSR2a}$ = component due to fault inception.

$i_{FSR3a}$ = component due to capacitor flashover.

$i_{FSR4a}$ = component due to current interruption.

At this stage the total time domain response of the current through the bypass switch (across the 'a' phase receiving end capacitor, say) is:

$$i_{RRTa}(t) = i_{RR3a}(t-t_2) + i_{RR4a}(t-t_3) + i_{RR5a}(t-t_4)$$

Components due to the steady state and fault inception ($i_{RR1a}$ , $i_{RR2a}$) are zero.

3.4.3.1.5 Capacitor reinsertion simulation

During the dead interval (after fault break off) the capacitor is reinserted back into the system. With reference to eqn. A1.34 the known zero valued transforms are $\bar{I}_{FSRka,b,c}$, $\bar{I}_{SSka,b,c}$, $\bar{I}_{RRkb,c}$, $\bar{I}_{BSka}$, $\bar{I}_{BRka}$, $\bar{E}_{BSkb,c}$ and $\bar{E}_{BRkb,c}$. Hence a matrix relationship of equation 3.19 is obtained, which in turn is inverted to give equation 3.20. (Equation 3.19 is to be found overleaf.)

$$\begin{bmatrix} \bar{E}_{FFka} \\ \bar{E}_{FFkb} \\ \bar{E}_{FFkc} \\ \bar{E}_{Ska} \\ \bar{E}_{Skb} \\ \bar{E}_{Skc} \\ \bar{E}_{Rka} \\ \bar{E}_{Rkb} \\ \bar{E}_{Rkc} \\ \bar{E}_{BSka} \\ \bar{E}_{BRka} \end{bmatrix} = \begin{bmatrix} B_{1,7} \\ B_{2,7} \\ B_{3,7} \\ B_{4,7} \\ B_{5,7} \\ B_{6,7} \\ B_{7,7} \\ B_{8,7} \\ B_{9,7} \\ B_{10,7} \\ B_{11,7} \end{bmatrix} \begin{bmatrix} \bar{I}_{RRka} \end{bmatrix} \quad \ldots(3.20)$$

$\bar{I}_{RRka}$ is the known transform and is given by:

$$\bar{I}_{RRka} = \int_{t_5}^{TOB} (i_{RR3a} + i_{RR4a} + i_{RR5a})\, e^{-j\omega t}\, dt$$

$i_{RR3a}$ = component due to capacitor flashover

$i_{RR4a}$ = component due to current interruption

$i_{RR5a}$ = component due to fault break off

$$\begin{bmatrix} 0 \\ 0 \\ 0 \\ 0 \\ 0 \\ 0 \\ \overline{I}_{RRka} \\ 0 \\ 0 \\ 0 \\ 0 \end{bmatrix} = \begin{bmatrix} A_{1,1} & A_{1,2} & A_{1,3} & A_{1,4} & A_{1,5} & A_{1,6} & A_{1,7} & A_{1,8} & A_{1,9} & A_{1,10} & A_{1,13} \\ A_{2,1} & A_{2,2} & A_{2,3} & A_{2,4} & A_{2,5} & A_{2,6} & A_{2,7} & A_{2,8} & A_{2,9} & A_{2,10} & A_{2,13} \\ A_{3,1} & A_{3,2} & A_{3,3} & A_{3,4} & A_{3,5} & A_{3,6} & A_{3,7} & A_{3,8} & A_{3,9} & A_{3,10} & A_{3,13} \\ A_{4,1} & A_{4,2} & A_{4,3} & A_{4,4} & A_{4,5} & A_{4,6} & A_{4,7} & A_{4,8} & A_{4,9} & A_{4,10} & A_{4,13} \\ A_{5,1} & A_{5,2} & A_{5,3} & A_{5,4} & A_{5,5} & A_{5,6} & A_{5,7} & A_{5,8} & A_{5,9} & A_{5,10} & A_{5,13} \\ A_{6,1} & A_{6,2} & A_{6,3} & A_{6,4} & A_{6,5} & A_{6,6} & A_{6,7} & A_{6,8} & A_{6,9} & A_{6,10} & A_{6,13} \\ A_{7,1} & A_{7,2} & A_{7,3} & A_{7,4} & A_{7,5} & A_{7,6} & A_{7,7} & A_{7,8} & A_{7,9} & A_{7,10} & A_{7,13} \\ A_{8,1} & A_{8,2} & A_{8,3} & A_{8,4} & A_{8,5} & A_{8,6} & A_{8,7} & A_{8,8} & A_{8,9} & A_{8,10} & A_{8,13} \\ A_{9,1} & A_{9,2} & A_{9,3} & A_{9,4} & A_{9,5} & A_{9,6} & A_{9,7} & A_{9,8} & A_{9,9} & A_{9,10} & A_{9,13} \\ A_{10,1} & A_{10,2} & A_{10,3} & A_{10,4} & A_{10,5} & A_{10,6} & A_{10,7} & A_{10,8} & A_{10,9} & A_{10,10} & A_{10,13} \\ A_{13,1} & A_{13,2} & A_{13,3} & A_{13,4} & A_{13,5} & A_{13,6} & A_{13,7} & A_{13,8} & A_{13,9} & A_{13,10} & A_{13,13} \end{bmatrix} \begin{bmatrix} \overline{E}_{FFka} \\ \overline{E}_{FFkb} \\ \overline{E}_{FFkc} \\ \overline{E}_{SKa} \\ \overline{E}_{Skb} \\ \overline{E}_{Skc} \\ \overline{E}_{Rka} \\ \overline{E}_{Rkb} \\ \overline{E}_{Rkc} \\ \overline{E}_{BSka} \\ \overline{E}_{BRka} \end{bmatrix}$$

. . . (3.19)

At this stage, the total time domain response of the voltage across the say 'a' phase sending and receiving end breaker is:

$$e_{BSTa}(t) = e_{BS4a}(t-t_3) + e_{BS5a}(t-t_4) + e_{BS6a}(t-t_5)$$

$$e_{BRTa}(t) = e_{BR4a}(t-t_3) + e_{BR5a}(t-t_4) + e_{BR6a}(t-t_5)$$

Components due to steady state, fault inception and capacitor flashover ($e_{BS1a}$ , $e_{BS2a}$ , $e_{BS3a}$ , $e_{BR1a}$ , $e_{BR2a}$ and $e_{BR3a}$) are zero.

3.4.3.1.6 Line reclosure simulation

In order to deionise the line fault, a dead interval is commonly required before line breaker auto-reclosure sequence takes place. Again as before, both the sending and the receiving end breaker poles are simultaneously closed. With reference to equation A1.35 the known zero valued transforms are $\bar{E}_{BSkb,c}$ , $\bar{E}_{BRkb,c}$ , $\bar{I}_{FSRka,b,c}$ , $\bar{I}_{SSka,b,c}$ , $\bar{I}_{RRka,b,c}$ which is represented by a matrix relationship of equation 3.21 which in turn is inverted to give equation 3.22.

$$\begin{bmatrix} \bar{E}_{BSka} \\ 0 \\ 0 \\ \bar{E}_{BRka} \\ 0 \\ 0 \end{bmatrix} = \begin{bmatrix} a_{10,10} & a_{10,11} & a_{10,12} & a_{10,13} & a_{10,14} & a_{10,15} \\ a_{11,10} & a_{11,11} & a_{11,12} & a_{11,13} & a_{11,14} & a_{11,15} \\ a_{12,10} & a_{12,11} & a_{12,12} & a_{12,13} & a_{12,14} & a_{12,15} \\ a_{13,10} & a_{13,11} & a_{13,12} & a_{13,13} & a_{13,14} & a_{13,15} \\ a_{14,10} & a_{14,11} & a_{14,12} & a_{14,13} & a_{14,14} & a_{14,15} \\ a_{15,10} & a_{15,11} & a_{15,12} & a_{15,13} & a_{15,14} & a_{15,15} \end{bmatrix} \begin{bmatrix} \bar{I}_{BSka} \\ \bar{I}_{BSkb} \\ \bar{I}_{BSkc} \\ \bar{I}_{BRka} \\ \bar{I}_{BRkb} \\ \bar{I}_{BRkc} \end{bmatrix} \quad \ldots (3.21)$$

$$\begin{bmatrix} \bar{I}_{BSka} \\ \bar{I}_{BSkb} \\ \bar{I}_{BSkc} \\ \bar{I}_{BRka} \\ \bar{I}_{BRkb} \\ \bar{I}_{BRkc} \end{bmatrix} = \begin{bmatrix} b_{1,1} & b_{1,4} \\ b_{2,1} & b_{2,4} \\ b_{3,1} & b_{3,4} \\ b_{4,1} & b_{4,4} \\ b_{5,1} & b_{5,4} \\ b_{6,1} & b_{6,4} \end{bmatrix} \begin{bmatrix} \bar{E}_{BSka} \\ \bar{E}_{BRka} \end{bmatrix} \quad \ldots (3.22)$$

$\bar{E}_{BSka}$ , $\bar{E}_{BRka}$ are the known transforms and are given by:

$$\bar{E}_{BSka} = \int_{t_6}^{TOB} (e_{BS4a} + e_{BS5a} + e_{BS6a})\, e^{-j\omega t}\, dt$$

$$\bar{E}_{BRka} = \int_{t_6}^{TOB} (e_{BR4a} + e_{BR5a} + e_{BR6a})\, e^{-j\omega t}\, dt$$

$e_{BS4a}$ , $e_{BR4a}$ = component due to current interruption

$e_{BS5a}$ , $e_{BR5a}$ = component due to fault break off

$e_{BS6a}$ , $e_{BR6a}$ = component due to capacitor reinsertion

3.4.3.2 Phase-to-phase fault

3.4.3.2.1 Fault inception simulation

With reference to equation A1.45 the zero valued transforms for a 'b'-'c' phase fault (say) are $\overline{E}_{BSka,b,c}$ , $\overline{E}_{BRka,b,c}$ , $\overline{I}_{Fkab,ca}$ , $\overline{I}_{SSka,b,c}$ and $\overline{I}_{RRka,b,c}$ . Again adopting the procedure of the previous Section the matrix relationship as shown in equation 3.23 is obtained, which in turn is inverted to give equation 3.24.

$$\begin{bmatrix} \overline{E}_{FFkbc} \\ 0 \\ 0 \\ 0 \\ 0 \\ 0 \\ 0 \end{bmatrix} = \begin{bmatrix} N_{2,2} & p_{2,10} & p_{2,11} & p_{2,12} & p_{2,13} & p_{2,14} & p_{2,15} \\ N_{10,2} & n_{10,10} & n_{10,11} & n_{10,12} & n_{10,13} & n_{10,14} & n_{10,15} \\ N_{11,2} & n_{11,10} & n_{11,11} & n_{11,12} & n_{11,13} & n_{11,14} & n_{11,15} \\ N_{12,2} & n_{12,10} & n_{12,11} & n_{12,12} & n_{12,13} & n_{12,14} & n_{12,15} \\ N_{13,2} & n_{13,10} & n_{13,11} & n_{13,12} & n_{13,13} & n_{13,14} & n_{13,15} \\ N_{14,2} & n_{14,10} & n_{14,11} & n_{14,12} & n_{14,13} & n_{14,14} & n_{14,15} \\ N_{15,2} & n_{15,10} & n_{15,11} & n_{15,12} & n_{15,13} & n_{15,14} & n_{15,15} \end{bmatrix} \begin{bmatrix} \overline{I}_{Fkbc} \\ \overline{I}_{BSka} \\ \overline{I}_{BSkb} \\ \overline{I}_{BSkc} \\ \overline{I}_{BRka} \\ \overline{I}_{BRkb} \\ \overline{I}_{BRkc} \end{bmatrix} \quad \ldots (3.23)$$

$$\begin{bmatrix} \overline{I}_{Fkbc} \\ \overline{I}_{BSka} \\ \overline{I}_{BSkb} \\ \overline{I}_{BSkc} \\ \overline{I}_{BRka} \\ \overline{I}_{BRkb} \\ \overline{I}_{BRkc} \end{bmatrix} = \begin{bmatrix} C_{1,1} \\ C_{2,1} \\ C_{3,1} \\ C_{4,1} \\ C_{5,1} \\ C_{6,1} \\ C_{7,1} \end{bmatrix} \begin{bmatrix} \overline{E}_{FFkbc} \end{bmatrix} \quad \ldots (3.24)$$

$\bar{E}_{FFkbc}$ is the known transform which is given by:

$$\bar{E}_{FFkbc} = \int_{t_1}^{TOB} e_{FF1bc} \; e^{-j\omega t} \, dt$$

where $e_{FF1bc}$ = time domain variation of prefault steady state component.

At this stage, the total time domain response of, say, the sending end 'c' phase capacitor voltage would be:

$$e_{STc}(t) = e_{S1c}(t) + e_{S2c}(t-t_1)$$

3.4.3.2.2 Capacitor flashover simulation

With reference to equation A1.45 the zero valued transforms are $\bar{E}_{FFkbc}$ , $\bar{E}_{BSka,b,c}$ , $\bar{E}_{BRka,b,c}$ , $\bar{I}_{Fkab,ca}$ , $\bar{I}_{SSka,b}$ and $\bar{I}_{RRka,b,c}$ . As mentioned earlier, the matrix relationship of equation 3.25 is obtained, which in turn is inverted to give equation 3.26.

$$\begin{bmatrix} 0 \\ \bar{E}_{Skc} \\ 0 \\ 0 \\ 0 \\ 0 \\ 0 \\ 0 \end{bmatrix} = \begin{bmatrix} N_{2,2} & p_{2,6} & p_{2,10} & p_{2,11} & p_{2,12} & p_{2,13} & p_{2,14} & p_{2,15} \\ N_{6,2} & n_{6,6} & n_{6,10} & n_{6,11} & n_{6,12} & n_{6,13} & n_{6,14} & n_{6,15} \\ N_{10,2} & n_{10,6} & n_{10,10} & n_{10,11} & n_{10,12} & n_{10,13} & n_{10,14} & n_{10,15} \\ N_{11,2} & n_{11,6} & n_{11,10} & n_{11,11} & n_{11,12} & n_{11,13} & n_{11,14} & n_{11,15} \\ N_{12,2} & n_{12,6} & n_{12,10} & n_{12,11} & n_{12,12} & n_{12,13} & n_{12,14} & n_{12,15} \\ N_{13,2} & n_{13,6} & n_{13,10} & n_{13,11} & n_{13,12} & n_{13,13} & n_{13,14} & n_{13,15} \\ N_{14,2} & n_{14,6} & n_{14,10} & n_{14,11} & n_{14,12} & n_{14,13} & n_{14,14} & n_{14,15} \\ N_{15,2} & n_{15,6} & n_{15,10} & n_{15,11} & n_{15,12} & n_{15,13} & n_{15,14} & n_{15,15} \end{bmatrix} \begin{bmatrix} \bar{I}_{Fkbc} \\ \bar{I}_{SSkc} \\ \bar{I}_{BSka} \\ \bar{I}_{BSkb} \\ \bar{I}_{BSkc} \\ \bar{I}_{BRka} \\ \bar{I}_{BRkb} \\ \bar{I}_{BRkc} \end{bmatrix}$$

. . . (3.25)

$$\begin{bmatrix} \bar{I}_{Fkbc} \\ \bar{I}_{SSkc} \\ \bar{I}_{BSka} \\ \bar{I}_{BSkb} \\ \bar{I}_{BSkc} \\ \bar{I}_{BRka} \\ \bar{I}_{BRkb} \\ \bar{I}_{BRkc} \end{bmatrix} = \begin{bmatrix} C_{1,2} \\ C_{2,2} \\ C_{3,2} \\ C_{4,2} \\ C_{5,2} \\ C_{6,2} \\ C_{7,2} \\ C_{8,2} \end{bmatrix} \begin{bmatrix} \bar{E}_{Skc} \end{bmatrix} \quad \ldots (3.26)$$

The known transform $\bar{E}_{Skc}$ is given by:

$$\bar{E}_{Skc} = \int_{t_2}^{TOB} (e_{S1c} + e_{S2c})\, e^{-j\omega t}\, dt$$

where $e_{S1c}$ = time domain variation of prefault steady state component.

$e_{S2c}$ = component due to fault inception.

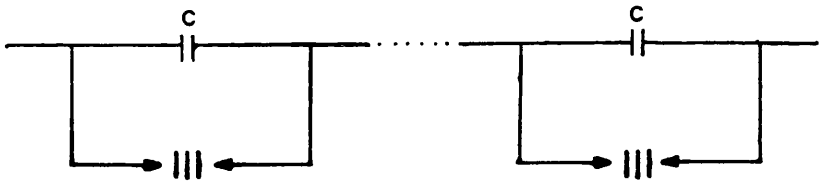


Figure 3.1 Multiple segment, complicated gaps

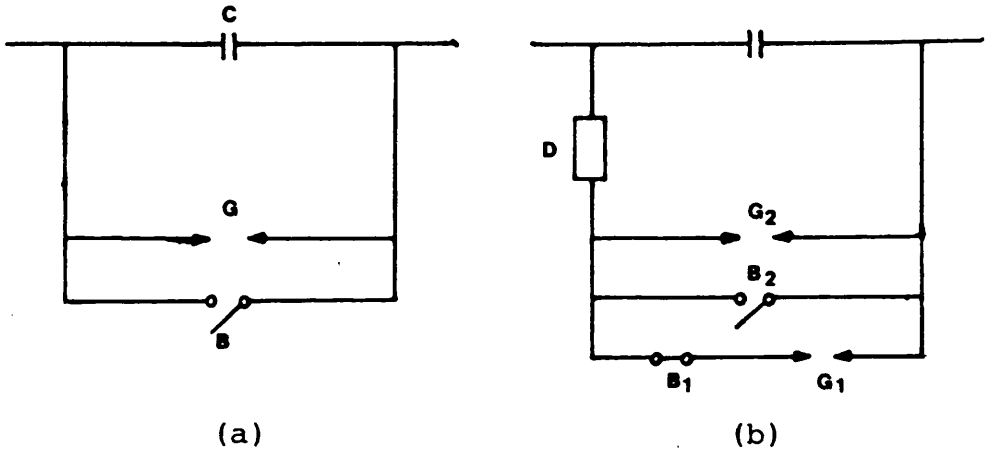


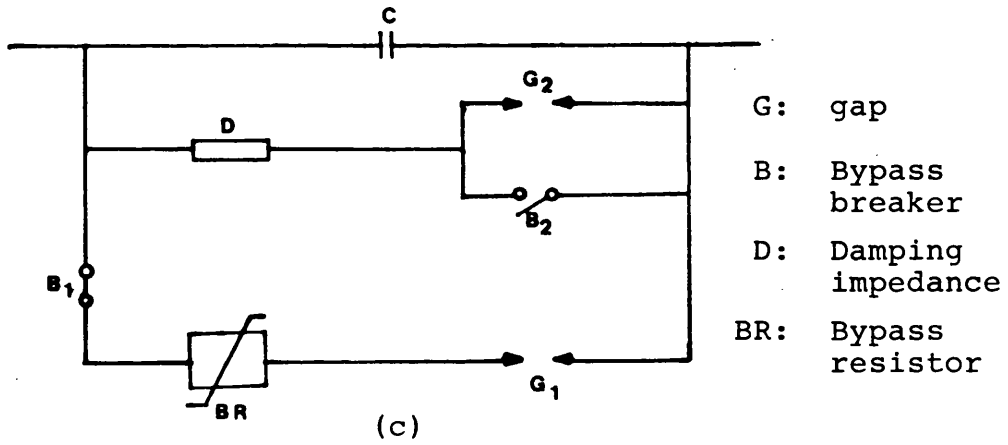


Figure 3.2 Non-self-clearing type gap

(a) single gap scheme
(b) dual gap or 'flip-flop' scheme
(c) dual gap or 'booster' scheme

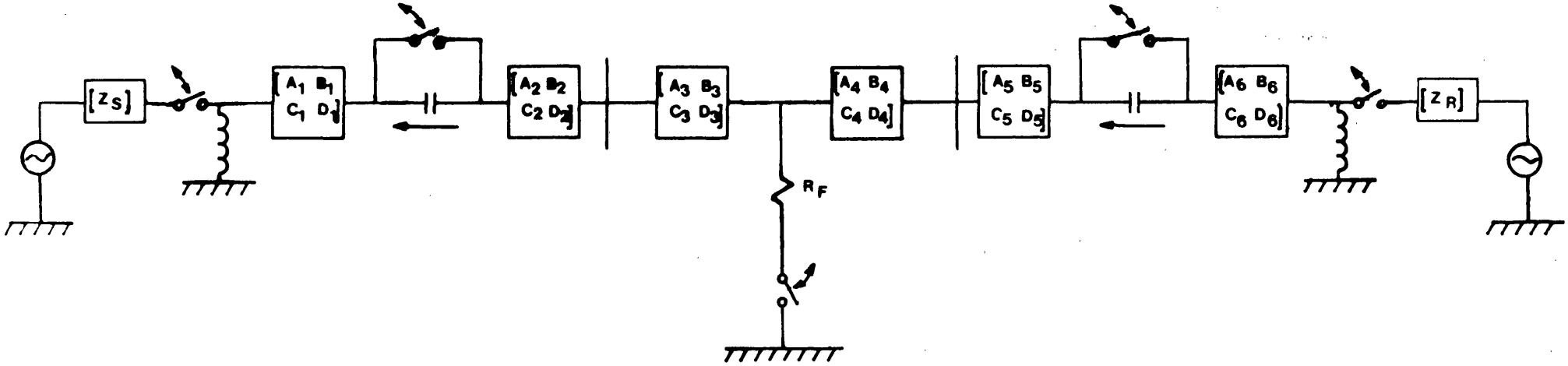


Figure 3.3 Basic System

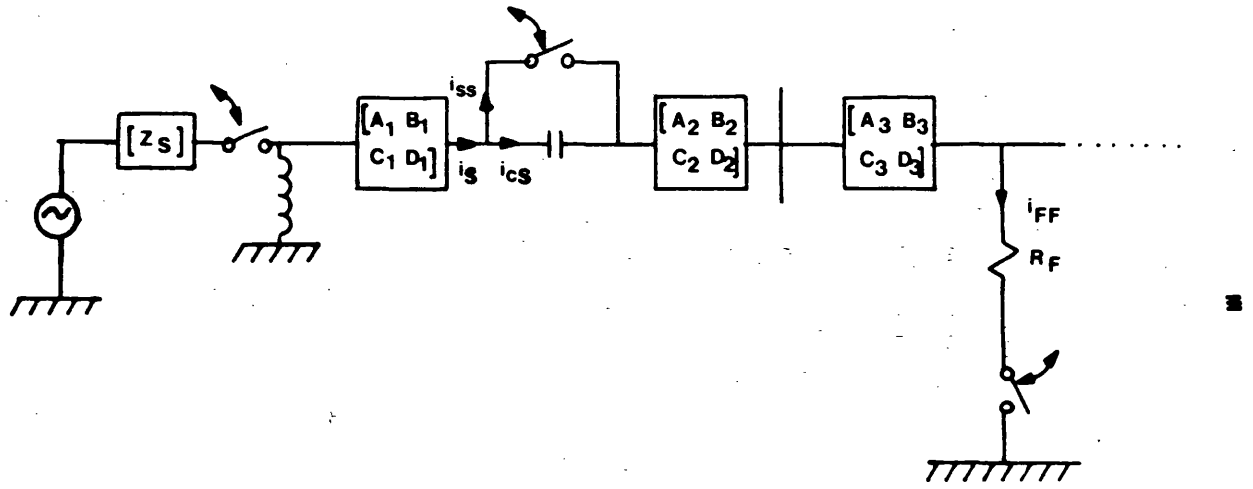


(a)

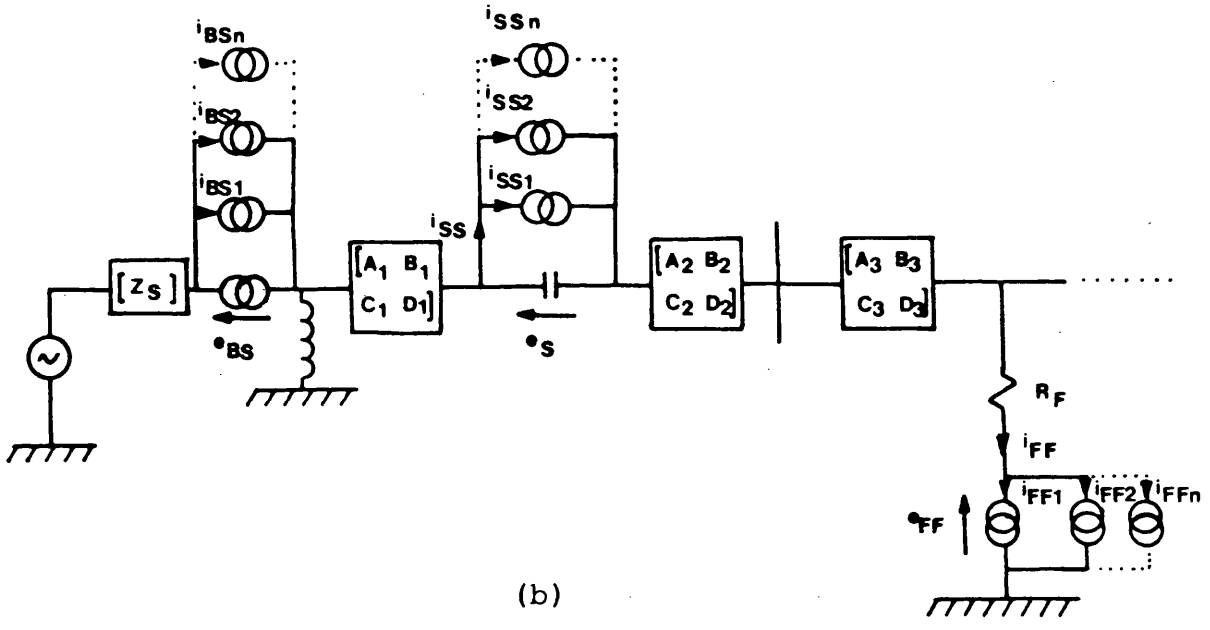


(b)

Figure 3.4 Simulation of network time non-linearities

(a) physical arrangement

(b) equivalent using parallel current generators

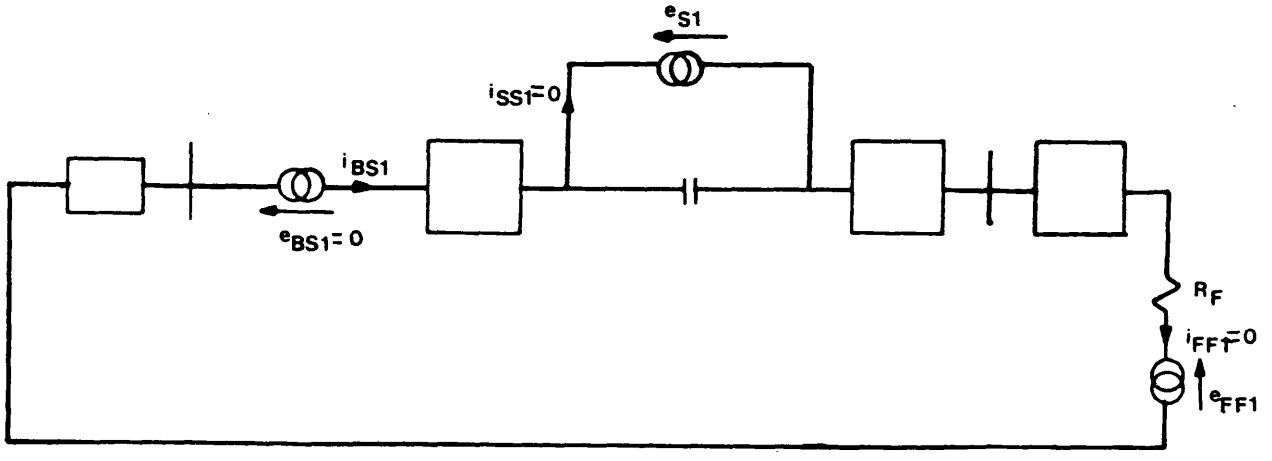
$e_{S1}$
$i_{SS1}=0$
$i_{BS1}$
$e_{BS1}=0$
$R_F$
$i_{FF1}=0$
$e_{FF1}$

(a)

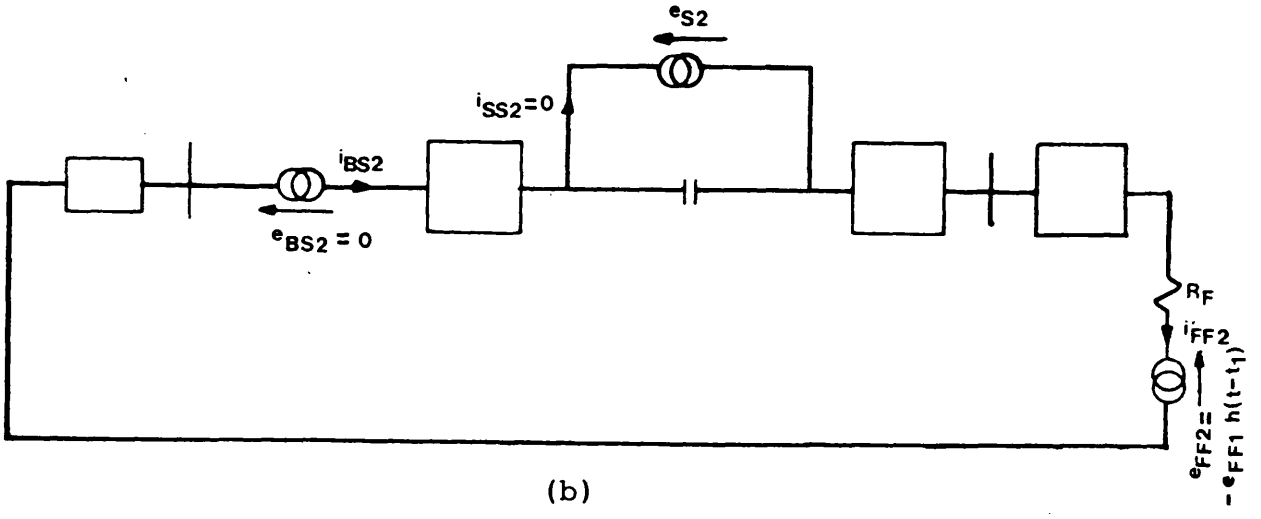
$e_{S2}$
$i_{SS2}=0$
$i_{BS2}$
$e_{BS2}=0$
$R_F$
$i_{FF2}$
$e_{FF2}=-e_{FF1}\,h(t-t_1)$

(b)

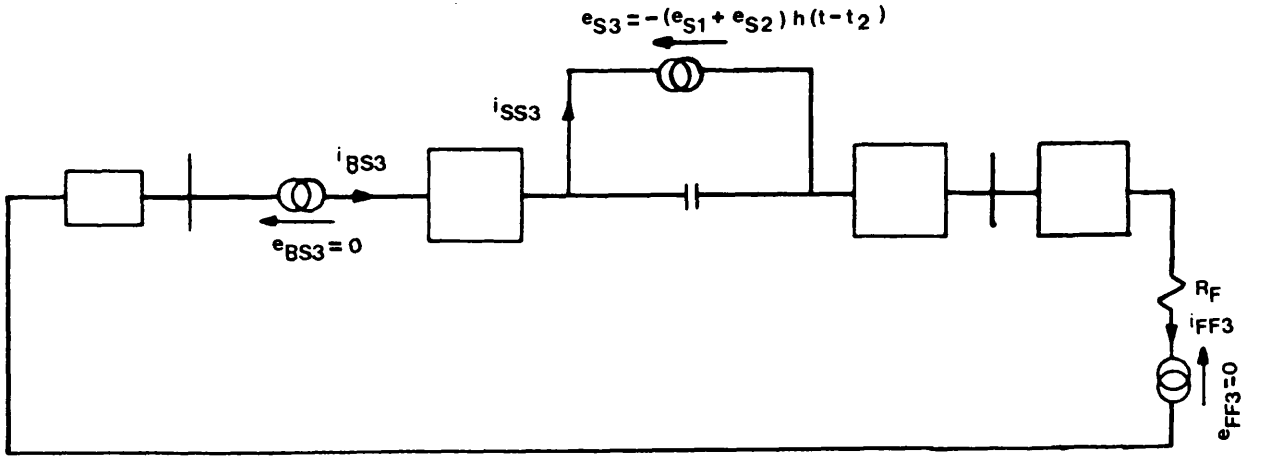
$e_{S3}=-(e_{S1}+e_{S2})\,h(t-t_2)$
$i_{SS3}$
$i_{BS3}$
$e_{BS3}=0$
$R_F$
$i_{FF3}$
$e_{FF3}=0$

(c)

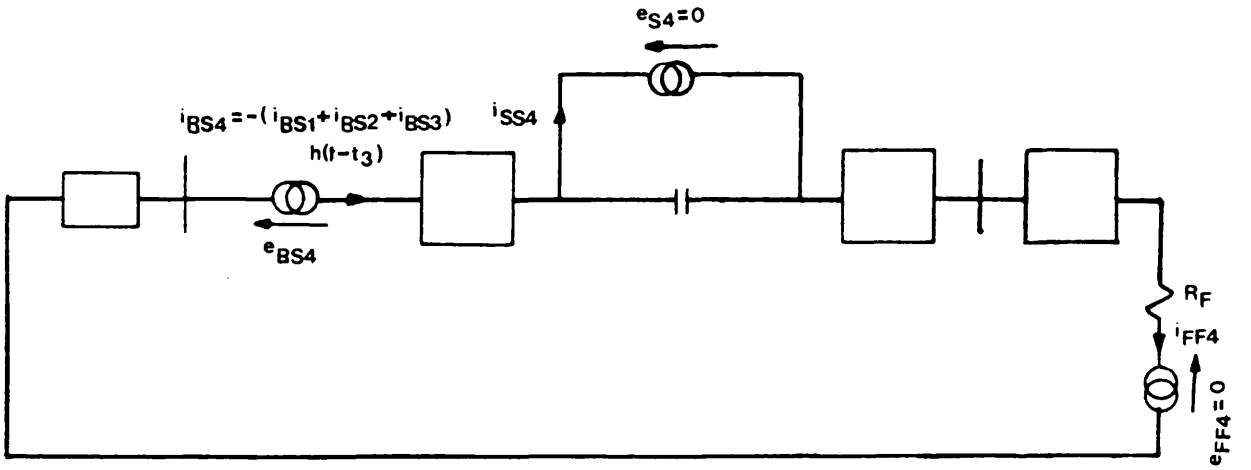
$e_{S4}=0$
$i_{BS4}=-(i_{BS1}+i_{BS2}+i_{BS3})$
$h(t-t_3)$
$i_{SS4}$
$e_{BS4}$
$R_F$
$i_{FF4}$
$e_{FF4}=0$

(d)

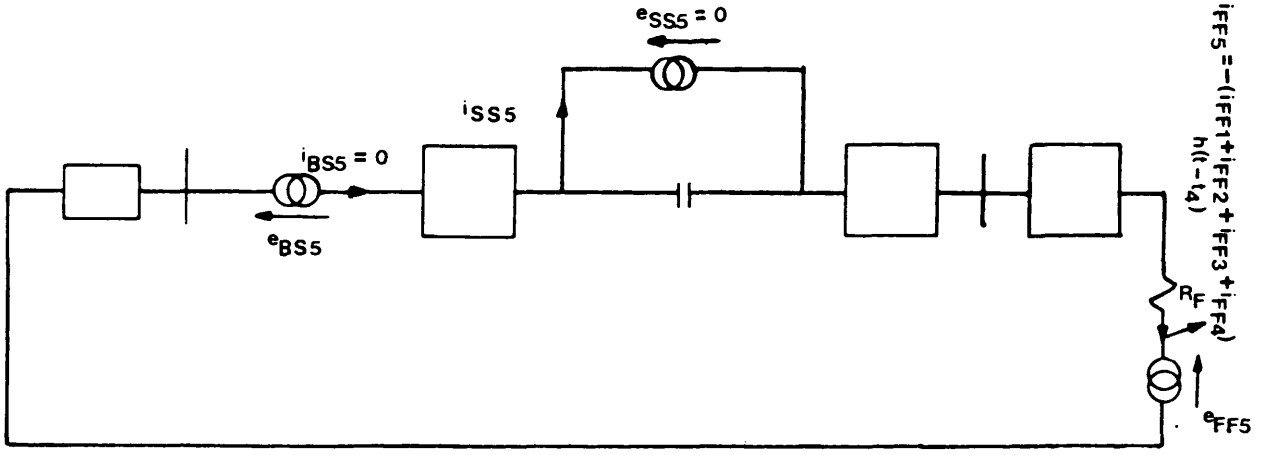
$e_{SS5}=0$
$i_{SS5}$
$i_{BS5}=0$
$e_{BS5}$
$i_{FF5}=-(i_{FF1}+i_{FF2}+i_{FF3}+i_{FF4})$
$h(t-t_4)$
$R_F$
$e_{FF5}$

(e)

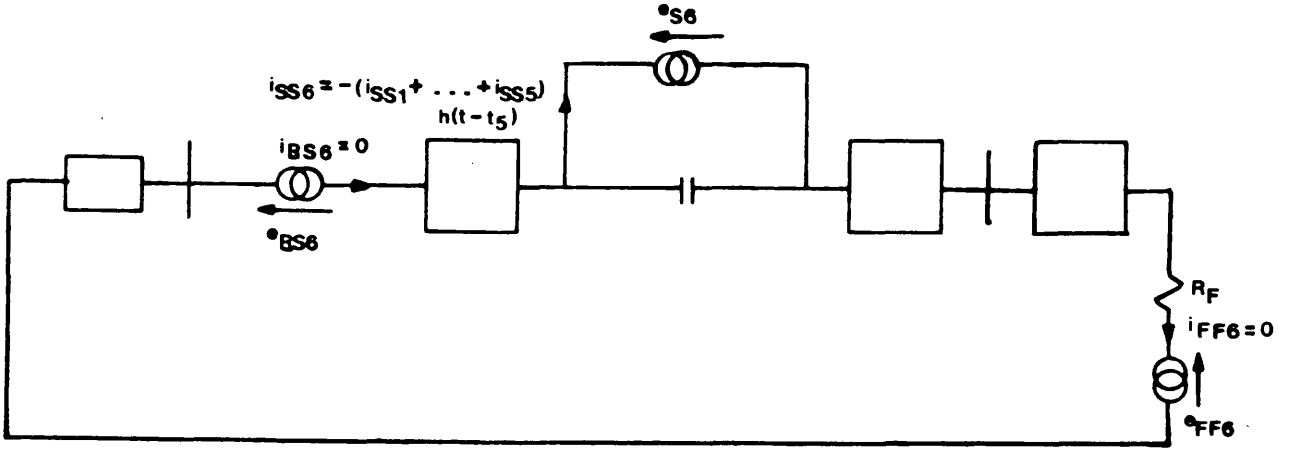
$e_{S6}$
$i_{SS6}=-(i_{SS1}+\ldots+i_{SS5})$
$h(t-t_5)$
$i_{BS6}=0$
$e_{BS6}$
$R_F$
$i_{FF6}=0$
$e_{FF6}$

(f)

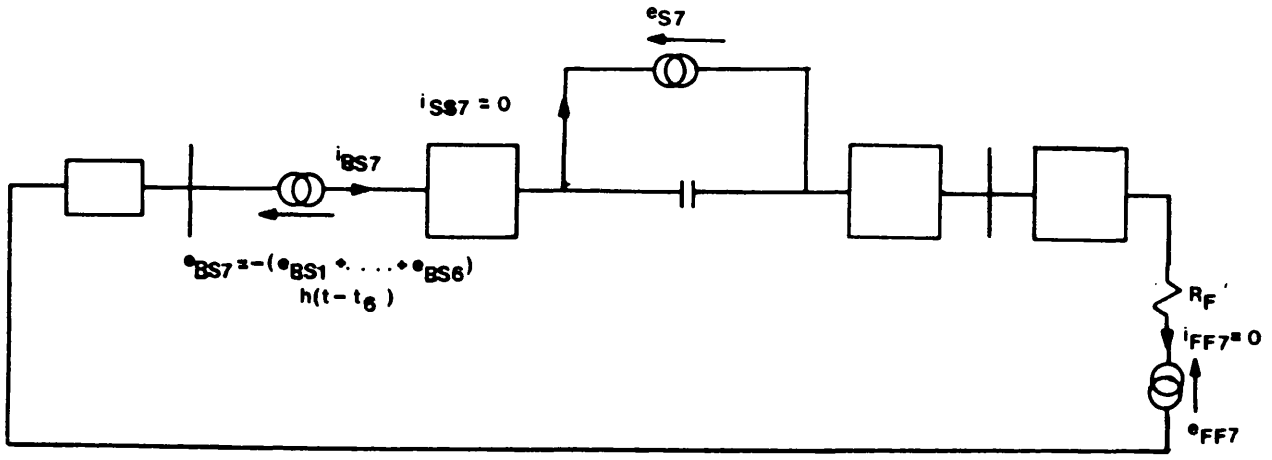


(g)

Figure 3.5 Illustrative example

(a) Steady state circuit
(b)-(g) Superimposed circuits
(b) Fault inception
(c) Capacitor flashover
(d) Breaker current interruption
(e) Fault break off
(f) Capacitor reinsertion
(g) Line reclosure

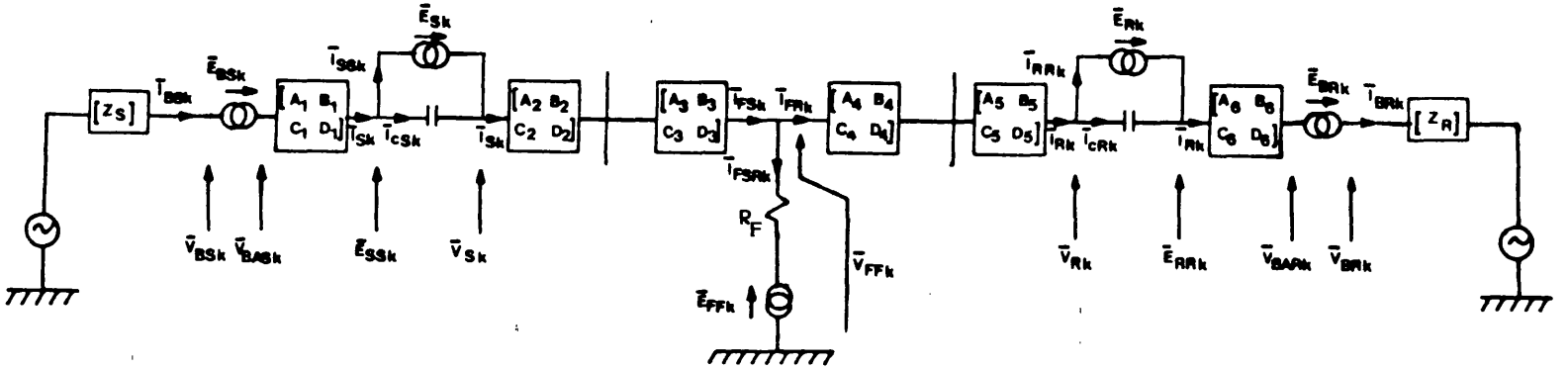


Figure 3.6 Superimposed system model

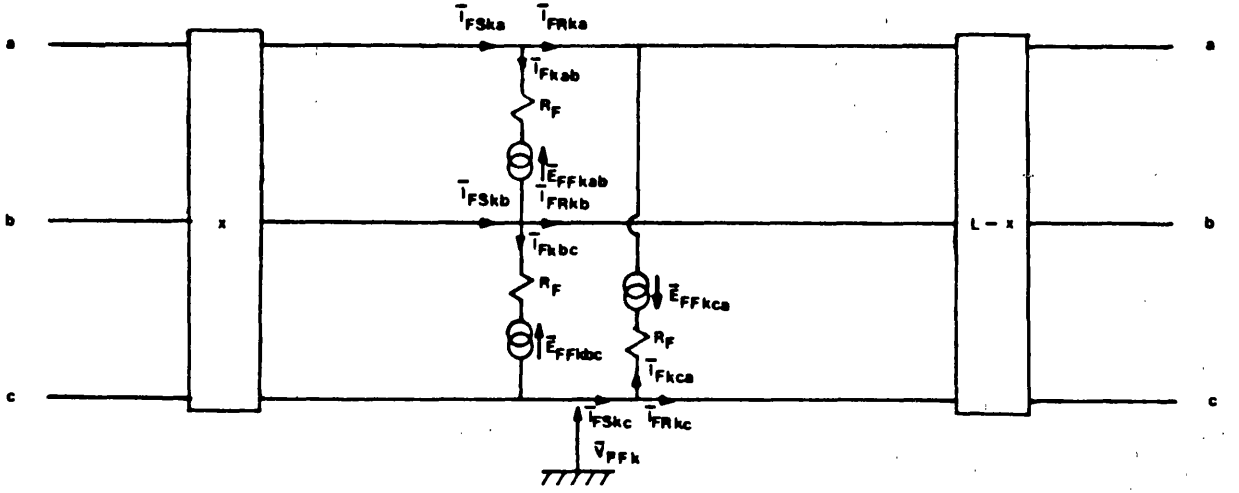


Figure 3.7 Simulation of phase-phase fault

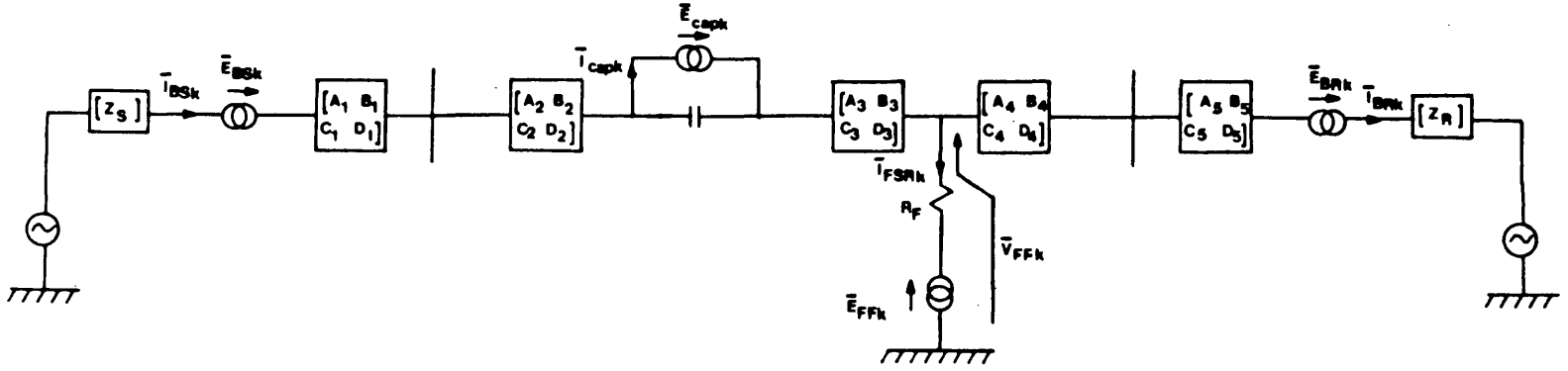


Figure 3.8 Superimposed system model with a single capacitor located at mid-point

# CHAPTER 4 CIRCUIT PARAMETERS

## 4.1 Introduction

The simulation results presented in Chapters 5 to 8 are for two different systems. In one system, the busbars at each end are terminated in relatively simple sources comprising of series lumped impedances based on the main source generations only, and in the second system, complex source side models comprising of infeeding lines with their local generations together with the main generations are considered. Both systems comprise 500kV, single circuit transmission lines. The line sections, both the line model and the infeeding lines, are discretely transposed at regular intervals using the scheme as shown in Chapter 2. Two most common series compensated schemes are considered, one in the form of two capacitors banks along the line, and the other being a single capacitor at the middle of the line. The total amount of compensation for the former is taken as 70% and for the latter, two separate cases with degrees of series compensation of 50% and 30% are considered. In the case of shunt compensation, schemes with both three-reactor bank and four-reactor bank have been considered and these have been incorporated at the ends of the line model only. The shunt reactor compensation is taken as 75% p.p.s. and 67.4% z.p.s, the latter being based on zero secondary

arc current. The simulation of the various capacitor and reactor schemes has already been described in Chapter 2.

In this Chapter the parameters of the transmission line model (including the infeeding line), series capacitors, shunt reactors, main sources and local sources associated with each infeeding lines and the Fourier transform parameters are presented. Also the parameters of the two main types of protective schemes considered one based on the block average principle[69] and the second employing the sequence comparator principle[84] (both schemes consider the independent and dependent mode of operation, the latter being with respect to permissive overreach and blocking) are presented.

## 4.2 Transmission Line Parameters

### 4.2.1 Circuit Studied

The fault studies apply to a typical horizontal construction, twin conductor, 500kV single circuit line as shown in Figure 4.1. The data which applies to both the line model and the infeeding line is as follows:

(a) phase conductors are 2 x 84/19/0.25cm SCA with 0.45m bundle spacing.

(b) earth wires are 7/0.35 cm A.W.

(c) earth resistivity is 100Ωm.

(d) conductor resistance = 0.03387Ω/km (at power frequency).

(e) earth wire resistance = 1.882Ω/km (at power frequency).

(f) conductor reactance = 0.007865Ω/km (at power frequency).

(g) earth wire reactance = 0.388Ω/km (at power frequency).

(h) conductor overall radius = 9.1cm.

(i) earth wire overall radius = 0.64cm.

(j) line lengths for the two systems considered are:

(1) 1st system - length of line model = 300km.

(2) 2nd system -
Length of main line model = 300km.
Infeeding line on the sending end source of length = 300km.
Two infeeding lines on the receiving end source of length = 150km each.

### 4.2.2 Basic Computed Parameters

The power frequency parameters of the line models presented here are not only essential from the steady state part of the analysis, but are also necessary for determining the parameters for shunt reactor, series capacitor, etc. These computed parameters are for the per unit length of impedance and admittance matrices, propagation constant and the line surge impedance and the admittance. They are evaluated using the same principle as suggested by Galloway et al[41]. Velocities of different modal components are also presented.

The parameters at power frequency are as follows:

Impedance matrix (Z)

$$[Z] = \begin{bmatrix} 0.1216+j0.5366 & 0.0866+j0.1988 & 0.0885+j0.2408 \\ 0.0866+j0.1988 & 0.1216+j0.5366 & 0.0885+j0.2408 \\ 0.0885+j0.2408 & 0.0885+j0.2408 & 0.1238+j0.5342 \end{bmatrix} * 10^{-3} \ \Omega/m \quad \ldots (4.1)$$

Admittance matrix (Y)

$$[Y] = \begin{bmatrix} j\ 0.3529 & -j\ 0.0087 & -j\ 0.0404 \\ -j\ 0.0087 & j\ 0.3529 & -j\ 0.0404 \\ -j\ 0.0404 & -j\ 0.0404 & j\ 0.3576 \end{bmatrix} * 10^{-8} \ \mho/m \quad \ldots (4.2)$$

From equations 4.1 and 4.2, the propagation constant matrix ($\gamma$) is:

$$[\gamma] = [0.2544 + j\ 0.1726 \quad 0.0571 + j\ 1.1070 \quad 0.06448 + j\ 1.0690] * 10^{-6} \text{ diag} \quad \ldots (4.3)$$

The surge impedance matrix ($Z_0$) is:

$$[Z_0] = \begin{bmatrix} 385.8 - j39.04 & 79.74-j23.25 & 110.9-j23.64 \\ 79.74-j23.25 & 385.8 - j39.04 & 110.9-j23.64 \\ 110.9 - j23.64 & 110.9 - j23.64 & 383.6-j39.11 \end{bmatrix} \Omega \quad \ldots (4.4)$$

and the corresponding surge admittance matrix ($Y_0$) is:

$$[Y_0] = \begin{bmatrix} 2.8600+j0.2112 & -0.3992+j0.0430 & -0.7274+j0.0024 \\ -0.3992+j0.0430 & 2.8600+j0.2112 & -0.7274+j0.0024 \\ -0.7274+j0.0024 & -0.7224+j0.0024 & 3.0040+j0.2215 \end{bmatrix} * 10^{-3} \mho \quad \ldots (4.5)$$

The different mode velocity propagation is given by equations 4.6 and 4.7.

For earth modes $V_1 = 2.38 \times 10^5$ km/s . . . (4.6)

For aerial modes $V_2 = V_3 = 2.92 \times 10^5$ km/s . . . (4.7)

## 4.3 Series Capacitor Parameters

In this Section, the calculated capacitor parameters at power frequency are presented alongwith the calculated threshold voltage for capacitor spark gap operations.

### 4.3.1 The Compensating Capacitor

As mentioned in Section 4.1, basically two series compensated schemes are considered. In the case where two capacitors are employed per phase, of the total 70% compensation, 35% is associated with each of the two capacitors.

The ABCD matrix representation of the series capacitor bank is as described in Chapter 2 and the value of $X_{cap}$, the capacitive reactance, used in the representation of the various aforementioned cases is as shown in Table 4.1

| Type of scheme | Percentage of compensation | $X_{cap}$ ($\Omega$) |
|---|---|---|
| Two capacitor banks | Total 70% (35% for each) | 64.9 (32.45) |
| Single capacitor bank | 50% | 46.36 |
| | 30% | 27.82 |

Table 4.1 Value of $X_{cap}$ for different levels of compensation

4.3.2 Determination of the threshold voltage

Typical loading of the 500kV line = 1,000 MVA

Full load current $(I_{f\ell}) = \frac{1000.10^6}{\sqrt{3}.500.10^3}$

$= 1.15kA$

For 70% compensation, with a capacitor at each end

Rating of each capacitor = $(I_{f\ell})^2 X_{cap}$ = 42.92 MVAR

Voltage across each capacitor = $X_{cap} I_{f\ell}$

= 32.45 x 1.15

= 37.318 kV r.m.s.

Sparkover voltage (2.75 p.u) = 2.75 x 37.318

= 102.645 kV r.m.s

Capacitor is designed to withstand = 102.645 x $\sqrt{2}$

= 145.139 kV peak

For the case of single capacitor at the middle, working on similar basis it can be shown that the value of threshold voltages

= 207.34 kV peak for 50% compensation,

or = 124.42 kV peak for 30% compensation.

## 4.4 Shunt Reactor Parameters

The calculation of the shunt reactor parameters is based on the theory developed by Kimbark[95].

### 4.4.1 Calculation of $X_1$

$X_1$, the inductive reactance of the main reactors (used both for three reactor and four reactor schemes) depends on the unit chosen value of $h_1$, the p.p.s. degree of shunt compensation, in this case being 0.75.

From equation 4.2, the total p.p.s. shunt admittance $B_1'$ (at power frequency) for half the line = $36.52 \times 10^{-5}$ ℧ .

Now, if $B_1$ is the shunt admittance of each of the two shunt reactor banks, then:

$$B_1 = h_1 B_1' = 27.39 \times 10^{-5} \text{ ℧} \qquad \ldots (4.8)$$

Hence, $X_1 = 1/B_1 = 3.65\text{k}\Omega$.

### 4.4.2 Calculation of $X_n$

In the calculation of the neutral reactance of a four reactor bank, it is assumed that there is complete neutralisation of the interphase capacitances between the sound phases and the isolated phase for studies pertaining to single pole autoreclosure techniques, ie the magnitude of the secondary arc current is assumed to be zero.

Under these conditions, from equation 4.2, $B_0' = 28.01 \times 10^{-5}\ \upsilon$ is the total z.p.s shunt admittance (again for half the line).

For complete neutralisation of the interphase capacitances

$$(B_1 - B_0) = (B_1' - B_0') \qquad \ldots (4.9)$$

where $B_0$ is the equivalent z.p.s. admittance of the four reactor bank and is equal to $18.88 \times 10^{-5}\ \upsilon$.

Using equations 4.8 and 4.9, it can be shown that

$$X_n = \frac{X_0 - X_1}{3} = \frac{\frac{1}{B_0} - \frac{1}{B_1}}{3} = \frac{B_1' - B_0'}{3B_1(B_1 - B_1' + B_0')}$$

$$= 548.54\Omega$$

Furthermore, $h_0$, the z.p.s. degree of compensation, is such that $B_0 = h_0\ B_0'$, which gives $h_0 = 0.674$.

## 4.5 Source parameters

As mentioned previously, two types of practical source model used are:

(1) In the case of simple sources:

The source short circuit level = 5, 10, 35 GVA

Source $Z_{S0}/Z_{S1}$ ratio = 1.0

Source X/R ratio = 30.0

(2) In the case of complex source model:

The main source short circuit level = 5,6,7, 35 GVA

and corresponding $Z_{S0}/Z_{S1}$ ratio = 0.6,0.6,0.5,0.5

The short circuit level of local generation = 0.25, 1, 5 GVA

and corresponding $Z_{S0}/Z_{S1}$ ratio = 0.5, 0.5, 0.4

Source X/R ratio = 30.0

## 4.6 Fourier Transform Parameters

Observation time TOB = 32, 64, 128 ms.

Frequency shift constant $\alpha$ is such that:

for TOB of 32 ms, $\alpha$ = 200

for TOB of 64 ms, $\alpha$ = 100

for TOB of 128 ms, $\alpha$ = 50

Truncation frequency $\Omega$ = 2.0kHz and the number of samples considered are 128, 256 and 512.

## 4.7 Protective Relay Parameters

In this analysis, two different type of relays based on the block average principle and the sequence comparator operating in three different modes are used.

Zone 1 relay (or the independent mode) setting = 80%

Permissive overreach (the dependent mode) setting = 120%

Blocking (the dependent mode) setting = 150%

In all the three cases, the characteristics are arranged so that the diameter of the nominal mho circle has an argument which is 10° less than the p.p.s. line impedance argument. The nominal c.t. ratios are 1200/1 and the v.t. ratios are 500/0.11 for a 500kV system. Responses are obtained for a level of sound-phase polarisation equal to 10% of the sound-phase voltage or voltages and the comparators have a setting voltage equal to 0.1V.

From equation 4.1:

$$Z_{L1} = (0.0344 + j\ 0.3090) \times 10^{-3}\Omega/m$$

$$Z_{L0} = (0.2981 + j\ 0.9894) \times 10^{-3}\Omega/m$$

The impedance of the protected line is

$$= 0.8 \times 300 \times 10^{3}\ (0.03442+j0.3090) \times 10^{-3}\Omega$$

$$= 74.6187\Omega\ \angle 83.^{\circ}6$$

The mho characteristic argument is $73.^{\circ}6$.

4.7.1 Independent Mode Relay Parameters

Table 4.2 gives the detail of Zone 1 parameters used. The mho characteristic of the relay with different levels of compensation is shown in Figures 4.2 to 4.4 To illustrate an example of the calculation involved, a particular case with a capacitor at each end (70% total

compensation, 35% associated with each of the two capacitors) is shown.

(i) Block Average Relay

The current replica impedance (from Figure 4.2(a)) is $|Z_r| = 43.25\Omega$.

From equation A3.2 of Appendix (A3):

$$|Z_r'| = \frac{n_v}{n_c} |Z_r|$$

$$= \frac{110}{500.10^3} \times 1200 \times 43.25 = 11.418\Omega.$$

Knowing $\phi_T = 68°$ (from Figure 4.2(a))

$$X_m = \sqrt{1 + \cot^2 \phi_T}\ |Z_r'| = 12.3147\Omega$$

Therefore $L_m = 0.03919H$

and $R_b = X_m \text{ Tan } \phi_T = 30.47995\Omega.$

The residual compensating factor K is given by

$$K = \frac{1}{3}\left[\left|\frac{Z_{L0}}{Z_{L1}}\right| - 1\right] = 0.7745$$

(ii) Sequence Comparator Relay

Equation A3.9 of Appendix (A3) gives the value of $n_3$

$$n_3 = \frac{n_1 n_2}{2} = \frac{1}{800} \text{ as } n_1 = n_2 = 1/20$$

and $\omega_0 L_m = 1$ therefore $L_m = 0.0031831$ H.

From equation A3.11 of Appendix (A3):

$$\angle\theta = \angle \frac{v_o(t)}{i(t)} = 90° - \tan^{-1} \frac{Q'}{1} + \tan^{-1} \frac{Q}{-1} - \tan^{-1} \frac{Q}{1}$$

From design point of view $Q' = \sqrt{3}$

Therefore $\angle\theta = 210° - 2\tan^{-1} Q = \phi_T$ .

From Figure 4.2(a), $\phi_T = 68.^{\circ}0$

Therefore $68° = 210° - 2\tan^{-1}Q$

Therefore $Q = 2.9042.$

Equation A3.3 (Appendix A(3)) gives:

$$R = \frac{1}{n_1^2 Q} = \frac{400}{Q} = 137.7316\Omega$$

and from equation A3.10

$$|Z_r| = \left| \frac{v_o(t)}{i(t)} \right| = \frac{\omega_0 L_{m1} n_3}{n_2^2 \sqrt{1+Q'^2}}$$

Therefore

$$L_{m1} = \frac{|Z_r| \; 2.0 \; \sqrt{1+Q'^2}}{\omega_0}$$

as $\frac{n_3}{n_2^2} = \frac{1}{2}$ for $n_1 = n_2 = \frac{1}{20}$ and $n_3 = \frac{1}{800}$

Therefore $L_{m1} = \frac{4.0 \; |Z_r|}{\omega_0} = 0.1454H$

Equation A3.4 of Appendix (A3) also gives:

$$Q' = \frac{\omega_0 L_{m1}}{n_2^2 R_b}$$

Therefore $R_b = \frac{\omega_0 L_{m1} \; 400}{Q'} = 10549.047\Omega$

| Type of relay | Parameters | Level of compensation/capacitor | | | Without Compen-sation |
|---|---|---|---|---|---|
| | | 50% | 35% | 30% | |
| Block average | $X_{cap}$ (Ω) | 46.36 | 32.45 | 27.82 | - |
| | $\|Z_r\|$ (Ω) | 29.00 | 43.25 | 48.00 | 76.00 |
| | $\|Z_r'\|$ (Ω) | 7.656 | 11.418 | 12.672 | 20.064 |
| | $X_m$ (Ω) | 8.6312 | 12.3147 | 13.4853 | 20.9150 |
| | $\phi_T$ | 62.5 | 68.0 | 70.0 | 73.6 |
| | $L_m$ (H) | 0.027470 | 0.039190 | 0.042925 | 0.066575 |
| | $R_b$ (Ω) | 16.58040 | 30.47995 | 37.05045 | 71.06310 |
| | K | 0.7745 | 0.7745 | 0.7745 | 0.7745 |
| Se-quence compar-ator | Q | 3.43084 | 2.9042 | 2.74750 | 2.50018 |
| | $L_m$ (H) | 0.003183 | 0.003183 | 0.003183 | 0.003183 |
| | R(Ω) | 116.5895 | 137.7316 | 145.5869 | 159.9885 |
| | $L_{m1}$ (H) | 0.09748 | 0.14540 | 0.16130 | 0.25550 |
| | $R_b$ (Ω) | 7072.200 | 10549.047 | 11702.623 | 18537.023 |

Table 4.2 Zone 1 relay parameters

### 4.7.2 Dependent Mode Relay Parameters

For the permissive overreach and blocking mode cases, working on the similar basis as the previous Section, the associated parameters can be obtained as detailed in Table 4.3. The mho characteristic of such relay with different relay setting is shown in Figure 4.5.

| Type of relay | Parameters | Permissive overreach | Blocking |
|---|---|---|---|
| Block average | $\|Z_r\|$ (Ω) | 114.5 | 142.0 |
| | $\|Z_r'\|$ (Ω) | 30.228 | 37.488 |
| | $X_m$ (Ω) | 31.51 | 39.0779 |
| | $\phi_T$ | 73.6 | 73.6 |
| | $L_m$ (H) | 0.100299 | 0.124389 |
| | $R_b$ (Ω) | 107.061795 | 132.775415 |
| | K | 0.7745 | 0.7745 |
| Sequence comparator | Q | 2.500178 | 2.500178 |
| | $L_m$ (H) | 0.003183 | 0.003183 |
| | R (Ω) | 159.988586 | 159.988586 |
| | $L_{m1}$ (H) | 0.384875 | 0.477312 |
| | $R_b$ (Ω) | 27923.43026 | 34629.93101 |

Table 4.3 Permissive overreach and blocking mode parameters

## 4.8 Filter Parameters

The parameters of the low pass Butterworth type of filter (as described in Appendix A3.4) used are:

$$R_1 = 1.422 \times K_2 (k\Omega)$$

$$R_2 = 5.399 \times K_2 (k\Omega)$$

$$R_3 = 0$$

$R_4 = \infty$

$C_1 = 0.33 \times C_f(\mu F)$

gain = 1

where $C_f$ = 0.01μF, the cut-off frequency ($f_c$) = 500 Hz

and $K_2 = \frac{100}{f_c C_f}$

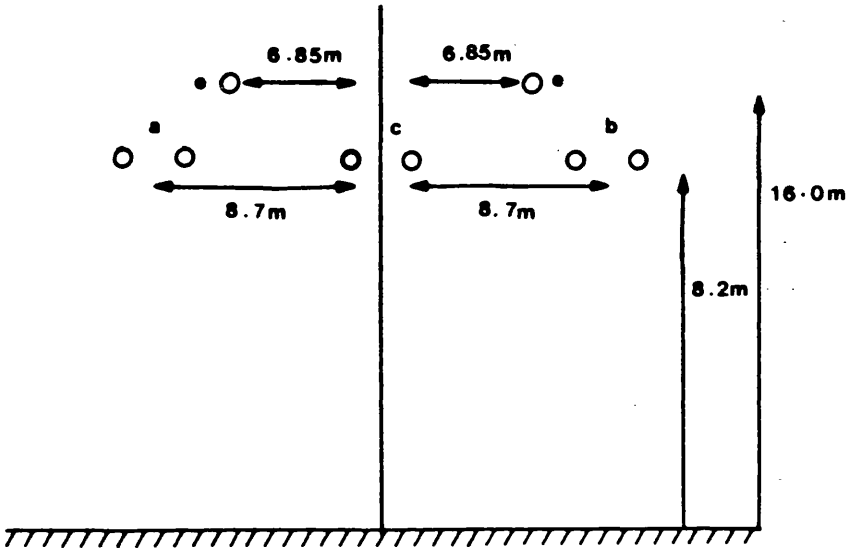


Figure 4.1 Line configuration.
500 kV twin conductor.

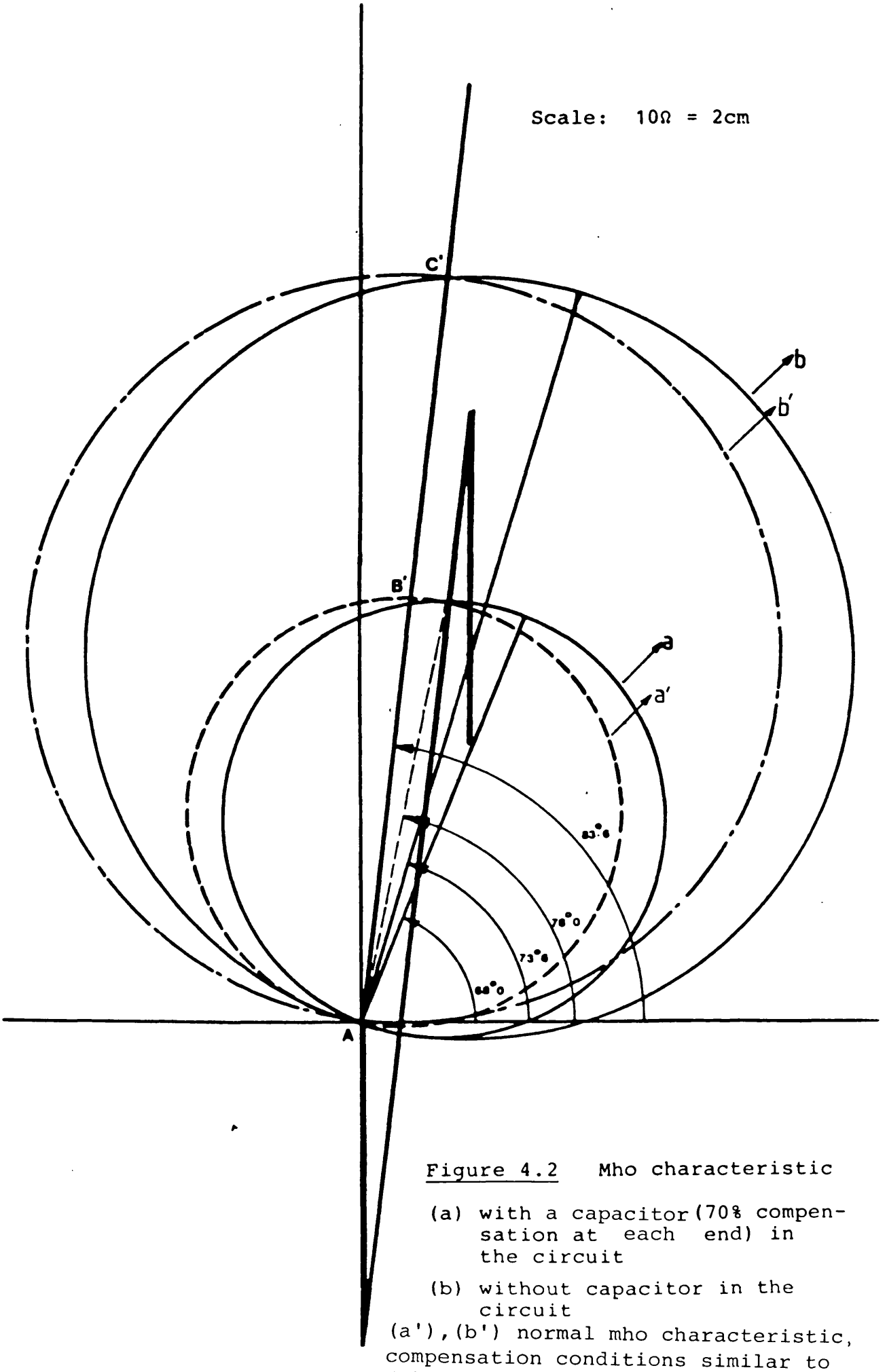


Figure 4.2 Mho characteristic

(a) with a capacitor (70% compensation at each end) in the circuit

(b) without capacitor in the circuit

(a'), (b') normal mho characteristic, compensation conditions similar to (a), (b)

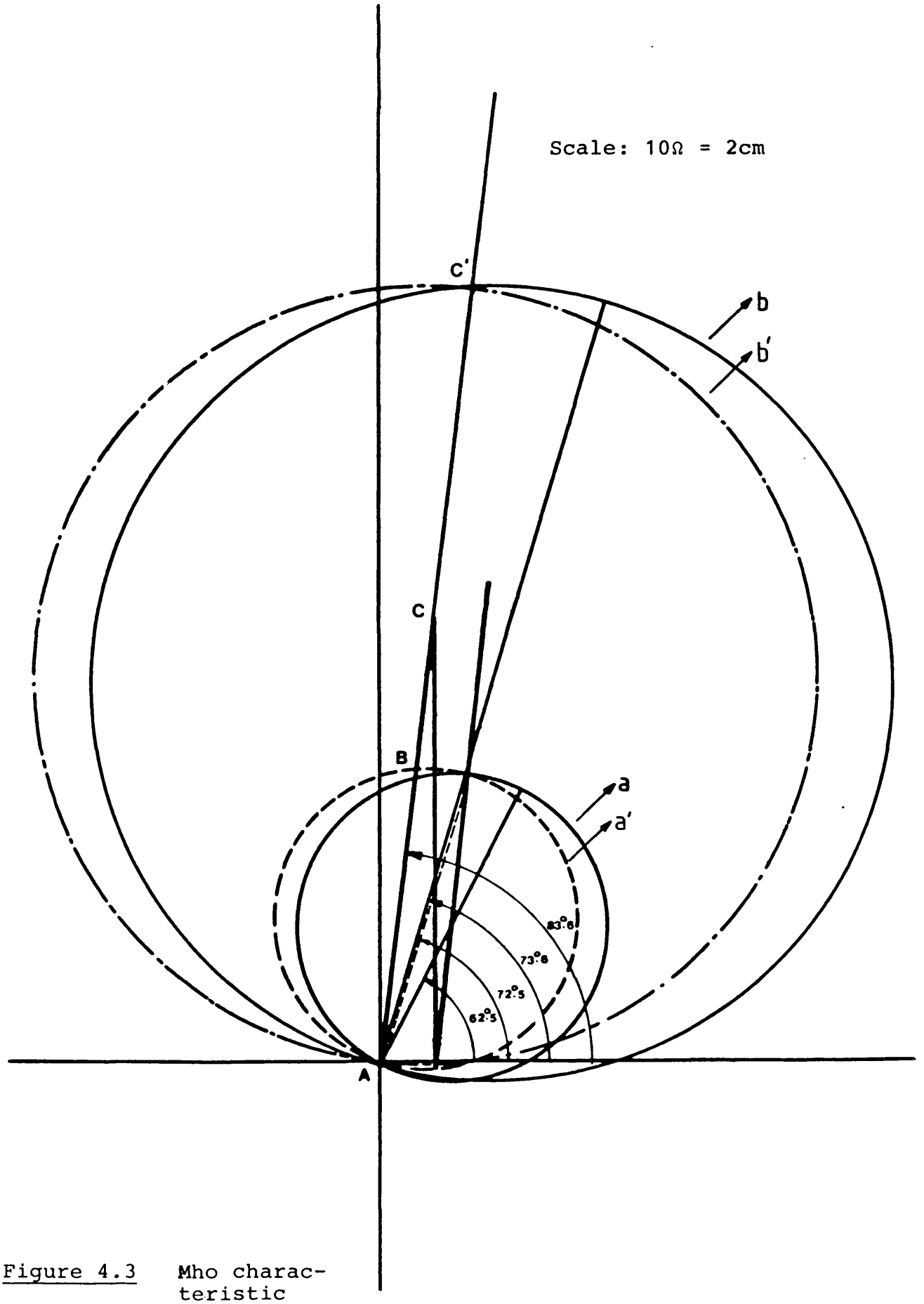


Figure 4.3 Mho characteristic

(a) with capacitor (50% compensation, at mid-point) in the circuit

(b) without capacitor in the circuit

(a'),(b') normal mho characteristic, compensation condition similar to (a),(b)

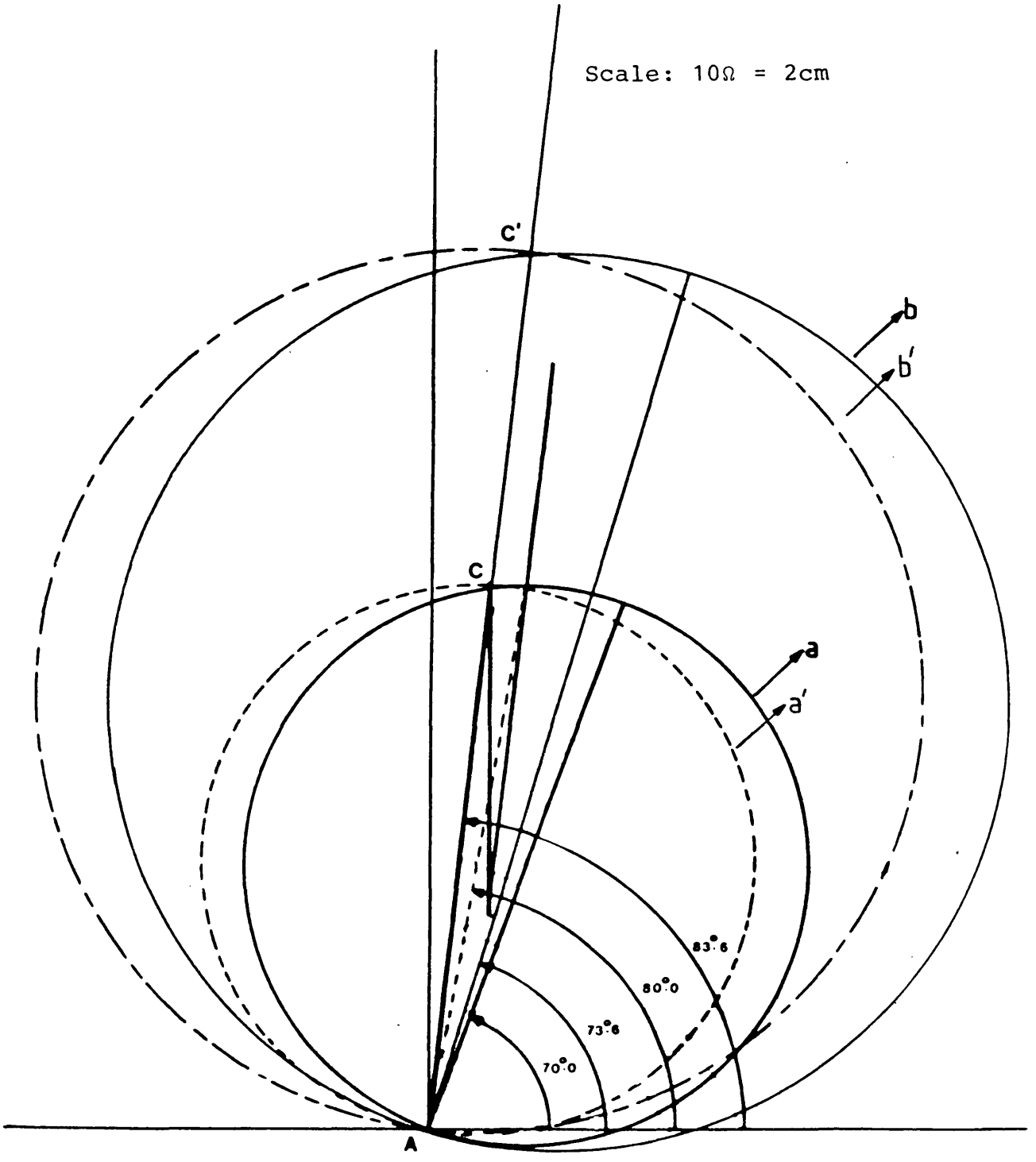


Figure 4.4 Mho characteristic

(a) with capacitor (30% compensation, at mid-point) in the circuit

(b) without capacitor in the circuit

(a'),(b') normal mho characteristic, compensation condition similar to (a),(b)

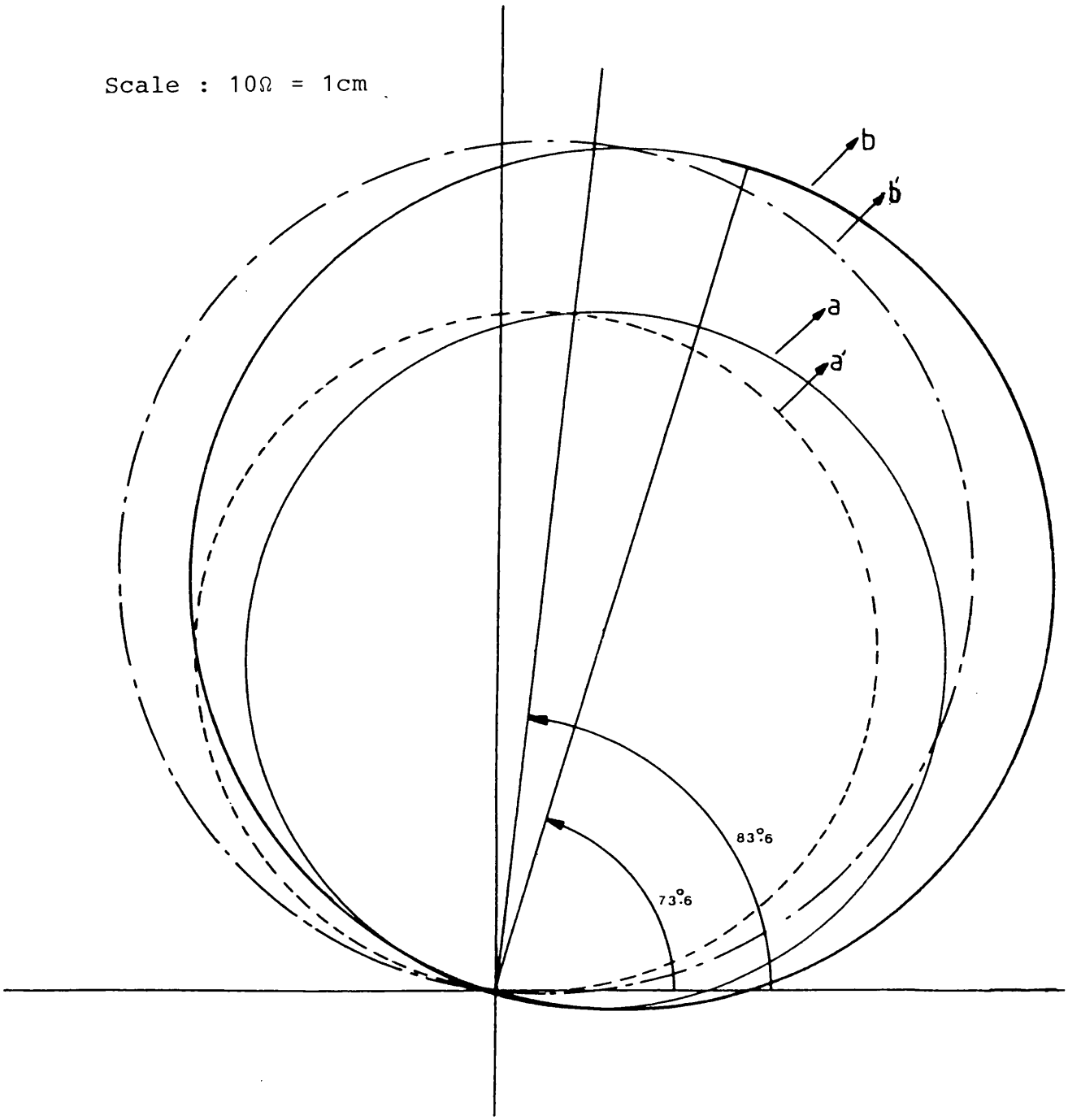


Figure 4.5 Mho characteristic

(a) Permissive overreach scheme
(b) Blocking scheme
(a'),(b') Normal mho characteristic, scheme similar to (a),(b)

# CHAPTER 5 DIGITAL EVALUATION OF THE GENERAL PRIMARY SYSTEM WAVEFORMS

## 5.1 Introduction

Johns and Aggarwal[37], in their studies associated with faults on uncompensated e.h.v. lines have shown that the frequency variance of line parameters, source parameters, fault position, etc considerably affect travelling wave distortion of both voltages and currents. Since such factors can also affect the fault induced overvoltage phenomena, the fault transients associated with the single pole autoreclosure sequences and the performance of system protective relays, it was felt necessary to consider some of the above-mentioned factors in the present study.

Two basic systems, the analysis of which has been developed in Chapter 2, are used to obtain the primary system responses. Initially, the relaying point responses (which are voltage and current waveforms mainly at the sending end) for a single-phase-to-earth fault on a single section feeder (simple source model as shown in Figure 2.7) are computed and presented in Section 5.2, followed by the presentation of results relating to faults on a multi-section compensated feeder (complex source model as shown in Figure 2.8) in Section 5.3. In the two systems simulated, identical line models are

considered in order to make a direct comparison of the results possible. The majority of the results presented are for the case where a capacitor is located at each end of the protected feeder, and some responses for a single capacitor for location at the mid-point are also given. All the cases considered have shunt compensation. The parameters used are as described in Chapter 4, and the types of fault simulated have already been shown in Chapter 3.

## 5.2 Responses of the Single Section Feeder

### 5.2.1 Effect of Fault Inception

Figure 5.1 shows the sending end relaying point waveforms (voltages and currents) for a solid 'a' phase-to-earth mid-point fault on a feeder without series compensation and illustrates the frequency dependent reflection at the source. The high frequency leading edge of the initial surge reaching the source is presented, with a high impedance compared with that apparent in the prefault region and as can be seen in Figure 5.1(a), a voltage spike therefore occurs on the relaying point voltage waveforms with a consequent increase in the rise time of the reflected current surge (Figure 5.1(b)). On subsequent reflections at the sources, further distortion of the surge waveform occurs as the various frequencies presented are reflected with differing phase and amplitude.

Figure 5.2 shows the waveforms for a series compensated system (with a capacitor at each end of the line) for an identical fault condition. In this respect it should be noted that the inclusion of a series capacitor (or capacitors) in a power transmission line introduces a point of electrical discontinuity and an incident surge is partially reflected, the remainder being transmitted through the capacitor and propagated along the line section and beyond. As the reflection coefficient is frequency dependent, it is clear that the high frequency components will pass through the capacitors virtually unchanged, whereas low frequency components, which in general are predominantly at power frequency, will be significantly reflected. This is apparent from Figures 5.1 and 5.2, which show that both the voltage and current waveforms are identical in the two cases, except for the actual magnitudes of the faulted phase voltages and currents, which are shown in Table 5.1.

| | Uncompensated | | Compensated | |
|---|---|---|---|---|
| | Computed | Analytical | Computed | Analytical |
| Voltage (kV) | 320 | 294 | 275 | 230 |
| Current (kA) | 3.7 | 4.56 | 6.1 | 6.18 |

Table 5.1 Computational and analytical magnitudes of currents and voltages

The Table also shows the analytical results obtained using an approximate model (see Appendix (A2)). As can be seen, the two sets of results are close to each other, showing the correctness of the computational process.

### 5.2.2 Effect of Source Capacities

The source capacities significantly affect the fault transient waveforms. Figures 5.3 and 5.4 show a comparison between the responses for a mid-point fault for both small and large source capacities at the sending end. The low source capacity introduces high frequency spikes into the voltage waveforms (faulted as well as the healthy phases). This is due to the relatively large impedance associated with low source capacity adjacent to the observation point and which constitutes a major point of electrical discontinuity, from which high frequency components are easily reflected. Also, the post-fault healthy phase currents have the same polarity as the faulty phase (Figure 5.3(b)). The reason for this later feature is that the faulty phase current fed from the remote (receiving end) source is considerably larger than that fed from the sending source (this being due to much larger receiving end source capacity), thus inducing a significant voltage in the healthy phases, which in turn forces a current to flow between ends. However, in the case of a large sending end source capacity, the

voltage waveforms in particular are much smoother (Figure 5.4(a)). This is due to the fact that the source impedance associated with this condition is low, resulting in the busbar voltage being held nearly constant and not easily distorted.

### 5.2.3 Effect of Prefault Loading

In the case of short uncompensated feeders, the waveforms are not significantly affected by prefault loading, as the prefault voltage at any point is almost independent of the circuit loading and so also are the high frequency components in the currents[37]. This is so even in the case of compensated systems, especially where combined shunt and series compensation is used. This is evident by comparing Figures 5.2 and 5.5. Figure 5.5 shows the waveforms for a system for conditions similar to those in Figure 5.2, except that a prefault load angle of $\delta = 30°$ is assumed for the former. As can be seen, the voltage waveforms are not very different. However, the current waveforms are significantly different from the

loaded case, especially the sound phase currents whose magnitude becomes quite comparable with the faulted phase current (Figure 5.5(b)). This is primarily due to an increase in the electromagnetic coupling between the faulted and healthy phases.

### 5.2.4 Effect of Fault Position

The transit time of travelling waves between the fault and source discontinuities varies in particular with fault position, and it follows that the apparent frequency of the superimposed travelling wave components decreases as the fault position becomes more distant from the observation point. Figures 5.6 and 5.7 show the sending end relaying point waveforms for a solid 'a'-phase-to-earth fault (on a compensated system) for different fault positions. For a close up fault (Figure 5.6(a)), as expected the faulted 'a' phase voltage collapses to zero with a small time delay (which is inherent to the modified Fourier transform technique) after fault inception. From the corresponding currents in Figure 5.6(b) it can be seen that the faulted phase current reaches a peak value of about 17 kA. In fact, the correctness of this figure can be verified from a knowledge of the system peak voltage ($\cong$ 408kV) and the sending end source impedance $Z_{S1}$ ($\cong$ 25$\Omega$). As can be seen, the sound phase currents are slightly distorted. As the fault position moves further away

from the sending end, the travelling wave phenomena becomes more prominent and this effect can be seen by comparing Figures 5.6 and 5.7 (the latter being for a fault at the receiving end). In this respect, it must be mentioned that the faulted phase waveforms are dominated by the earth mode and the sound phases by the aerial modes. From Figure 5.7(a) and looking at the faulted phase voltage, it is evident that initially the transit time is about 2.5 ms, which is the time taken for an earth mode to travel from the sending end to the fault point and back. This figure corresponds to an effective propagation velocity of approximately 240 km/ms.

### 5.2.5 Effect of Type of Fault

Faults not involving earth give rise to waveforms which generally are very distorted. Figure 5.8 shows the waveforms for an 'a'-'b' phase fault, and comparing this with an 'a' phase-to-earth fault for corresponding source conditions as shown in Figure 5.2, it is apparent that the travelling waves persist for considerably longer in the former, especially in the faulted phases. This is due to the fact that the lower attenuation of the aerial modes associated with phase faults take relatively longer time to disappear.

### 5.2.6 Effect of Fault Instant

The two possible worst cases, from the travelling wave point of view, are the faults at an instant of time corresponding to voltage maximum and voltage minimum (ie zero voltage) in the faulted phase or phases. In the former the travelling wave distortion is effectively increased, producing high frequency spikes as shown in Figure 5.2, whilst in the latter, travelling wave distortion is significantly reduced because there is not a large and sudden voltage change at the point of fault. Figure 5.9 shows the waveforms for 'a'-phase-to-earth mid-point fault at voltage minimum. It can be clearly seen that the distortion is extremely small, and the well-known offset nature of the current waveform is observed.

### 5.2.7 Effect of Degree of Series Compensation and Location of Capacitor

As one of the prime objectives of the thesis is to examine the effect of series compensation on primary system waveforms, studies for conditions similar to those in Figure 5.2 are carried out. Initially the amount of series compensation is reduced to 50%, and secondly the capacitors at each end are replaced by a single capacitor in the middle (associate 50% series compensation). Figures 5.10 and 5.11 show such responses and it can be seen that the waveforms are

not very different to Figure 5.2. However, the magnitudes of the faulted phase current waveforms are different.

### 5.2.8 Primary System Waveforms at other Relaying Points

In order to examine the effect of the aforementioned factors at the other relaying point (ie receiving end), similar studies have been carried out, and some of the results are presented here. It has been found out that the effect of various factors as mentioned in Section 5.2.1 to 5.2.7 is also applicable in this case. For example, Figures 5.12 and 5.13 are the receiving end responses for a fault at the sending end busbar, the former being for a capacitor located at each end and the latter being for a single capacitor at the mid-point. Comparing Figure 5.12 with the corresponding cases for the sending end (Figure 5.7) it can be seen that the waveforms are more or less identical.

## 5.3 Response Evaluation of a Multi-section Feeder System

In this Section, similar studies to that presented in Section 5.2 have been carried out, mainly to determine the differences between the responses of a single and multi-section feeder respectively, the faulted line model being the same in both cases.

5.3.1 Effect of Fault Inception

Figures 5.14 and 5.15 show the results at the sending end relaying point for a solid 'a' phase-to-earth fault at the mid-point (without and with series compensation respectively). Like in the single section feeder, both the voltage and current waveforms are identical in the two cases (Figures 5.14 and 5.15), except for the actual magnitudes of the faulted phase voltages and currents.

Also, comparing this with the results of an identical fault condition for a single section feeder (Figures 5.1 and 5.2), it can be clearly seen that both voltage and current waveforms are significantly different in the two cases, especially the current waveforms which are apparently more distorted in the case of the multi-section feeder arrangement. This is so because in the case of the multi-section feeder arrangement (Figure 2.8) the travelling waves of currents set up on fault inception travel through S towards $G_S$ and are partially reflected by the latter back to S to produce these very significant current distortions. Furthermore, in the case of the single section feeder, the frequency of the travelling wave components is largely dependent on the wave transit time between the source discontinuity and fault point. They consequently have a relatively higher frequency distortion compared

with those produced in the multi-section feeder, where the wave transit time between the points of major discontinuity and fault point is much longer, resulting in travelling wave components being lower in frequency and also persisting for a much longer period.

### 5.3.2 Effect of Main Source Capacities

The studies of Section 5.2.2 have indicated that for a smaller source capacity the waveforms produced are considerably more distorted with high frequency components, whereas when the source capacities are large the magnitudes of the superimposed travelling wave components are relatively low and they are damped more quickly. Similar sorts of effects, but to a much lesser extent, are found to be true when considering the multi-section feeder, as shown by Figures 5.16 and 5.17.

### 5.3.3 Effect of Prefault Loading

Figure 5.18 shows the response at the sending end relaying point, when a mid-point 'a' phase-to-earth fault under identical conditions as those of Figure 5.15 is considered, except that in this case the line has a prefault loading of 30°. As expected, the line loading has a significant effect on the waveforms, especially the magnitude of the currents, which go up quite sharply. The substantial increase in the magnitude of the healthy phase currents again is attributed to the

increased electromagnetic coupling between the phases. Comparing Figure 5.18 with Figure 5.5, the latter being for an identical fault condition for a single section feeder, the differences are clearly observed.

### 5.3.4 Effect of Fault Position

As already mentioned in Section 5.2.4, when the fault position becomes more distant from the observation point, the frequency of the superimposed travelling components decreases and the transit time between the source discontinuities and fault point in particular varies with fault position. This phenomena can also be observed from Figures 5.19 and 5.20 for a solid 'a' phase-to-earth fault. Again, as expected in the case of a close up fault, Figure 5.19(a), the faulted phase voltage collapses to zero. Comparing these two figures with its single section feeder counterpart (Figures 5.6 and 5.7), there are marked differences between the two system responses. Both voltage and current waveforms are seen to differ significantly in the two cases, again primarily because of the different transit times involved in the two cases. From Figure 5.20(a), the total transit time between the observation point and main generating source at the sending end S - $G_S$ - S is 2 ms, which corresponds to an effective propagation velocity of approximately 300km/ms. Also, the transit time between ends S and R (ie fault point) is about 2 ms.

### 5.3.3 Effect of Type of Fault

Figure 5.21 shows the response at the relaying point for a solid 'a'-'b' fault. The fault conditions are similar to those of Figure 5.15. Comparing with its single section counterpart, following identical fault conditions of Figure 5.8, the differences can be observed. In the case of the single section feeder, travelling wave produces more higher frequency (particularly in the voltage waveforms) initially than the multi-section feeder. This, again, is due to the fact that the transit time between the points of major discontinuity is longer in the multi-section feeder, as such the travelling wave components are not all that predominant during that period.

### 5.3.6 Effect of Fault Instant

The effect of fault instant is shown by comparing Figures 5.22 and 5.15 for a mid-point, solid 'a' phase-to-earth fault. As expected, for a fault at voltage zero the travelling wave distortion is minimal, both in the case of voltage and current waveforms as compared with a fault at voltage maximum. The result of this is that the waveforms are not very different for an identical fault condition on a single section feeder, as shown in Figure 5.9.

### 5.3.7 Effect of Degree of Compensation and Location of Capacitor

In order to see the effect of the degree of compensation and location of series capacitor, studies for conditions similar to those in Figure 5.15 are carried out, except that for the former the amount of compensation is changed to 50%, and for the latter the capacitors at each end are replaced by a single capacitor in the middle, with 50% series compensation. It can be observed from Figures 5.23 and 5.24 that the waveforms are not very different from Figure 5.15, except for a small variation in the magnitude of the faulted phase current and voltage. Also, comparing these with identical fault conditions on a single section feeder, as shown in Figures 5.10 and 5.11, the waveforms are completely different.

### 5.3.8 Primary Responses at other Relaying Points

To examine the effect of the above-mentioned factors on the receiving end voltage and current waveforms, a similar series of studies has been carried out and some of the responses are presented. Figures 5.25 and 5.26 are the receiving end responses for a fault at the sending end busbar, the former being for a capacitor located at each end and the latter for a single capacitor at the mid-point. Comparing these with the corresponding cases for the single section

feeder (Figures 5.12 and 5.13), the differences between the waveforms can be observed.

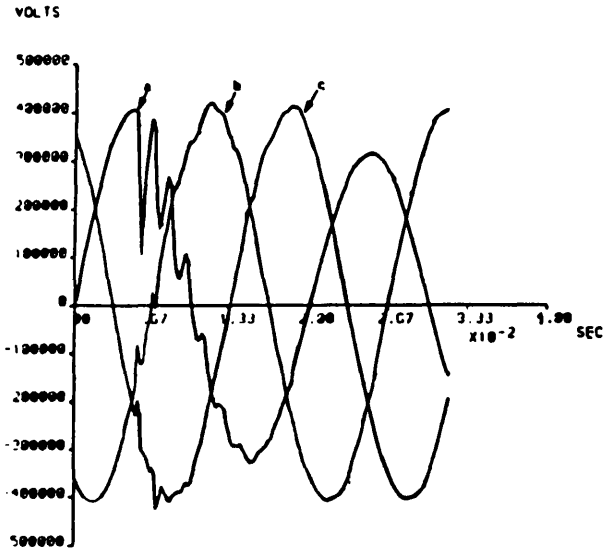


(a)

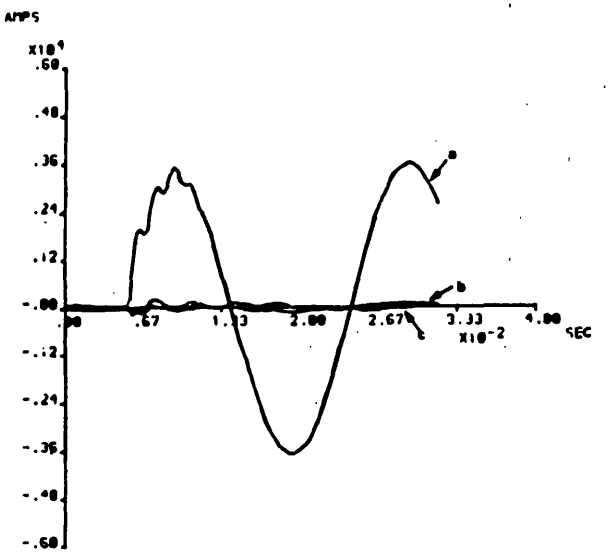


(b)

Figure 5.1 Voltage and current waveforms at the S.E. of the single section feeder. Without series compensation, 'a'-earth fault, x = 150 km, $G_S = G_R$ = 10GVA, FT = 5ms, $V_S/V_R = \angle 0°$

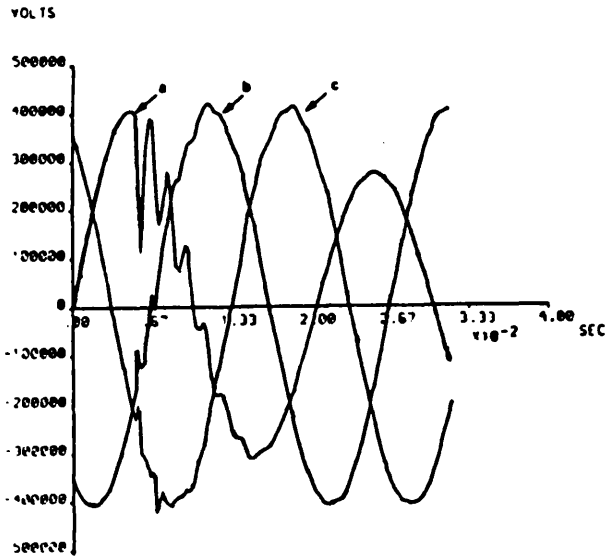


(a)

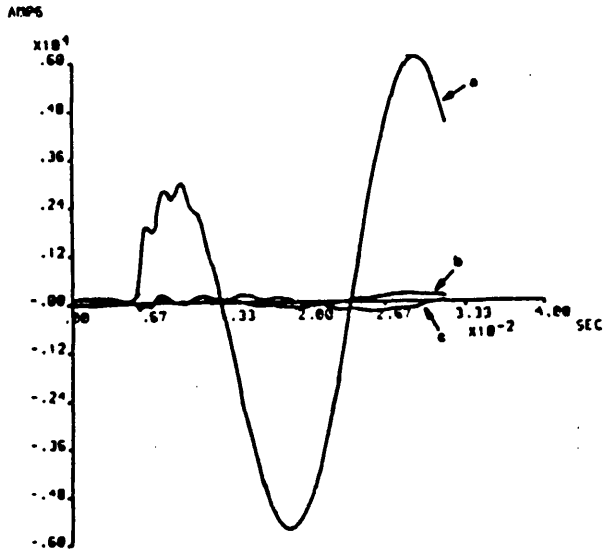


(b)

Figure 5.2 Voltage and current waveforms at the S.E. of the single section feeder. A capacitor at each end, 'a'-earth fault, x = 150 km, $G_S = G_R$ = 10GVA, FT = 5ms, $S_{cap}$ = 0.7 $V_S/V_R = \angle 0°$

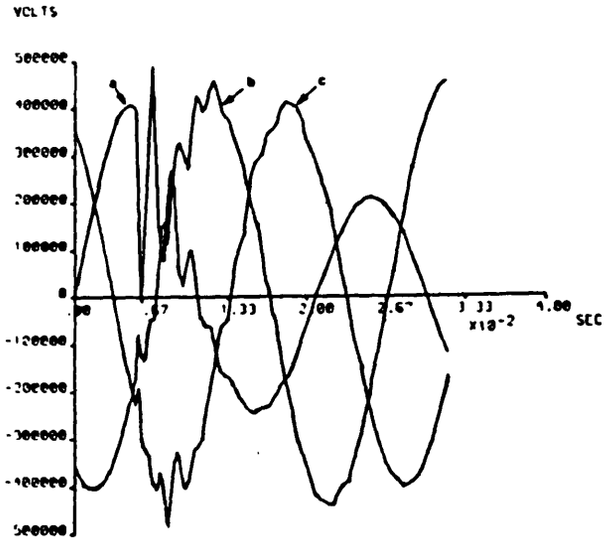


(a)

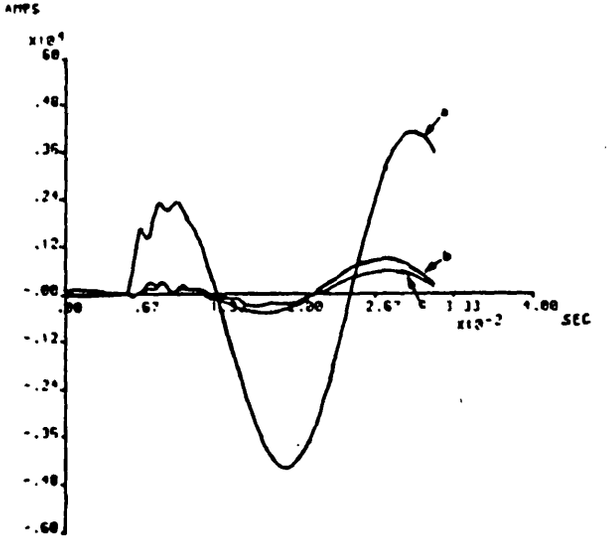


(b)

Figure 5.3 Voltage and current waveforms at S.E. of the single section feeder. A capacitor at each end, 'a'-earth fault, x = 150km, $G_S$ = 5GVA, $G_R$ = 35GVA, FT = 5ms, $S_{cap}$ = 0.7, $V_S/V_R = \angle 0°$

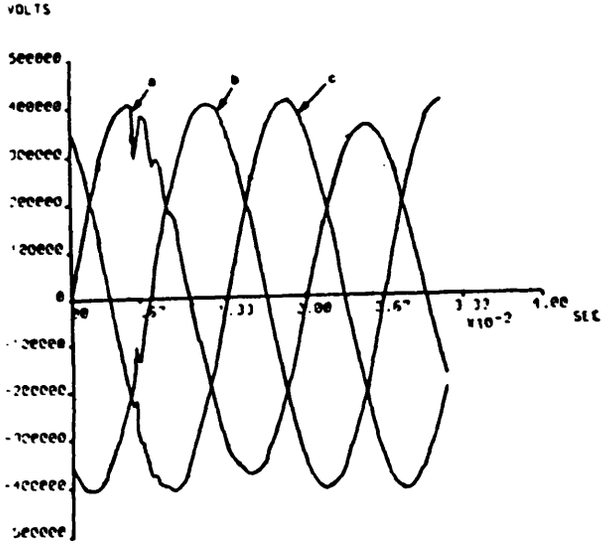


(a)

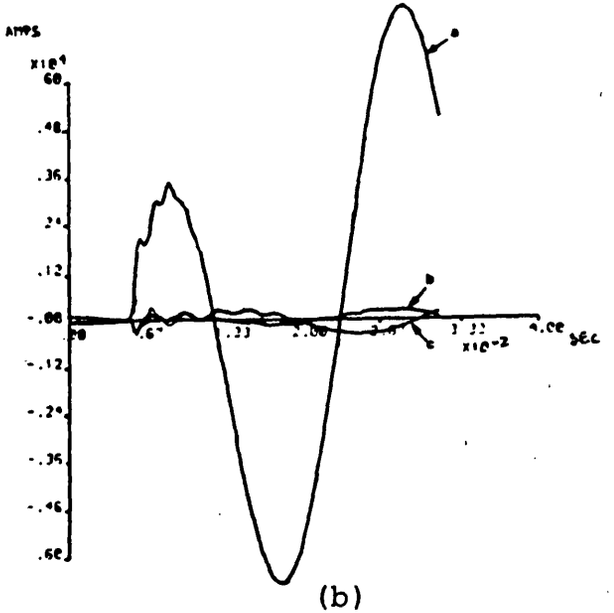


(b)

Figure 5.4 Voltage and current waveforms at S.E. of the single section feeder. A capacitor at each end, 'a'-earth fault, x = 150km, $G_S$ = 35GVA, $G_R$ = 35 GVA, FT = 5ms, $S_{cap}$ = 0.7, $V_S/V_R = \angle 0°$

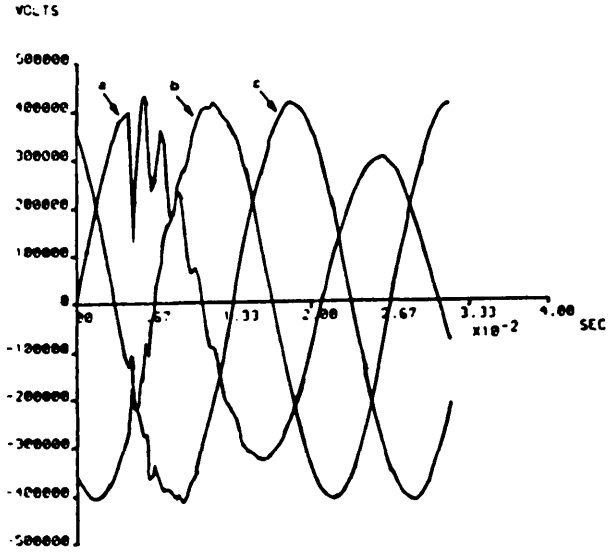


(a)

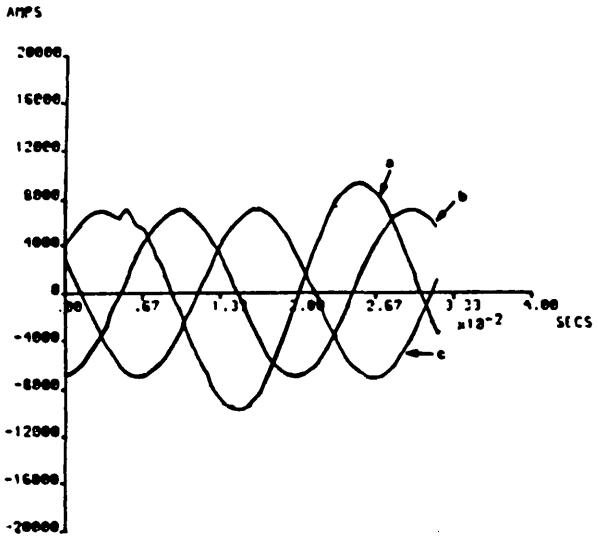


(b)

Figure 5.5 Voltage and current waveforms at the S.E. of the single section feeder. A capacitor at each end, 'a'-earth fault, x = 150km, $G_S$ = 10GVA = $G_R$, FT = 4.16ms, $S_{cap}$ = 0.7, $V_S/V_R = \angle 30°$

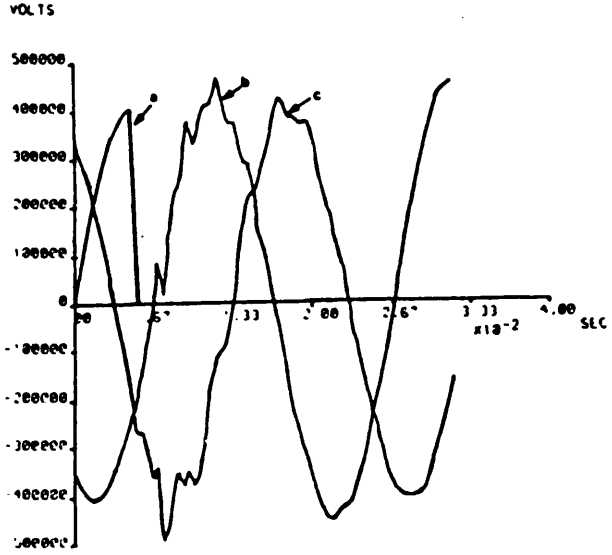


(a)

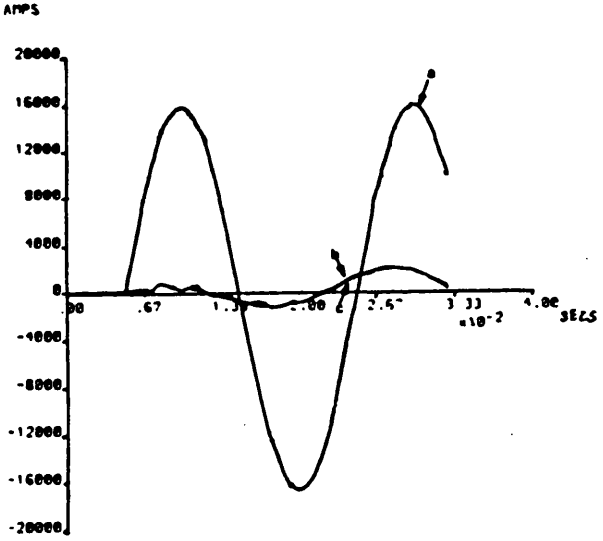


(b)

Figure 5.6 Voltage and current waveforms at the S.E. of the single section feeder. A capacitor at each end, 'a'-earth fault, x = 0km, $G_S$ = $G_R$ = 10GVA, FT = 5ms, $S_{cap}$ = 0.7, $V_S/V_R = \angle 0°$

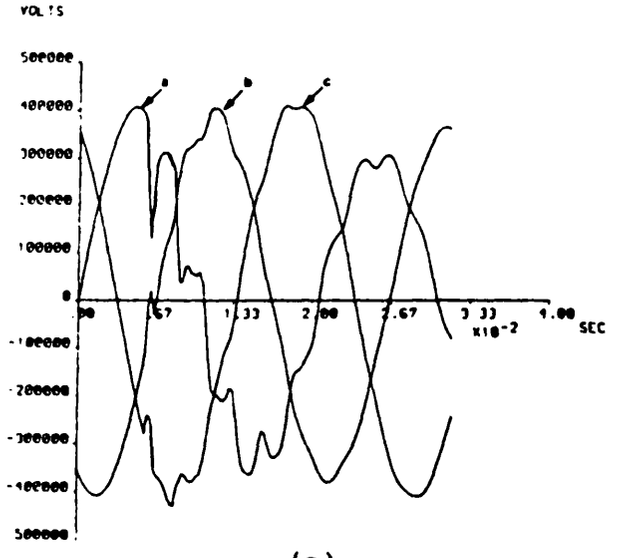


(a)

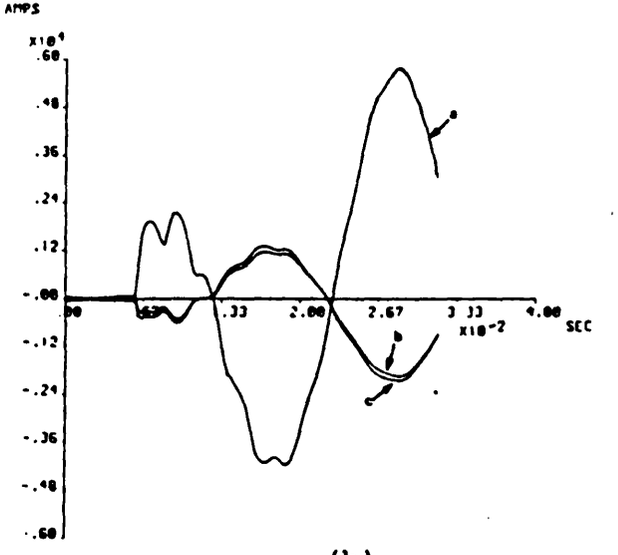


(b)

Figure 5.7 Voltage and current waveforms at the S.E. of the single section feeder. A capacitor at each end, 'a'-earth fault, x = 300km, $G_S = G_R$ = 10GVA, FT = 5ms, $S_{cap}$ = 0.7, $V_S/V_R = \angle 0°$

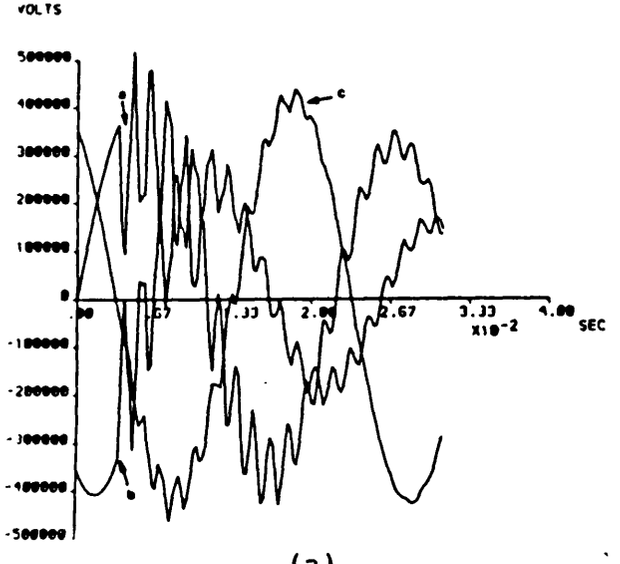


(a)

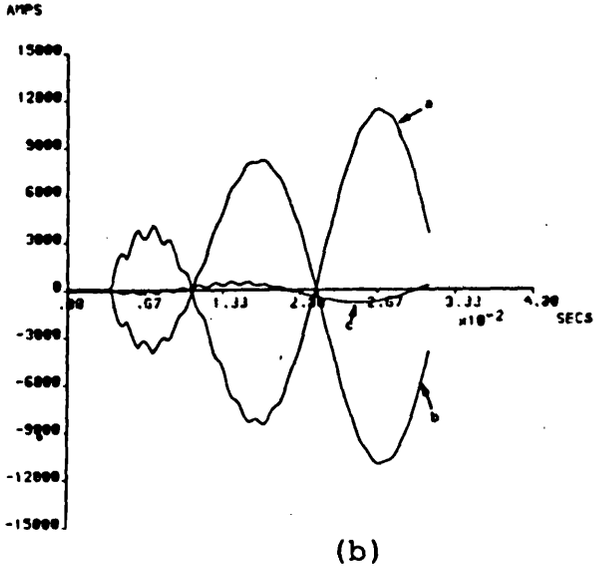


(b)

Figure 5.8 Voltage and current waveforms at the S.E. of the single section feeder, a capacitor at each end, 'a'-'b' phase fault, x = 150km, $G_S$ = 10GVA = $G_R$, FT = 3.33ms, $S_{cap}$ = 0.7, $V_S/V_R = \angle 0°$

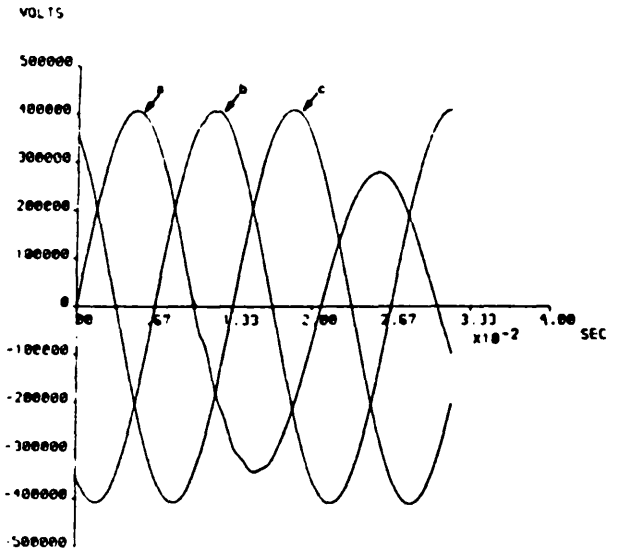


(a)

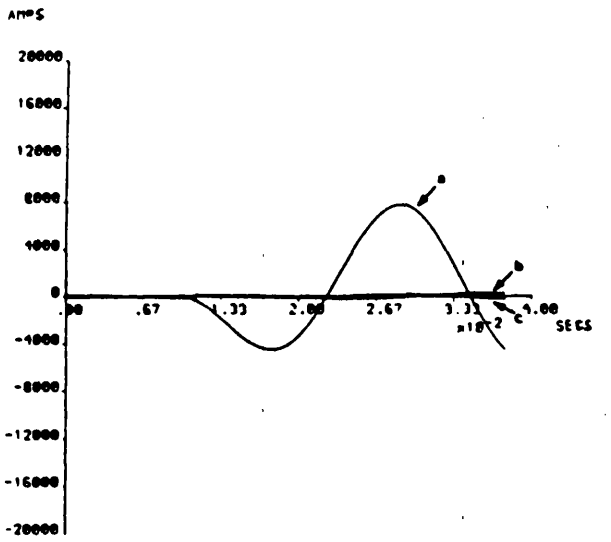


(b)

Figure 5.9 Voltage and current waveforms at the S.E. of the single section feeder, a capacitor at each end, 'a'-earth fault, x = 150km, $G_S = G_R$ = 10GVA, FT = 10ms, $S_{cap}$ = 0.7, $V_S/V_R = \angle 0°$

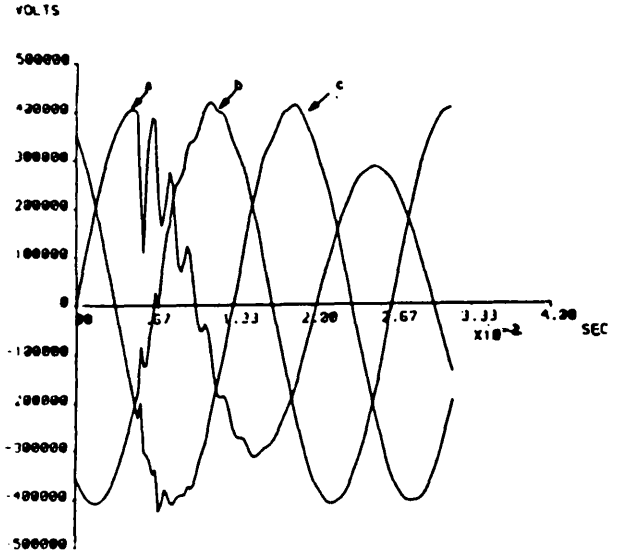


(a)

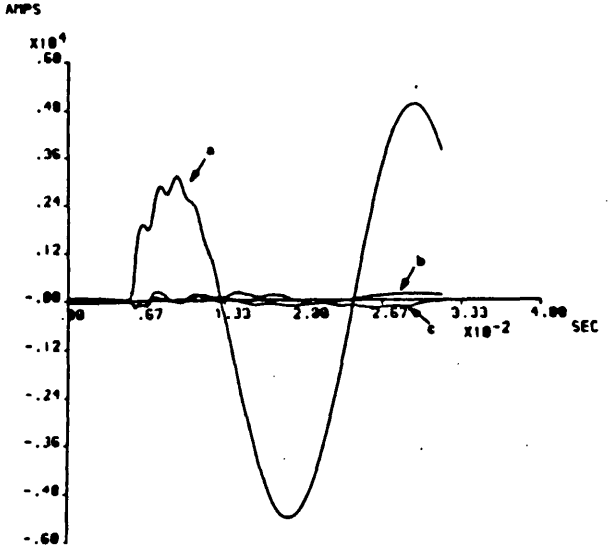


(b)

Figure 5.10 Voltage and current waveforms at the S.E. of the single section feeder, a capacitor at each end, 'a'-earth fault, x = 150km, $G_S = G_R$ = 10GVA, FT = 5ms, $S_{cap}$ = 0.5, $V_S/V_R = \angle 0°$

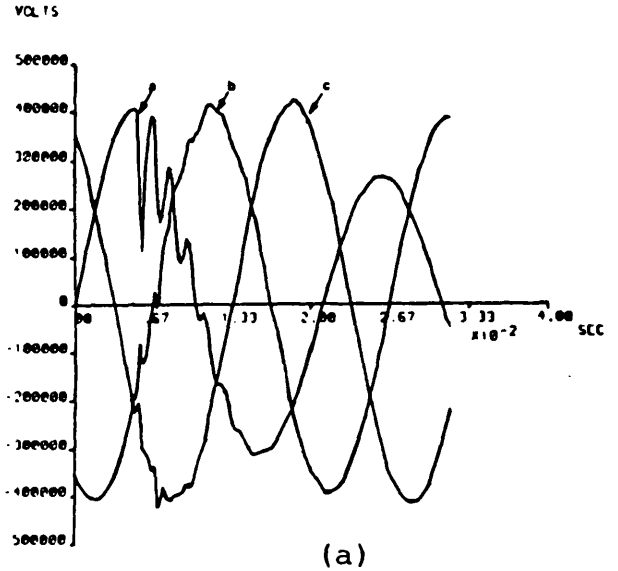


(a)

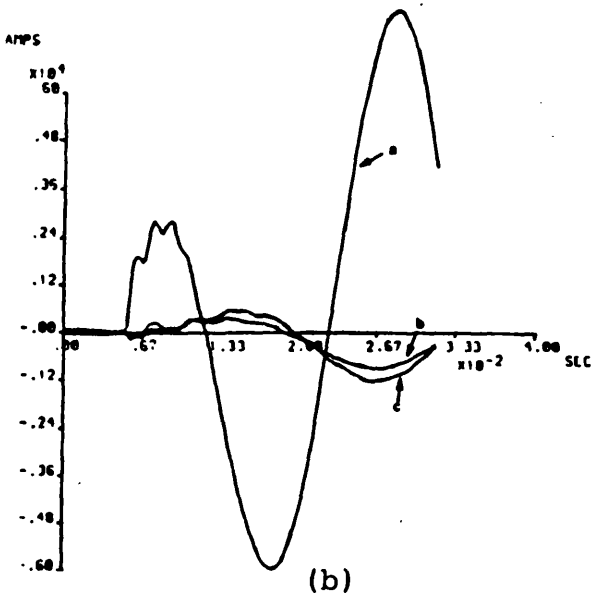


(b)

Figure 5.11 Voltage and current waveforms at the S.E. of the single section feeder, capacitor at mid-point, 'a'-earth fault, x = 150km, $G_S = S_R$ = 10GVA, FT = 5ms, $S_{cap}$ = 0.5, $V_S/V_R = \angle 0°$

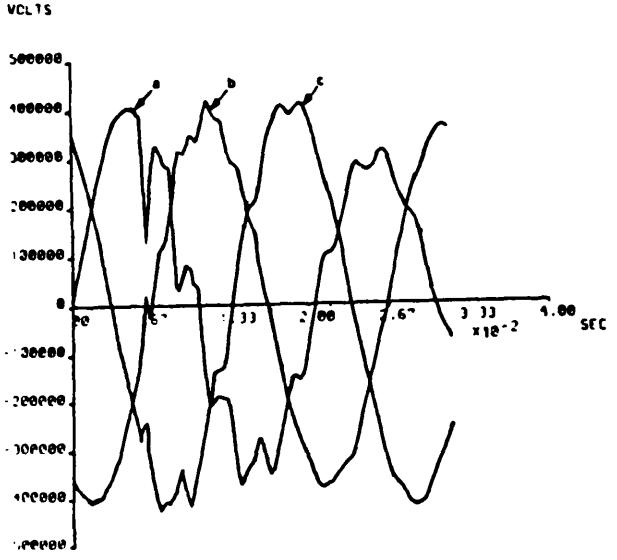


(a)

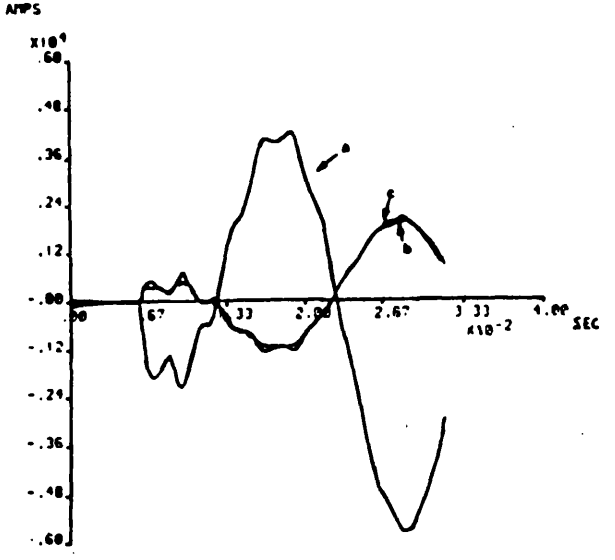


(b)

Figure 5.12 Voltage and current waveforms at the R.E. of the single section feeder, capacitor at each end, x = 0km. Other conditions similar to Figure 5.2.

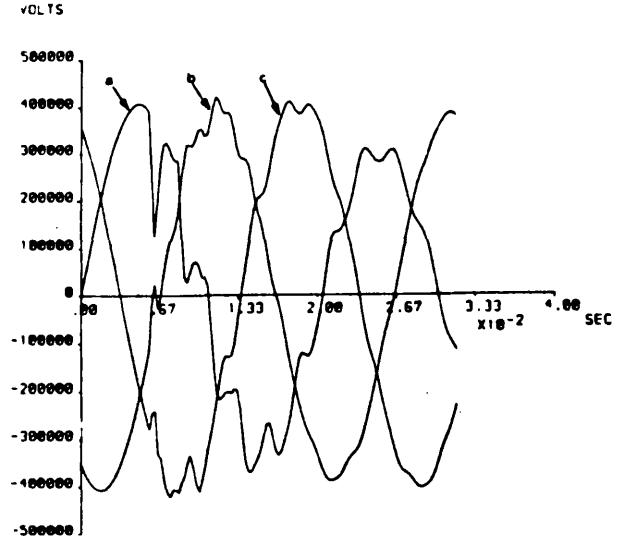


(a)

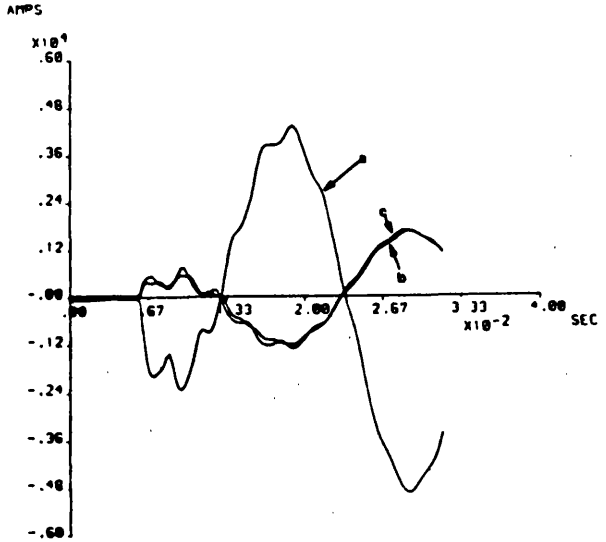


(b)

Figure 5.13 Voltage and current waveforms at the R.E. of the single section feeder, capacitor at mid-point, x = 0km, other conditions similar to Figure 5.11.

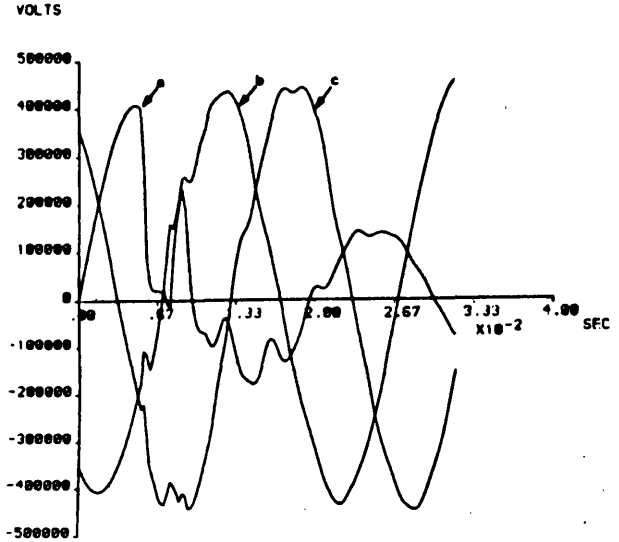


(a)

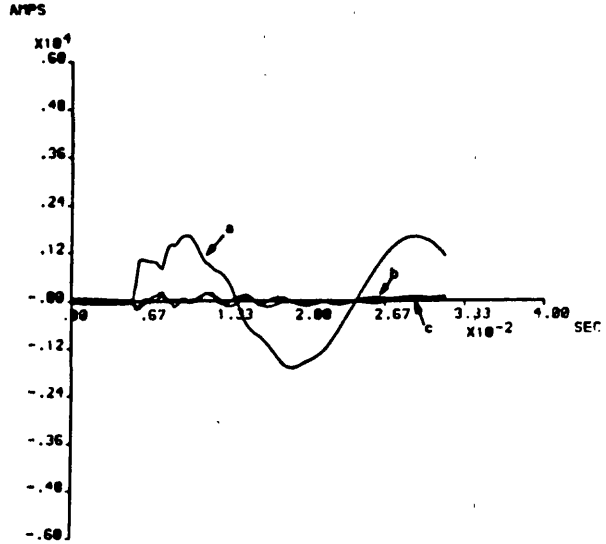


(b)

Figure 5.14 Voltage and current waveforms at the S.E. of the multisection feeder. Fault and source conditions similar to Figure 5.1 and Figure 2.8 respectively.

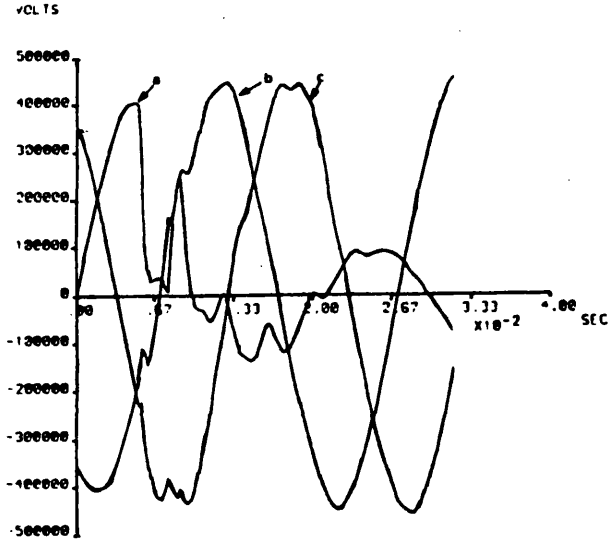


(a)

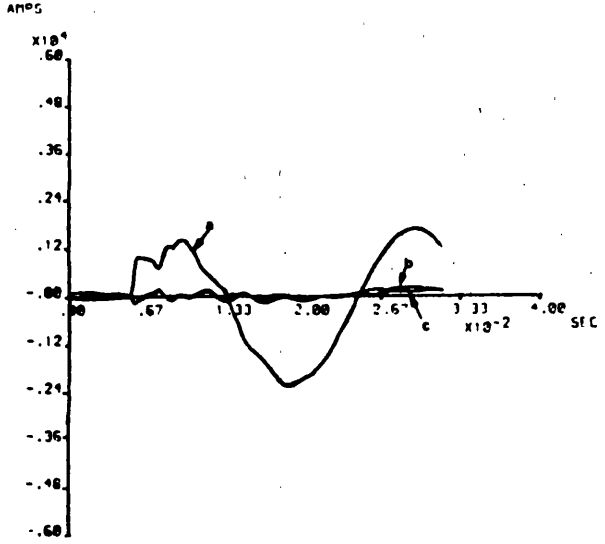


(b)

Figure 5.15 Voltage and current waveforms at the S.E. of the multisection feeder. Fault and source conditions similar to Figure 5.2 and Figure 2.8 respectively.

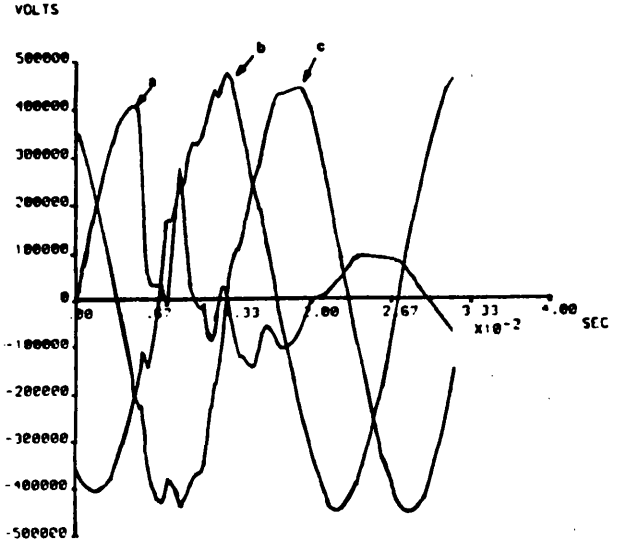


(a)

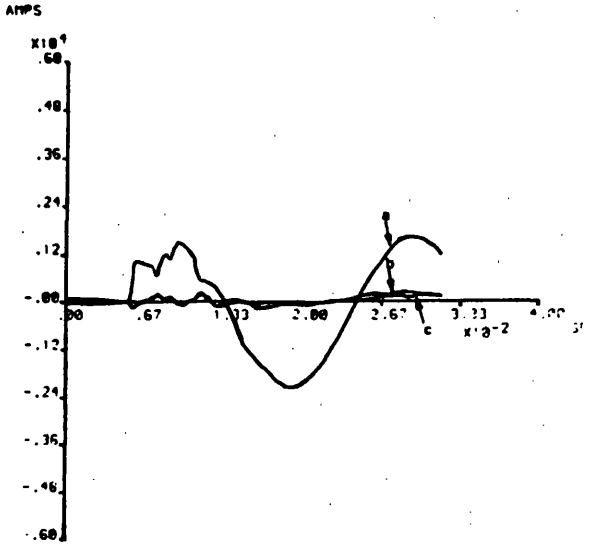


(b)

Figure 5.16 Voltage and current waveforms at the S.E. of the multisection feeder, $G_S$ = 5GVA, $G_R$ = 35GVA. Other fault and source conditions similar to Figure 5.3 and Figure 2.8 respectively.

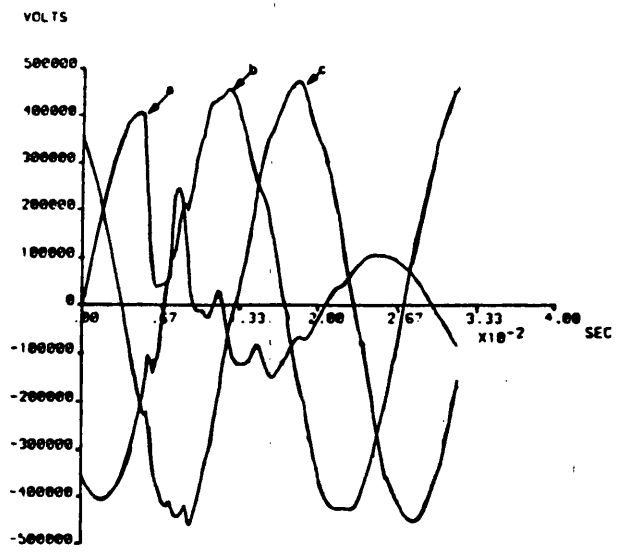


(a)

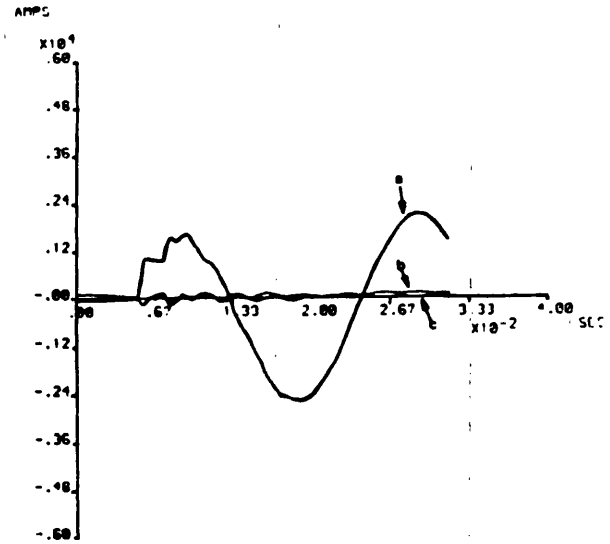


(b)

Figure 5.17 Voltage and current waveforms at the S.E. of the multisection feeder, $G_S$ = 35GVA, $G_R$ = 35GVAV. Other fault and source conditions similar to Figure 5.4 and Figure 2.8 respectively.

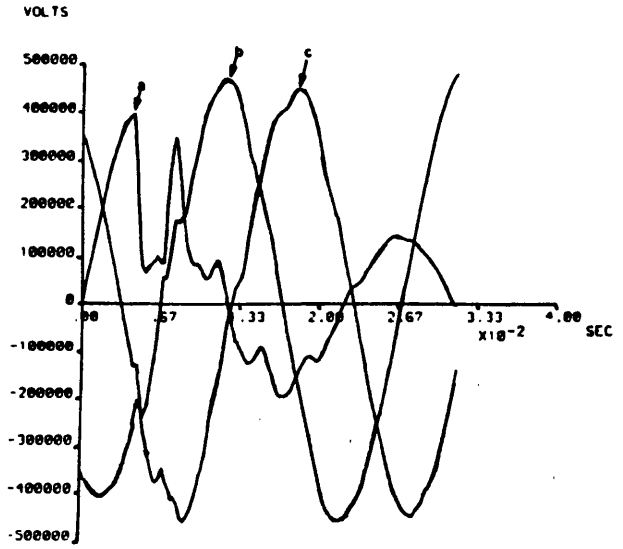


(a)

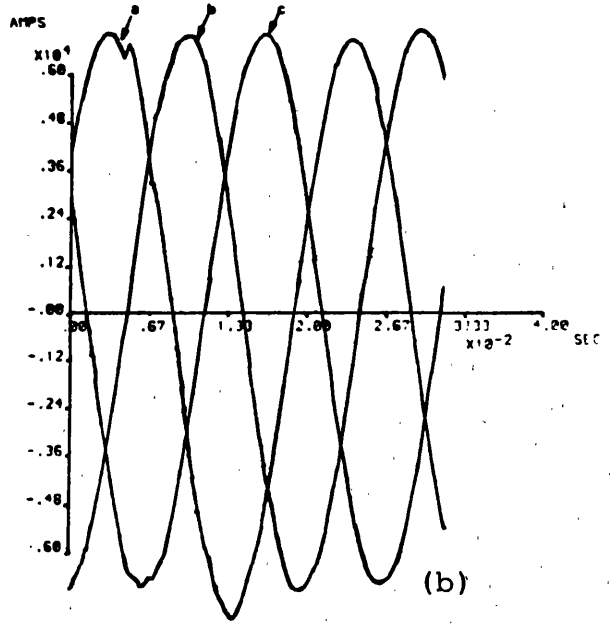


(b)

Figure 5.18 Voltage and current waveforms at the S.E. of the multisection feeder. Fault and source conditions similar to Figure 5.5 and Figure 2.8 respectively.

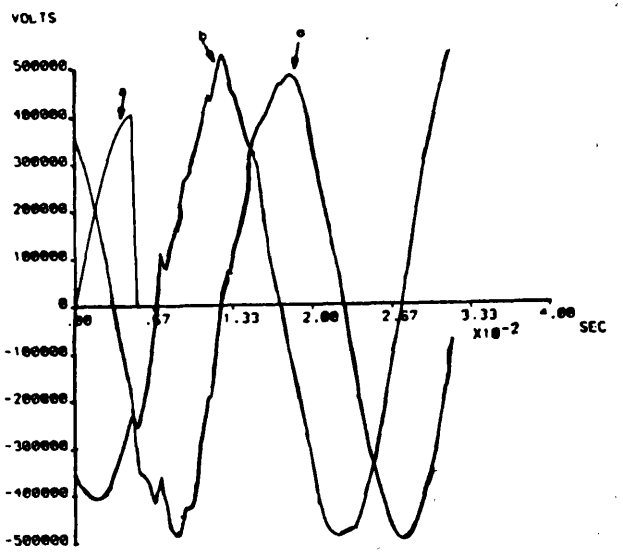


(a)

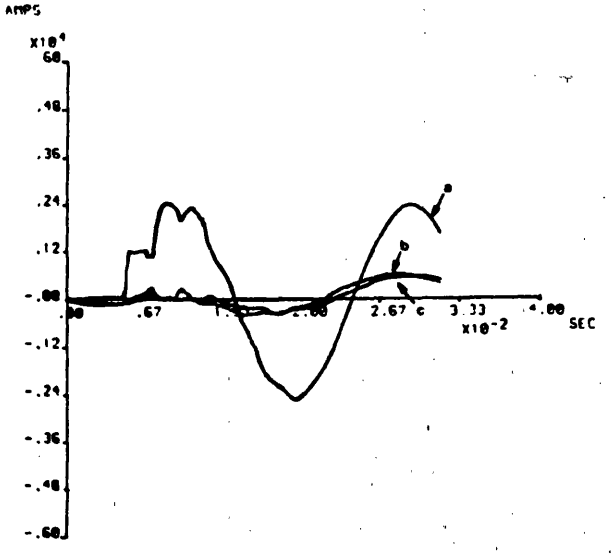


(b)

Figure 5.19 Voltage and current waveforms at the S.E. of the multisection feeder. Fault and source conditions similar to Figure 5.6 and Figure 2.8 respectively.

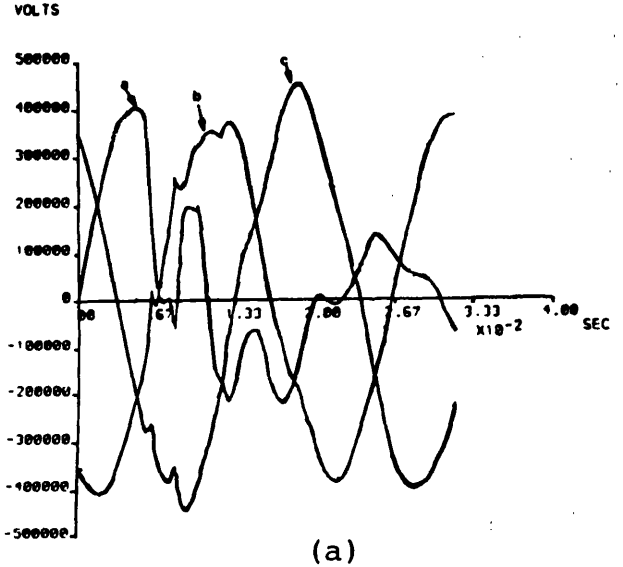


(a)

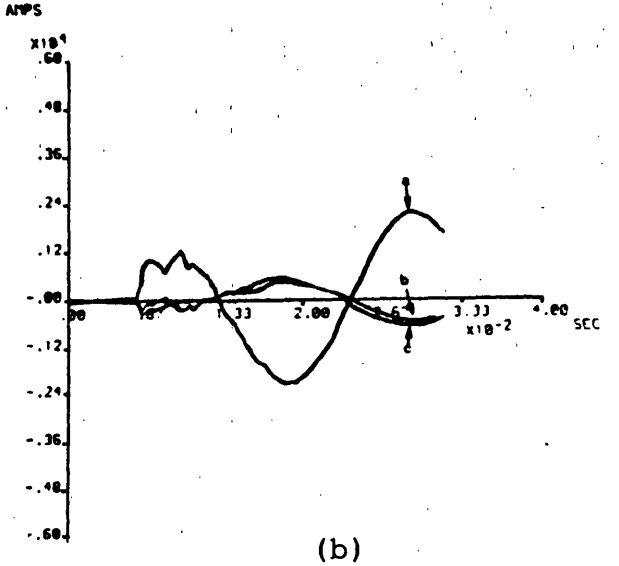


(b)

Figure 5.20 Voltage and current waveforms at the S.E. of the multisection feeder. Fault and source conditions similar to Figure 5.7 and Figure 2.8 respectively.

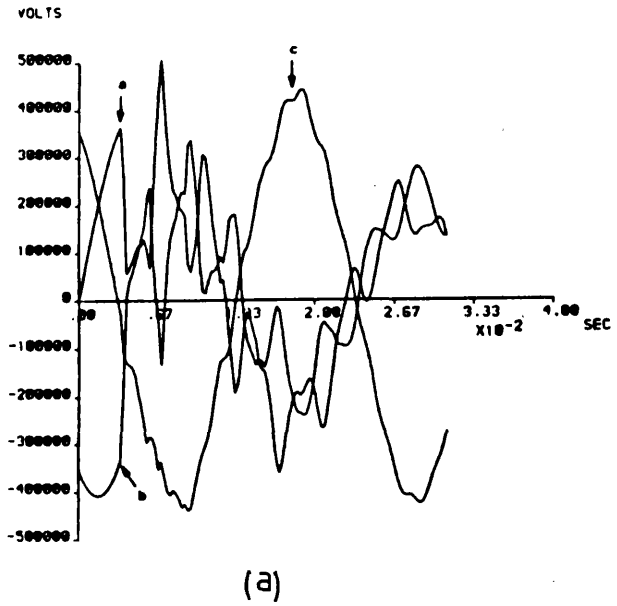


(a)

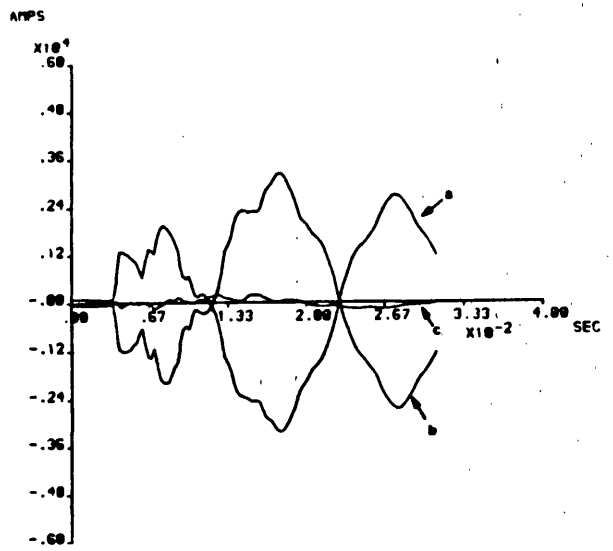


(b)

Figure 5.21 Voltage and current waveforms at the S.E. of the multisection feeder. Fault and source conditions similar to Figure 5.8 and Figure 2.8 respectively.

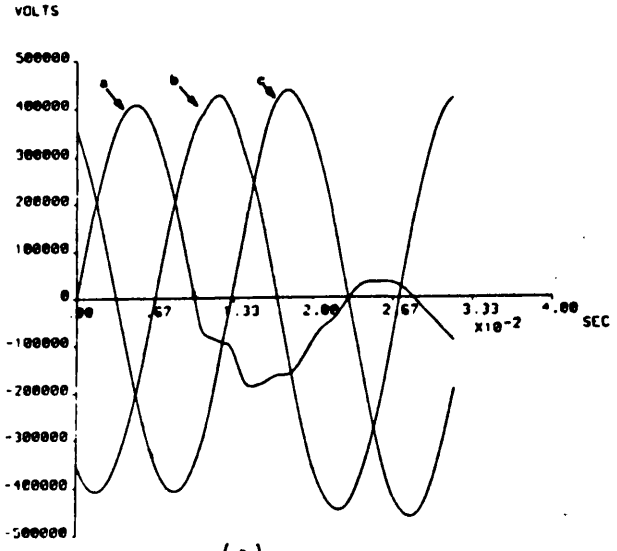


(a)

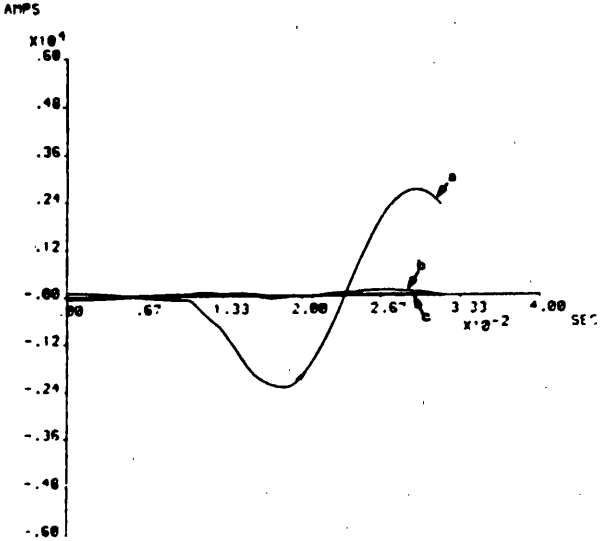


(b)

Figure 5.22 Voltage and current waveforms at the S.E. of the multisection feeder. Fault and source conditions similar to Figure 5.9 and Figure 2.8 respectively.

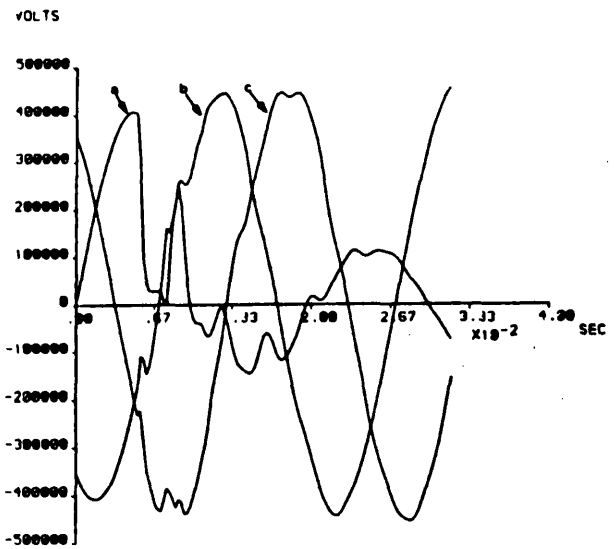


(a)

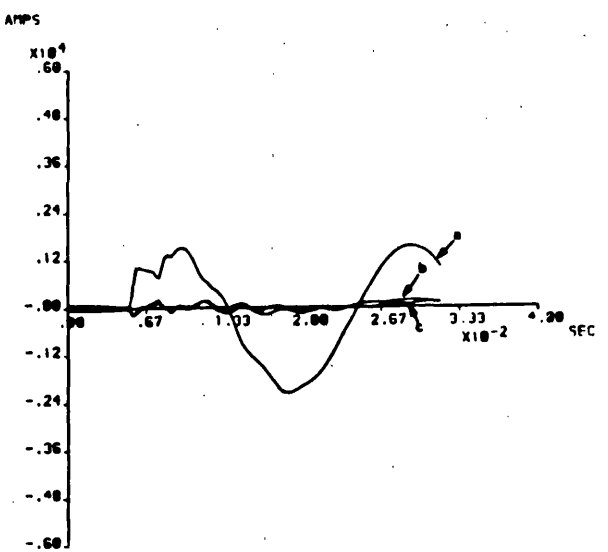


(b)

Figure 5.23 Voltage and current waveforms at the S.E. of the multisection feeder. Fault and source conditions similar to Figure 5.10 and Figure 2.8 respectively.

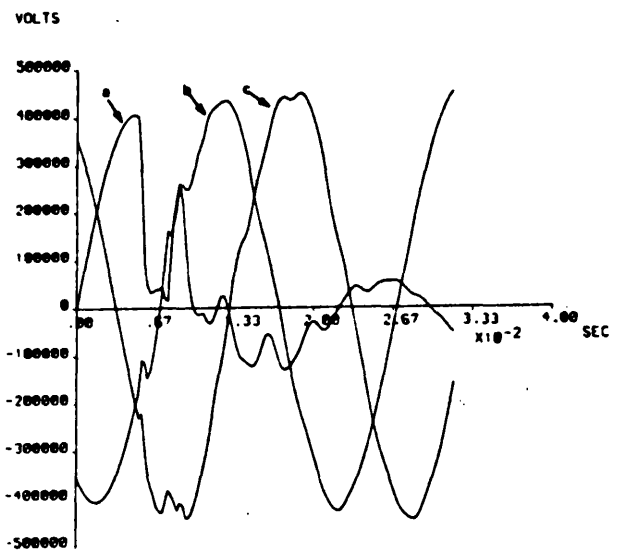


(a)

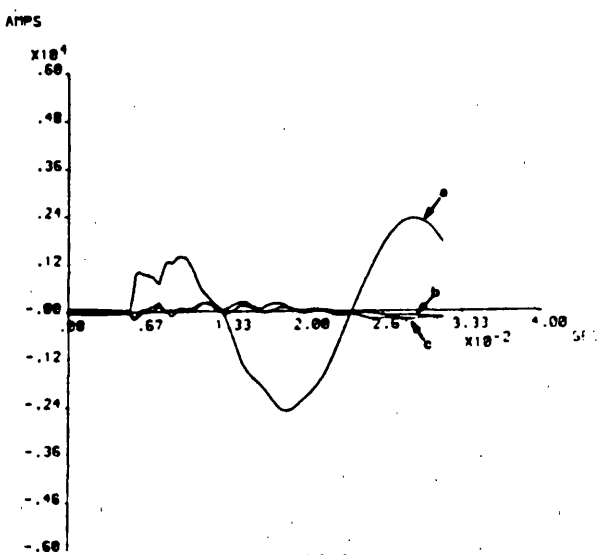


(b)

Figure 5.24 Voltage and current waveforms at the S.E. of the multisection feeder. Fault and source conditions similar to Figure 5.11 and Figure 2.8 respectively.

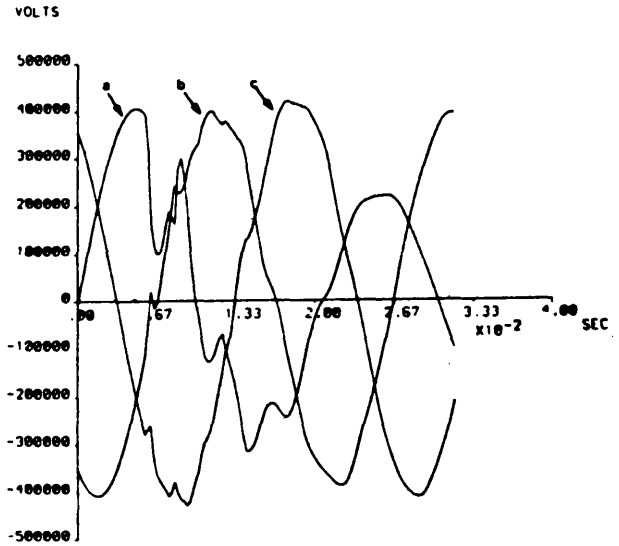


(a)

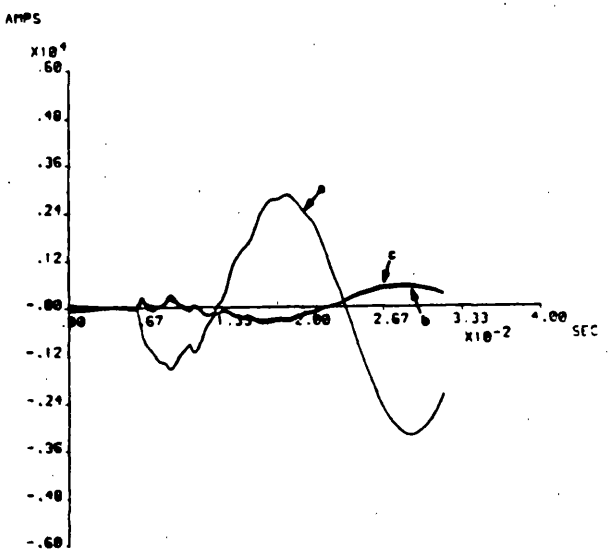


(b)

Figure 5.25 Voltage and current waveforms at the R.E. of the multisection feeder. Fault and source conditions similar to Figure 5.12 and Figure 2.8 respectively.

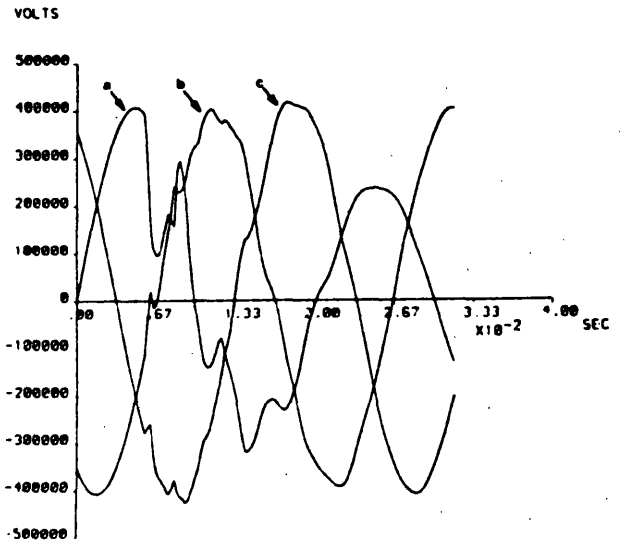


(a)

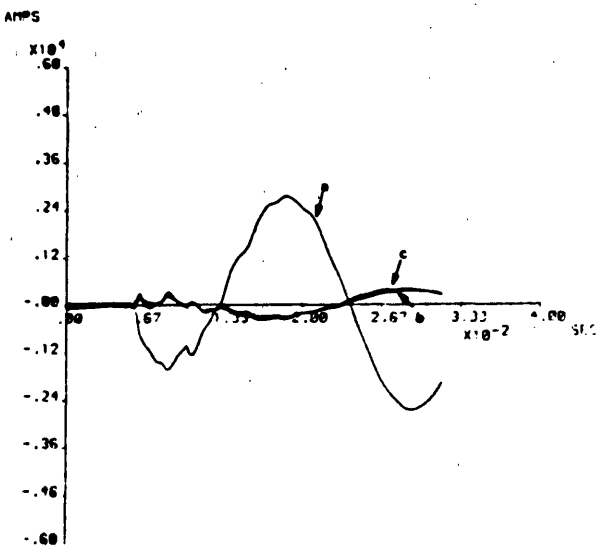


(b)

Figure 5.26 Voltage and current waveforms at the R.E. of the multisection feeder. Fault and source conditions similar to Figure 5.13 and Figure 2.8 respectively.

# CHAPTER 6 DIGITAL EVALUATION OF THE OVERVOLTAGE PHENOMENA IN SERIES COMPENSATED LINES WITH CAPACITOR PROTECTIVE GAP IN OPERATION

## 6.1 Introduction

Earlier computer studies associated with fault induced overvoltages phenomena have been largely concerned with either short lines or long lines having shunt compensation only[64,70,77], and not much work has been reported on examining the overvoltages on series compensated lines, especially the overvoltage phenomena across the capacitor banks, under various fault conditions[78,79]. Also, in the case of lines employing shunt compensation only, it has been found that the overvoltages developed under fault conditions can be quite high, and in certain cases can approach the permissible insulation levels for which the system is designed[76].

Section 6.2 of this Chapter is concerned with examining in some detail the overvoltage phenomena across the capacitors during various fault conditions, followed by a brief look at the possible overvoltage due to fault inception at the relaying point (mainly at the sending end).

## 6.2 Transient Capacitor Overvoltages due to Fault Inception

As mentioned in Chapter 3, capacitor banks in a series compensated line have to be protected against excessive voltages, especially during fault conditions. All the studies have indicated that depending on the system configuration and fault conditions, there can be a wide variation in the actual magnitudes of these overvoltages, which means that if the capacitor protective spark gaps are set to flashover for a certain preset threshold voltage level, then it is possible that in certain cases the fault induced overvoltages across the capacitor banks would reach this threshold level, resulting in the shorting out of the capacitors, and in other cases this may not be so. Furthermore, studies have indicated that when the capacitors do flashover, the actual times at which they do so are very random. The results presented here give some insight into these two aforementioned very non-linear effects, which can be very onerous from a protection point of view, as shown in some detail in Chapter 8.

In most practical systems, a threshold value of the voltage which would result in the shorting out of the capacitor bank is about 2.75 p.u. (the base value for this being different for different systems as shown in Chapter 4), and this is the value assumed in the

results presented here. In order to produce the highest overvoltages across the capacitors, fault is applied at voltage maximum. Again, as the majority of the faults occurring in nature are single-phase-to-earth faults, hence this fault condition is particularly considered.

Studies have indicated that with a single section feeder and simple sources on either side, irrespective of fault and capacitor location, the protective gap for all tested fault positions flashes over. An example to illustrate such a case is shown in Figures 6.1 (a,b), which show the voltages across capacitors (located one at each side) for a fault at 165km. Also shown is another set of responses for voltage across capacitor and current through the bypass switch for a 30% mid-point located capacitor and fault at 110km (Figures 6.1 (c,d)). These Figures clearly show that the capacitor/capacitors on the faulted phase flash over for such system configuration, but the times at which they do so is different for different fault positions.

In the case of the multi-section feeder, with complex source model, the protective gap operations behave randomly depending on the fault position, location of capacitor, amount of compensation, gap setting, complexity of the source side network, etc. Some of the results covering faults on the multi-section

feeder are summarised in Table 6.1. Also shown in it is the time when the threshold level of 2.75 p.u. is reached. The profile of maximum overvoltage across series capacitor, prior to spark gap operation, for both capacitor location and its associate level of compensation, is shown in Figure 6.2.

For all such fault conditions, when the capacitor flashes over it does so only on the faulted phase and within a time interval of one cycle after fault inception. However, the times of flash over are different. Also, it can be observed from Figure 6.2 that the flashover is very random, as there are many instances when the capacitor/capacitors do not reach the preset threshold level.

As it is not possible to present all the studies used in Figure 6.2, however, few responses of the voltage across the capacitor and the current through the bypass switch are shown in Figure 6.3. Figures 6.3 (a,b and c,d) are voltage across capacitor responses for fault at 40 and 240 km respectively, withacapacitor located at each end. From these Figures it can be seen that only the sending end capacitor flashes over for the former fault location and the receiving end capacitor flashes over for the latter position. Figures 6.3 (e,f) are the responses of the voltage across the capacitor when located at the mid-point (50% compensation)

| Distance in km | Voltage across Cap./Time for Cap. to F/O (after fault inception) | | | |
|---|---|---|---|---|
| | A Cap. at each end | | A Cap. in middle | |
| | S.E. (1pu=52.7kV,70%comp) | R.E. | 30% comp (1pu=45.5kV) | 50% comp (1pu=75.3kV) |
| 0.0 | 2.51 | 2.51 | 1.98 | 2.34 |
| 40.0 | 2.75/18.50 | 2.17 | 2.06 | 2.58 |
| 60.0 | - | - | 2.23 | 2.70 |
| 75.0 | 2.45 | 2.45 | 2.39 | 2.75/18.00 |
| 80.0 | - | - | - | 2.75/18.00 |
| 85.0 | 2.29 | 2.57 | - | 2.75/17.75 |
| 90.0 | 2.23 | 2.63 | 2.51 | 2.75/17.50 |
| 95.0 | 2.20 | 2.64 | - | - |
| $100.0^{+}$ | 2.11 | 2.72 | 2.56 | 2.75/17.25 |
| 105.0 | 2.05 | 2.75/19.25 | - | - |
| 110.0 | 2.02 | 2.75/18.75 | 2.72 | - |
| 115.0 | 1.98 | 2.75/18.25 | - | 2.75/16.50 |
| 120.0 | 1.95 | 2.75/18.00 | - | 2.75/16.25 |
| 125.0 | - | - | 2.75/18.50 | - |
| 135.0 | - | - | 2.75/18.00 | - |
| $150.0^{-}$ | - | - | 2.75/17.50 | 2.75/16.00 |
| $150.0^{+}$ | 1.77 | 2.75/17.00 | 1.65 | 2.06 |
| 155.0 | - | - | 1.73 | - |
| 165.0 | 1.67 | 2.75/16.50 | 1.65 | - |
| 185.0 | 1.55 | 2.75/16.00 | 1.57 | 1.87 |
| 205.0 | 1.51 | 2.75/15.50 | 1.48 | - |
| 225.0 | 1.49 | 2.75/7.0 | 1.32 | 1.74 |
| 240.0 | 1.43 | 2.75/6.25 | 1.32 | 1.69 |
| 275.0 | - | - | 1.40 | - |
| 290.0 | - | - | 1.32 | - |
| 300.0 | 1.86 | 1.86 | 1.32 | 1.67 |

Table 6.1 Voltage across capacitor for different levels of compensation (multiple section feeder)

and the current flowing through the bypass switch, for a fault at 75 km. The voltage across capacitor responses for 30% compensation mid-point located capacitor with identical fault position of Figure 6.3(e) are shown in Figure 6.3(g), from which it can be seen that the capacitors do not flashover.

For all cases considered the voltage detected across the healthy phase capacitors were up to 0.5p.u. These voltages could be of significance since a single-phase-to-earth fault could develop, depending on the insulation level, to a phase-to-phase-to-earth fault[64]. This is a very severe fault, not only for system stability, but also because of higher overvoltages produced in the system. Also, when single pole autoreclosure technique is used, clearing any other type of faults besides the single-phase-to-earth faults is undesirable.

## 6.3 Relaying Point Overvoltages

As shown in Chapter 5, low source capacity introduces considerable voltage waveform distortion in the faulted and healthy phases, which is due to the relatively large impedance associated with such source capacity adjacent to the point of observation and being a major point of electrical discontinuity high frequency components are reflected. So, in order to get considerable

waveform distortion, small sending end source capacity of 5 GVA has been particularly considered in this Section. As mentioned previously, in the case of capacitor spark gap operation, a threshold value of 2.75 p.u. is assumed.

### 6.3.1 Single Section Feeder

#### 6.3.1.1 A Capacitor at each end

The mid-point 'a' phase-to-earth fault at voltage maximum with line loading corresponding to about 12° for a line without series compensation induces an overvoltage of 1.21, 1.11 and 1.21 p.u. (where 1 p.u. = 408kV) on 'a', 'b' and 'c' phase respectively (Figure 6.4(a)). Whereas, for identical fault and source conditions for a line with total series compensation of 70% produces an overvoltage of 1.26, 1.16 and 1.16 p.u. on the 'a', 'b' and 'c' phase respectively. The sending end and receiving end capacitor on the faulted phase conductor get shorted out at approximately 4 and 15 ms after fault inception (time $T_2$ and $T_3$ respectively) as shown in Figure 6.4(b). At this point it must be mentioned that the overvoltage generally occurs after a very short period of time following fault inception, and prior to capacitor shorting out (in case of flashover).

Faults not involving earth, say 'a'-'b' phase faults with identical source and fault conditions as

Figure 6.4(b), but without any line loading, induce an overvoltage of 1.225 and 1.07 p.u. on the faulted 'a' and healthy 'c' phase respectively. The receiving end capacitors on the faulted phase conductor flashover at time $T_2$, which is approximately 5 ms after fault inception, whereas the 'a' and 'b' phase sending end capacitor get shorted out at about 7 and 16 ms after fault inception (time $T_3$ and $T_4$ respectively) as shown in Figure 6.5.

Faults at voltage minimum involving 'a' phase-to-earth fault under identical fault and source conditions, as Figure 6.5, is illustrated by Figure 6.6. The receiving end and sending end faulted phase capacitor get shorted out at 7 and 8 ms after fault inception (time $T_3$ and $T_4$ respectively). No significant over-voltage is observed under such conditions.

6.3.1.2 A Capacitor at mid-point

The mid-point, beyond capacitor location 'a' phase-to-earth fault at voltage maximum with line loading corresponding to about 12° for a line with 50% series compensation (single capacitor at the middle) induces an overvoltage of 1.27, 1.1 and 1.2 p.u. on the 'a', 'b' and 'c' phase respectively (Figure 6.7). The faulted phase capacitor flashes over at time $T_2$, which corresponds to 14 ms after fault inception. Comparing

with Figure 6.4(a), which is for an identical source and fault conditionsbut without series compensation, it is observed that the faulted phase overvoltage is more in the compensated case.

The worst tested case from an overvoltage point of view for such feeder configuration is the phase-to-phase fault. Figure 6.8 shows such a case with identical source and fault conditions as Figure 6.5; the faulted phase capacitors get shorted out at approximately 14 ms after fault inception (time $T_2$). The overvoltage on the faulted 'a' and healthy 'c' phase is 1.41 and 1.11 p.u. respectively.

Faults at voltage minimum do not produce any significant overvoltage as shown in Figure 6.9, where the fault and source conditions are identical to Figure 6.6. The faulted phase capacitor flashover at time $T_2$, corresponds to about 8 ms after fault inception.

### 6.3.2 Multi-Section Feeder

#### 6.3.2.1 A Capacitor at each end

The mid-point 'a' phase-to-earth fault at voltage maximum with a line loading corresponding to about 12° without any series compensation on a multi-section feeder does not produce any significant overvoltage (Figure 6.10(a)). Compared with Figure 6.4(a), it can

be seen that the overvoltage on a single section feeder is relatively more. Whereas, for a 70% capacitor compensated case under identical fault and source conditions of Fig 6.10(a), induces a slight overvoltage on the healthy phases (Figure 6.10(b)). For such a case only the receiving end faulted phase capacitor flashover at time $T_2$, which corresponds to approximately 18 ms after fault inception.

Phase-to-phase faults involving 'a' and 'b' phase induce an overvoltage of 1.25 p.u. on the faulted 'a' phase, and 1.10 on the healthy 'c' phase, as shown in Figure 6.11. The receiving end faulted phase capacitors get shorted out at about 16 ms after fault inception (time $T_2$).

Figure 6.12 shows the sending end voltage response for a fault at voltage minimum. No significant overvoltage is observed. The receiving end and sending end faulted phase capacitor gets shorted out at time 8 ms and 10 ms after fault inception (time $T_2$ and $T_3$ respectively).

6.3.2.2 A Capacitor at mid-point

When the capacitor is located at the middle (50% series compensation), for a mid-point beyond capacitor location 'a' phase-to-earth fault at voltage maximum

with line loading corresponding to about 12°, an overvoltage of about 1.17 and 1.11 p.u. is induced on the healthy 'b' and 'c' phase respectively (Figure 6.13). For such fault conditions none of the capacitors flashover.

The worst possible tested case for such feeder arrangement is the 'a'-'b' phase fault, which induces an overvoltage of 1.29 and 1.05 p.u. on the faulted 'a' and healthy 'c' respectively, as shown in Figure 6.14. Again, for this case, none of the capacitors flashover.

Faults at voltage minimum induce an overvoltage of 1.16 p.u. on the healthy 'c' phase, as shown in Figure 6.15. The capacitor on the faulted phase flashover at time $T_2$ which corresponds to about 10.5 ms after fault inception.

All the above studies have been carried out up to a maximum frequency of 2kHz. However, in order to get a true picture of the overvoltage phenomena, it is desirable to go up to very large frequency.

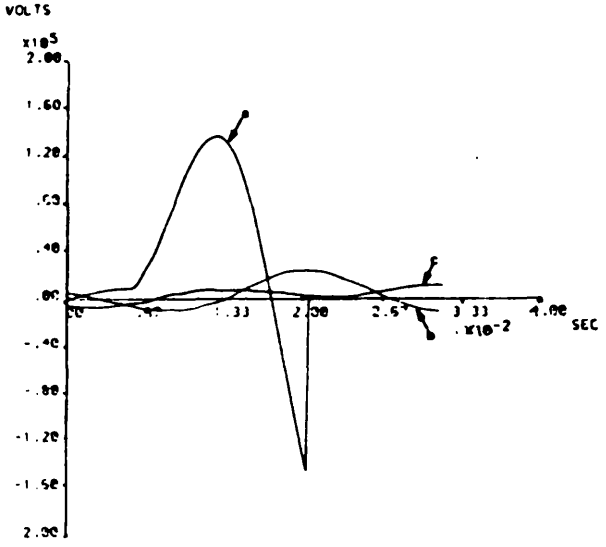


(a)

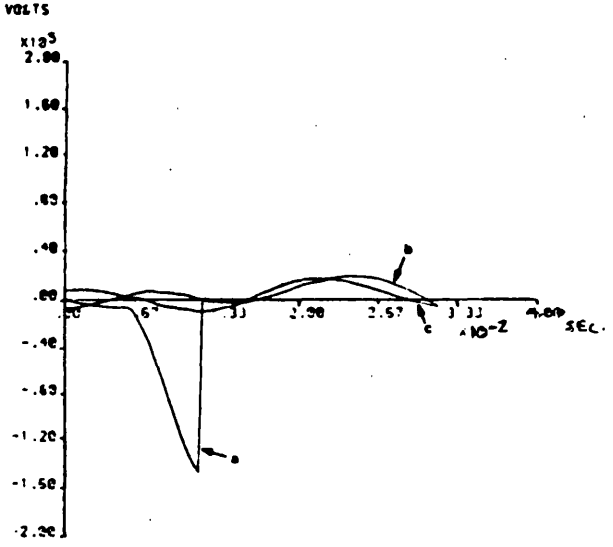


(b)

Figure 6.1(a,b)
Voltages across capacitors (located one at each end) waveforms of single section feeder;
$G_S = G_R = 10GVA$, $S_{cap} = 0.7$,
$x = 165km$, $FT = 5ms$

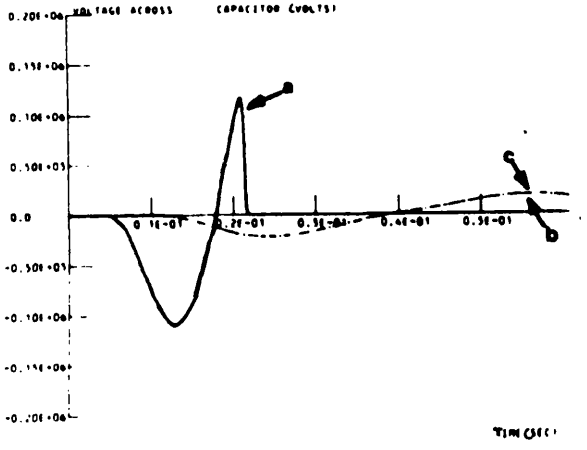

(c)

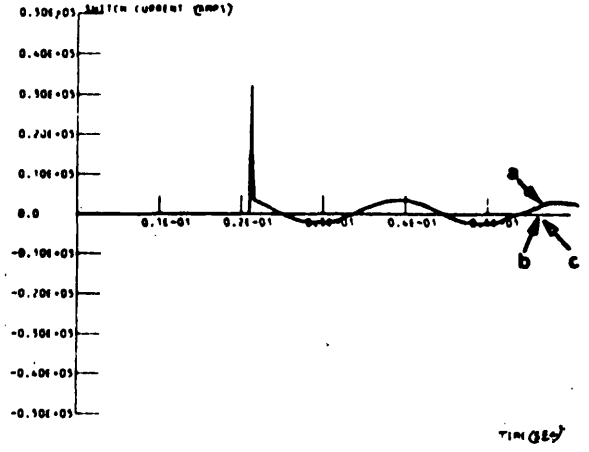

(d)

Figure 6.1(c,d)

Voltage across capacitor (located at mid-point) and current through the bypass switch waveforms of single section feeder;
$G_S = G_R = 10GVA$, $S_{cap} = 0.3$,
$x = 110km$, $FT = 5ms$

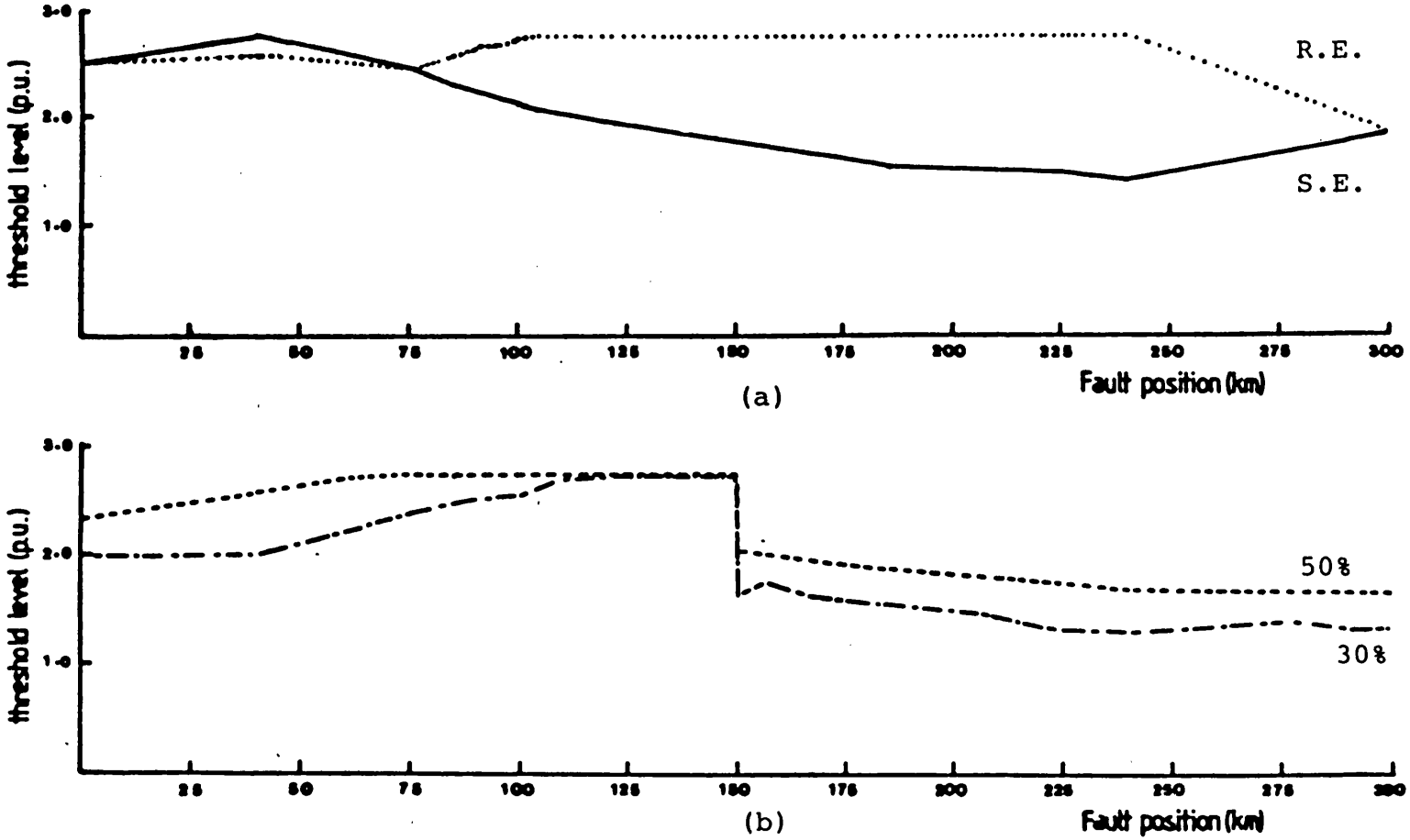


Figure 6.2 Maximum overvoltages across capacitors for multi-section feeder, 'a'-earth fault.

(a) a capacitor at each end (total 70% compensation)

(b) a capacitor at mid-point

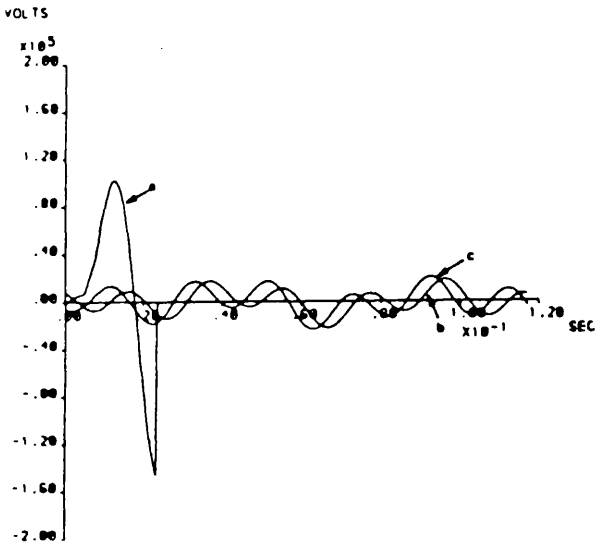


(a)

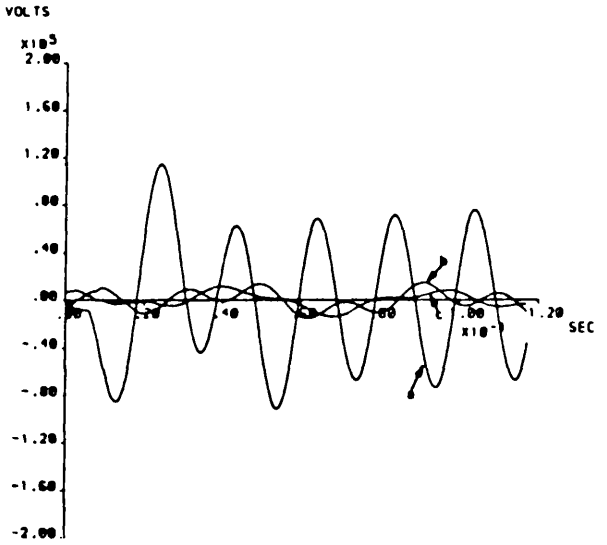


(b)

Figure 6.3(a,b)

Voltages across capacitors (a cap. at each end) waveforms of multisection feeder; $S_{cap}$ = 0.7, x = 40km, FT = 5ms

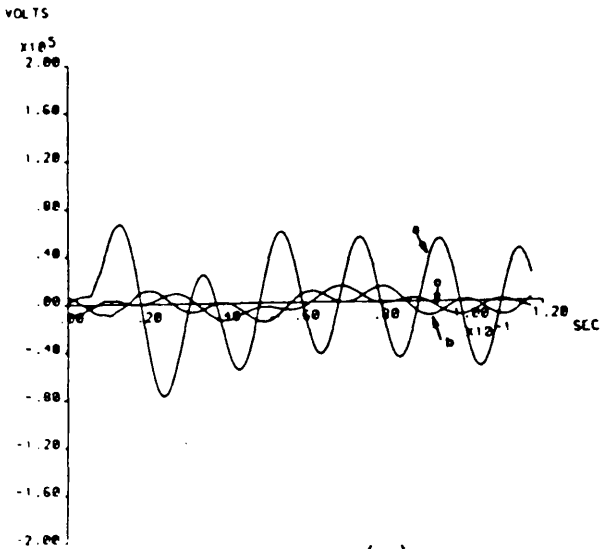


(c)

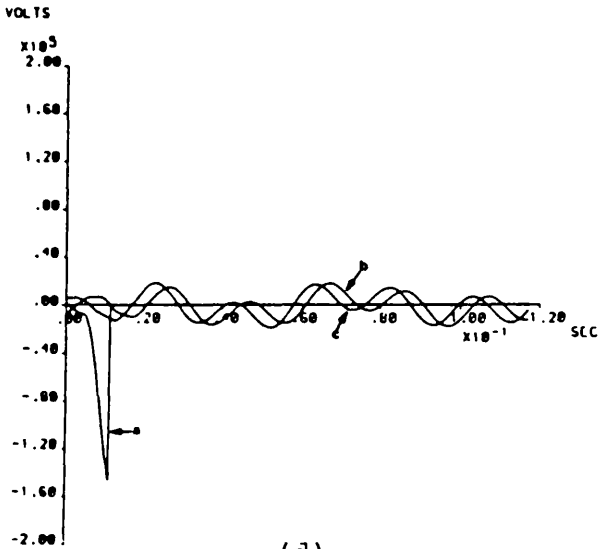


(d)

Figure 6.3(c,d)

Voltage across capacitor (a cap. at each end) waveforms of multisection feeder; $S_{cap}$ = 0.7, x = 240km, FT = 5ms

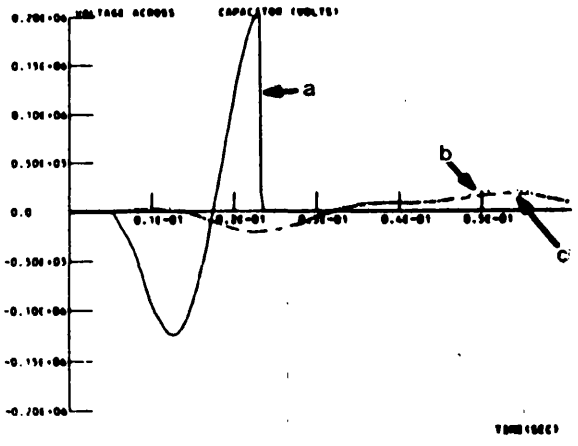


(e)

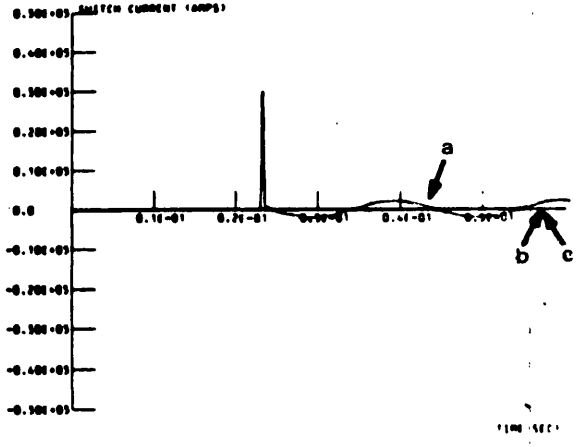


(f)

Figure 6.3(e,f)

Voltage across capacitor (located at mid-point) and current through the bypass switch waveforms of multisection feeder. $S_{cap}$ = 0.5, x = 75km, FT = 5ms.

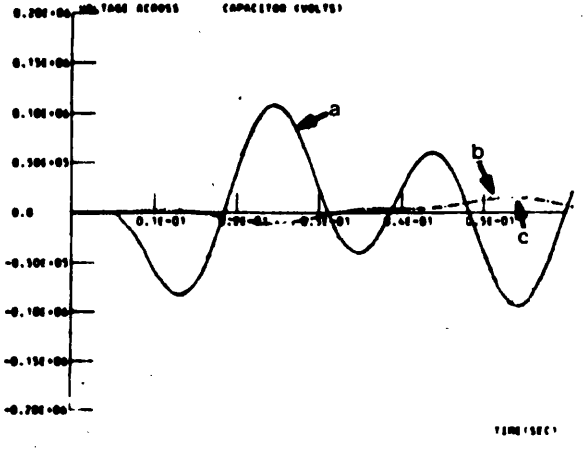


(g)

Figure 6.3(g)

Voltage across capacitor (located at mid-point) waveforms of multi-section feeder. $S_{cap}$ = 0.3, x = 75km, FT = 5ms.

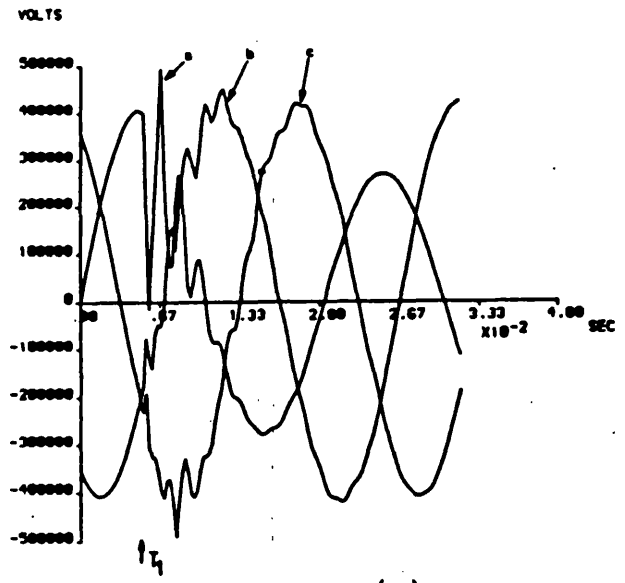


Figure 6.4 System overvoltages at the S.E. of the single section feeder; 'a'-earth fault; x = 150km; $V_S/V_R = \angle 12°$; $G_S$ = 5GVA; $G_R$ = 35GVA; $T_1$ = 4.67ms.

(a) without compensation

(b) with a capacitor at each end, $S_{cap}$ = 0.7, $T_2$ = 9ms, $T_3$ = 20ms.

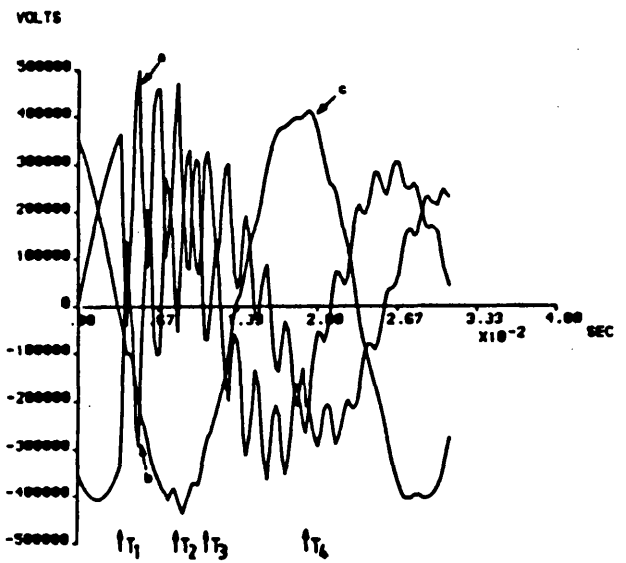


Figure 6.5

Figure 6.5 System overvoltages at the S.E. of the single section feeder; 'a'-'b' phase fault, x = 150km, $V_S/V_R = \angle 0°$; $G_S$ = 5GVA, $G_R$ = 35GVA, $T_1$ = 3.33ms, $T_2$ = 8.33ms, $T_3$ = 10.33ms, $T_4$ = 19.33ms.

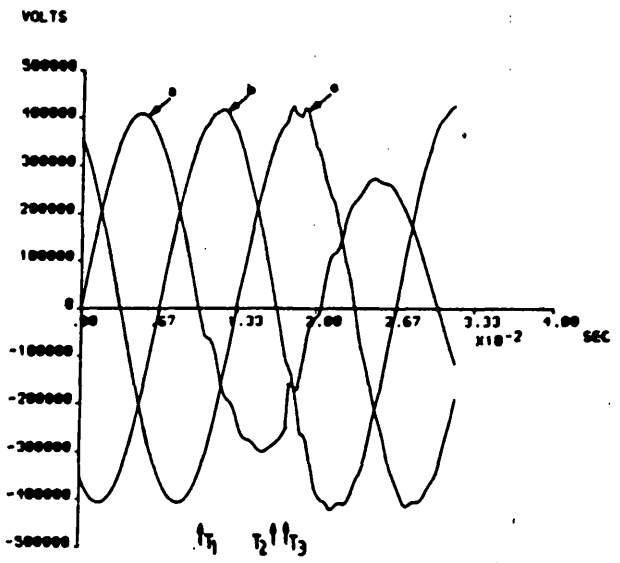


Figure 6.6

Figure 6.6 System overvoltages at the S.E. of the single section feeder; 'a'-earth fault, x = 150km, $V_S/V_R = \angle 0°$, $G_S$ = 5GVA, $G_R$ = 35GVA, $T_1$ = 10ms

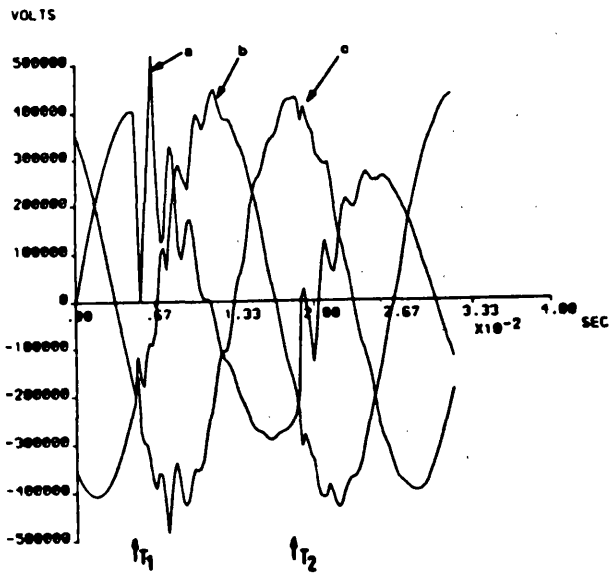


Figure 6.7

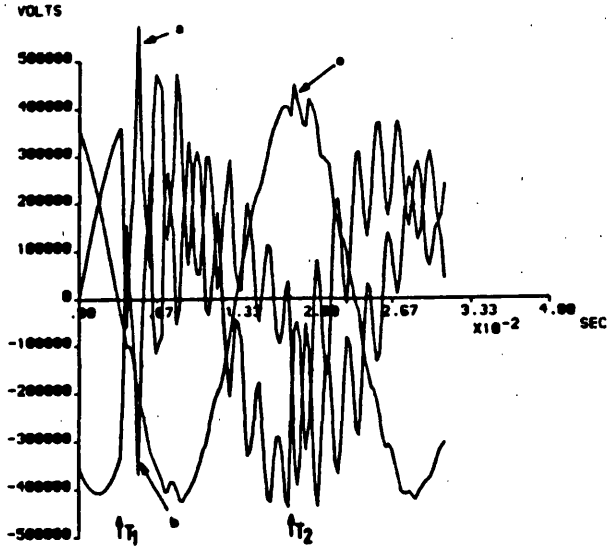


Figure 6.8

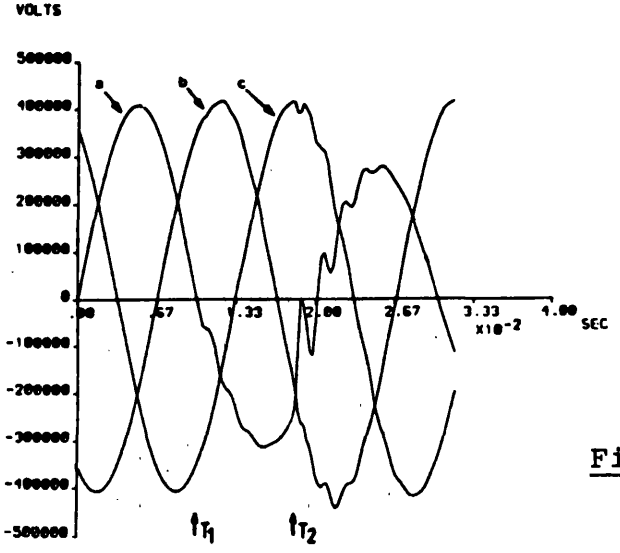


Figure 6.9

Figure 6.7 System over-voltages at the S.E. of the single section feeder with capacitor at mid-point; $S_{cap}$ = 0.5. Fault and source conditions similar to Figure 6.4(b), $T_1$ = 4.67ms, $T_2$ = 18.67ms.

Figure 6.8 System over-voltages at the S.E. of the single section feeder with capacitor at mid-point; $S_{cap}$ = 0.5. Fault and source conditions similar to Figure 6.5, $T_1$ = 3.33ms, $T_2$ = 17.33ms.

Figure 6.9 System over-voltages at the S.E. of the single section feeder with capacitor at mid-point; $S_{cap}$ = 0.5. Fault and source conditions similar to Figure 6.6. $T_1$ = 10ms, $T_2$ = 18ms.

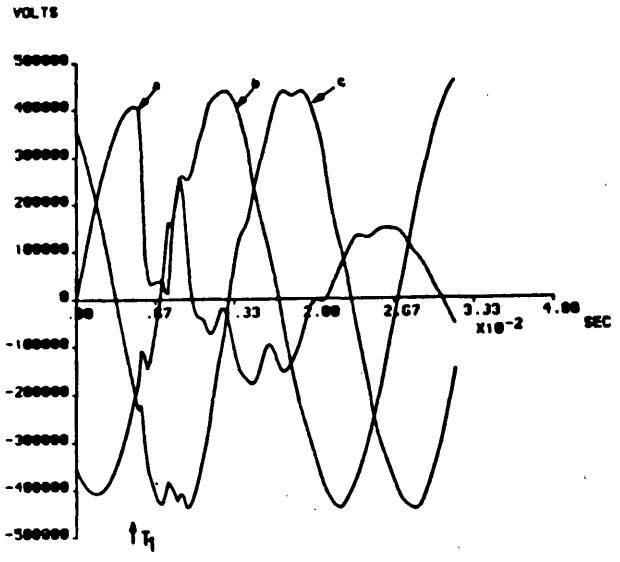


(a)

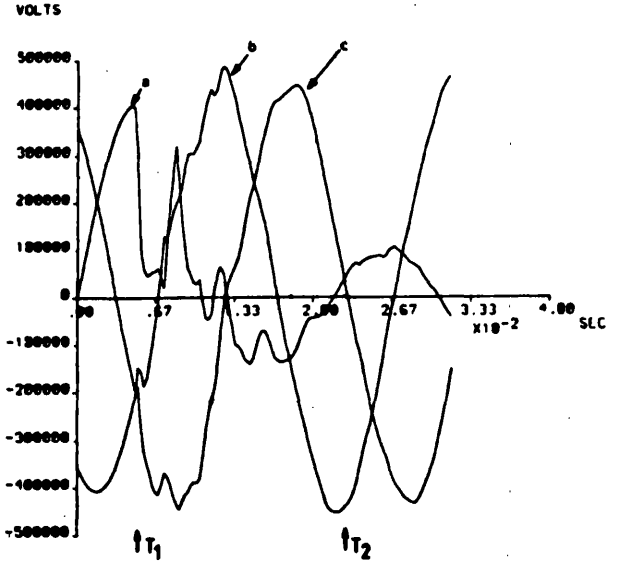


(b)

Figure 6.10(a,b)

System overvoltages at the S.E. of the multi-section feeder. Fault and source conditions similar to Figure 6.4 and Figure 5.16 respectively.

(a) $T_1$ = 4.67ms

(b) $T_1$ = 4.67ms, $T_2$ = 22.67ms

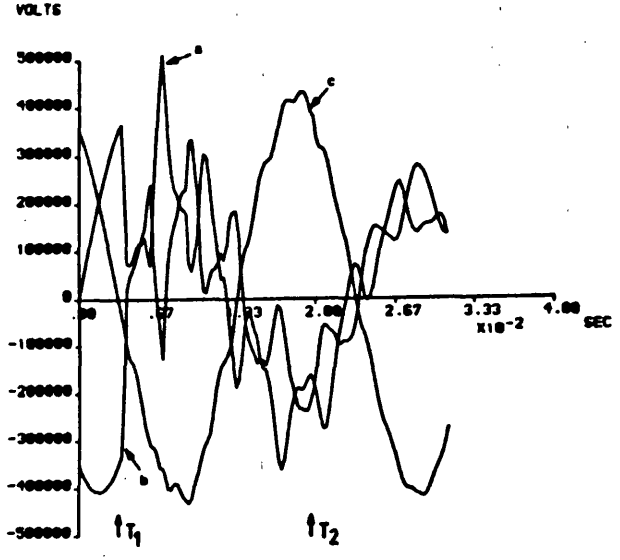


Figure 6.11

Figure 6.11

System overvoltages at the S.E. of the multi-section feeder. Fault and source conditions similar to Figure 6.5 and Figure 5.16 respectively. $T_1$ = 3.33ms, $T_2$ = 19.33ms.

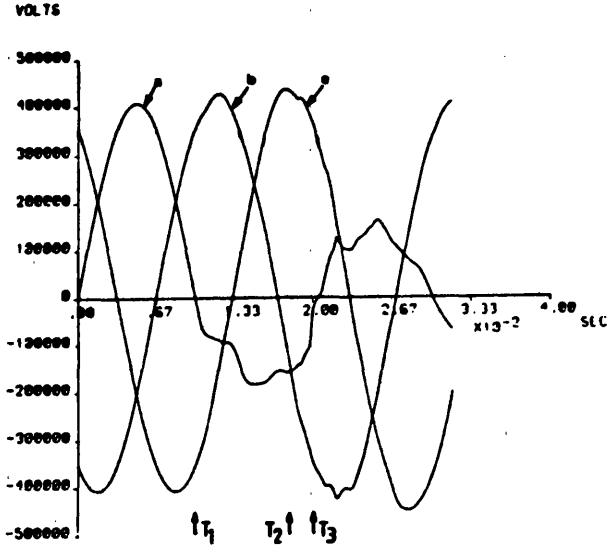


Figure 6.12

Figure 6.12

System overvoltages at the S.E. of the multi-section feeder. Fault and source conditions similar to Figure 6.6 and Figure 5.16 respectively. $T_1$ = 10ms, $T_2$ = 18ms, $T_3$ = 20ms.

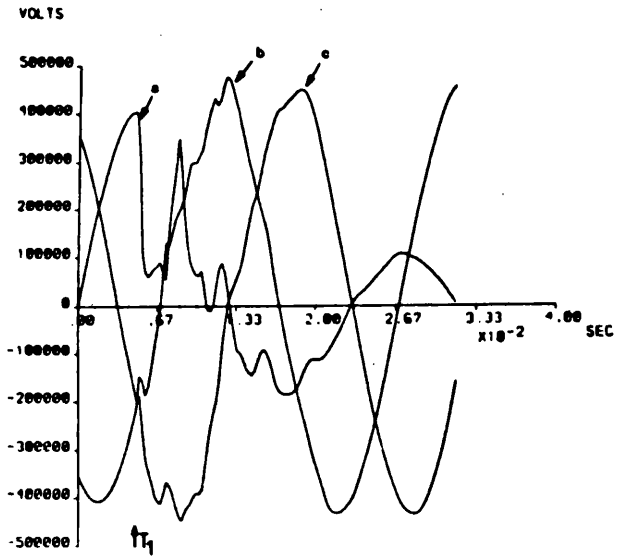


Figure 6.13

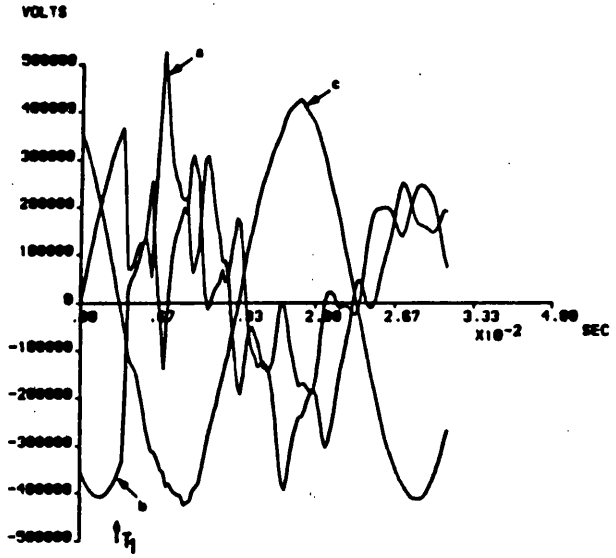


Figure 6.14

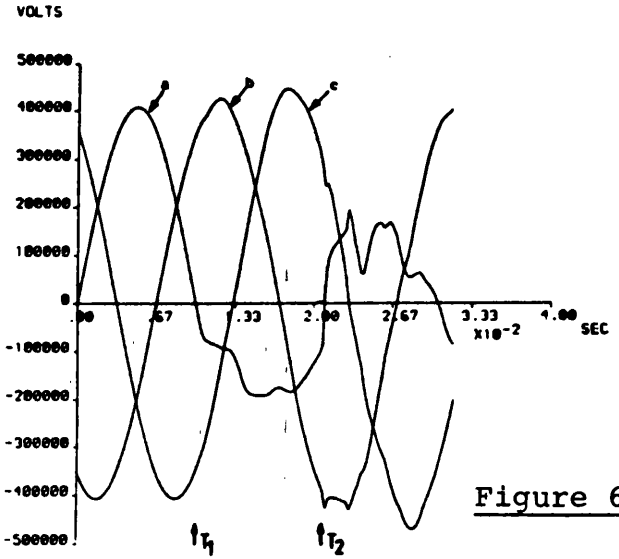


Figure 6.15

Figure 6.13 System over-voltages at the S.E. of the multi-section feeder. Fault and source conditions similar to Figure 6.7 and Figure 5.16 respectively, $T_1$ = 4.67ms.

Figure 6.14 System over-voltages at the S.E. of the multi-section feeder. Fault and source conditions similar to Figure 6.8 and Figure 5.16 respectively, $T_1$ = 3.33ms.

Figure 6.15 System over-voltages at the S.E. of the multi-section feeder. Fault and source conditions similar to Figure 6.9 and Figure 5.16 respectively, $T_1$ = 10ms, $T_2$ = 20.5ms.

# CHAPTER 7 EVALUATION OF THE PRIMARY SYSTEM WAVEFORMS ASSOCIATED WITH SINGLE POLE AUTORECLOSURE SEQUENCES

## 7.1 Introduction

The most common faults encountered on e.h.v. a.c. transmission lines are of the single-phase-to-earth type and the majority of these are transitory in nature[63]. Single pole autoreclosure sequences which involve opening and reclosing only the faulted phase can be used to clear such faults, especially on long line applications. The majority of work reported so far has been primarily concerned with the application of such techniques to long lines having shunt compensation only[65,66], and not much has been reported on single pole autoreclosure techniques as applied to series compensated (or combined series/shunt compensated) lines. In this respect, it must be mentioned that in the latter case, apart from the primary system waveforms being affected by the various discontinuities introduced by the operation of the capacitor protection equipment to short out the capacitor/capacitors (in the majority of cases this sequence occurs before the line protection relay operating times), there are also the additional discontinuities introduced by the various autoreclosure sequences (which can further affect the waveforms) during a complete cycle of events, and the implications of incorrect operation of line

protection at any time throughout the process of fault clearance can often be quite serious. It was in the light of this that it was decided to develop frequency domain methods for simulating the complete fault clearance sequences for a series compensated line, and a few of these results are presented in this Chapter.

In most practical systems, the total time taken for the line breaker poles to open on the faulted phase is about 4 to 5 cycles after fault inception, and a dead time of about 20 to 25 cycles is generally required before a successful reclosure of these breakers can take place; primarily to allow sufficient time for the current in the fault path to deionise. The studies have indicated that in the majority of cases the capacitor spark gaps operate within a cycle of fault inception and during the dead time interval, the air across the protective spark gap also deionises and regains its flashover voltage withstand strength. The capacitor bypass breaker is automatically reopened within the dead time interval, which means that the capacitor is in full service well before the line breaker autoreclosure sequence[67]. In the case of an unsuccessful autoreclosure, as for example for a sustained fault, the aforementioned sequences are repeated and the line breakers permanently lock out.

The digital techniques developed here for simulating the single pole autoreclosure techniques as applied to a series compensated line with shunt reactors are quite flexible, in that they can be used to provide realistic fault waveforms for a variety of conditions, eg different autoreclosure dead time, etc. In this respect, the number of possible times between the initial fault inception and all the steps throughout the whole fault clearance process is extremely large, but in order to simply illustrate some typical applications studies, the results presented here are confined to:

(i) Overall relay operating time of 1 cycle for both ends.

(ii) An arbitrary fault break-off time of about 1 cycle (which does not necessarily ensure secondary arc extinction) after breaker contact separation.

(iii) Simulating reclosure of sending end and receiving end breakers after fault of about 4 cycles.

(iv) Minimum value of voltage across capacitor for spark gap operation of 2.75 p.u.

The mathematical analysis and the simulation technique developed for applying single pole autoreclosure

techniques to series compensated lines have already been discussed in Chapter 3. In this Chapter, the primary system waveforms for systems employing such techniques are presented for both a single and multi-section feeder, as shown in Figures 2.7 and 2.8. Both systems employ four reactor shunt compensation schemes where $h_1 = 0.75$ and $h_0 = 0.674$.

## 7.2 Single Section Feeder

### 7.2.1 A Capacitor at Each End

Figure 7.1 shows a fault transient sequence following a mid-point 'a' phase-to-earth fault at voltage maximum for a line with a total series compensation of 70%. It can be seen from the faulted phase voltages of Figures 7.1 (a,c) that during the initial post-fault period the transit time is approximately 1ms, corresponding to an aerial mode velocity of 292 km/ms. Both the capacitors on the faulted phase conductor get shorted out almost simultaneously at approximately 8 ms (time $T_2$) after fault inception. This is evident from Figures 7.1(e,f) which show the voltage across the two faulted phase capacitors. The shorting out of the capacitors produces a slight distortion in the faulted phase relaying point voltage waveforms (Figures 7.1(a,c)). As expected, relaying point currents in the faulted phase increase sharply in magnitude on fault inception

and rings down slightly following the shorting out of the capacitors before being interrupted at $T_3$, which is approximately 10 ms (for both the ends) after the breaker contact separation time (Figures 7.1 (b,d)). The sound phase currents remain small in magnitude on opening of the line breaker poles, high frequency transients are set up particularly on the faulted phase voltages, and these gradually ring down until fault break-off at $T_4$ (Figures 7.1 (a,c)). The fault break-off time $T_4$ is about 2½ cycles after fault inception. Thereafter, a near power frequency voltage of peak value of about 66 kV is induced in the faulted phase due to the capacitive and inductive coupling with the healthy phases.

The reinsertion of the capacitors at time $T_5$, which is about 3½ cycles after fault inception, does not produce any significant changes in the relaying point voltages and currents, both for the sending end and the receiving end (Figures 7.1 (a-d)). However, a small amount of voltage develops across the capacitor on the now isolated conductor, as shown by Figures 7.1 (e,f), due to the coupling effects between the isolated and the energised conductors.

The line breakers are reclosed similarly at time $T_6$, which is about 4 cycles after fault inception.

This sequence produces small overvoltages which are quickly damped as shown in Figures 7.1 (a,c). As regards the currents, this sequence results into a significant amount of high frequency reclosing transients (Figures 7.1 (b,d)), and so far as the capacitor voltages are concerned almost normal steady state voltage across all the six capacitors is observed (Figures 7.1 (e,f)).

7.2.2 A Capacitor at Mid-point

Figure 7.2 shows a typical fault transient sequence simulation involving 'a' phase-to-earth fault at the receiving end near peak fault voltage, with a series compensation of 50%. In this case, the effect of the electromagnetic coupling between the faulted and healthy phases is evident during the initial post-fault period as the faulted phase relaying point current induces a voltage in the healthy phases and this causes a significantly large current to flow in antiphase with the faulted phase current particularly at the sending end relaying point current, as shown in Figure 7.2(b). At the receiving end, because the fault is close to the point of obvservation, the coupling is relatively small and hence the magnitude of the sound phase current is small as shown by Figure 7.2(d). As expected, the receiving end relaying point current reaches a peak value of about 17 kA (Figure 7.2(c)), and this can be

verified to be about correct from a knowledge of the system peak voltage (≅ 408 kV) and the receiving end source impedance $Z_{R1}$ of about 25 ohms.

The faulted phase capacitor flashes over at a time $T_2$, which is about 16 ms after fault inception as shown by Figure 7.2(e). This sequence introduces a small amount of distortion in the faulted phase sending end relaying point voltage. The voltage across the healthy phase capacitors is relatively large and in phase with one another. As the faulted phase receiving end relaying point voltage has collapsed to zero on fault inception, the shorting out of the capacitor has no effect on it. The faulted phase currents at the two ends, especially at the sending end, ring down following capacitor flashover and, similar to the study in Section 7.2.1, are interrupted at approximately 10 ms after breaker contact separation time (Figures 7.2 (a,c)) and the faulted phase voltage at the sending end rings down until fault break-off. On current interruption the voltage across the healthy phase capacitor rings down.

The fault break-off and capacitor reinsertion are at about 52 ms and 75 ms respectively after fault inception. The fault break-off has little effect on the relaying point currents, whereas a near power frequency voltage of peak value of about 55 kV is induced

in the isolated conductor at both the ends (Figures 7.2 (a-d)). However, capacitor reinsertion has very little effect on the relaying point voltage and current waveforms.

The reclosing transient produced both on voltages and currents is similar to those in Figure 7.1.

## 7.3 Multi-Section Feeder (Complex Source)

### 7.3.1 A Capacitor at Each End

Figure 7.3 shows results for a typical fault transient sequence following a mid-point 'a' phase-to-earth fault at voltage maximum. As compared with Figure 7.1 (and also shown in Chapter 5), the post-fault waveforms associated with the multi-section feeder are more distorted and the lower frequency transients persist for a longer period than those in the single section feeder. As mentioned previously, this is because the travelling waves generated on fault inception have to travel rather a long distance through different infeeding line sections before being partially reflected towards the observation points from the electrical discontinuities associated with the various infeeds.

With reference to the voltage waveforms at the sending end relaying point S (Figure 7.3(a)), it can be

seen that during the initial post-fault period there are effectively two transit times involved, one associated with the distance S-F-S, and the other with distance S-$G_S$-S, these being approximately 1 ms and 2 ms respectively. The voltages across all six capacitors are scanned and the one to reach a pre-determined threshold value of about 2.75 p.u. is shorted out first. In this particular case, the faulted phase receiving end capacitor is the first to be shorted out at time $T_2$ which is 17ms after fault inception, as shown by Figures 7.3 (e,f), whereas the faulted phase sending end capacitor remains in the circuit. It can be seen that this scheme is quite different from an identical study involving a simple source model (Figure 7.1), where both the faulted phase capacitors get shorted out almost simultaneously. The shorting out of the capacitor produces a slight distortion in the relaying point voltage waveform, particularly at the receiving end as shown by Figure 7.3(c). This is more pronounced than the case for a simple source model. The relaying point currents in the faulted phases again ring down slightly before being interrupted at approximately 8 ms after breaker contact separation time, and on current interruption the faulted phase voltages ring down until fault breaks off at time $T_4$, which is about 65 ms after fault inception (Figures 7.3 (a-d)). In this case, comparing Figures 7.3 (a) and (c) it can be seen that

the sending end faulted phase voltage rings down to almost a steady d.c. level, whereas the receiving end voltage to almost zero level. As in the simple source case, the fault break-off again causes a near sine wave voltage (at power frequency) being induced in the isolated conductor due to the coupling effects, and one interesting point to note here is that the range of this voltage is about 160 kV peak, compared with about 66 kV for an identical study in the simple source model.

The reinsertion of series capacitor does not significantly affect the waveforms, but the line breaker reclosures, however, do produce small overvoltages of 1.2 p.u. and 1.14 p.u. at the sending end and receiving end respectively.

### 7.3.2 A Capacitor at Mid-Point

Figure 7.4 shows the system response following single-phase-to-earth fault at the receiving end again near voltage maximum. Many of the features associated with the previously considered fault study (Figure 7.3) are again observed. The transit time between the fault and source discontinuities varies with fault position and it follows that the apparent frequency of the superimposed travelling wave decreases as the fault is further away from the point of observation as shown

before. From Figure 7.4(a), which is the sending end relaying point voltage waveform, it is evident that during the initial post-fault period there are again effectively two transit times involved, one associated with the distance S-F-S (Figure 2.8) and the other with the distance S-$G_S$-S, these being 2 ms each. In this case the capacitors do not flashover as shown by Figure 7.4(e), but the voltage across the healthy phase capacitor is large and in phase with one another, similar to the simple source model. The relaying point current is interrupted just after line breaker contact separation time, thereafter the faulted phase voltage again rings down until fault break-off at about 65 ms after fault inception (Figures 7.4 (a-d)).

On fault break-off, the induced voltages in the faulted phase due to coupling effects causes a near sine wave voltage and, as in Section 7.3.3, the range of the voltage is about 145 kV as compared to about 55 kV for identical simple source model study. The opening of the breakers reduces the voltage across the capacitors, whereas on line reclosures the voltage across the faulted phase capacitor reaches to about 2 p.u.

Fig. 7.1

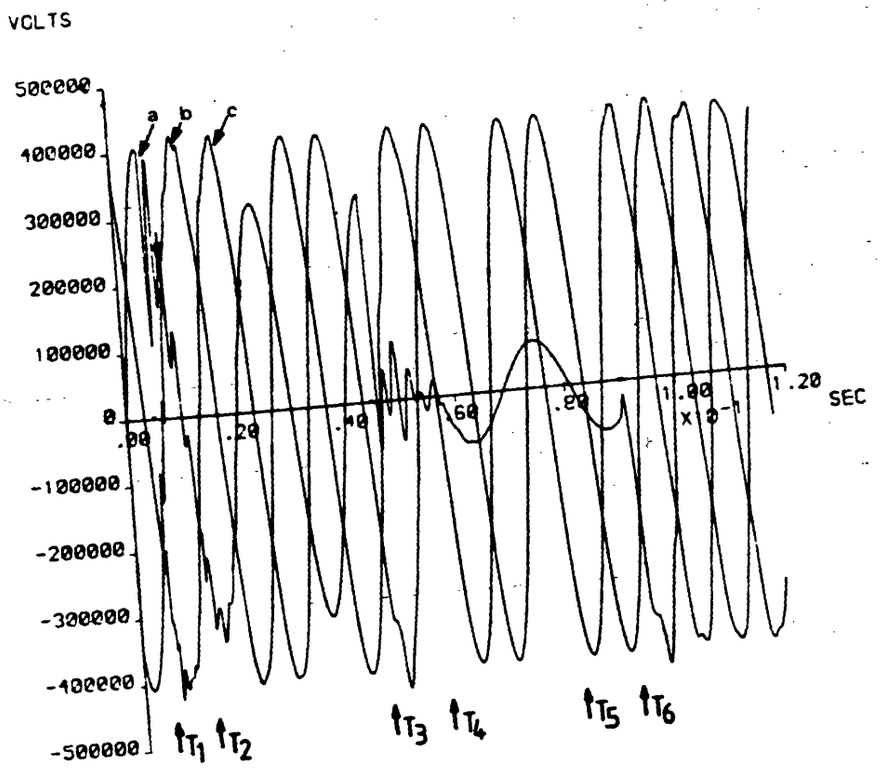
VOLTS
500000
400000
300000
200000
100000
0
-100000
-200000
-300000
-400000
-500000
a
b
c
.00
.20
.40
.60
.80
1.00
1.20
SEC
X 10-1
T1
T2
T3
T4
T5
T6

(a)

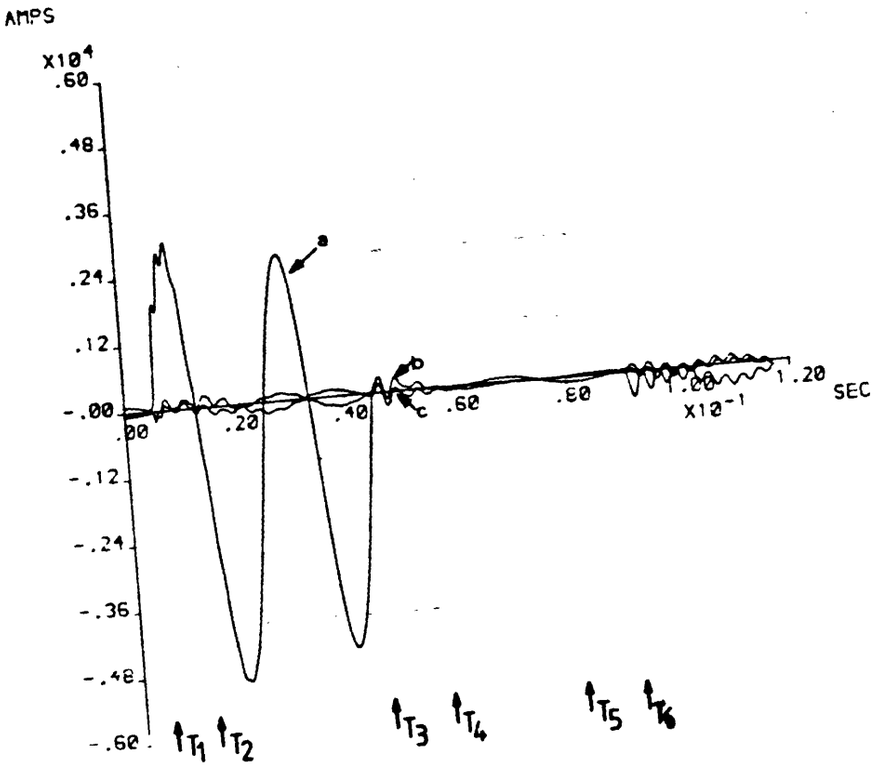
AMPS
X10^4
.60
.48
.36
.24
.12
-.00
-.12
-.24
-.36
-.48
-.60
a
b
c
.00
.20
.40
.60
.80
1.00
1.20
SEC
X10-1
T1
T2
T3
T4
T5
T6

(b)

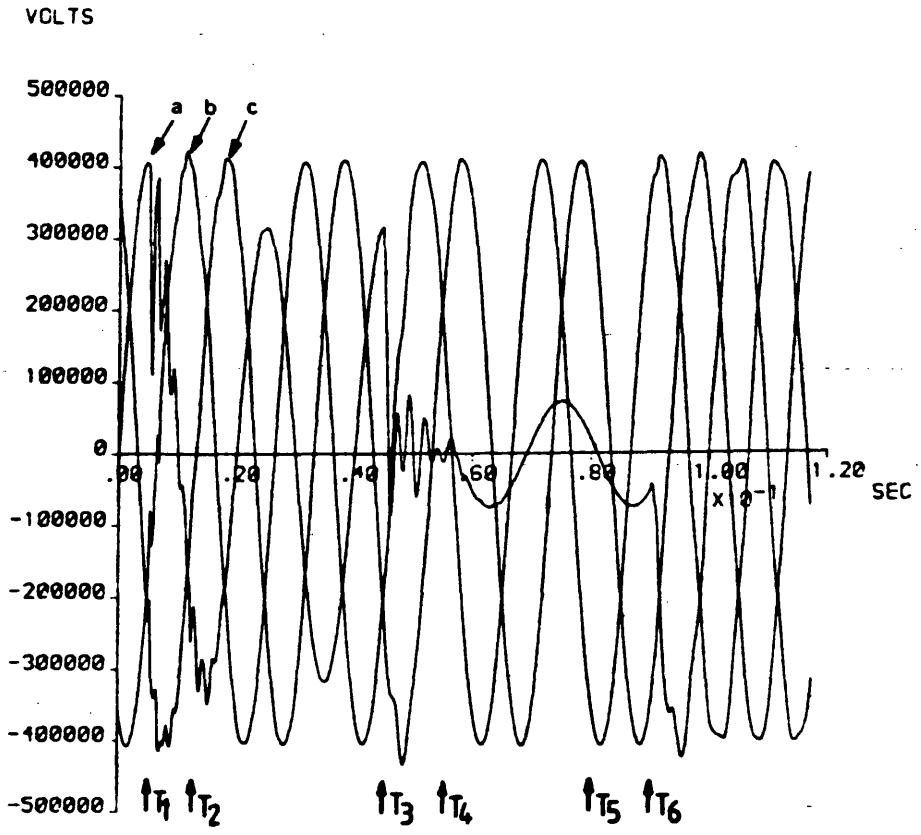
VOLTS
500000
400000
300000
200000
100000
0
-100000
-200000
-300000
-400000
-500000
a
b
c
.00
.20
.40
.60
.80
1.00
1.20
X10-1
SEC
T1
T2
T3
T4
T5
T6

(c)

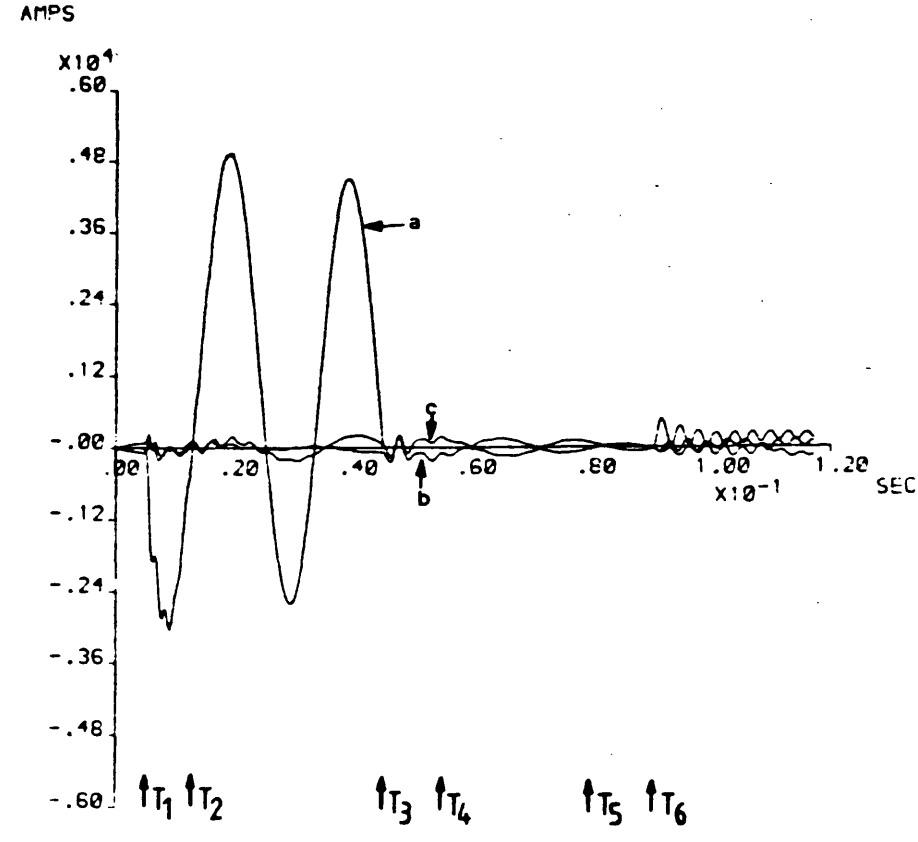
AMPS
X10⁴
.60
.48
.36
.24
.12
-.00
-.12
-.24
-.36
-.48
-.60
a
b
c
.00
.20
.40
.60
.80
1.00
1.20
X10-1
SEC
T1
T2
T3
T4
T5
T6

(d)

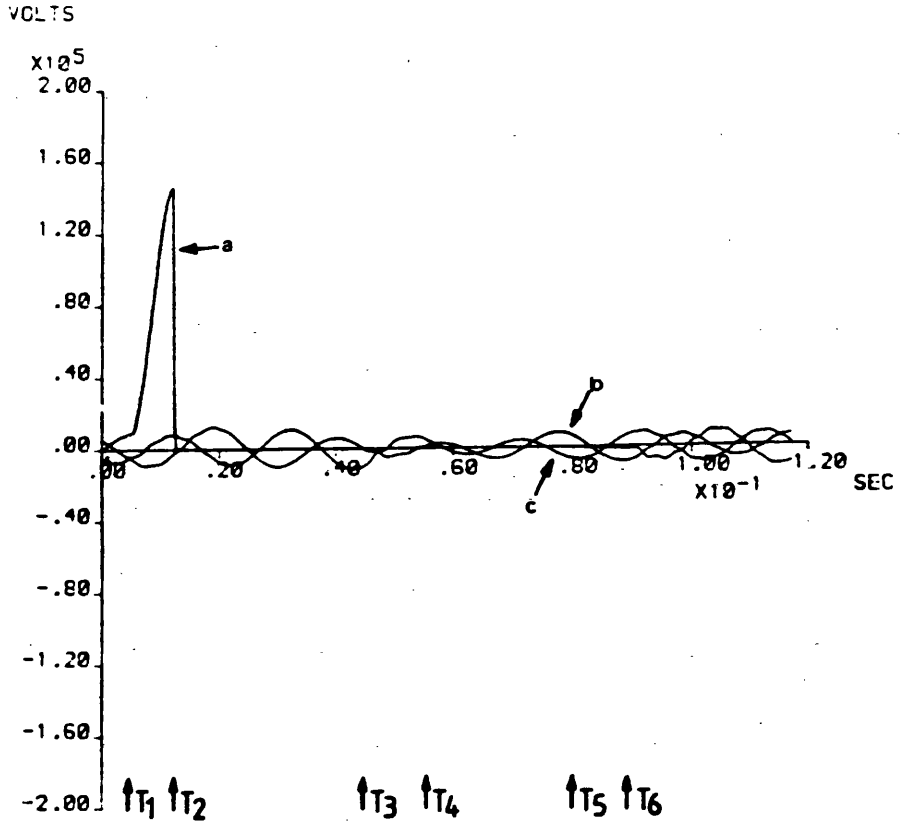
VOLTS
X10^5
2.00
1.60
1.20
.80
.40
.00
-.40
-.80
-1.20
-1.60
-2.00
a
b
c
.00
.20
.40
.60
.80
1.00
1.20
X10^-1
SEC
T1 T2
T3 T4
T5 T6

(e)

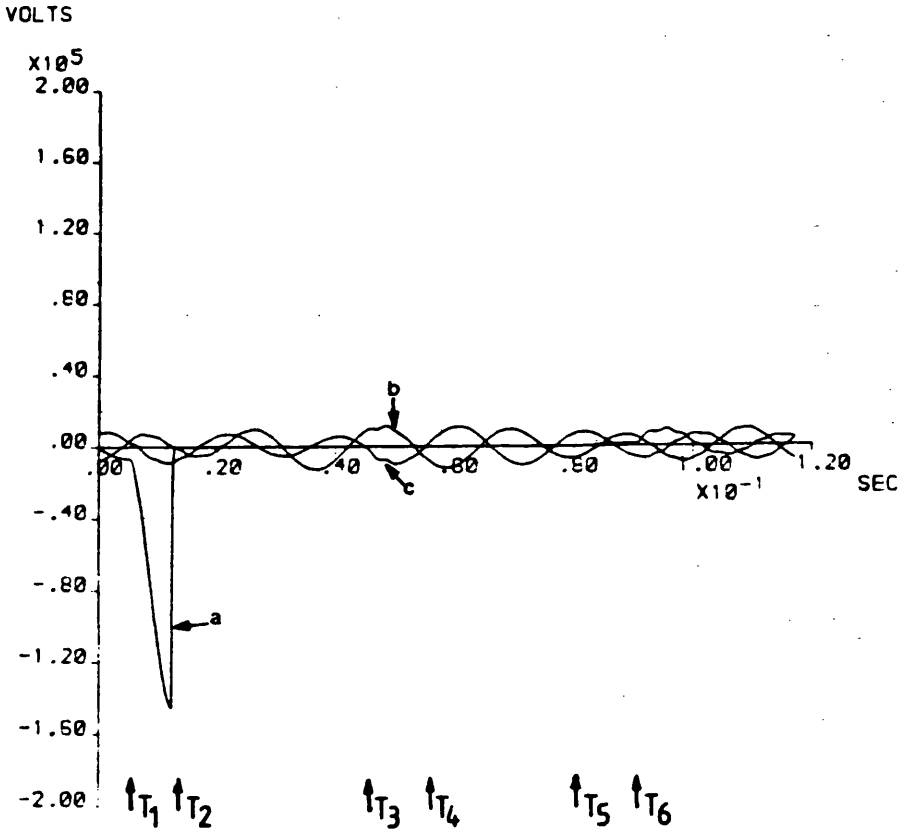
VOLTS
X10^5
2.00
1.60
1.20
.80
.40
.00
-.40
-.80
-1.20
-1.60
-2.00
b
c
a
.00
.20
.40
.60
.80
1.00
1.20
X10^-1
SEC
T1 T2
T3 T4
T5 T6

(f)

Figure 7.1

Mid-point 'a'-earth fault (x = 150km); Single section feeder. Source conditions similar to Figure 5.2.A Capacitor at each end. $S_{cap}$ = 0.7, $h_1$ = 0.75, $h_0$ = 0.674; $T_1$ = fault inception (5ms); $T_2$ = 'a'-phase S.E. and R.E. capacitors flashes over (13ms); $T_3$ = 'a'-phase breaker poles separate (45ms); $T_4$ = fault break-off (55ms); $T_5$ = 'a'-phase S.E. and R.E. capacitors reinsert (80ms); $T_6$ = 'a'-phase breaker poles reclose (90ms).

(a) Voltages on line side of breaker at end S.
(b) Line currents at end S.
(c) Voltages on line side of breaker at end R.
(d) Line currents at end R.
(e) Voltages across S-end capacitors.
(f) Voltages across R-end capacitors.

Fig. 7.2

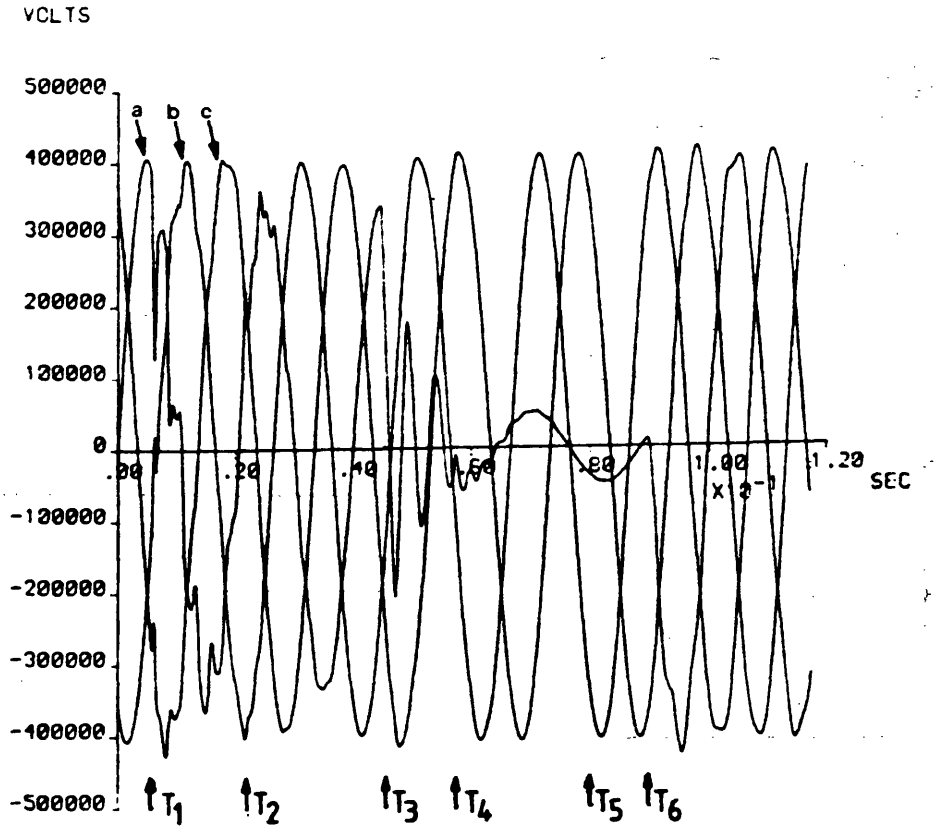
VOLTS
500000
400000
300000
200000
120000
0
-120000
-200000
-300000
-400000
-500000
a
b
c
.00
.20
.40
.60
.80
1.00
1.20
SEC
$T_1$
$T_2$
$T_3$
$T_4$
$T_5$
$T_6$

(a)

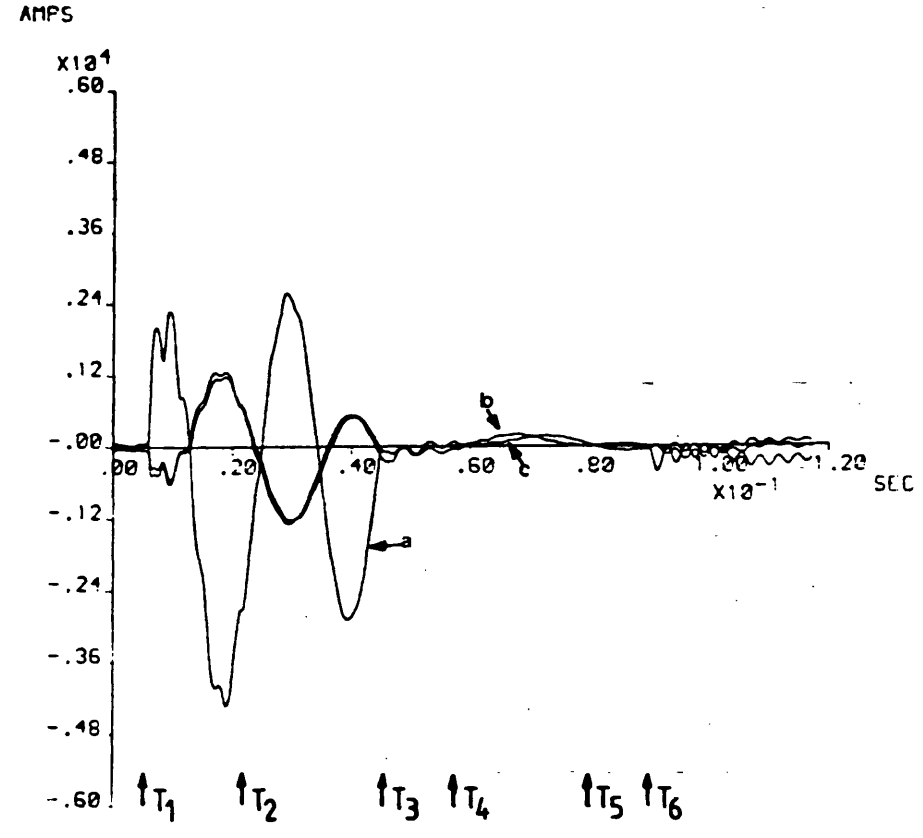
AMPS
X10⁴
.60
.48
.36
.24
.12
-.00
-.12
-.24
-.36
-.48
-.60
a
b
c
.00
.20
.40
.60
.80
1.00
1.20
X10⁻¹
SEC
$T_1$
$T_2$
$T_3$
$T_4$
$T_5$
$T_6$

(b)

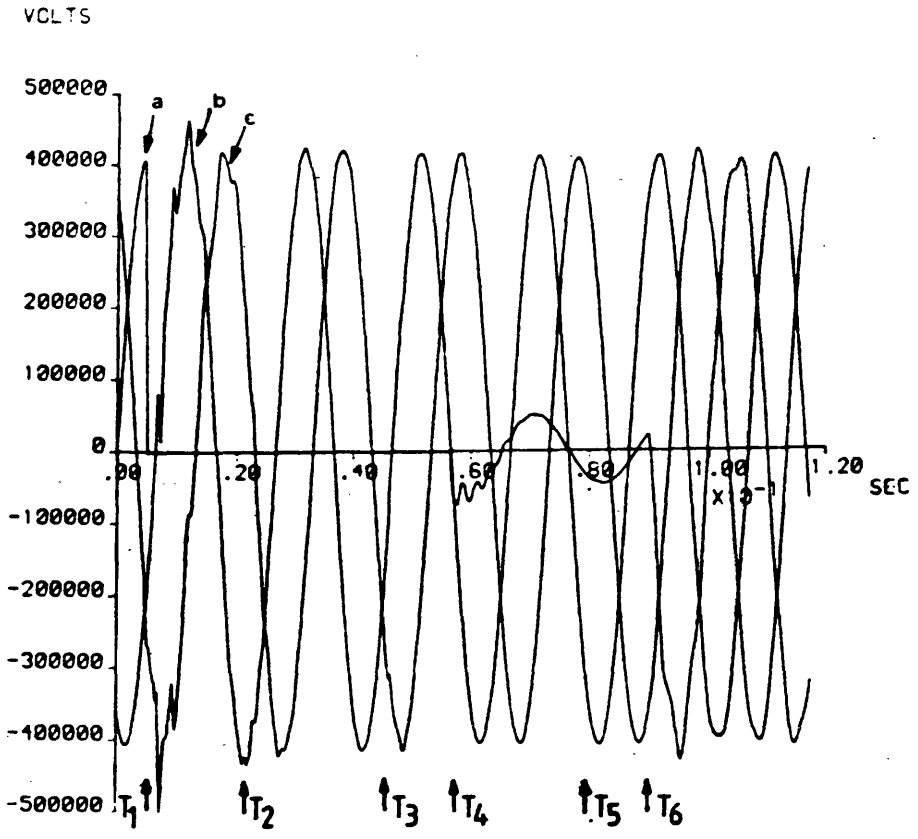
VOLTS
500000
400000
300000
200000
100000
0
-100000
-200000
-300000
-400000
-500000
a
b
c
.00
.20
.40
.60
.80
1.00
1.20
SEC
$T_1$
$T_2$
$T_3$
$T_4$
$T_5$
$T_6$

(c)

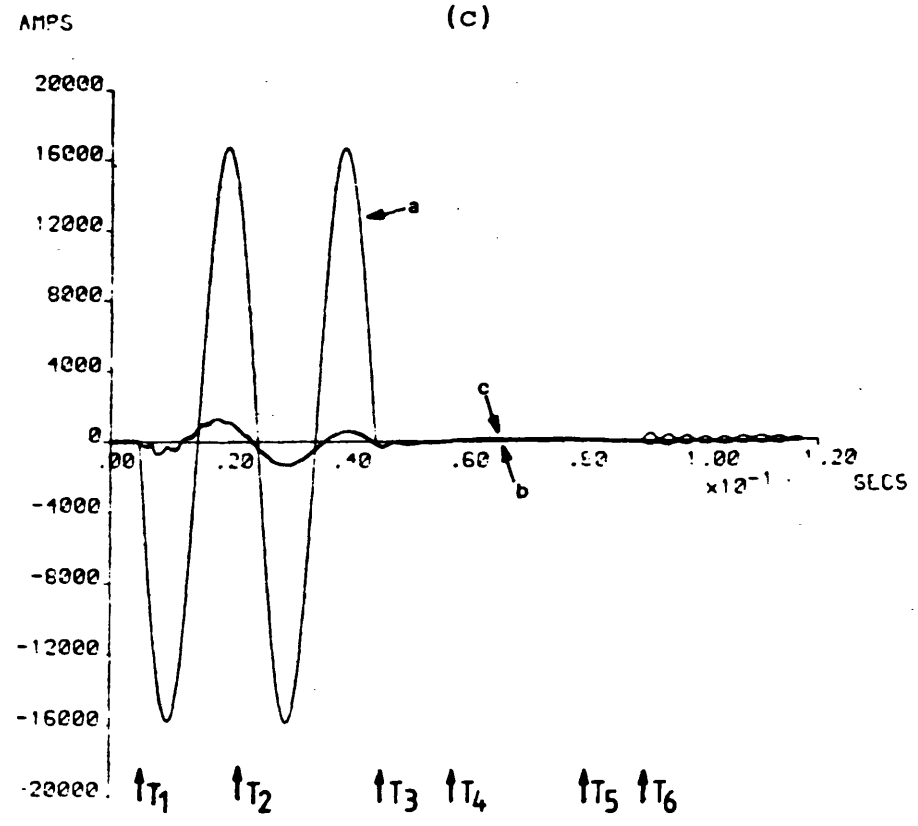
AMPS
20000
16000
12000
8000
4000
0
-4000
-8000
-12000
-16000
-20000
a
b
c
.00
.20
.40
.60
1.00
1.20
SECS
$T_1$
$T_2$
$T_3$
$T_4$
$T_5$
$T_6$

(d)

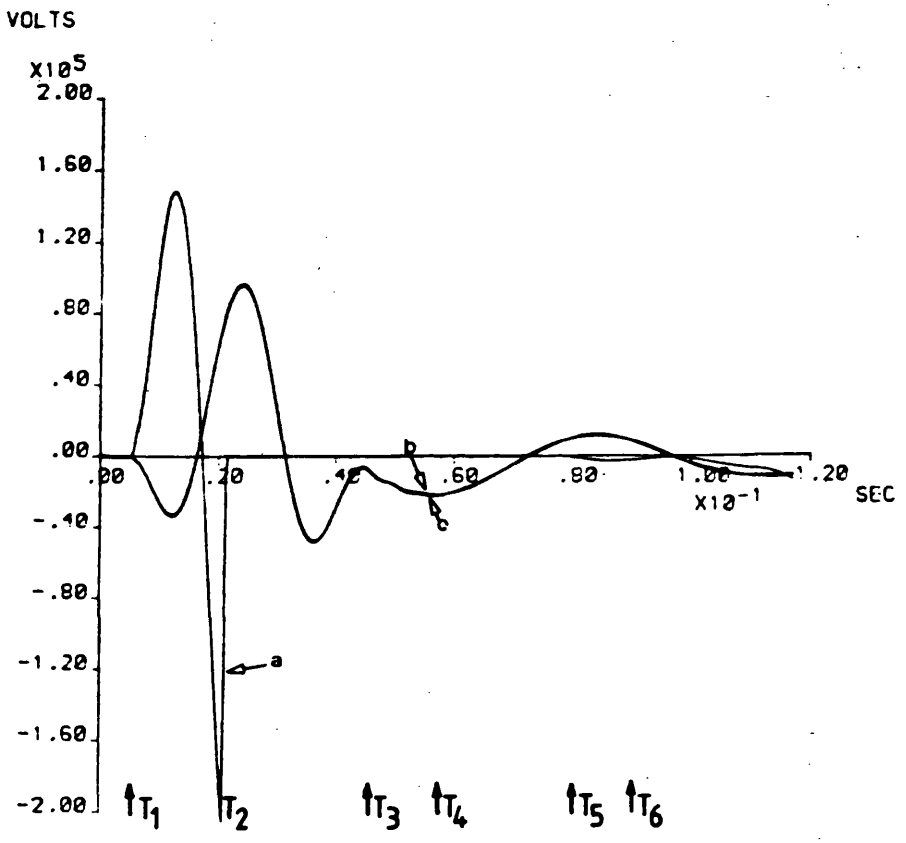
VOLTS
X10^5
2.00
1.60
1.20
.80
.40
.00
-.40
-.80
-1.20
-1.60
-2.00
.00
.20
.60
.80
1.20
X10^-1
SEC
a
b
c
T1
T2
T3
T4
T5
T6

(e)

Figure 7.2

'a'-earth remote-end fault (x = 300km); Single section feeder; source conditions similar to Figure 5.2. A Capacitor at mid-point. $S_{cap}$ = 0.5, $h_1$ = 0.75, $h_0$ = 0.674; $T_1$ = fault inception (5ms); $T_2$ = 'a'-phase capacitor flashes over (21ms); $T_3$ = 'a'-phase breaker poles separate (45ms); $T_4$ = fault break-off (57ms); $T_5$ = 'a'-phase capacitor reinsert (80ms); $T_6$ = 'a'-phase breaker poles reclose (90ms).

(a) Voltages on line side of breaker at end S.
(b) Line currents at end S.
(c) Voltages on line side of breaker at end R.
(d) Line currents at end R.
(e) Voltages across capacitors.

Fig. 7.3

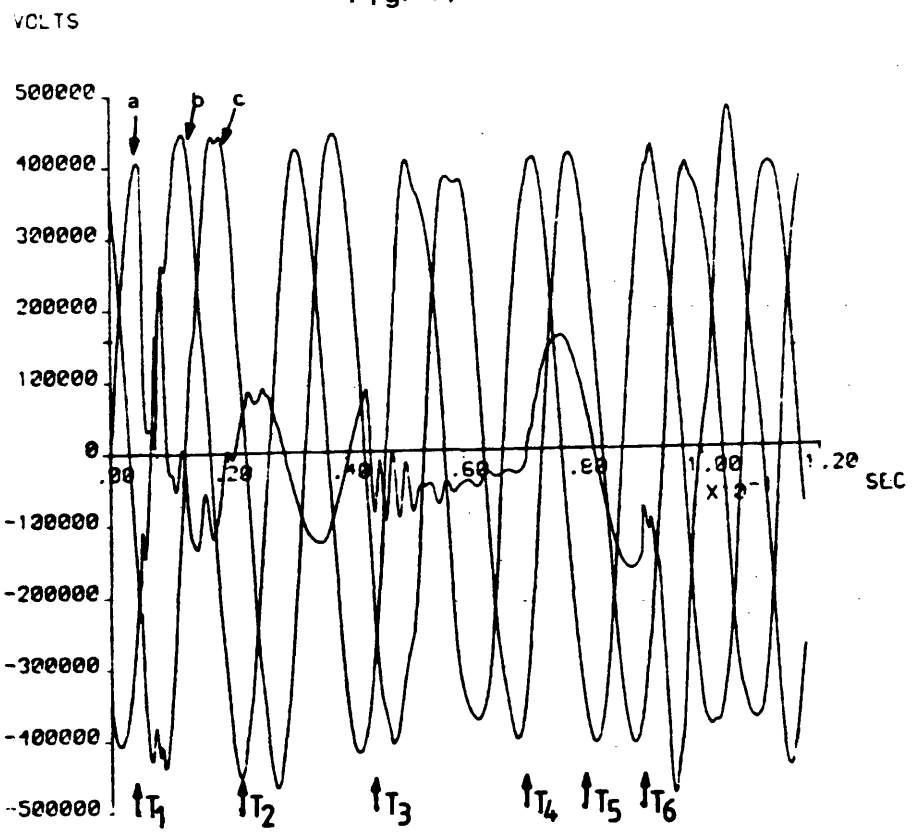
VOLTS
500000
400000
300000
200000
120000
0
-120000
-200000
-300000
-400000
-500000
a
b
c
.00
.20
.40
.60
.80
1.00
1.20
SEC
T1
T2
T3
T4
T5
T6

(a)

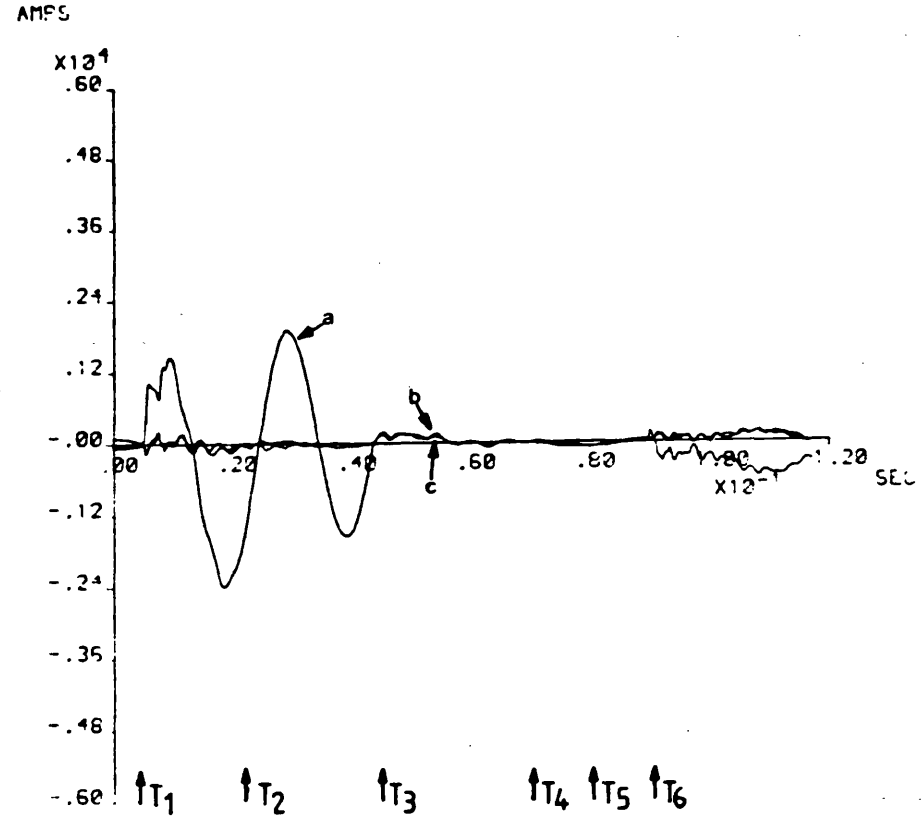
AMPS
X10⁴
.60
.48
.36
.24
.12
-.00
-.12
-.24
-.36
-.48
-.60
a
b
c
.00
.20
.40
.60
.80
1.20
SEC
T1
T2
T3
T4
T5
T6

(b)

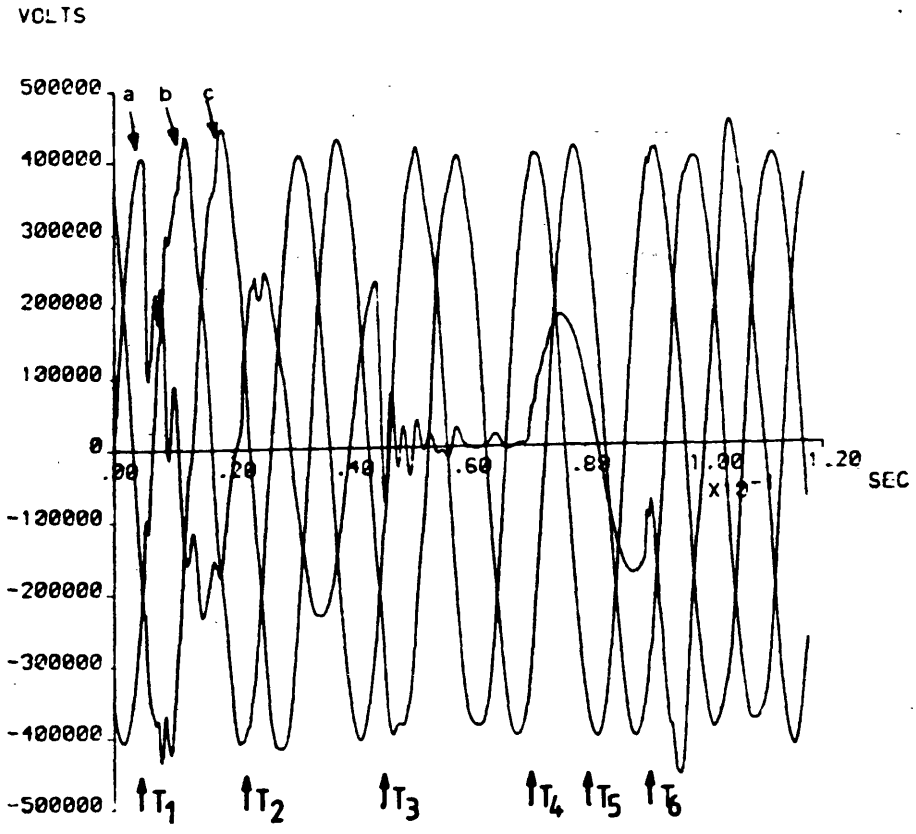
VOLTS
500000
400000
300000
200000
100000
0
-100000
-200000
-300000
-400000
-500000
a
b
c
.00
.20
.40
.60
.80
1.00
1.20
SEC
$T_1$
$T_2$
$T_3$
$T_4$
$T_5$
$T_6$

(c)

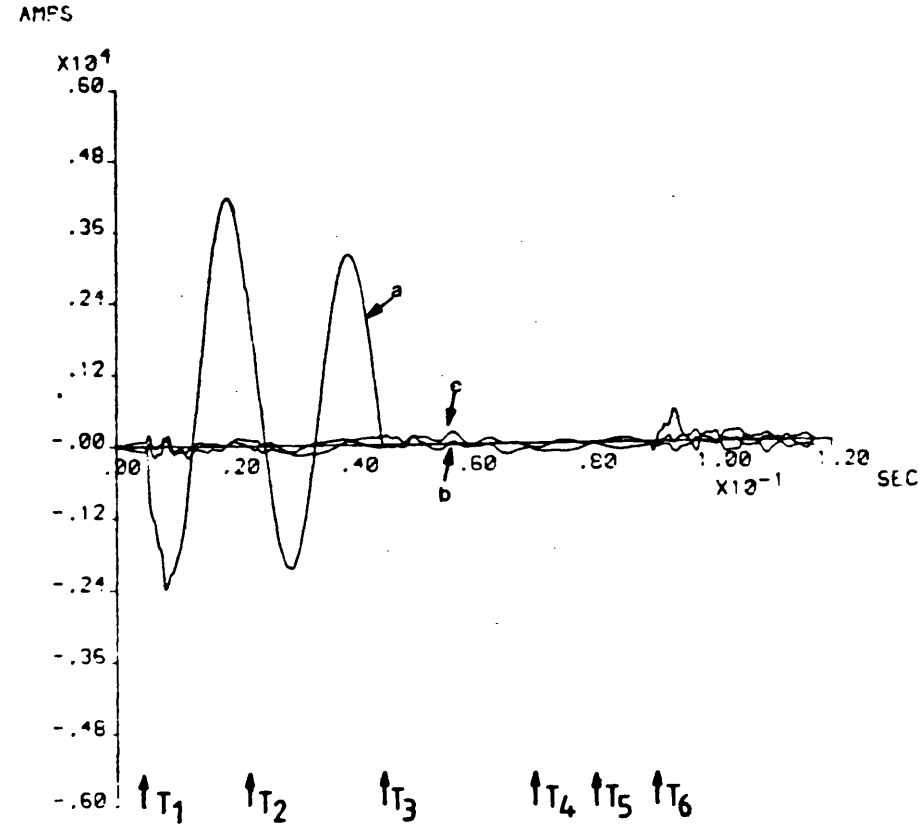
AMPS
X10⁴
.60
.48
.36
.24
.12
-.00
-.12
-.24
-.36
-.48
-.60
a
b
c
.00
.20
.40
.60
.80
1.00
1.20
SEC
$T_1$
$T_2$
$T_3$
$T_4$
$T_5$
$T_6$

(d)

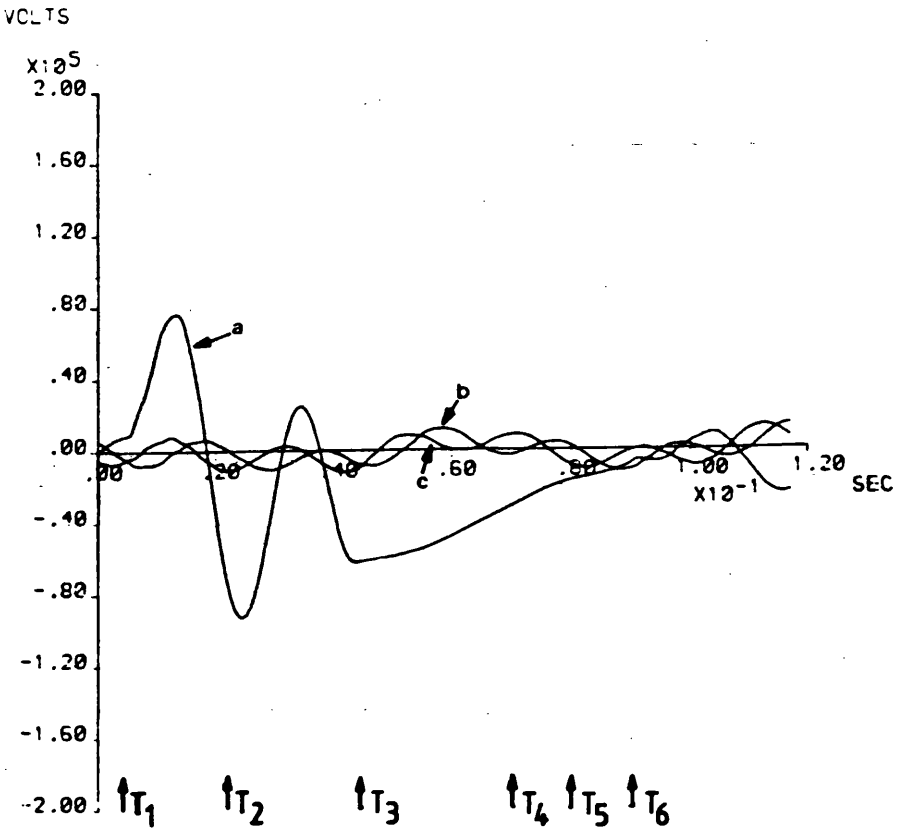
VOLTS
X10^5
2.00
1.60
1.20
.80
.40
.00
-.40
-.80
-1.20
-1.60
-2.00
a
b
c
.60
1.00
1.20
X10^-1
SEC
T1
T2
T3
T4
T5
T6

(e)

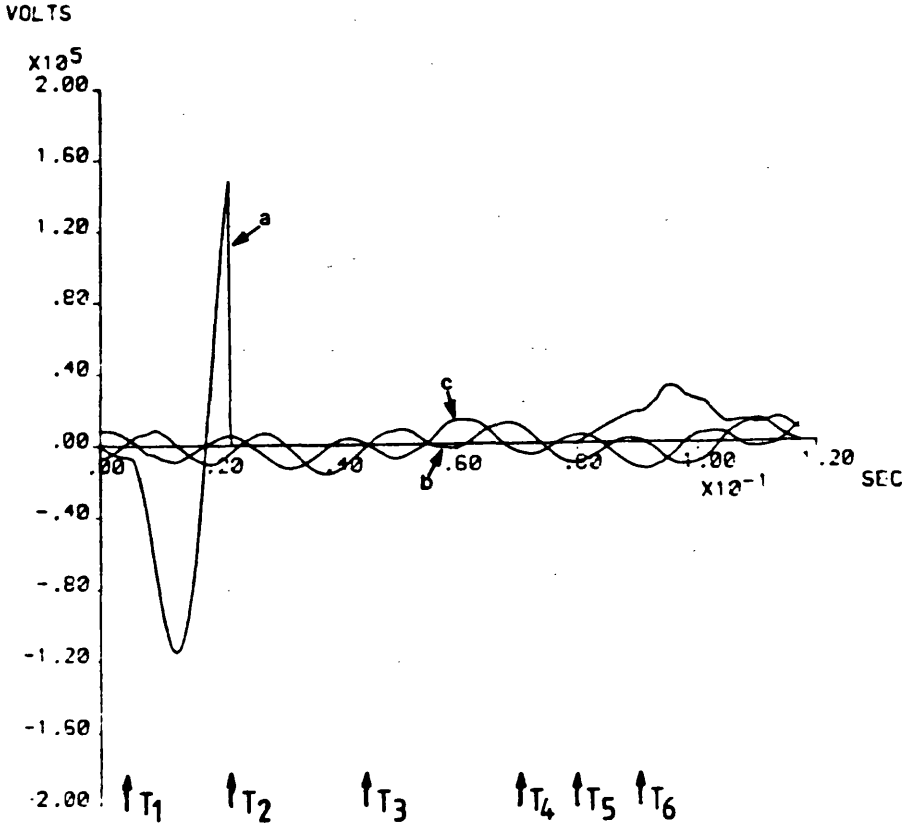
VOLTS
X10^5
2.00
1.60
1.20
.80
.40
.00
-.40
-.80
-1.20
-1.60
-2.00
a
b
c
.60
1.00
1.20
X10^-1
SEC
T1
T2
T3
T4
T5
T6

(f)

Figure 7.3

Mid-point 'a'-earth fault (x = 150km); Multi-section feeder; Source conditions similar to Figure 2.8; A Capacitor at each end. $S_{cap}$ = 0.7, $h_1$ = 0.75, $h_0$ = 0.674. $T_1$ = fault inception (5ms); $T_2$ = 'a'-phase R-end capacitor flashes over (22ms); $T_3$ = 'a'-phase breaker poles at ends S and R separate (43ms); $T_4$ = fault break-off (70ms); $T_5$ = 'a'-phase R-end capacitor reinsert (80ms); $T_6$ = 'a'-phase brekaer poles at ends S and R reclose (90ms).

(a) Voltages on line side of breaker at end S.
(b) Line currents at end S.
(c) Voltages on line side of breaker at end R.
(d) Line currents at end R.
(e) Voltages across end S capacitors.
(f) Voltages across end R capacitors.

Fig. 7.4

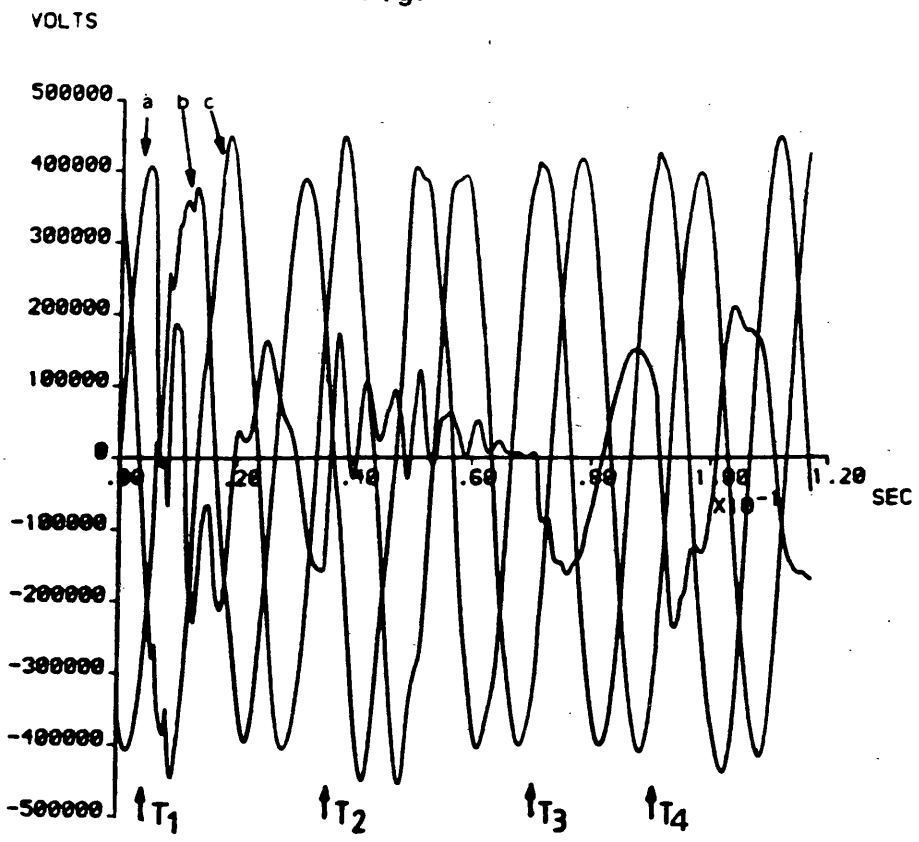
VOLTS
500000
400000
300000
200000
100000
0
-100000
-200000
-300000
-400000
-500000
a
b
c
.20
.40
.60
.80
1.00
1.20
SEC
$T_1$
$T_2$
$T_3$
$T_4$

(a)

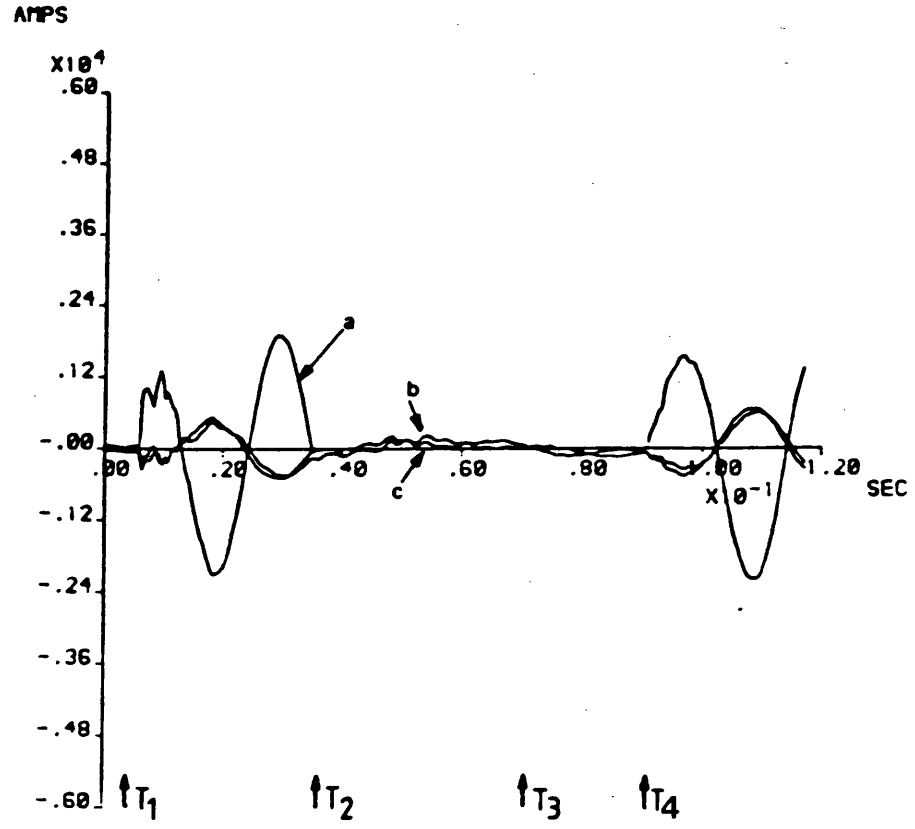
AMPS
X10⁴
.60
.48
.36
.24
.12
-.00
-.12
-.24
-.36
-.48
-.60
a
b
c
.20
.40
.60
.80
1.00
1.20
SEC
$T_1$
$T_2$
$T_3$
$T_4$

(b)

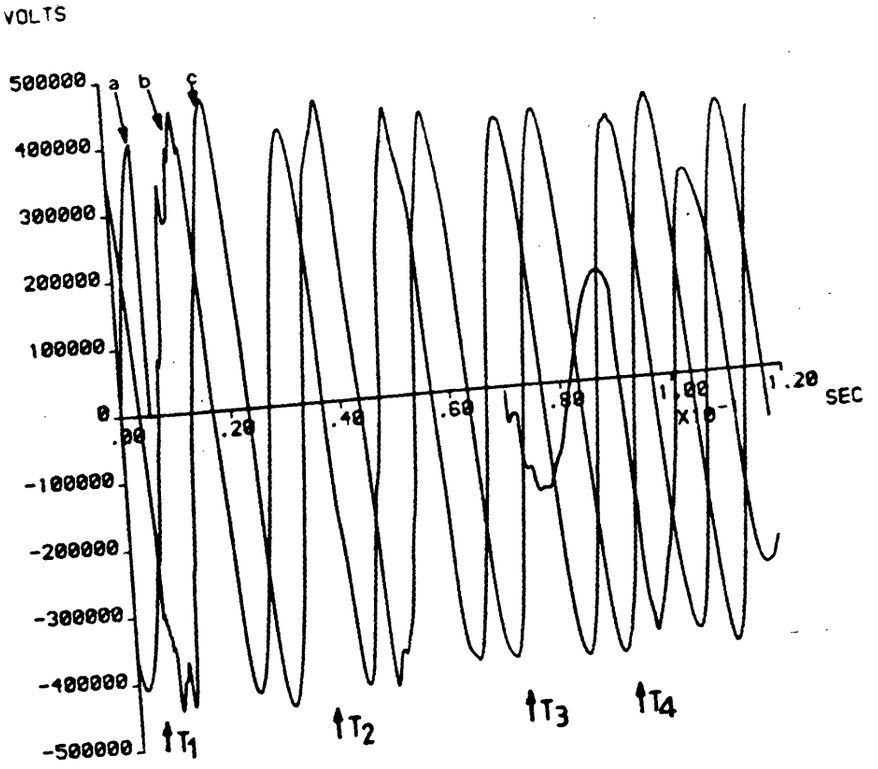
VOLTS
500000
400000
300000
200000
100000
0
-100000
-200000
-300000
-400000
-500000
a
b
c
.00
.20
.40
.60
.80
1.00
1.20
SEC
X10-
T1
T2
T3
T4

(c)

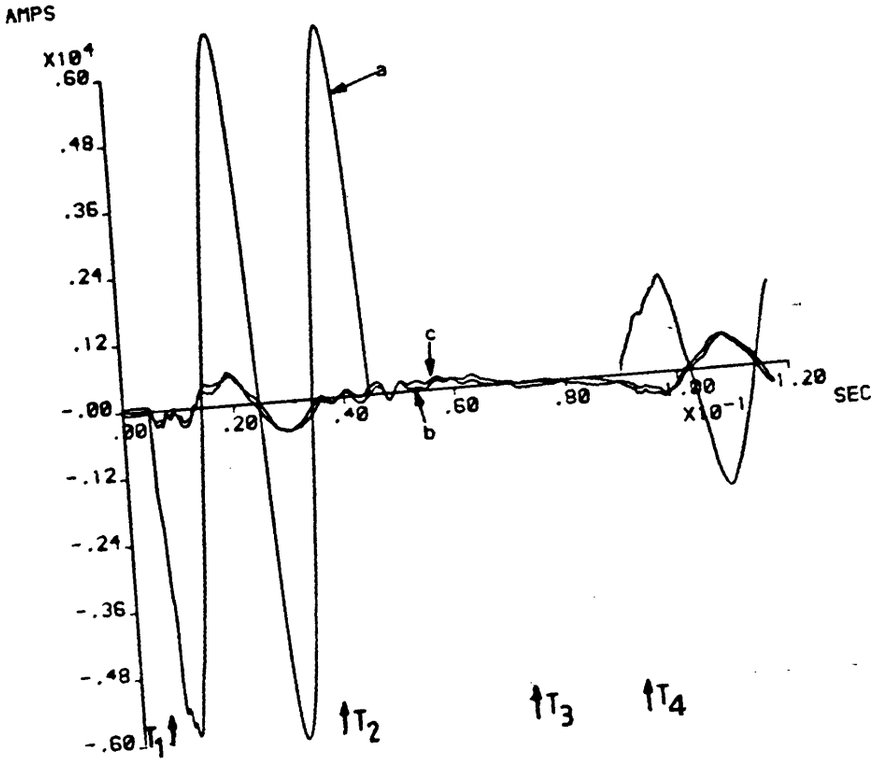
AMPS
X10⁴
.60
.48
.36
.24
.12
-.00
-.12
-.24
-.36
-.48
-.60
a
b
c
.00
.20
.40
.60
.80
1.00
1.20
SEC
X10-1
T1
T2
T3
T4

(d)

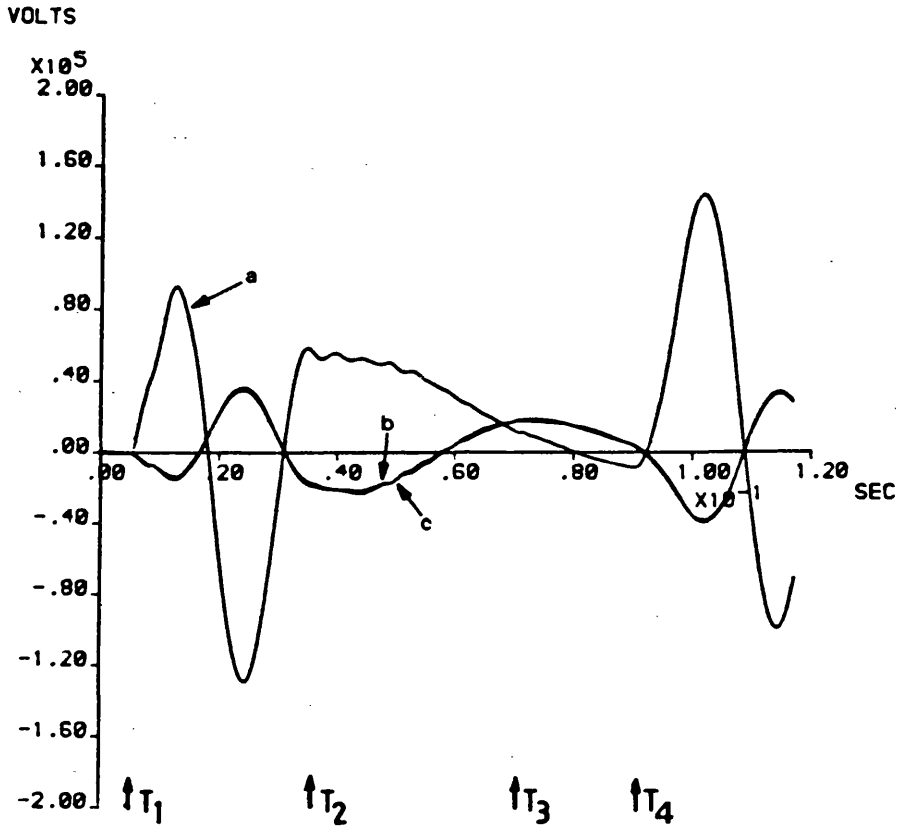
VOLTS
X10^5
2.00
1.60
1.20
.80
.40
.00
-.40
-.80
-1.20
-1.60
-2.00
.00
.20
.40
.60
.80
1.00
1.20
X10^-1
SEC
a
b
c
T1
T2
T3
T4

(e)

Figure 7.4

'a'-earth remote-end fault (x = 300km). Multi-section feeder. Source conditions similar to Figure 2.8. A Capacitor at mid-point. $S_{cap}$ = 0.5, $h_1$ = 0.75, $h_0$ = 0.674; $T_1$ = fault inception (5ms); $T_2$ = 'a' phase breaker poles at ends S and R separate (37ms); $T_3$ = fault break-off (70ms); $T_4$ = 'a' phase breaker poles reclose (90ms).

(a) Voltages on line side of breaker at end S.
(b) Line currents at end S.
(c) Voltages on line side of breaker at end R.
(d) Line currents at end R.
(e) Voltages across capacitors.

# CHAPTER 8 DIGITAL EVALUATION OF DISTANCE RELAY PERFORMANCE

## 8.1 Introduction

It is now widely accepted that an accurate and realistic knowledge of the fault transient phenomena, particularly in relation to e.h.v. transmission systems, is essential not only for the successful development of any future high speed protection equipment, but also for fully assessing the performance of existing modern, high speed relays, in particular of the 'distance' type. The results shown in Chapters 5-7 clearly indicate that the primary system waveforms have a considerable amount of travelling wave distortion, which can persist for an appreciable time after fault inception, and the studies relating to both uncompensated short lines[69] and long lines with shunt compensation only[34] have clearly indicated that these travelling waves can significantly affect the distance relay performance both in terms of speed and accuracy.

In long line applications where series and shunt compensation is a technical necessity, additional relay problems are introduced due to the transients and distorted waveforms caused by the compensation. However, in the case of lines having shunt compensation only, it has been shown[34] that it is the system configuration

rather than the compensation which is the principal factor which determines the performance of modern distance protection. As regards long lines with series compensation, the situation is quite different in that sudden circuit impedance changes take place as a result of the firing of the gap across the capacitor bank to protect it from overvoltages, and this can have an adverse effect on the performance of the distance relay which is essentially an impedance measuring device[90]. As mentioned previously, the capacitor spark gap operation is very random in nature and depends on a number of factors, such as capacitor location, degree of compensation, gap setting, etc. This clearly means that if the relay is preset with the assumption that the capacitor (or capacitors) stays in the circuit after the occurrence of a fault, and subsequently there is a shorting out of the capacitor soon after the fault and before the protective relay has time to operate, then this could result in a substantial amount of under-reaching (and vice versa). Not much work has been reported so far on the combined effect these various aforementioned factors can have on the performance of modern distance relays and, as mentioned in Chapter 1, the majority of the studies have been related to steady-state fault calculations or without considering the spark gap operation.

The prime objective of the work presented in this Chapter is therefore to examine in some detail the performance of the cross-polarised mho relays[69] with different polarising quantities (as applied to a series compensated line with single spark gap scheme) both in the independent and dependent modes of operation using the well-known block average principle[69] and comparing its performance with a relatively new distance scheme based on the sequence comparator principle[84], the latter being chosen for its much superior performance especially in terms of speed which has been shown to be in the range of 0.35 - 0.5 cycles for the majority of faults on an uncompensated system. This can be particularly important in the case of series compensated lines where the correct relay performance is very much dependent on the capacitor spark gap operation. Results so far have indicated that in the majority of cases the capacitors which do flashover do so within 0.5 - 1.0 cycles after fault inception, and this means that the second distance scheme based on the sequence comparator principle could be used to advantage in series compensated lines and therefore help to solve some of the protection problems encountered on series compensated lines.

This Chapter, in particular reveals the effect on

the two types of distance protection relays as applied to both series compensated e.h.v. single section and multi-section feeders (Figures 2.7 and 2.8). The results presented are for two schemes, one employing two capacitors per phase (one at either end) and the other in which there is a single capacitor in the middle, the former having a fixed compensation of 70% and the latter for different degrees of compensation. All cases considered have shunt compensation based on a 3-reactor scheme. The voltage and current transformers are assumed to be located on the busbar side of the shunt reactors.

Digital methods of simulating the responses of the mixing and relay circuits used in the block average comparator arrangement, and as described by Johns and Aggarwal[69], are briefly outlined in Appendix 3, which also includes the simulation of the responses of the various circuits associated with the sequence comparator arrangement. All the parameters associated with this study have already been presented in Chapter 4.

Initially, the various signals simulated (as applied to block average arrangement) are described in Section 8.2, followed by the principles underlying the sequence comparator arrangement in Section 8.3. Section 8.4 briefly describes the two permissive schemes

considered here, mainly the permissive overreach and the blocking scheme. The Zone 1 relay responses (independent mode) are presented in Section 8.5, followed by the responses involving the permissive overreach and the blocking schemes (dependent mode).

## 8.2 Block Average Arrangement

The relaying signals compared in a block average comparator arrangement to produce the polarised mho characteristics are of the well-known form of equation 8.1.

$$S_1 = IZ_r - V$$

$$S_2 = V + V_p \qquad \ldots (8.1)$$

I, V are the relaying current at c.t. secondaries and the relaying voltage at the v.t. secondaries respectively. $V_p$ is the sound phase polarising voltage and $Z_r$ is the replica impedance; the former is obtained using the polarising circuit and the latter is associated with a transformer-reactor arrangement (Appendix A3.2.1).

The signal $S_1$ is of a standard form and varies according to the type of fault, eg for an 'a'-earth fault, is of the form as shown in equation 8.2.

$$S_{1a} = (I_a + KI_{res})\, Z_r - V_a \qquad \ldots (8.2)$$

where $I_{res}$ is the zero sequence current and K is the residual compensating factor, as given by equation 8.3:

$$K = \frac{1}{3}\left[\left|\frac{Z_{L0}}{Z_{L1}}\right| - 1\right] \qquad \ldots (8.3)$$

where $Z_{L0}$ and $Z_{L1}$ are the z.p.s. and p.p.s. line impedances.

As regards signal $S_2$, there are essentially three basic types:

(a) self-polarised:

(b) fully cross-polarised

and (c) using the memory circuit.

8.2.1 Self-polarised type

In this case, the polarising signal is obtained from the same faulted phase and is not very satisfactory, mainly because for close-up earth faults the faulted phase voltage is close to zero, which gives unsatisfactory $S_2$ signal. However, it can have certain advantages for other fault positions. For an 'a'-earth fault, for example, the $S_2$ signal is given by equation 8.4:

$$S_{2a} = V_a + k_p V_a \qquad \ldots (8.4)$$

where $k_p$ is a constant.

8.2.2 Fully Cross-Polarised Type

The fully cross-polarised type is the most commonly used. In this case, the polarising signal is obtained from the healthy phases and for an 'a'-earth fault, for example, it is given by equation 8.5:

$$S_{2a} = V_a + k_p V_{bc} \quad \ldots (8.5)$$

where $k_p$ is the polarising constant and is equal to $k_p \angle 90°$.

8.2.3 Use of the Memory Circuit

In the case of series compensated lines, it has been found that the signal $S_2$ obtained using the memory circuit can have certain advantages[85]. In this type a mixture of the faulted and/or healthy phase voltage with a voltage from a memory circuit is used as the polarising signal. As, for example, for 'a'-earth fault, the signal is as expressed in equation 8.6:

$$S_{2a} = E_a$$

$$\text{or} \quad S_{2a} = E_a + k_p V_{bc} \quad \ldots (8.6)$$

where $E_a$ is the prefault steady state component of voltage and $k_p$ is the polarised voltage constant which is equal to $|k_p| \angle 90°$.

Second order low pass filter (as shown in Appendix A3.4) preconditions the $S_1$ and $S_2$ signals before

going into the block average comparator.

## 8.3 Fundamental Principles of the Sequence Comparator Arrangement

Distance relays based on the sequence comparator arrangement are a relatively new form of protection equipment and, as mentioned before, have a superior response both in terms of speed and accuracy to those based on the block average comparator arrangement.

The underlying principles[84] can best be explained by (ignoring cross-polarising) assuming that the comparator has input quantities A and B, such that:

$$A = V - IZ$$

$$B = V \angle -\pi/2$$

and the criterion for operation is that:

$$\pi > \arg (B/A) > 0$$

ie. A lags B by 0 to 180°. As the operation of the comparator is required to be independent of the magnitude of A and B, these two quantities are converted into square waveforms before being supplied to the comparator. To understand the operation of the comparator, the input square waves may be regarded as logic variables. At any instant of time signal A can be either high or low, ie either

A or $\overline{A}$ and likewise either B or $\overline{B}$. If both signals are unity mark space of equal periods but differing phases, then the four states occur in a cyclic manner. There are only two possible sequences of these states as shown in Figures 8.1 and 8.2. These are:

(1) If A leads B:- $A.B$, $\overline{A}.\overline{B}$, $\overline{A}.\overline{B}$, $A.\overline{B}$ (in one cycle). It follows that when A changes it gains the opposite polarity to B, and when B changes it gains the same polarity as A.

(2) If A lags B:- $A.B$, $A.\overline{B}$, $\overline{A}.\overline{B}$, $\overline{A}.B$ (in one cycle). Again, it follows that when A changes it gains the same polarity as B, but when B changes it gains the opposite polarity to A.

The comparator has a logic circuit which examines the input signals at each polarity change to see which of the two statements is true and thus determines whether the sequence is progressing in a trip or a restrain direction.

In order to ensure the comparator is foolproof against spurious noise and so on, the following criteria are employed in determining the tripping output:

(a) When the counter is incremented to a count of one (ie there is an upward count of 1 due to a polarity change), the trip output is inhibited for 6 ms.

(b) Subsequently, if there is an upward count of 1 as soon as the 6 ms have elapsed, a trip signal is given by the comparator, provided there is no change of state in a restrain sequence (down count) during this period of 6 ms. If a down count is, however, detected in this period of 6 ms, then the tripping condition is changed to a count of three.

(c) There should always be a gap of at least 4 ms between the new count and the last count for the tripping counter to register 1 upwards.

(d) Once the comparator gives a trip output, the output can only reset when the counter is decremented to zero.

### 8.3.1 Modelling on a Digital Computer

Here again, essentially there are two signals to be compared. Taking an 'a'-earth fault as an example, they are essentially of the form of equation 8.7:

$$S_{1a} = V_a - IZ_r = V_a - (I_a + K\, I_{res})\, Z_r$$

$$\text{and } S_{2a} = V_a + k_p V_{bc} + k_s E_a \qquad \ldots (8.7)$$

$IZ_r$ is a component of the voltage associated with the transphasor circuit (as shown in Appendix A3.2.2) and $k_p V_{bc}$, $k_s E_a$ are the sound phase polarising and synchronous polarising voltages respectively, as shown in Appendix A3.3.

In order to eliminate the effects of travelling wave distortion of the voltage signal, a second order low-pass filter with a cut-off frequency of 500Hz preconditions the voltage signal (Appendix A3.4). As mentioned previously, in order to make the two signals $S_1$ and $S_2$ independent of the magnitudes, they are converted into squared waveforms and in order to comply with the criteria for comparison, the second signal ($S_2$) is advanced by -90°, ie delayed by 5 ms. The complete arrangement is shown in Figure 8.3. The logic as described previously is then applied to obtain the up and down counts for the trip signal and the previously described tripping criterion is used.

## 8.4 Principles of the Permissive Schemes (Dependent Mode)

One of the main disadvantages of conventional time-stepped distance protection (Figure 8.4) is the fact

that the instantaneous Zone 1 of the protection at each end of the protected line cannot be set to cover the whole of the feeder length, and is usually set to about 80%. This leaves two 'end zones', each being about 20% of the protected feeder length, in which faults are cleared instantaneously (Zone 1 time) by the protection at one end of the feeder, but in Zone 2 time (0.3 - 0.4 sec) by the protection at the other end of the feeder. In some applications this situation cannot be tolerated for the following three main reasons:

(1) Faults remaining on the feeder for Zone 2 time may cause the system to become unstable.

(2) Where high speed autoreclosing is used, the non-simultaneous opening of the circuit breakers at both ends of the faulted sections results in no 'dead time' during the auto-reclosure cycle for the secondary arc to be extinguished and for ionised gases to clear. This can result in a permanent lockout of the circuit breakers at each end of the line section for a transient fault.

(3) In series compensated lines where speed of relay operation can be quite important (due

to the capacitor spark gap operation), this delayed relay operation for certain fault conditions can be quite onerous.

Unit schemes of protection which compare the conditions at the two ends of the protected feeder simultaneously can positively identify whether the fault is internal or external to the protected section, and are capable of providing high speed protection for the whole feeder length. This advantage is, however, offset by the fact that the unit scheme does not provide back-up protection to adjacent feeders given by a distance scheme. The most desirable scheme is obviously one which combines the best features of both arrangements, ie instantaneous tripping over the whole feeder length, plus back-up protection to adjacent feeders. This can be achieved by interconnecting the distance protections at each end of the protected feeder by a signalling channel. This signalling channel may be high frequency signalling over the overhead line conductors, or voice frequency using either pilots, a power line carrier communications channel, a radio link or a microwave channel. The purpose of the signalling channel is to transmit information about the system conditions at one end of the protected line to the other end; it can also be arranged so as to initiate or prevent tripping of the remote circuit breaker.

The former arrangement is generally referred to as a 'transfer trip scheme', whilst the latter is known as a 'blocking scheme'.

In this work, the performances of two permissive schemes, namely the 'permissive overreach' and the 'blocking' schemes as applied to series compensated lines, have been evaluated (both using the block average and sequence comparator arrangement) in order to find out whether such schemes offer any added advantages.

### 8.4.1 Transfer Tripping (Permissive Overreach) Scheme

A prime example of transfer tripping is the permissive overreach scheme. In such a scheme, a relay is set so that it covers faults beyond the remote terminal, normally set for 120% of the line length is used to send an intertripping signal, as shown in Figure 8.5(a). In this case, however, it is essential that the receive relay contact be monitored by a directional mho type relay contact to ensure that tripping does not take place unless the fault is within the protected section. The situation as regards the tripping circuits at the two ends are concerned is shown in Figure 8.5(b).

With reference to Figure 8.5(a) and considering a fault at point X(say), close to end S, it can be seen that because of the nature of the directional relay settings, the fault although close to end S, would still be picked up almost simultaneously by the two directional mho relays at ends S and R, resulting in contact $Z_{2S}$, $Z_{2R}$ closing, which in turn transmit an inter-tripping signal from each end of the line and this controls the receive relay contact at the remote end. The tripping times of the relays at each end are thus not only dependent on the operating times of the mho relays, but also on the times taken to send the tripping signal, typically between 5 and 15 ms. If the lower 5 ms is taken, then the tripping time $T_S$ from the end S is:

$$= T_{2S} \text{ (if } T_{2S} \geq T_{2R} + 5 \text{ ms)}$$

$$\text{or} \quad = T_{2R} + 5 \text{ ms (if } T_{2S} < T_{2R} + 5 \text{ ms)}$$

Again, the tripping time $T_R$, from end R is:

$$= T_{2R} \text{ (if } T_{2R} \geq T_{2S} + 5 \text{ ms)}$$

$$\text{or} \quad = T_{2S} + 5 \text{ ms (if } T_{2R} < T_{2S} + 5 \text{ ms)}$$

As regards the fault at point $X_1$ (say) this would result in $Z_{2S}$ closing and sending a carrier signal to end R. However, because of the directional relay at end R, the closing of contact $Z_{2R}$, and hence transmission

of carrier to end S, would be prevented. Hence, tripping for external faults is not possible. The same principle applies to fault at point $X_2$.

8.4.2 Blocking Scheme

A normally closed receive relay contact is used in the tripping circuit, allowing instantaneous tripping via the forward looking directional Zone 2 starting units $Z_{2S}$ and $Z_{2R}$, as shown in Figure 8.6(a).

A blocking instruction has to be sent by the reverse-looking offset directional units $Z_{SS}$, $Z_{RR}$ to prevent instantaneous tripping for out of zone faults. To achieve this, the reverse looking units $Z_{SS}$, $Z_{RR}$ must operate faster than forward looking $Z_{2S}$ and $Z_{2R}$ units and the signalling channel must also be extremely fast in operation. In practice, this is seldom the case and to ensure discrimination,a short time '$T_{lag}$' is generally introduced into the blocking mode trip circuit. In order to ensure that no blocking signal is sent for an internal fault (especially for a fault in the region X or Y), a forward looking $Z_2$ contact in the signalling channel start circuit is connected as shown in Figure 8.6(b).

The situation as far as the tripping circuits at the two ends is concerned, when considering a fault at

point $X_1$ (say) close to end S of Figure 8.6(a), is as follows.

A fault at point $X_1$ could result in the operation of $Z_{2S}$, $Z_{SS}$ and $Z_{2R}$. As the fault is in the forward direction as regards $Z_{2S}$, this would result in the normally closed contact $C_2$ being opened, thus preventing the carrier to be transmitted to end R when $Z_{SS}$ operates. This means that the receive relay contact at end R remains closed and hence tripping occurs at end R. As regards the carrier transmission from end R, because the fault is outside the reach of $Z_{RR}$, therefore $Z_{RR}$ contacts do not close and hence no carrier transmission to end S. Naturally, when the fault is anywhere in the region $P_1$ - $P_2$, neither $Z_{SS}$ nor $Z_{RR}$ contacts close and hence no blocking signal is sent.

If a fault occurs external to the protected zone, say at $X_2$, then as regards the end S, relay $Z_{2S}$ sees it as a reverse fault and hence no trip signal. In the case of transmission from end S, $C_2$ remains closed and because $Z_{SS}$ operates, therefore a blocking signal is transmitted to end R, opening contact $C_3$ and hence there is no trip signal at end R either. The same principle applies for faults at end R.

## 8.5 Relay Responses Evaluation

The majority of studies presented here are for faults at an instant of time corresponding to voltage maximum, and some studies corresponding to voltage minimum (ie zero voltage) are also presented. Relay performance in the independent mode of operation is examined first as applied to the two different systems (Figures 2.7 and 2.8), followed by a limited study involving the dependent mode of operation as applied to the multi-section feeder configuration only.

### 8.5.1 Single Section Feeder

#### 8.5.1.1 A capacitor at each end

Figure 8.7(a) shows a typical coincidence detector Zone 1 relay output of the relaying signals $S_1$ and $S_2$ using the block average arrangement, the

fault being at 75 km from the sending end. The relay settings as shown by Figure 4.2(a) assume that none of the capacitors flashover. It can be seen that the integrator output (Figure 8.7(b)) builds up gradually and the sending end relay gives a trip signal at about 15ms after fault inception. This is so in spite of the fact that the sending end capacitor flashover at 4.75 ms after fault inception. Figure 8.7(c) shows the corresponding integrator output for the receiving end relay again for a fault at 75 km from the receiving end and this also indicates a similar sort of trip time. However, for a mid-point fault (150 km), relays at both end fail to reach the set level due to the sudden change of system parameters, the latter resulting from capacitor gap operation at the two ends (Figures 8.7 (d, e)).

Figure 8.8 shows a typical response of the relay employing the sequence comparator arrangement. In this case, slightly slower trip times of 16 ms and 15.5 ms (for the sending end and receiving end relays respectively) are obtained for an identical fault at 75 km. Here again the relays fail to operate for a mid-point fault, primarily because the capacitor spark gap operating times are faster than the relay operating times. Figure 8.9 shows how the two relays respond when the relay settings assume no flashover of the capacitors. It can be seen that the sequence comparator has a

slightly better performance in terms of the operating times than the block average arrangement. However, in both the cases, there is a considerable amount of underreaching - 52% for the block average and about 60% for the sequence comparator, this being due to the capacitor spark gap operations. This can be verified to be approximately correct by looking at Figure 4.2, which clearly shows that the relays would detect faults only in the region AB' if there is a capacitor flashover (corresponding to a fault point of 130 km). The primary system waveforms have indicated that for a feeder terminated in relatively simple sources (ie the configuration of Figure 2.7) the capacitors at both end do flashover for a majority of fault conditions (again shown in Table 8.1), and they do so in a relatively short time after fault inception. Figure 8.10 shows the relay responses when the relays are set assuming that there are no capacitors in the circuit (corresponding mho characteristic shown in Figure 4.2(b)). Here again the relatively faster response of the sequence comparator, especially at the boundary, is evident but the interesting point to note here is that the underreaching effects are considerably reduced (in fact there is a slight overreaching of about 1.7% in the case of the sequence comparator), this being about 6% and 10% for the block average sending end and receiving end relays respectively. Table 8.1 summarises the relay performance.

| Distance from SE or RE(km) | Cap.F/O instant (ms) | Setting with capacitor in the circuit | | | | Setting with no capacitor in the circuit | | | |
|---|---|---|---|---|---|---|---|---|---|
| | | Sending End | | Receiving End | | Sending End | | Receiving End | |
| | | B/A trip time(ms) | S/C trip time(ms) | B/A trip time(ms) | S/C trip time(ms) | B/A trip time(ms) | S/C trip time(ms) | B/A trip time(ms) | S/C trip time(ms) |
| 0.00 | 10.50 | 13.00 | 12.00 | 12.75 | 11.75 | 12.50 | 11.50 | 12.25 | 11.50 |
| 60.00 | 4.50 | 14.50 | 16.00 | 13.24 | 11.50 | - | - | - | - |
| 75.00 | 4.75 | 14.68 | 16.00 | 14.56 | 15.50 | 11.44 | 10.50 | 11.68 | 10.25 |
| 85.00 | 5.00 | 14.92 | 15.75 | 19.24 | 15.25 | - | - | - | - |
| 100.00 | 5.50 | 19.00 | 15.75 | - | - | 11.44 | 10.25 | 11.68 | 10.25 |
| 115.00 | 6.00 | 24.40 | 21.25 | 23.56 | restrain | 11.20 | 10.50 | 11.68 | 10.25 |
| 120.00 | 6.25 | restrain | restrain | restrain | " | 11.68 | 10.50 | - | - |
| 150.00 | 15.25 | " | " | " | " | 13.25 | 10.50 | 12.40 | 10.25 |
| 185.00 | 16.50 | " | " | " | " | 18.52 | 10.50 | 17.44 | 10.00 |
| 205.00 | 16.50 | " | " | " | " | 19.96 | 10.50 | 21.00 | 12.00 |
| 215.00 | - | " | " | " | " | - | - | 22.24 | 12.00 |
| 225.00 | 17.00 | " | " | " | " | 24.76 | 10.50 | restrain | 20.25 |
| 240.00 | 17.50 | " | " | " | " | restrain | 10.50 | " | 20.25 |
| 244.00 | - | " | " | " | " | " | 10.50 | " | 20.25 |
| 252.00 | - | " | " | " | " | " | restrain | " | restrain |

Table 8.1 A Capacitor at each end. Single section feeder. $G_S = G_R = 10.0$ GVA.
Block average and sequence comparator relay operating time.

As far as the voltage minimum (ie voltage zero) faults are concerned, results have shown that the faulted phase capacitors flashover for a majority of fault positions, and this means that if the relays are set with the capacitor in the circuit then like the corresponding case for voltage maximum faults, a considerable amount of underreaching is produced for both types of relays. When the relays are set without the capacitors in the circuit, the responses are as shown in Figure 8.11. It can be seen that unlike the case for voltage maximum faults (Figure 8.10), the block average relay has a better performance (in terms of both speed and relay reach) than the sequence comparator relays, this being so both for the sending end and receiving end relays. Figure 8.12 shows a typical output response of the two arrangements for a fault at 165 km.

8.5.1.2 A Capacitor at the mid-point

Similar sorts of relay responses, both for the block average and sequence comparator relays as above are obtained when considering a single capacitor in the middle of the line with a series compensation of 30%. Table 8.2 gives details of their operating times at different fault locations, along with capacitor flashover times. In the case of the relay setting without capacitor flashover, it can be seen that

| Distance from SE or RE(km) | Cap.F/O instant (ms) | Setting with capacitor in the circuit | | | | Setting with no capacitor in the circuit | | | |
|---|---|---|---|---|---|---|---|---|---|
| | | Sending End | | Receiving End | | Sending End | | Receiving End | |
| | | B/A trip time(ms) | S/C trip time(ms) | B/A trip time(ms) | S/C trip time(ms) | B/A trip time(ms) | S/C trip time(ms) | B/A trip time(ms) | S/C trip time(ms) |
| 0.00 | no F/O | 13.25 | 12.25 | 13.25 | 12.25 | 12.25 | 11.50 | 12.25 | 11.50 |
| 60.00 | 17.50 | 13.43 | 16.00 | 13.10 | 11.50 | 12.30 | 11.00 | 12.00 | 11.00 |
| 75.00 | 17.00 | - | - | 13.24 | 11.75 | 12.30 | 11.00 | 12.10 | 11.00 |
| 110.00 | 16.50 | 15.40 | 16.75 | - | - | - | - | - | - |
| 135.00 | 15.75 | 32.65 | 18.00 | 32.65 | 28.75 | 14.00 | 11.50 | 13.20 | 11.25 |
| 138.00 | - | - | - | 44.00 | - | - | - | - | - |
| 140.40 | - | 44.80 | 50.25 | restrain | 30.00 | - | - | - | - |
| 143.30 | - | 45.00 | 50.50 | " | 50.00 | - | - | - | - |
| $150.00^-$ | 7.75 | restrain | restrain | " | restrain | 13.43 | 12.00 | 13.80 | 12.00 |
| $150.00^+$ | 7.00 | " | " | " | " | 12.45 | 10.50 | 12.84 | 10.50 |
| 165.00 | 7.50 | " | " | " | " | 13.43 | 10.50 | 12.84 | 10.00 |
| 190.00 | - | " | " | " | " | - | - | 17.75 | 10.00 |
| 225.00 | 17.00 | " | " | " | " | 20.10 | 12.25 | 20.50 | 10.00 |
| 231.00 | - | " | " | " | " | 24.20 | - | restrain | 12.25 |
| 234.00 | - | " | " | " | " | 25.60 | - | " | 12.25 |
| 236.25 | - | " | " | " | " | restrain | 20.50 | " | 20.50 |
| 240.00 | 17.50 | " | " | " | " | " | restrain | " | restrain |

Table 8.2 A Capacitor at mid-point (amount of compensation = 30%). Single section feeder $G_S = G_R = 10.0$ GVA. Block average and sequence comparator relay operating time.

irrespective of the flashover, the sending and receiving end block average relay operates for faults up to about 143 km and 138 km respectively. The operating times of the sequence comparator relay are slightly reduced (especially the receiving end relay) and in this case both the sending end and receiving end relays operate for faults up to about 143 km. The relay responses are shown in Figure 8.13, which indicate 41.5% and 40% underreach for the block average and sequence comparator respectively. This can again be verified to be correct by looking at the mho characteristic of Figure 4.4, where the locus AC corresponds to a maximum fault point of 150 km and which is the maximum reach point of a relay (with this particular setting) if there is a capacitor flashover. The slight disagreement between the two reaches is due to the effects of the travelling wave distortion at the boundaries of relay operation.

If the relay setting is changed to that of capacitor flashover, then the relay performance is again vastly improved, primarily due to the fact that here again the faulted phase capacitor flashes over for the majority of fault positions as shown by Table 8.2. It is observed that the sequence comparator relay has faster and better performance than the block average counterpart. The underreaching being 1.6% and 2.3% respectively for the two ends (Figure 8.14).

Studies have also indicated that the relay remains stable for reverse faults.

### 8.5.2 Multi-Section Feeder

#### 8.5.2.1 A Capacitor at each end

The primary system waveforms have indicated that the random behaviour of the capacitor protective gap operation is more noticeable in the case of a line terminated in complex source models, and this is apparent by comparing Tables 8.1 and 8.3. It can be clearly seen that in the former case (which is for a simple source model) both the faulted phase capacitors flashover almost simultaneously for a majority of fault positions, whereas in the latter case (which is for a complex source model) it is very random in nature. With relays initially set without capacitor flashover, Figures 8.15 and 8.16 show typical output of the block average and sequence comparator arrangement for a fault at 185 km from the sending end. It can be seen that both types of relay for end S operate for faults up to about 185 km and 195 km, showing an underreach of about 23% and 18% respectively, and this is in spite of the fact that the end S capacitor never flashes over (as shown by Table 8.3). This can be put down firstly to the effect on the end S relay due to the shorting out of the end R capacitor, and secondly due to the complexity of the source side networks. Figure 8.17 shows

| Distance from S.E. or R.E. (km) | F/O instant (ms) | | Fully cross-polarised | | | | Use of Memory | |
|---|---|---|---|---|---|---|---|---|
| | | | Block Average | | Sequence Comparator | | Block Average | |
| | For S.E. Cap. | For R.E. Cap. | S.E. trip time (ms) | R.E. trip time (ms) | S.E. trip time (ms) | R.E. trip time (ms) | S.E. trip time (ms) | R.E. trip time (ms) |
| 0.00 | | no F/O | 16.25 | 16.50 | 12.00 | 11.75 | 12.50 | 12.75 |
| 60.00 | N | 6.25 | 20.00 | 15.50 | 11.00 | 10.50 | 13.72 | 11.80 |
| 75.00 | O | 7.00 | 21.40 | 15.16 | 10.50 | 10.25 | 13.24 | 12.82 |
| 95.00 | | 15.50 | 19.96 | 19.48 | 11.00 | 10.25 | 14.20 | 17.56 |
| 115.00 | F | 16.00 | 19.48 | 20.92 | 11.50 | 10.50 | 17.08 | 18.52 |
| 120.00 | L | 16.00 | 19.00 | 22.85 | 11.50 | 13.50 | 17.08 | - |
| 131.73 | A | - | - | 25.25 | - | " | - | - |
| 135.00 | S | 16.50 | - | restrain | - | " | - | 24.28 |
| 150.00 | H | 17.00 | 20.92 | " | 20.50 | 20.25 | 19.96 | restrain |
| 156.00 | O | - | - | " | " | " | - | " |
| 165.00 | V | 17.75 | 24.76 | " | " | restrain | 23.80 | " |
| 185.00 | E | 18.25 | 100.60 | " | " | " | 55.00 | " |
| 195.00 | R | 19.25 | restrain | " | " | " | restrain | " |
| 195.50 | | - | " | " | " | " | " | 24.76 |
| 200.00 | | no F/O | " | 24.76 | restrain | " | " | 24.76 |
| 205.00 | | " | " | restrain | " | " | " | restrain |

Table 8.3 A Capacitor at each end. Multi-section feeder. Relay setting with capacitor in the circuit. Block average and sequence comparator relay operating time.

the relay responses. One interesting point to note here is the behaviour of the end R block average relay. It can be clearly seen in this particular case that the relay operates for faults up to about 132 km, restrains for faults up to about 195 km and then again operates for faults in a small region of 195-200 km. This can be put down to the fact that the end R capacitor sparks over in a random fashion (as shown by Table 8.3) and the rather peculiar behaviour of the relay can best be explained with reference to the mho characteristic of Figure 4.2, which shows that if the relay is set with the capacitor in the circuit then irrespective of whether the capacitor flashover or not, all faults would be picked up in the region AB' (which correspond to a maximum fault point of 130 km) and would fail to pick up faults beyond this if the capacitor flashes over. However, Table 8.3 shows that the R-end capacitor flashover for faults only up to about 195 km and this means that theoretically the relay which has been set without capacitor flashover should also pick up faults between 195 and 240 km (locus B'C' in Figure 4.2), the latter being its 80% reach point. In this particular case,because the relay performance is also affected by the system configuration, it picks up faults between 195-200 km only. As far as the end R sequence comparator relay is concerned, it shows a better coverage (156 km) than the corresponding block

average relay whose reach point is reached at about 132 km. This is so because for faults between 132 and 156 km,the sequence comparator relay operation is faster than the spark over time of the R-end capacitor (as seen by Table 8.3). However, unlike the block average relay, the sequence comparator relay does not show the narrow band of operation for faults between about 195-200 km. As regards the reverse faults, the relay remains stable. The results concerning the block average relay have been obtained by utilising the signals as shown by equation 8.5.

In order to assess the advantages of the memory circuit considering signal $S_2$ of the block average comparator arrangement (as shown by equation 8.6), a new set of results is obtained, details of which are summarised in Table 8.3. It can be seen that the relay has a relatively faster response when such a circuit is employed (typical output of the block average arrangement using memory circuit for faults at 185 km is shown in Figure 8.18). However, in spite of the faster response, the block average relay at end R still has the restraining condition for faults between about 135-195 km and as in the previous case, operates again for faults between 195-200 km.

As regards the using of the self-polarising signal in choosing $S_2$ (equation 8.4), it was found that the results obtained are very similar to those obtained using equation 8.5.

On changing the setting of the relays assuming that flashover occurs at all times, a new set of operating times are obtained, as summarised in Table 8.4, and again as shown by the relay response in Figure 8.19. It can be clearly seen that both the sending end and receiving end block average relays overreach substantially. This is also the case for the sequence comparator relay.

All the above results are for voltage maximum faults. As far as the voltage minimum faults are concerned, studies have shown that both the sending end and receiving end capacitors flashover for a majority of fault positions and, unlike the voltage maximum faults, both the sending end and receiving end capacitors flashover for not only the simple source models, but also for the complex source models. Therefore, for complex source models and with the relays set assuming no capacitor flashover, there is a substantial amount of underreaching as shown by Table 8.5 for the two types of relays. However, when the two relays are set with no capacitor in the circuit,

| Distance from S.E. or R.E. (km) | Sending End | | | Receiving End | | |
|---|---|---|---|---|---|---|
| | Cap. F/O instant (ms) | B/A trip time (ms) | S/C trip time (ms) | Cap. F/O instant (ms) | B/A trip time (ms) | S/C trip time (ms) |
| 0.00 | | 12.50 | 11.50 | no F/O | 12.75 | 11.50 |
| 60.00 | N | 11.32 | 10.50 | 6.25 | 11.32 | 10.25 |
| 75.00 | O | 12.28 | 10.75 | 7.00 | " | " |
| 100.00 | | 12.76 | 11.00 | 15.50 | " | " |
| 110.00 | F | 12.28 | " | 16.00 | " | 10.75 |
| 120.00 | L | 13.24 | 11.25 | " | " | " |
| 150.00 | A | 14.68 | 11.75 | 17.00 | " | 11.00 |
| 165.00 | S | 17.08 | " | 17.75 | - | - |
| 185.00 | H | 18.52 | 12.00 | 18.25 | 18.52 | 11.25 |
| 225.00 | O | 19.48 | 20.50 | no F/O | 19.00 | 20.25 |
| 240.00 | V | 21.40 | " | " | 20.92 | " |
| 300.00 | E R | 25.72 | " | - | 26.75 | " |

Table 8.4 A Capacitor at each end. Multi-section feeder. Relay setting with no capacitor in the circuit. Block average and sequence comparator relay operation time.

these underreachings are significantly reduced (Table 8.5).

| Relay | Setting with cap. in circuit | | Setting with no cap. in circuit | |
|---|---|---|---|---|
| | B/A | S/C | B/A | S/C |
| Sending end | 46.6% | 58.0% | 3.8% | 11.1% |
| Receiving end | 46.0% | 45.3% | 4.1% | 2.7% |

Table 8.5 A Capacitor at each end. Multiple source. Voltage minimum. Block average and sequence comparator relays underreach

This is in marked contrast to the corresponding case for voltage maximum faults (Figure 8.19) which shows that when the relays are set without the capacitor in the circuit, the relays tend to overreach quite considerably.

Figure 8.20 shows a typical output response of the two arrangements for a fault at 165 km and Figure 8.21 shows the relay responses. As in the corresponding case for the simple source model, it can be seen that the block average relay has an overall better performance than the sequence comparator relay.

8.5.2.2 A Capacitor at the mid-point

In this study first 30% series compensation is assumed. Here again, the very random nature of the capacitor spark gap operation is apparent (Table 8.6) and this in turn significantly affects the relay performance. With the Zone 1 relay setting assuming no flashover of the capacitor, the response characteristics are shown in Figure 8.22 which clearly shows the various bands of relay operations due to capacitor flashover. In the case of end S block average relay, for example, it can be seen that the relay operates for faults up to about 135 km, restrains for faults up to about 150 km and then operates again for faults between 150-200 km. This phenomena can again best be explained with reference to Figure 4.4, which shows the mho characteristic of the relay both with and without the capacitor in the circuit. It can be seen that for a relay set with capacitor in circuit, irrespective of whether the capacitor flashover or not, the relay would always pick up faults in the region AC (corresponding to a maximum fault position of 150 km) and would fail to pick up faults beyond this if the capacitor flashover. Table 8.6 shows that the capacitor flashover for faults between about 125-150km and then stays in the circuit and this means that a relay with this particular setting would have a no-operate band around 150 km and should pick up

| Distance from S.E. or R.E. (km) | F/O instant (ms) | | Setting with capacitor in the circuit | | | | Setting with no capacitor in the circuit | | | |
|---|---|---|---|---|---|---|---|---|---|---|
| | | | Sending End | | Receiving End | | Sending End | | Receiving End | |
| | For cap. from S.E. | For cap. from R.E. | B/A trip time (ms) | S/C trip time (ms) | B/A trip time (ms) | S/C trip time (ms) | B/A trip time (ms) | S/C trip time (ms) | B/A trip time (ms) | S/C trip time (ms) |
| 0.00 | no F/O | no F/O | 12.50 | 12.00 | 12.75 | 11.75 | 12.50 | 11.50 | 12.00 | 11.50 |
| 60.00 | " | " | 12.92 | 11.75 | 14.08 | 15.50 | 11.10 | 11.50 | 12.25 | 10.50 |
| 75.00 | " | " | 14.29 | 12.00 | 14.48 | 15.75 | 11.56 | 12.00 | 12.34 | 10.75 |
| 100.00 | " | " | 18.57 | 15.75 | - | - | 12.53 | " | - | - |
| 125.00 | 18.50 | " | 24.00 | 29.50 | - | - | - | - | - | - |
| 135.00 | 18.00 | " | 35.32 | 50.50 | 32.65 | 29.50 | 14.60 | 15.50 | 11.70 | 10.75 |
| 142.40 | - | - | restrain | restrain | restrain | restrain | - | - | - | - |
| $150.00^{-}$ | 17.50 | no F/O | " | " | " | " | 14.87 | 12.75 | 12.53 | 15.50 |
| $150.00^{+}$ | no F/O | 17.50 | 17.60 | 12.50 | " | 20.25 | " | 11.75 | 11.17 | 11.00 |
| 165.00 | " | 18.00 | 20.50 | 20.50 | " | 20.25 | 16.00 | 11.00 | 13.04 | " |
| 175.00 | " | 18.50 | - | - | " | " | - | - | - | - |
| 185.00 | " | no F/O | 48.77 | 20.25 | 24.60 | restrain | 16.50 | 13.50 | - | - |
| 200.00 | " | " | 55.60 | 20.50 | 54.85 | " | - | - | - | - |
| 225.00 | " | " | restrain | restrain | restrain | " | 19.24 | 20.50 | 19.16 | 20.25 |
| 240.00 | " | " | " | " | " | " | 20.70 | 20.50 | 20.50 | " |
| 252.00 | - | " | " | " | " | " | 24.20 | 20.25 | 22.50 | " |

Table 8.6 A Capacitor at mid-point (amount of compensation = 30%). Multi-section feeder. Block average and sequence comparator relay operating time.

all faults between 150-240 km. In this particular case, faults only up to about 200 km are picked up, because apart from the effect of capacitor flashover, the relay performance is also affected by the system configuration. As far as the end R block average relay is concerned, when considering the faults from the receiving end, unlike the case for the simple source model (as shown by Table 8.2, which shows that the capacitor spark gap operating times are identical for faults from either end) the behaviour of the capacitor spark gap is very different. Table 8.6 shows that there is no flashover for faults up to about 150 km, the capacitor flashes over for faults between 150-175 km and then stays in the circuit for faults subsequently. Theoretically, all faults up to about 150 km and again between 175-240 km should be picked up by the relay, but the results show that these limits are about 140 km and 185-200 km as shown by Figure 8.22.

The sequence comparator relay (again set with capacitor in the circuit) at end S has a similar performance to the block average, except that it operates faster for the majority of faults. Like the block average relay it has a similar sort of narrow band (between about 142-150 km) of no-operation and this is in contrast to the results of corresponding

case for the system with a capacitor at either end (Figure 8.17) which failed to show such a band. The relay then picks up faults up to about 200 km, similar to the block average relay. As regards the receiving end relay, the band of no-operation is similar to the end S and the relay then picks up faults for 150 km to only about 175 km. The results are again summarised in Table 8.6 and Figure 8.22 gives the corresponding response characteristic.

When the relays are set without the capacitor in the circuit, both types of relays tend to overreach, as shown by Table 8.6.

When the degree of series compensation is increased to 50%, the band of no-operation for the sending end relay (both for block average and sequence comparator) is increased very considerably as shown by the response curve of Figure 8.23. This again is attributed to the effect the flashing over of the capacitor has on a relay initially set with the capacitor in the circuit. With reference to the mho characteristic of Figure 4.3, it can again be seen that irrespective of whether the capacitor flashes over or not, the relay would always pick up faults in the region AB, which correspond to a maximum fault point of about 91 km and would fail to

do so if there is a capacitor flashover for subsequent faults. In this particular case Table 8.7 shows that for faults from the sending end the capacitor sparks over for faults between about 75-150 km and then stays in the circuit for the rest of the fault positions, and this means that the no-operation band should be between about 90-150 km. Figure 8.23 clearly shows this to be approximately the case for both the block average and sequence comparator sending end relays. The upper limits of operation for the two relays is, however, reached at about 175 km as opposed to the limit of 240 km, this discrepancy again is due to the effect the system configuration has on relay performances.

In the case of end R relay (when considering faults from the receiving end), Table 8.7 shows that the capacitor does not flashover for faults up to about 150 km and then flashes over for all faults subsequently. This means that the relay should theoretically pick up all faults up to about 150 km and restrain subsequently. However, as shown by Figure 8.23, this is not quite the case and it can be seen that both the block average and sequence comparator relays reach the limit for faults up to 80 km.

| Distance from S.E. or R.E. (km) | Sending End | | | Receiving End | | |
|---|---|---|---|---|---|---|
| | Cap.F/O instant (ms) | B/A trip time (ms) | S/C trip time (ms) | Cap.F/O instant (ms) | B/A trip time (ms) | S/C trip time (ms) |
| 0.00 | no F/O | 13.25 | 12.25 | no F/O | 12.75 | 12.00 |
| 40.00 | " | 18.5 | 16.50 | - | - | - |
| 60.00 | - | - | - | no F/O | 36.00 | 16.75 |
| 75.00 | 18.00 | 30.25 | 18.25 | " | 37.25 | 18.25 |
| 78.75 | - | 39.75 | - | - | 40.00 | 18.50 |
| 88.00 | - | restrain | 30.50 | - | - | - |
| 90.00 | 17.50 | " | restrain | - | - | - |
| 100.00 | 17.25 | " | " | - | - | - |
| 115.00 | - | - | - | no F/O | restrain | restrain |
| 150.00⁻ | 16.00 | restrain | restrain | " | " | " |
| 150.00 | no F/O | 37.25 | 20.50 | 21.00 | " | " |
| 165.00 | " | 68.00 | 20.50 | - | - | - |
| 173.00 | " | 70.50 | 20.50 | - | - | - |
| 180.00 | " | " | restrain | - | - | - |
| 185.00 | " | restrain | " | - | - | - |
| 200.00 | " | " | " | 22.25 | restrain | restrain |
| 240.00 | " | " | " | 23.25 | " | " |

Table 8.7 Capacitor at mid-point (amount of compensation = 50%). Multi-section feeder. Relay setting with capacitor in circuit. Block average and sequence comparator relay operating time.

### 8.5.3 Dependent Modes of Operation

#### 8.5.3.1 Permissive Overreach (Transfer Tripping) Scheme

##### 8.5.3.1.1 A capacitor at each end

Table 8.8 gives details of operating times obtained for the permissive overreach scheme, utilising both the block average and the sequence comparator relays, both relays being set to 120% as shown by Figure 4.5(a). The relay responses are as shown in Figure 8.24. It can be seen that the protection scheme employing both the block average and sequence comparator relays gives the full 100% coverage. As regards the operating times, however, there is a wide variation for both type of relays and this very much depends on the fault position. In the case of the scheme employing block average relays, the operating times for both sending end and the receiving end schemes are around 16-22ms for majority of faults, and rising to about 27ms for faults close to the busbar. This wide variation can be attributed not only to the interdependency of the sending end and receiving end protective schemes, but also due to the random nature of the capacitor spark gap operation as shown in Table 8.8. In the case of the scheme employing sequence comparator relays, the overall response is superior, in terms of operating times being about 17ms for the majority of faults. The end S scheme has a uniform operating time throughout except for faults at the remote end, where the operating time rises to about 20ms. However, the scheme employing sequence comparator at end R has an operating time of about 26ms for faults

| Distance from S.E. or R.E. (km) | F/O instant (ms) | | Sending End | | Receiving End | |
|---|---|---|---|---|---|---|
| | For S.E. Cap. | For R.E. Cap. | With B/A trip time (ms) | With S/C trip time (ms) | With B/A trip time (ms) | With S/C trip time (ms) |
| 0.00 | no F/O | no F/O | 26.75 | 17.50 | 26.50 | 25.5 |
| 40.00 | 18.50 | " | 22.25 | 17.25 | - | - |
| 60.00 | N | 6.25 | - | - | 20.25 | 19.75 |
| 75.00 | O | 7.00 | 21.50 | 16.75 | 21.25 | 19.50 |
| 100.00 | F | 15.50 | 18.25 | 16.00 | - | - |
| 150.00 | L | 17.00 | 16.25 | 16.00 | 18.50 | 16.50 |
| 200.00 | A S | no F/O | - | - | 16.25 | 16.50 |
| 225.00 | H | " | 16.50 | 15.25 | 16.50 | 16.00 |
| 240.00 | O | " | 16.25 | 15.25 | - | - |
| 260.00 | V | " | - | - | 17.25 | 15.75 |
| 300.00 | E R | " | 21.50 | 20.50 | 21.75 | 12.50 |

Table 8.8 A capacitor at each end. Multi-section feeder. Permissive overreach scheme operating times.

up to 20% of the line length and a shorter operating time of about 12.5ms for faults from about 85% of the line length onwards. It can be clearly seen that the scheme employing the block average relay is more affected by the random nature of the spark gap than the scheme employing the sequence comparator relays, this being more noticeable for faults close to the two ends of the protected feeder.

8.5.3.1.2 A capacitor at mid-point

When a single capacitor is placed at the mid-point with 30% series compensation, the relay responses are as shown in Figure 8.25, and the operating times are summarised in Table 8.9. Again, full coverage is attained using such a scheme (for both block average and sequence comparator relays). Similar sort of responses to the previous case (Figure 8.24) are obtained, except for responses close to the two ends. In the case of the block average relay in particular, the end S scheme for close up and remote end faults has operating times of about 24 and 25 ms respectively, compared to 26 and 21 ms for the previous case (Figure 8.24), and the end R scheme operating times for close up and remote end faults are about 20ms compared to 26 and 22 ms for the previous case.

When the amount of compensation is increased to 50%, the relay responses are as shown in Figure 8.26. The

| Distance from S.E. or R.E. (km) | Sending End | | | Receiving End | | |
|---|---|---|---|---|---|---|
| | Cap. F/O instant (ms) | With B/A trip time (ms) | With S/C trip time (ms) | Cap. F/O instant (ms) | With B/A trip time (ms) | With S/C trip time (ms) |
| 0.00 | no F/O | 24.25 | 17.75 | no F/O | 20.50 | 26.00 |
| 25.00 | - | - | - | " | 22.50 | 26.25 |
| 60.00 | no F/O | 22.00 | 16.75 | - | - | - |
| 75.00 | - | - | - | no F/O | 17.50 | 19.50 |
| 100.00 | no F/O | 18.25 | 16.50 | - | - | - |
| 150.00 | 17.50 | 15.75 | 16.00 | no F/O | 18.50 | 16.75 |
| 150.00 | no F/O | 16.25 | 16.25 | 17.50 | 18.50 | 17.25 |
| 200.00 | - | - | - | no F/O | 16.75 | 17.00 |
| 225.00 | no F/O | 17.50 | 15.75 | - | - | - |
| 240.00 | - | - | - | no F/O | 17.00 | 16.50 |
| 275.00 | no F/O | 17.75 | 21.25 | - | - | - |
| 300.00 | " | 25.50 | 21.00 | no F/O | 19.25 | 12.75 |

Table 8.9 A capacitor at mid-point (30% compensation). Multi-section feeder. Permissive overreach scheme operating time.

scheme employing both the block average and sequence comparator relays gives 100% coverage and the responses are similar to the case of a capacitor at each end, with 70% compensation (Figure 8.24). Table 8.10 summarises the relay operating times.

8.5.3.2 Blocking Schemes

8.5.3.2.1 A capacitor at each end

Table 8.11 gives details of the operating times for a blocking scheme employing both block average and sequence comparator relays set to 150%, as shown by the mho characteristic of Figure 4.5(b). The relay responses are shown in Figure 8.27. Comparing this with the corresponding case for the permissive overreach scheme (Figure 8.24), it can be seen that the blocking scheme, for majority of faults, has a much superior response than the latter, especially in terms of operating times (being 17-20ms as compared to 16-22 ms for the former). Also, for such faults the response remains uniform and the operating times do not vary a lot from one fault position to the other, unlike the permissive overreach scheme. This is particularly so for the scheme employing the block average relay. The end S block average relay operating time remains more or less uniform for the entire feeder length, whereas the end R remains so for faults up to 75% of the line length, and thereafter the operating time rises to about 26ms. As regards the scheme employing sequence comparator relay

| Distance from S.E. or R.E. (km) | Sending End | | | Receiving End | | |
|---|---|---|---|---|---|---|
| | Cap. F/O instant (ms) | With B/A trip time (ms) | With S/C trip time (ms) | Cap. F/O instant (ms) | With B/A trip time (ms) | With S/C trip time (ms) |
| 0.00 | no F/O | 26.25 | 17.50 | no F/O | 25.00 | 25.50 |
| 40.00 | " | 23.25 | 17.00 | - | - | - |
| 60.00 | - | - | - | no F/O | 19.25 | 19.25 |
| 75.00 | 18.00 | 23.50 | 16.50 | " | 18.75 | 15.50 |
| 100.00 | 17.25 | 18.25 | 16.25 | - | - | - |
| 150.00⁻ | 16.00 | 17.25 | 15.75 | no F/O | 18.00 | 15.50 |
| 150.00 | no F/O | 16.25 | 16.00 | 16.00 | 18.50 | 17.25 |
| 200.00 | - | - | - | 17.25 | 16.75 | 17.00 |
| 225.00 | no F/O | 17.50 | 15.75 | 18.00 | 18.50 | 16.75 |
| 240.00 | " | 17.75 | 15.75 | - | - | - |
| 260.00 | - | - | - | no F/O | 18.25 | 12.00 |
| 300.00 | no F/O | 20.00 | 20.50 | " | 21.25 | 12.50 |

Table 8.10 A capacitor at mid-point (50% compensation). Multi-section feeder. Permissive overreach scheme operating time.

| Distance from S.E. or R.E. (km) | F/O instant (ms) | | Sending End | | Receiving End | |
|---|---|---|---|---|---|---|
| | For S.E. Cap. | For R.E. Cap. | With B/A trip time (ms) | With S/C trip time (ms) | With B/A trip time (ms) | With S/C trip time (ms) |
| 0.00 | no F/O | no F/O | 17.25 | 11.50 | 17.00 | 11.50 |
| 40.00 | 18.50 | " | 16.50 | 15.75 | - | - |
| 60.00 | N | 6.25 | - | - | 16.25 | 15.25 |
| 75.00 | O | 7.00 | 19.50 | 16.00 | 16.25 | 15.25 |
| 100.00 | F | 15.50 | 17.75 | 16.00 | - | - |
| 150.00 | L | 17.00 | 18.00 | 16.50 | 15.75 | 16.00 |
| 200.00 | A | no F/O | - | - | 16.25 | 16.50 |
| 225.00 | S H | " | 19.25 | 15.50 | 15.75 | 16.50 |
| 240.00 | O | " | 18.25 | 19.75 | - | - |
| 260.00 | V E | " | - | - | 22.00 | 17.00 |
| 300.00 | R | " | 18.50 | 18.50 | 25.75 | 17.25 |

Table 8.11 A capacitor at each end. Multi-section feeder. Blocking scheme operating time.

at end S, for close up faults (ie up to about 20% of the line length), the operating time is lower and is about 11.5 ms. This is also the case for the end R scheme employing sequence comparator relay, the latter being in marked contrast to the permissive overreach scheme (Figure 8.24) where the operating time increases to about 26ms for close up faults.

8.5.3.2.2 A capacitor at mid-point

When a single capacitor in the middle is considered and with 30% compensation the relay responses are as shown in Figure 8.28, which are quite similar to Figure 8.27, except for faults close to the two ends of the protected feeder. The end R scheme employing block average relay operating time for such fault conditions reduces to about 21.5ms compared to 26ms (Figure 8.27) and the end R scheme employing sequence comparator scheme increases to about 26ms compared to 20ms (Figure 8.27). Also, comparing Figure 8.28 with the corresponding case for the permissive overreach scheme (Figure 8.25) it can be seen that the operating times utilising the blocking scheme are faster then the latter. Table 8.12 summarises both the relay operating times and it also shows the random nature of the capacitor flashover.

When the compensation is increased to 50%, the relay responses are as shown in Figure 8.29. In this case,

| Distance from S.E. or R.E. (km) | Sending End | | | Receiving End | | |
|---|---|---|---|---|---|---|
| | Cap.F/O instant (ms) | With B/A trip time (ms) | With S/C trip time (ms) | Cap.F/O instant (ms) | With B/A trip time (ms) | With S/C trip time (ms) |
| 0.00 | no F/O | 17.25 | 11.50 | no F/O | 17.00 | 11.25 |
| 25.00 | - | - | - | " | 17.75 | 16.00 |
| 60.00 | no F/O | 16.00 | 16.50 | - | - | - |
| 75.00 | - | - | - | no F/O | 17.25 | 15.75 |
| 100.00 | no F/O | 16.75 | 16.50 | - | - | - |
| 150.00⁻ | 17.50 | 18.00 | 17.00 | no F/O | 16.25 | 16.25 |
| 150.00 | no F/O | 18.00 | 16.75 | 17.50 | 15.75 | 16.00 |
| 200.00 | - | - | - | no F/O | 17.75 | 16.50 |
| 225.00 | no F/O | 20.25 | 15.50 | - | - | - |
| 240.00 | - | - | - | no F/O | 21.00 | 16.75 |
| 275.00 | no F/O | 20.00 | 20.25 | - | - | - |
| 300.00 | " | 20.00 | 26.00 | no F/O | 21.75 | 17.50 |

Table 8.12 A capacitor at mid-point (30% compensation). Multi-section feeder. Blocking scheme operating time.

the responses are quite similar to the case where a capacitor is located at each end and with associated 70% compensation. Here again the uniformity of the operating times for a majority of faults can be clearly seen unlike the corresponding case for the permissive overreach scheme as shown by Figure 8.26. Table 8.13 summarises the relay operating times.

| Distance from S.E. or R.E. (km) | Sending End | | | Receiving End | | |
|---|---|---|---|---|---|---|
| | Cap.F/O instant (ms) | With B/A trip time (ms) | With S/C trip time (ms) | Cap.F/O instant (ms) | With B/A trip time (ms) | With S/C trip time (ms) |
| 0.00 | no F/O | 17.25 | 11.50 | no F/O | 17.00 | 11.25 |
| 40.00 | " | 15.50 | 11.50 | - | - | - |
| 60.00 | - | - | - | no F/O | 17.25 | 16.00 |
| 75.00 | 18.00 | 16.25 | 16.50 | " | 17.25 | 15.75 |
| 100.00 | 17.25 | 16.25 | 16.50 | - | - | - |
| 150.00⁻ | 16.00 | 18.00 | 17.00 | no F/O | 16.25 | 16.25 |
| 150.00 | no F/O | 17.50 | 16.25 | 16.00 | 16.25 | 15.75 |
| 200.00 | - | - | - | 17.25 | 17.75 | 16.25 |
| 225.00 | no F/O | 18.75 | 15.50 | 18.00 | 22.00 | 16.50 |
| 240.00 | " | 18.25 | 15.50 | - | - | - |
| 260.00 | - | - | - | no F/O | 23.00 | 17.00 |
| 300.00 | no F/O | 19.50 | 19.25 | " | 23.75 | 17.75 |

Table 8.13 A capacitor at mid-point (50% compensation). Multi-section feeder. Blocking scheme operating time.

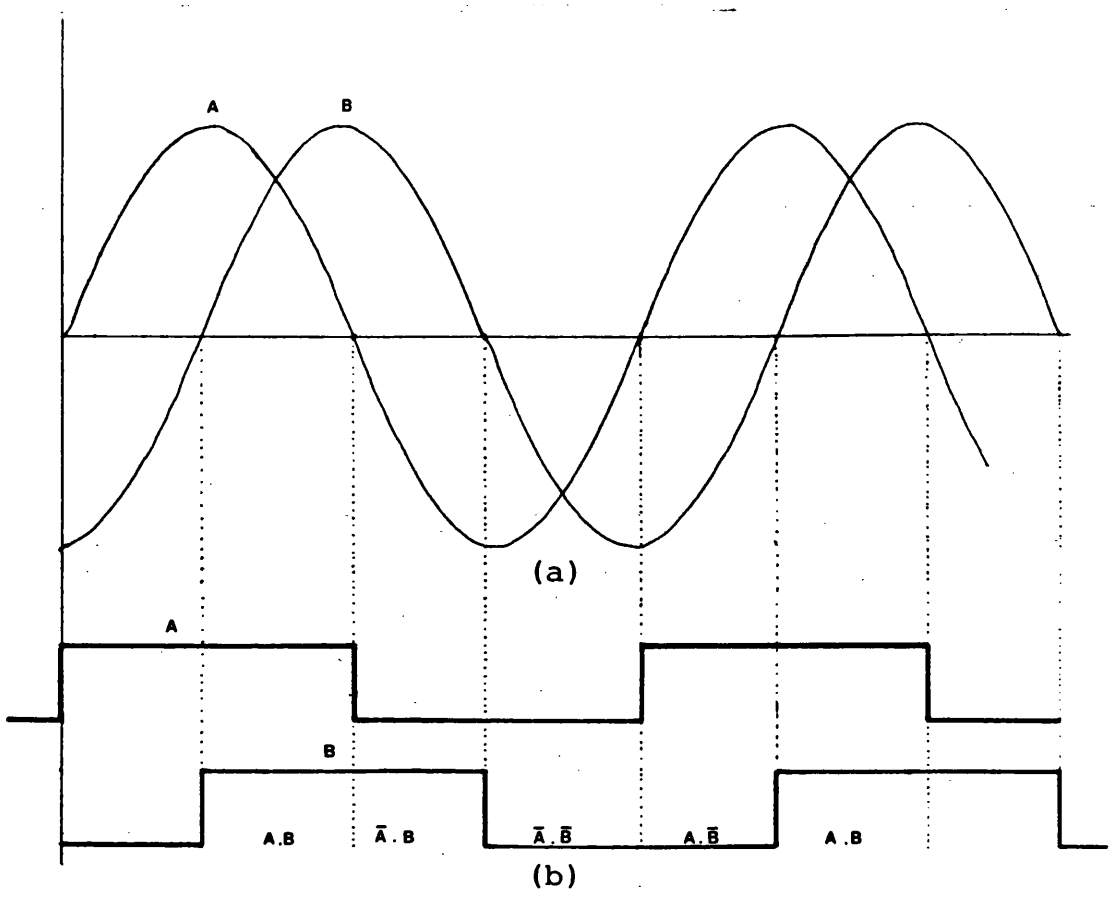


Figure 8.1 Effect of logic variables for comparator (restrain condition)

(a) squared inputs (b) logical states

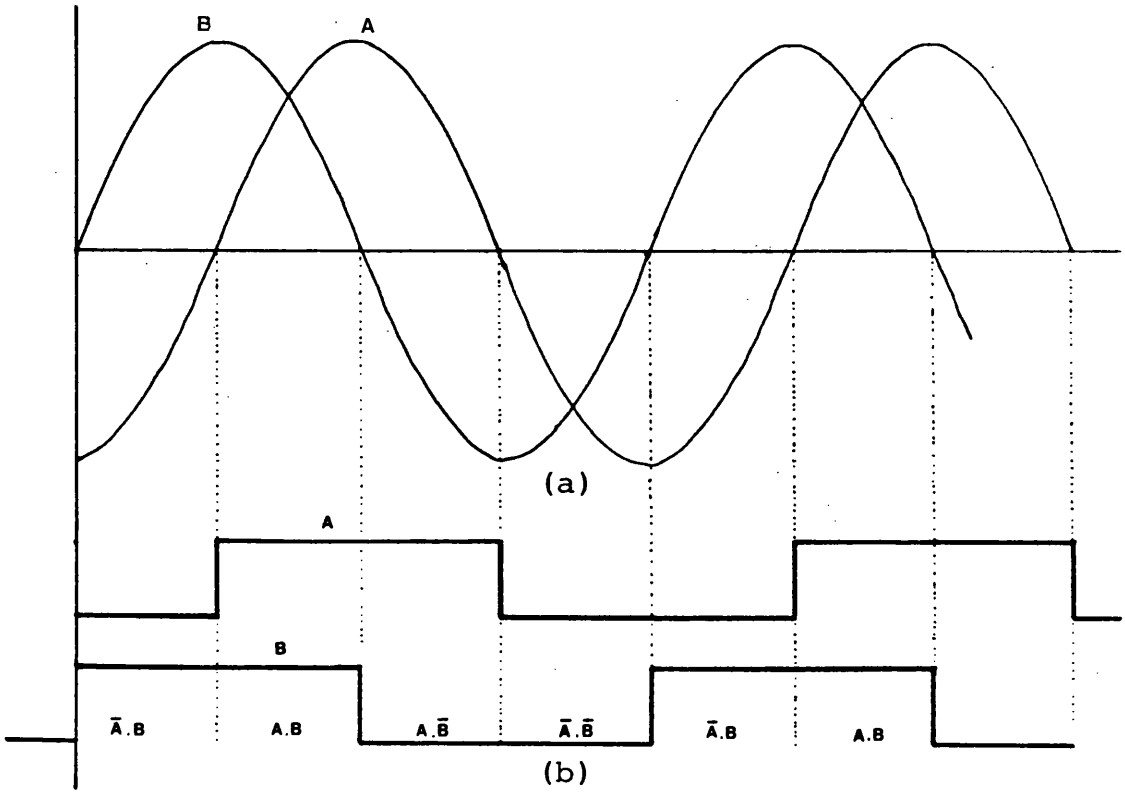


Figure 8.2 Effect of logic variables for comparator (operate condition)

(a) squared inputs

(b) logical states

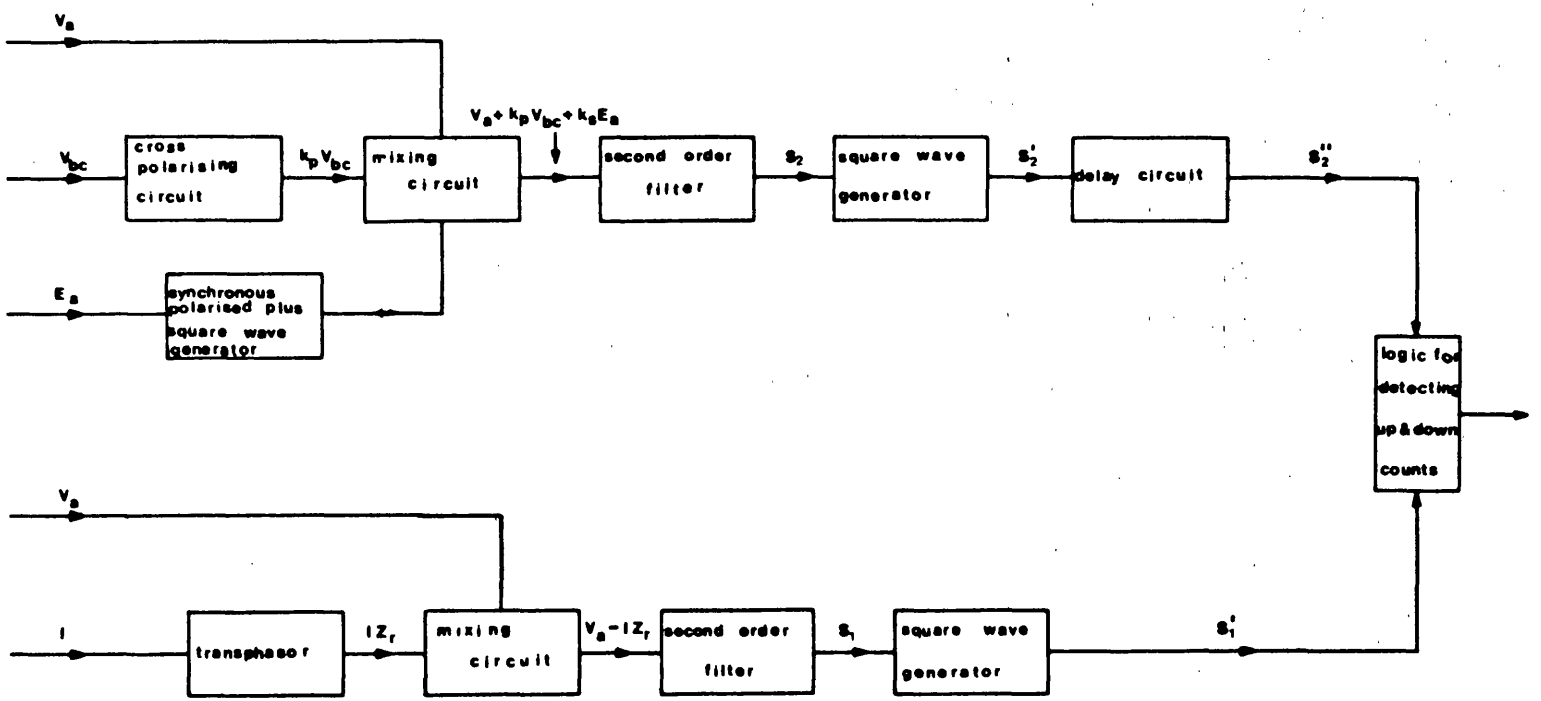


Figure 8.3 Sequence comparator arrangement

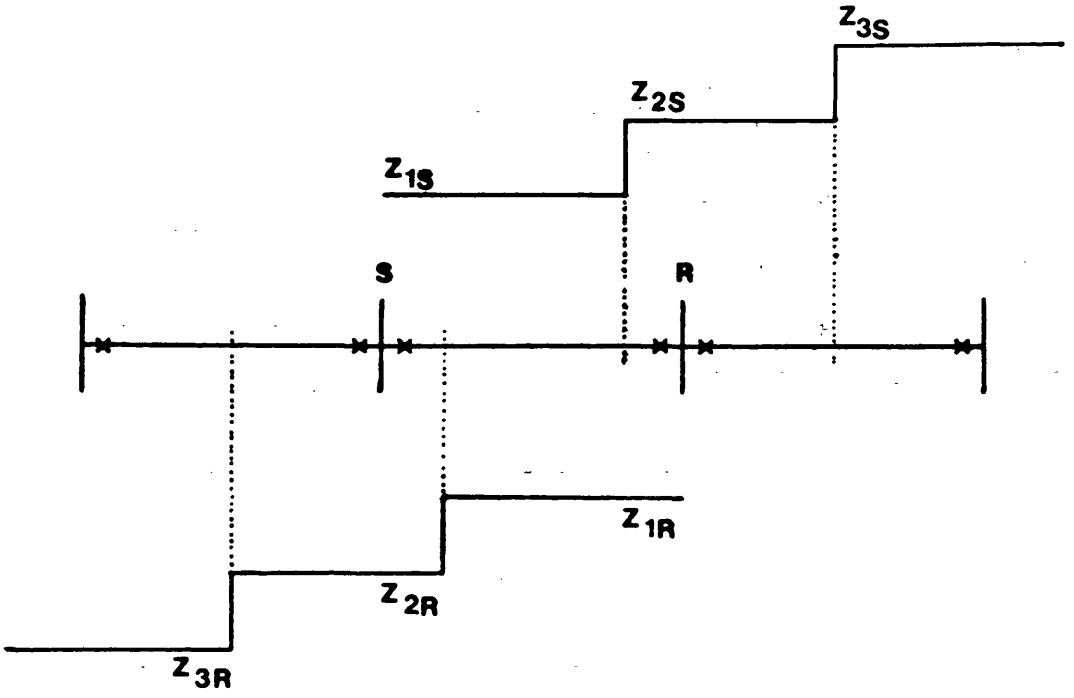


Figure 8.4 Zoning of distance relays

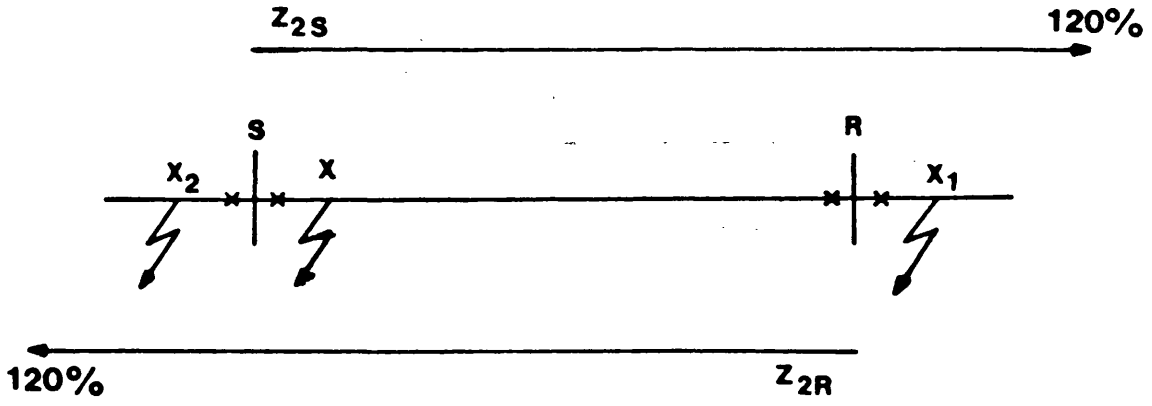


(a)

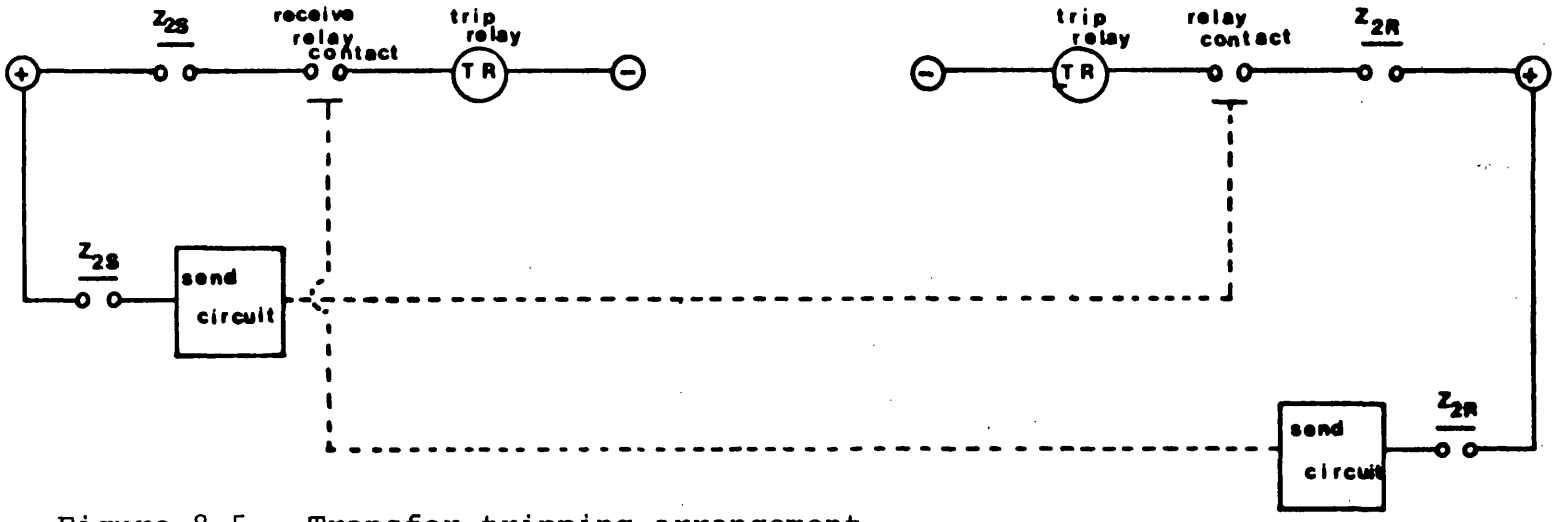


Figure 8.5 Transfer tripping arrangement
(a) Zoning (b) tripping circuit

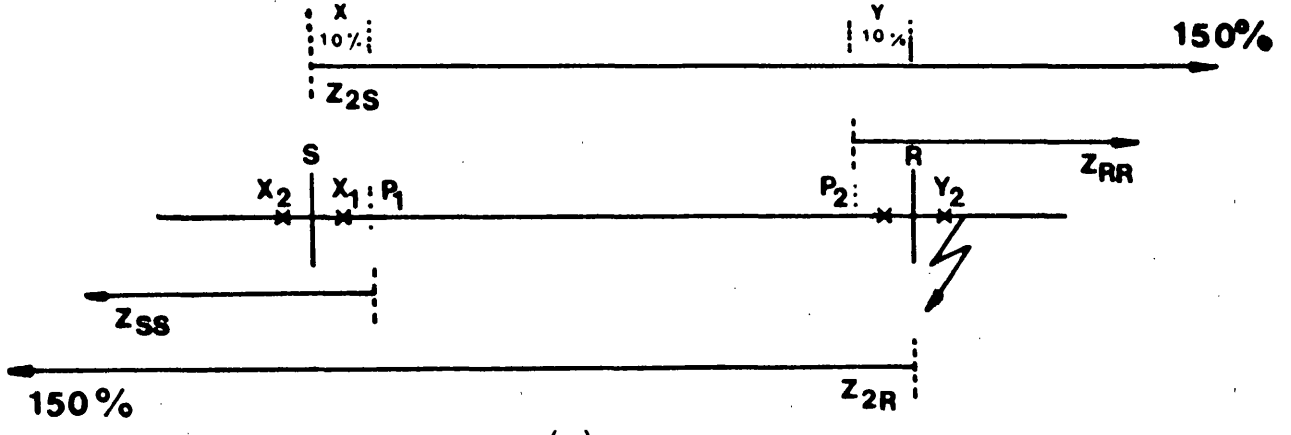


(a)

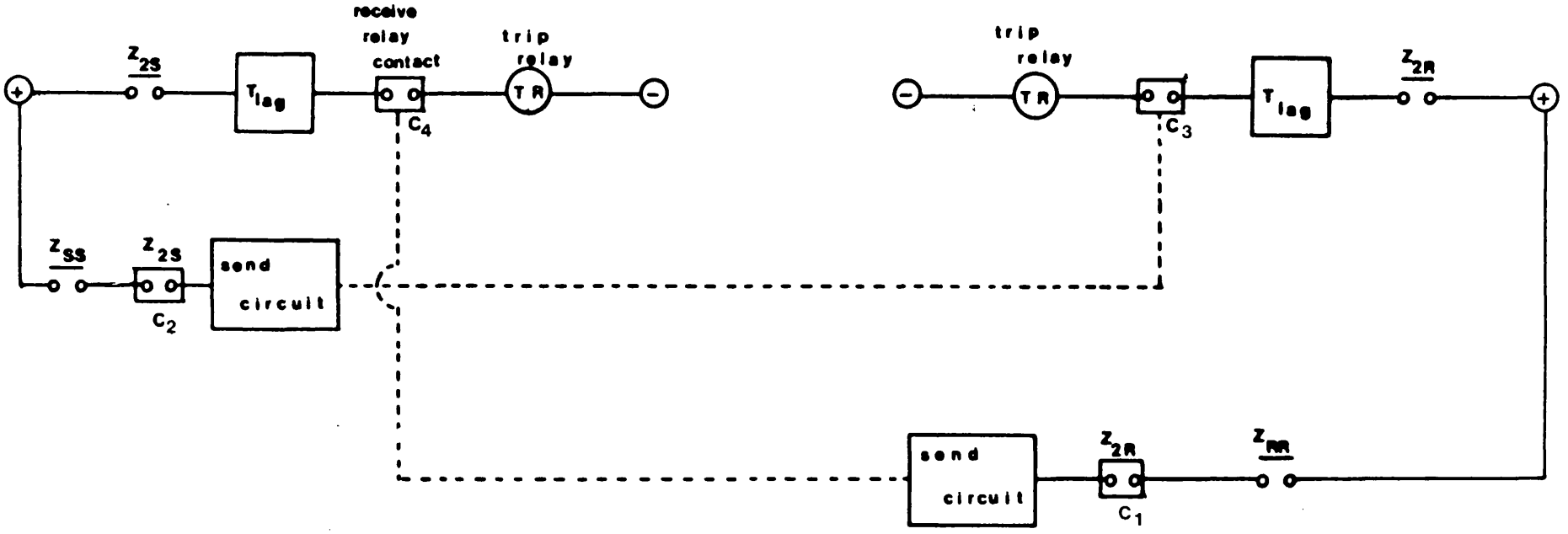


(b)

Figure 8.6 Blocking arrangement

(a) Zoning

(b) Tripping circuit

Fig. 8.7

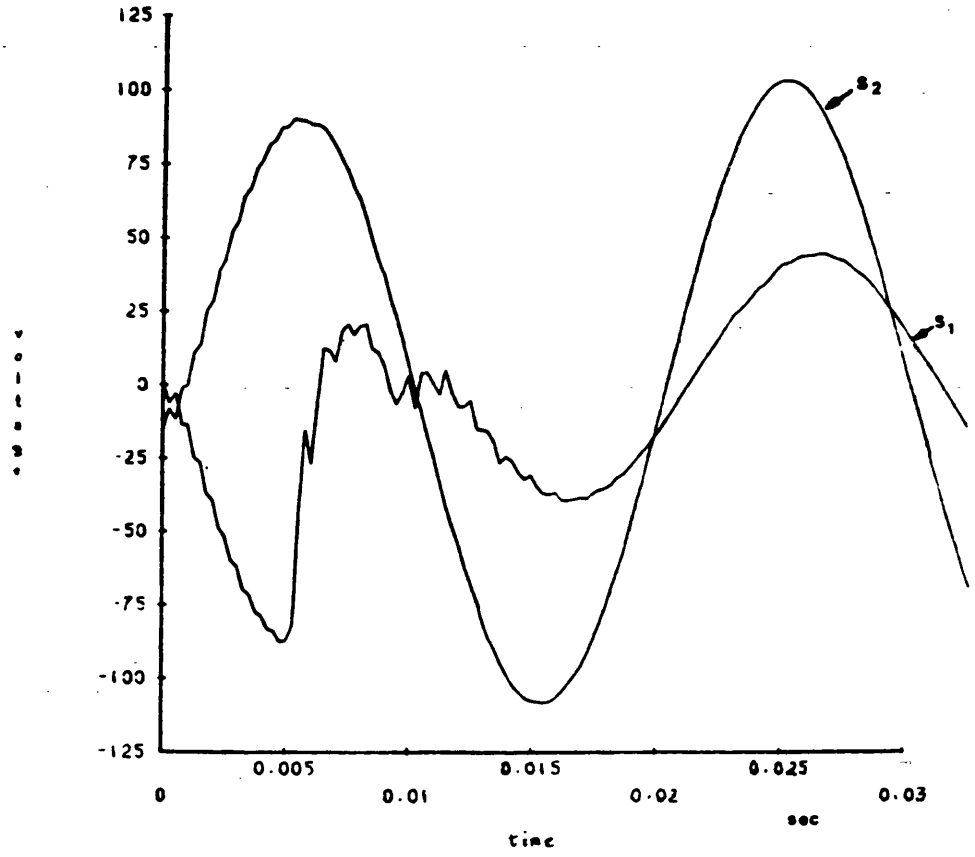
125
100
75
50
25
0
-25
-50
-75
-100
-125
0
0.005
0.01
0.015
0.02
0.025
0.03
sec
time
$S_2$
$S_1$

(a)

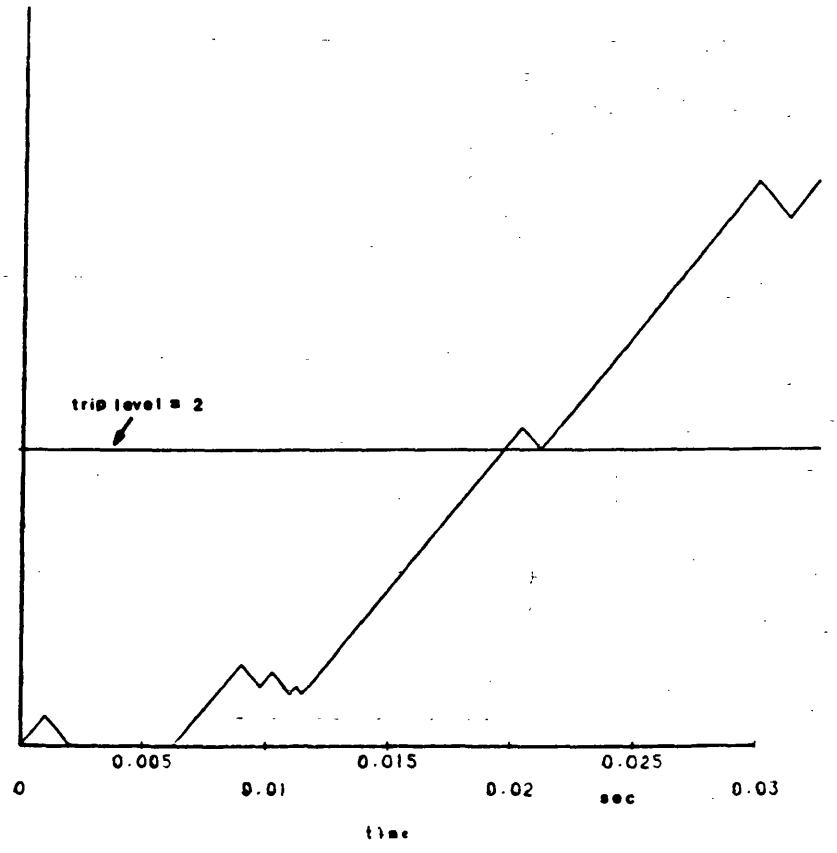
trip level = 2
0.005
0.015
0.025
0
0.01
0.02
sec
0.03
time

(b)

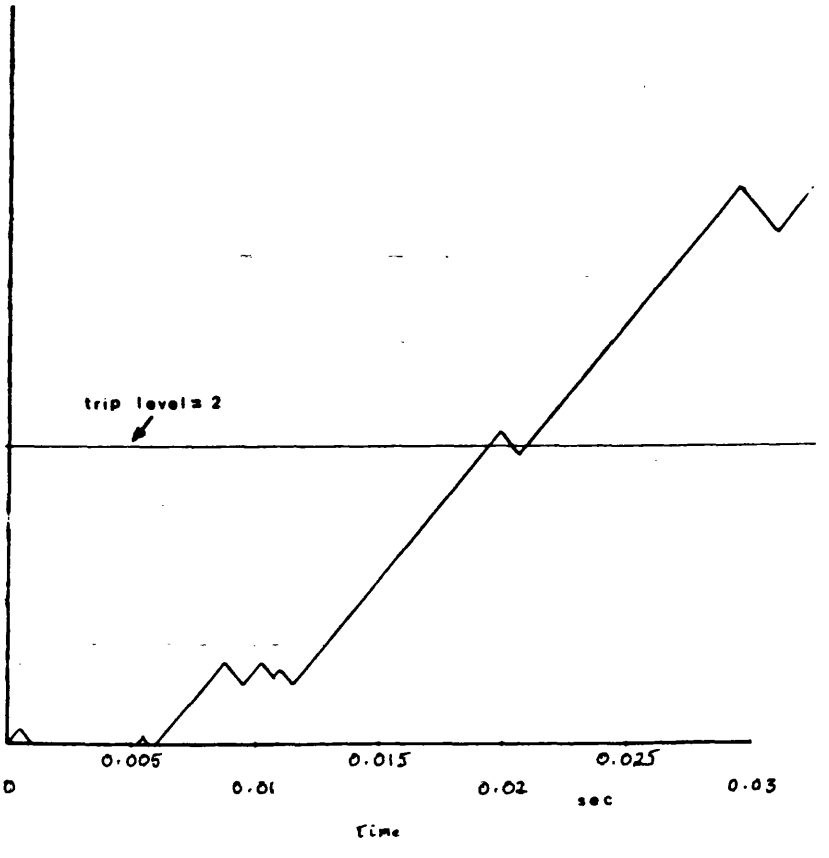
trip level = 2
0.005
0.015
0.025
0
0.01
0.02
sec
0.03
time

(c)

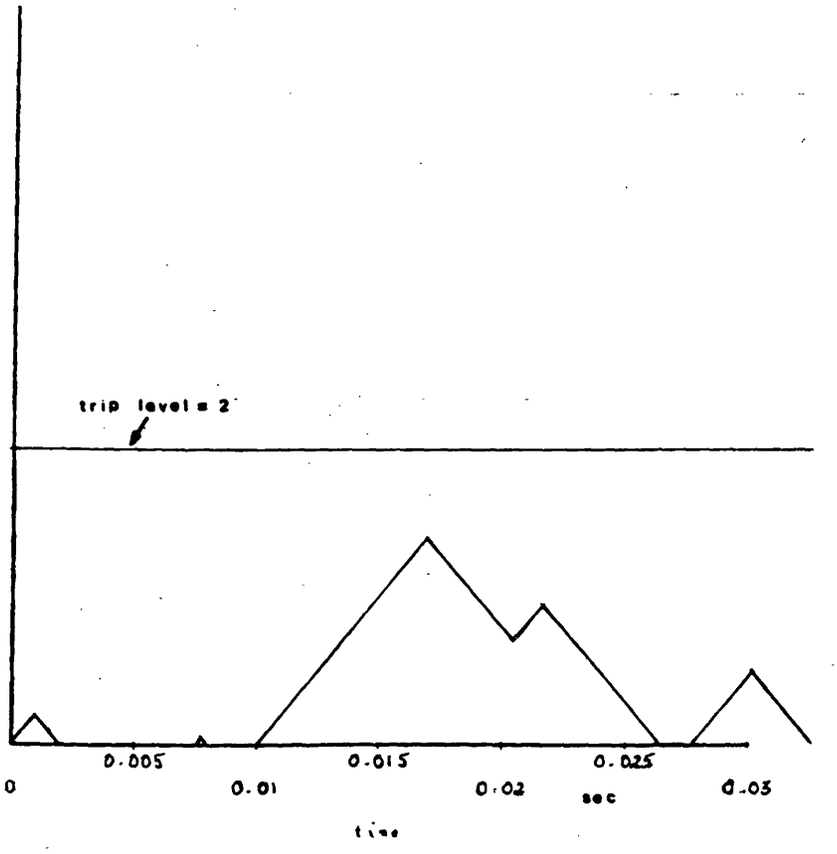
trip level = 2
0.005
0.015
0.025
0
0.01
0.02
sec
0.03
time

(d)

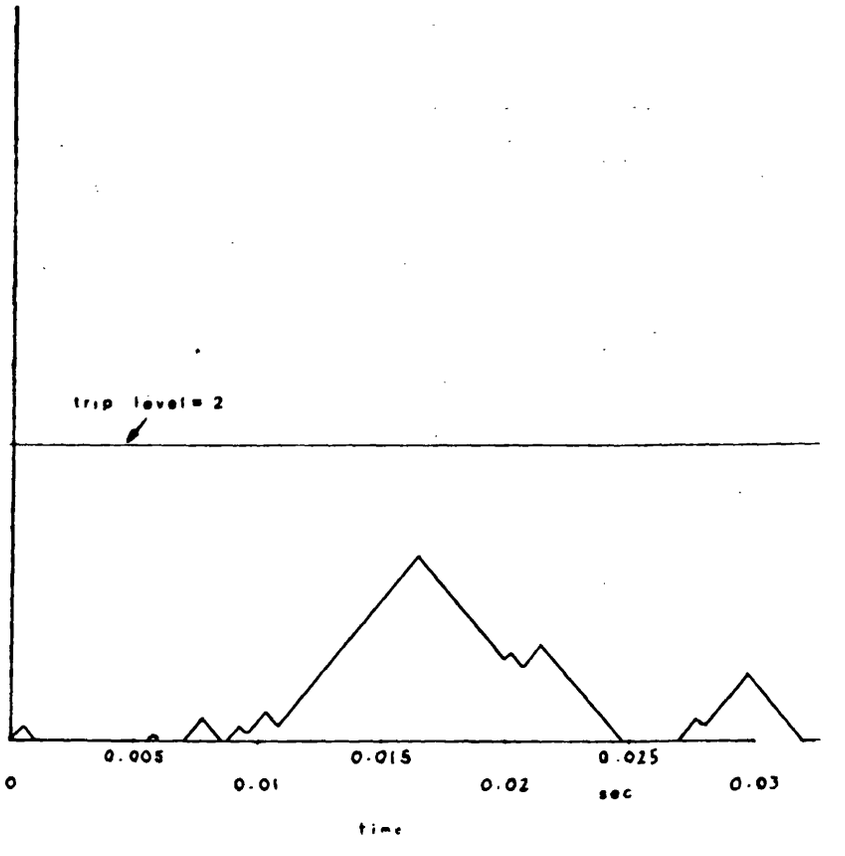
trip level = 2
0.005
0.015
0.025
0
0.01
0.02
sec
0.03
time

(e)

Figure 8.7

Single section feeder; a capacitor at each end.
B/A relay (setting with capacitor in the circuit).
Faults at voltage maximum.

(a) Relaying signals $S_1$ & $S_2$, fault at 75km from the S.E.

(b) S.E. relay integrator output, fault at 75km from the S.E.

(c) R.E. relay integrator output, fault at 75km from the R.E.

(d) S.E. relay integrator output, fault at mid-point.

(e) R.E. relay integrator output, fault at mid-point.

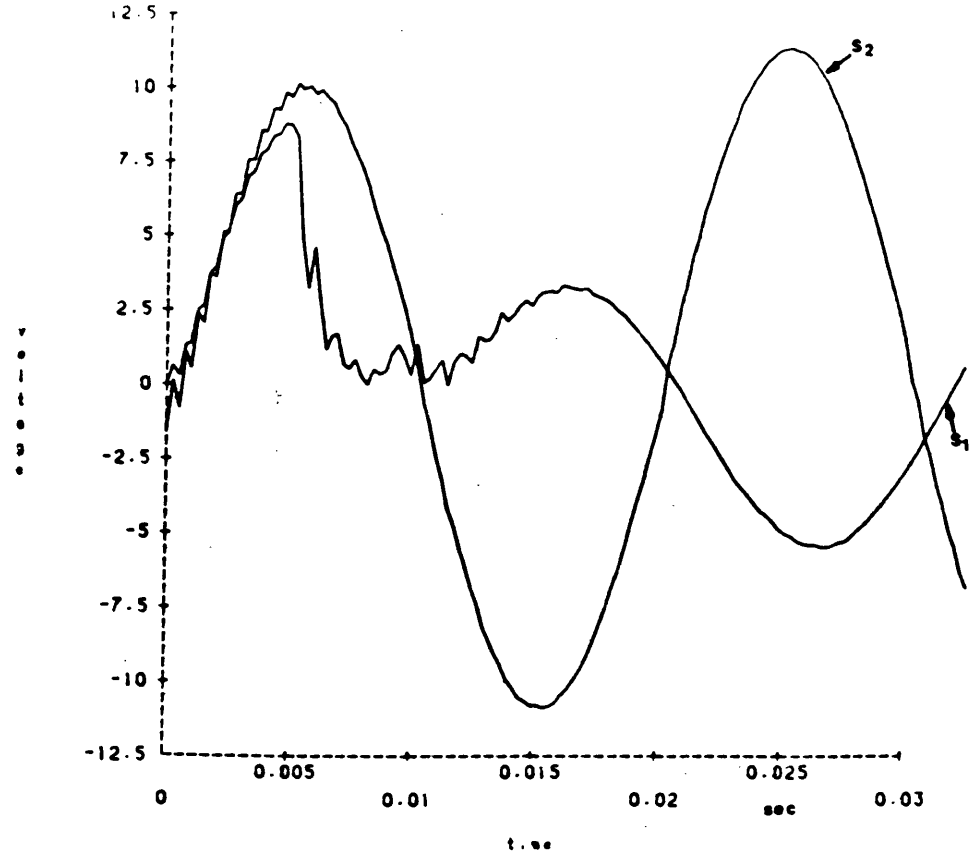


(a)

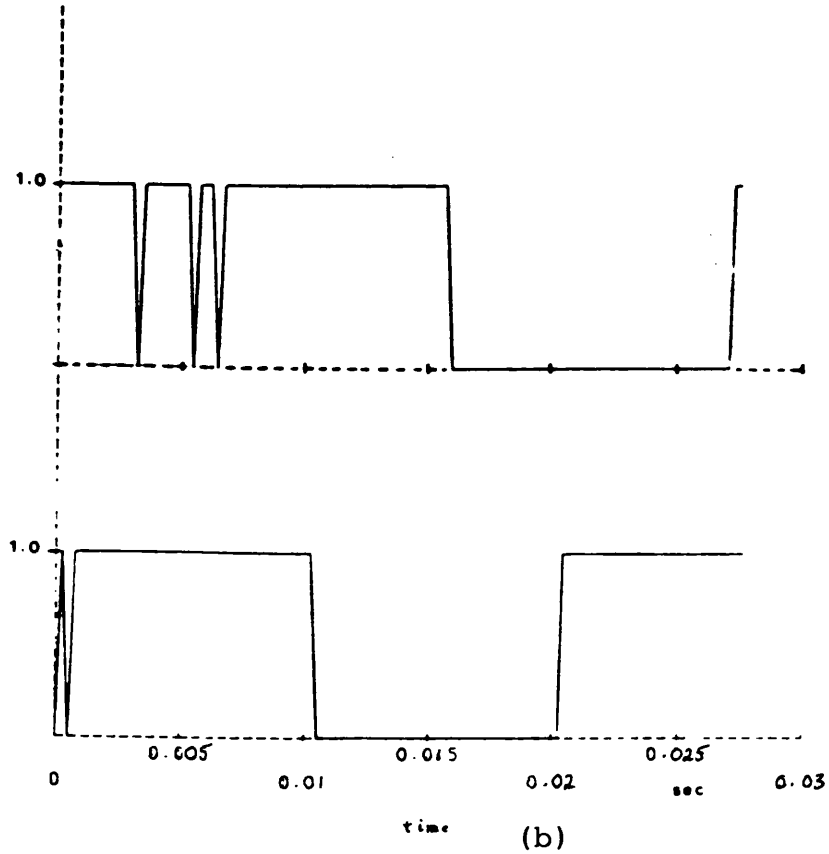


(b)

1 - upcount
2 - downcount

| Time | Count |
|---|---|
| 0.2500 E-03 | 2 |
| 0.5000 E-03 | 1 |
| 0.7500 E-03 | 2 |
| 0.3250 E-02 | 2 |
| 0.3500 E-02 | 1 |
| 0.5500 E-02 | 2 |
| 0.5750 E-02 | 1 |
| 0.6500 E-02 | 2 |
| 0.6750 E-02 | 1 |
| 0.1050 E-01 | 1 |
| 0.1600 E-01 | 1 |
| 0.2050 E-01 | 1 |
| 0.2750 E-01 | 1 |

Figure 8.8 Sequence comparator response, conditions similar to Fig. 8.7(b)

(a) squared inputs
(b) logical states

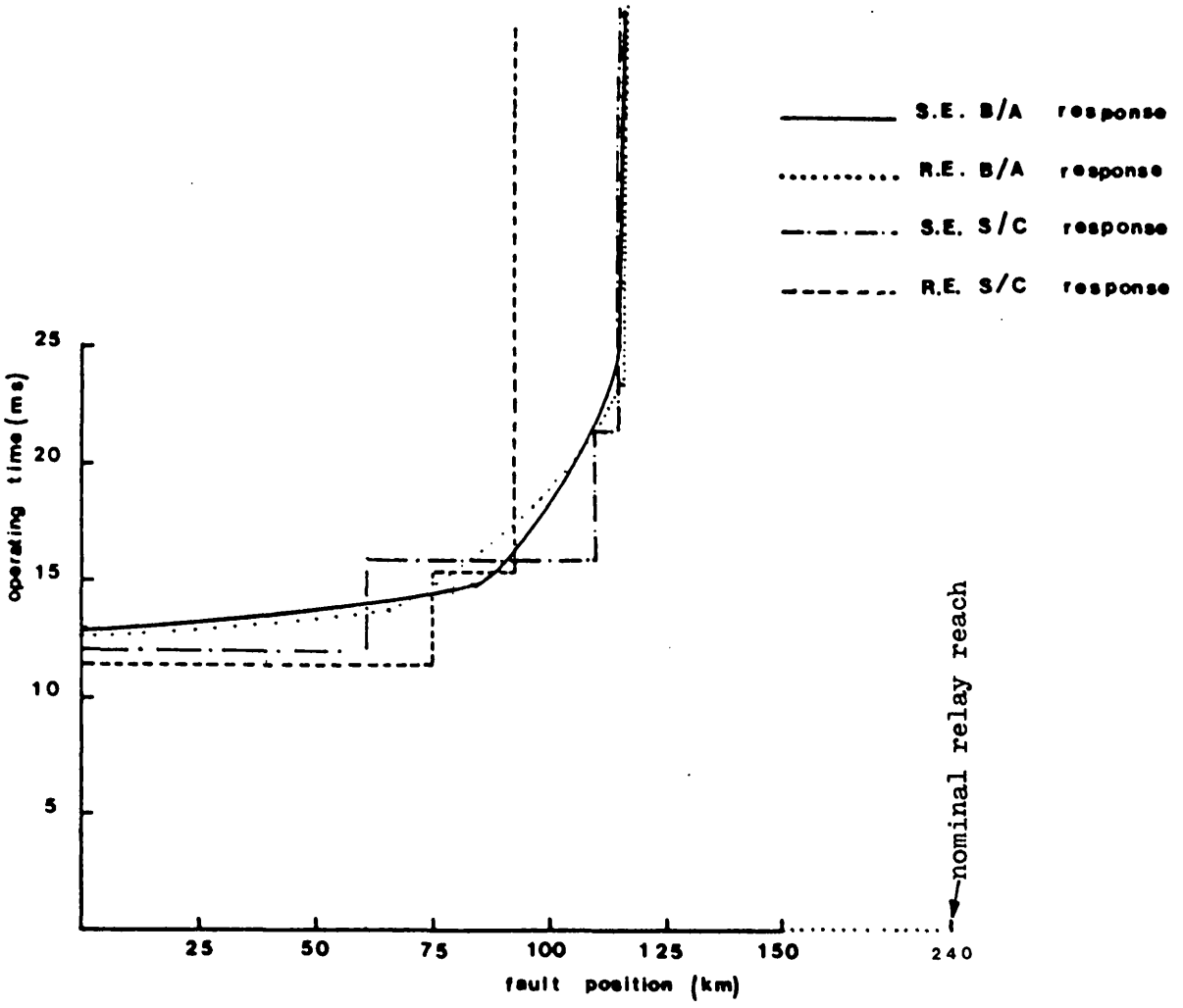


Figure 8.9 Operating characteristics of B/A and S/C relays (relay setting with capacitor in the circuit). Fault conditions are as shown in Table 8.1.

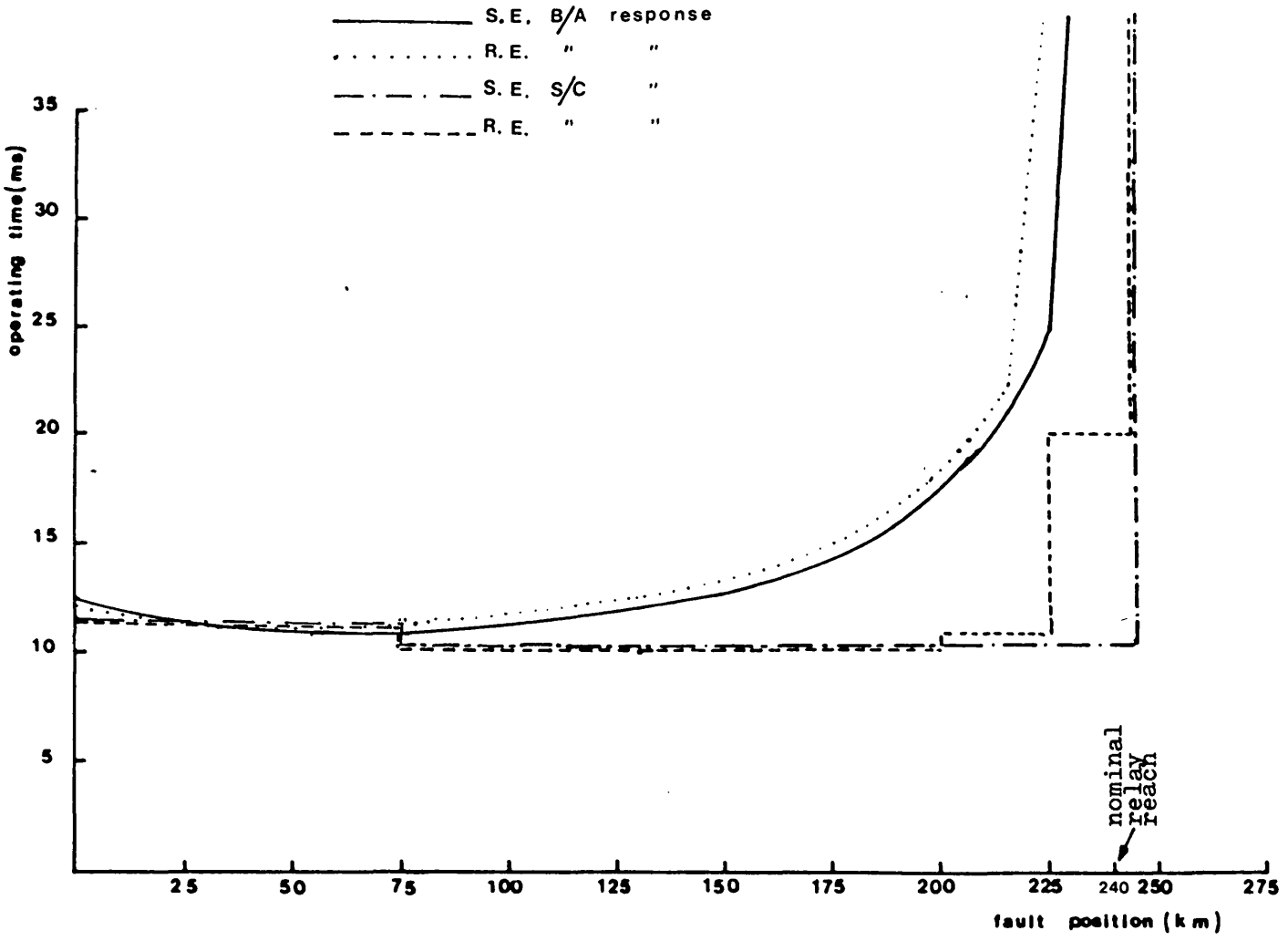


Figure 8.10 Operating characteristics of B/A and S/C relays (relay setting with no capacitor in the circuit). Fault conditions are as shown in Table 8.1.

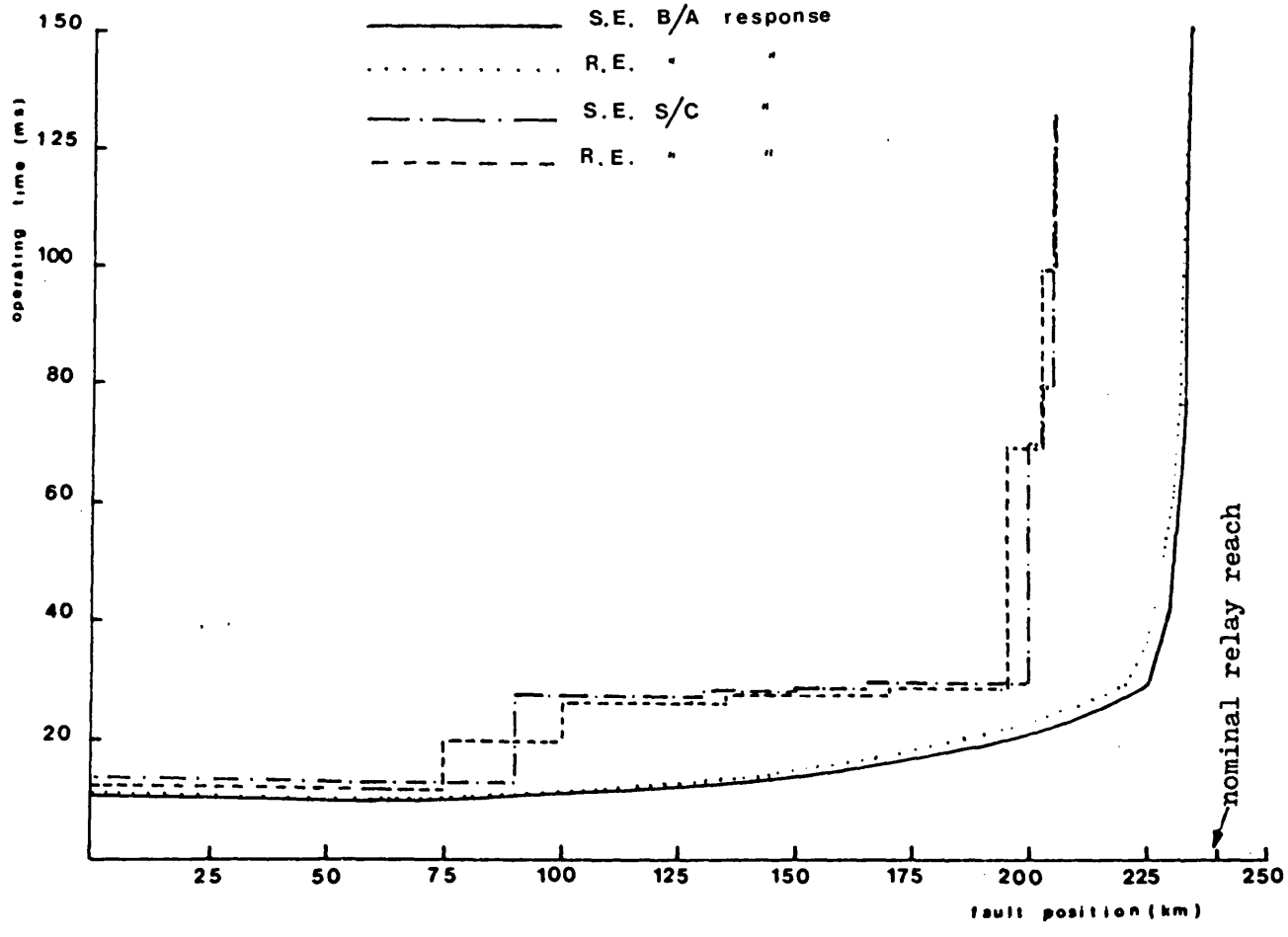


Figure 8.11 Operating characteristics of B/A and S/C relays (relay setting with no capacitor in the circuit). Voltage minimum faults.

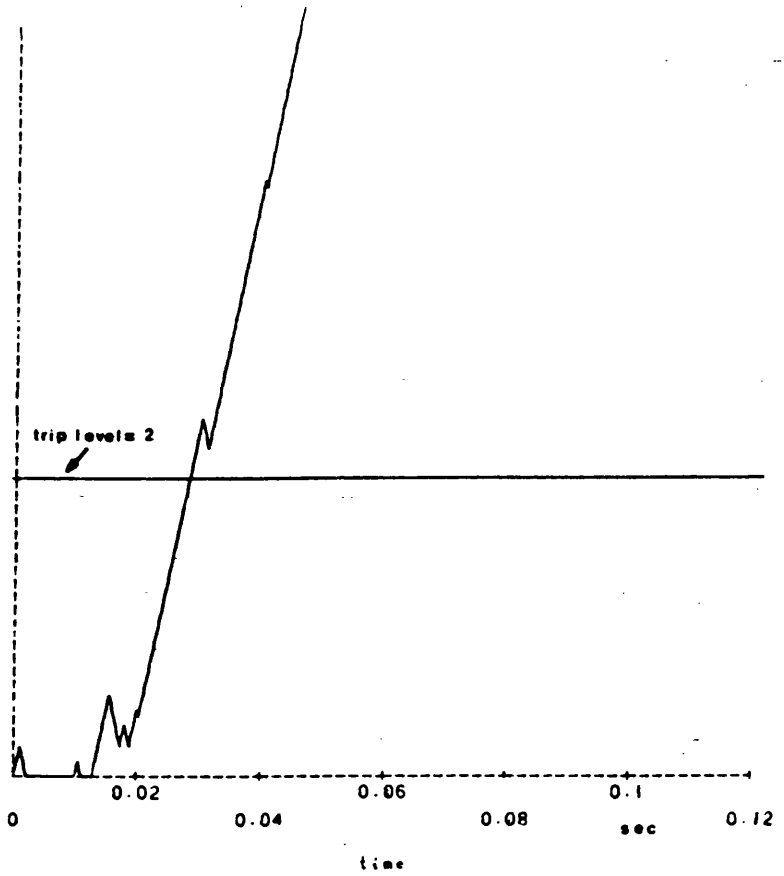


(a)

1 - Upcount
2 - Downcount

| Time | Count |
|---|---|
| 0.2500 E-03 | 2 |
| 0.5000 E-03 | 1 |
| 0.7500 E-03 | 2 |
| 0.5500 E-02 | 2 |
| 0.1050 E-01 | 2 |
| 0.2050 E-01 | 1 |
| 0.3000 E-01 | 1 |
| 0.3050 E-01 | 1 |
| 0.3275 E-01 | 1 |
| 0.4050 E-01 | 1 |
| 0.4850 E-01 | 1 |
| 0.5075 E-01 | 1 |
| 0.5400 E-01 | 1 |
| 0.6050 E-01 | 1 |
| 0.7075 E-01 | 1 |
| 0.7450 E-01 | 1 |
| 0.8050 E-01 | 1 |
| 0.8775 E-01 | 1 |
| 0.9075 E-01 | 1 |
| 0.9475 E-01 | 1 |
| 0.1005 E+00 | 1 |
| 0.1078 E+00 | 1 |
| 0.1107 E+00 | 1 |
| 0.1143 E+00 | 1 |

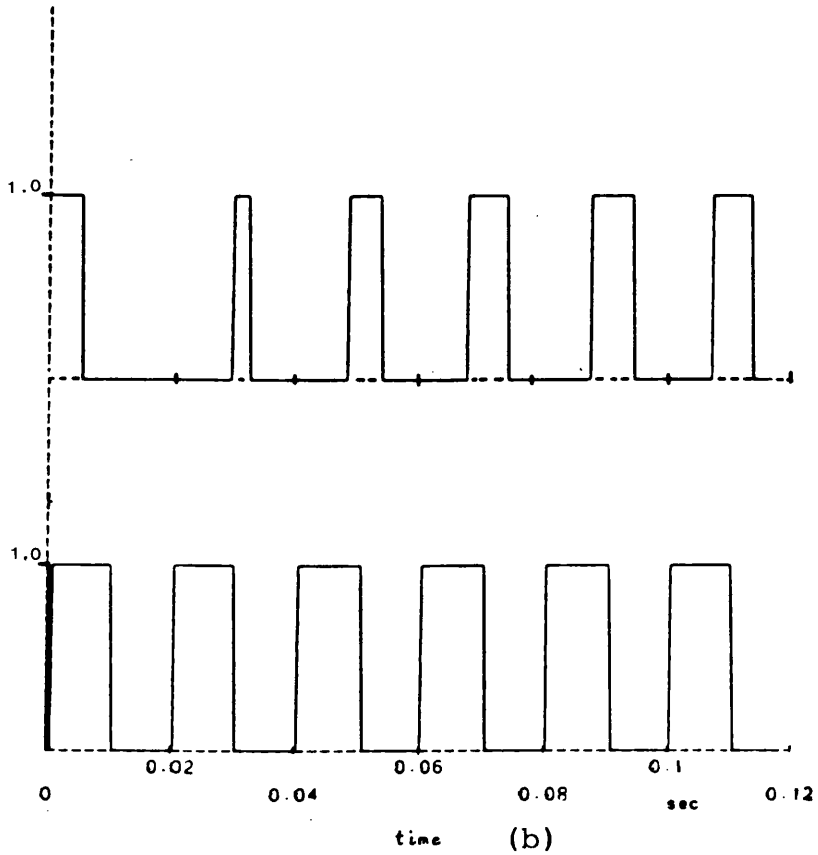


(b)

Figure 8.12 S.E. relay (set with cap. F/O) responses for a voltage minimum fault at 165km from the S.E. (single section feeder).

(a) block average (b) sequence comparator

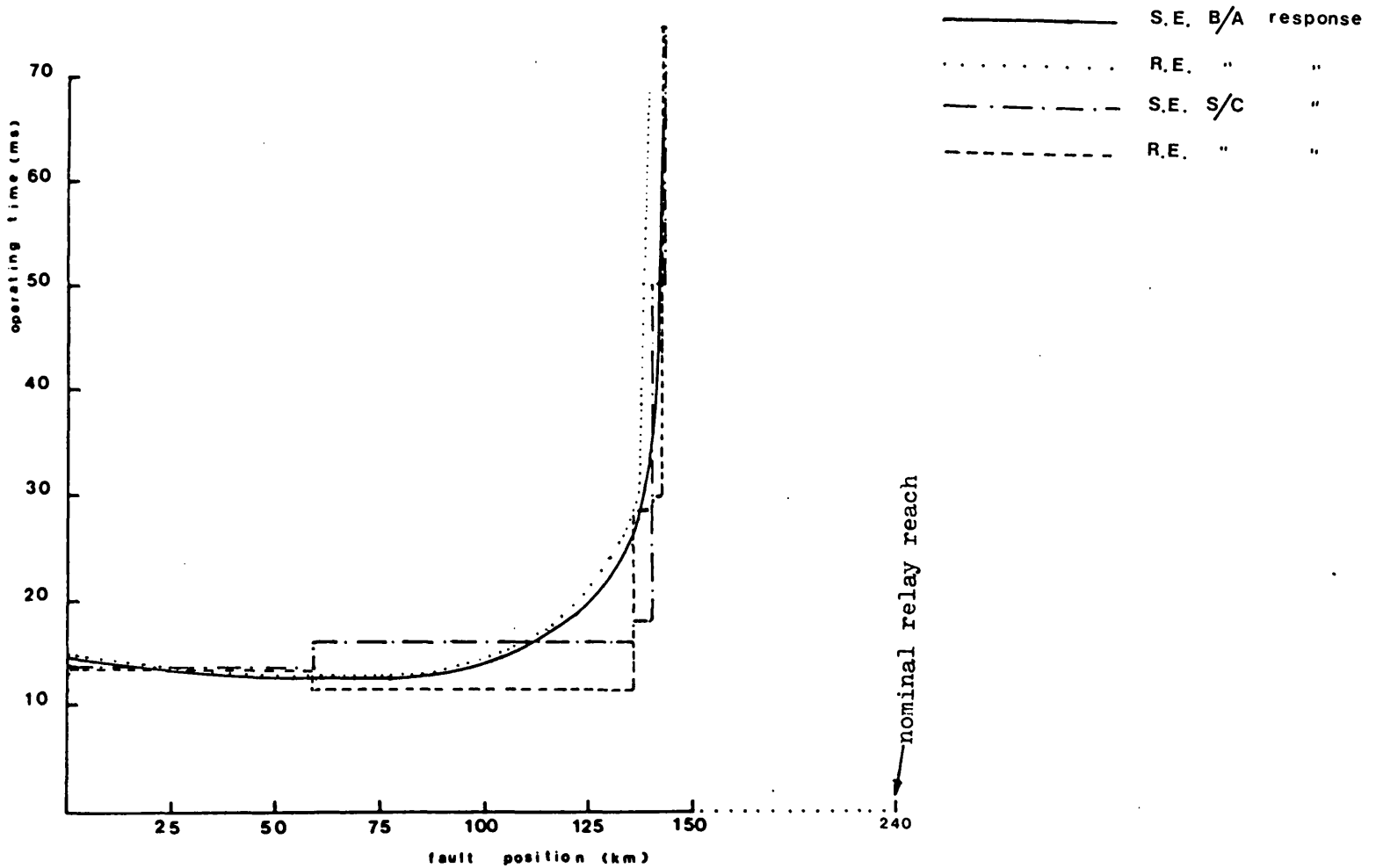


Figure 8.13 Operating characteristics of B/A and S/C relays (relay setting with capacitor in the circuit). Fault conditions are as shown in Table 8.2.

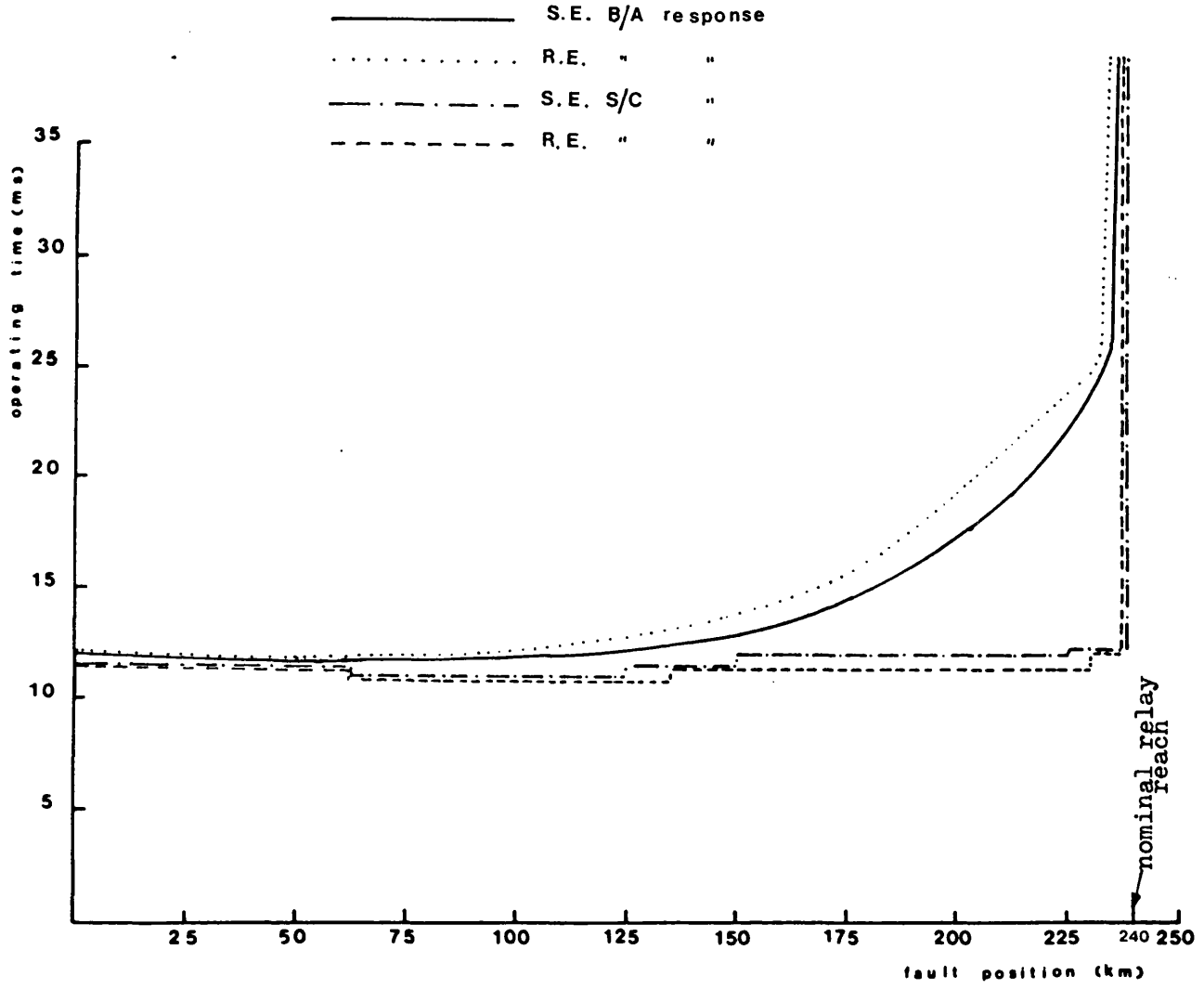


Figure 8.14 Operating characteristics of B/A and S/C relays (relay setting with no capacitor in the circuit). Fault conditions are as shown in Table 8.2.

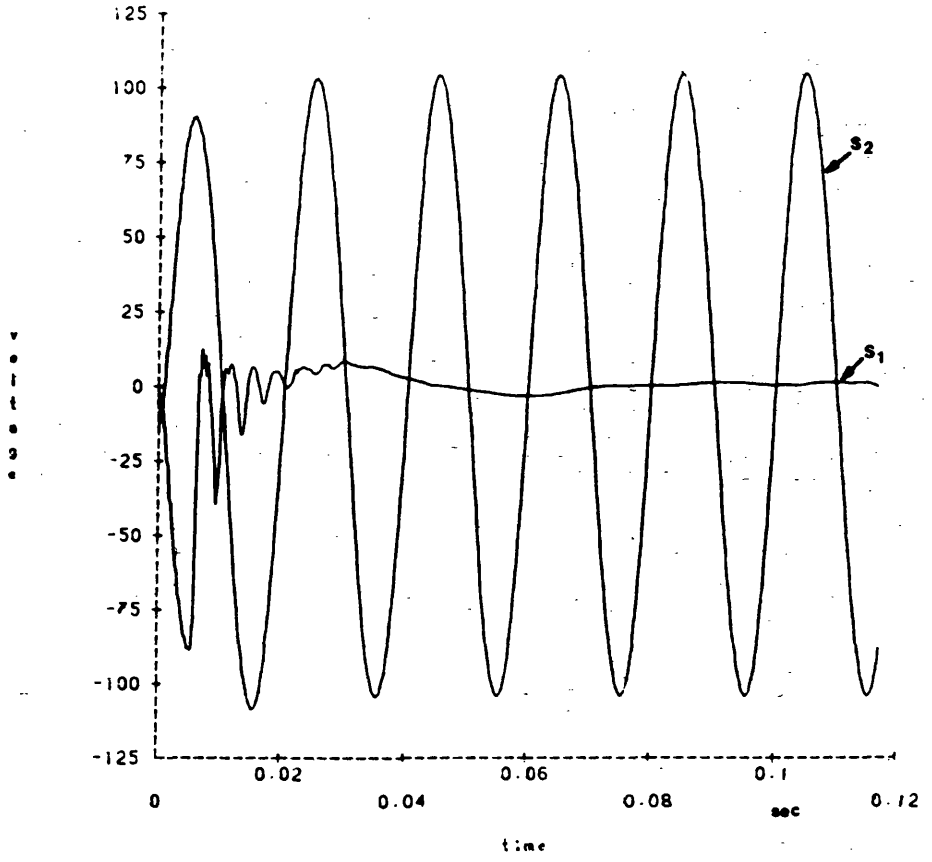


(a)

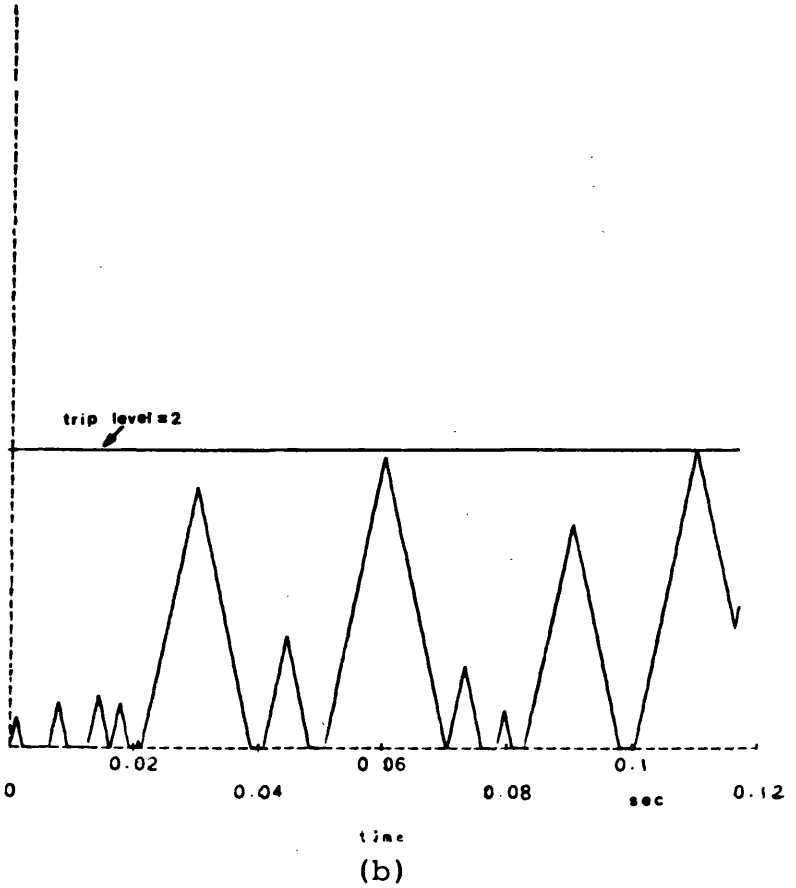


(b)

Figure 8.15 S.E. B/A relay (set with capacitor in the circuit) responses for voltage maximum fault at 185km from S.E. (multi-section feeder)

(a) relaying signals $S_1$ and $S_2$ ; (b) integrator output

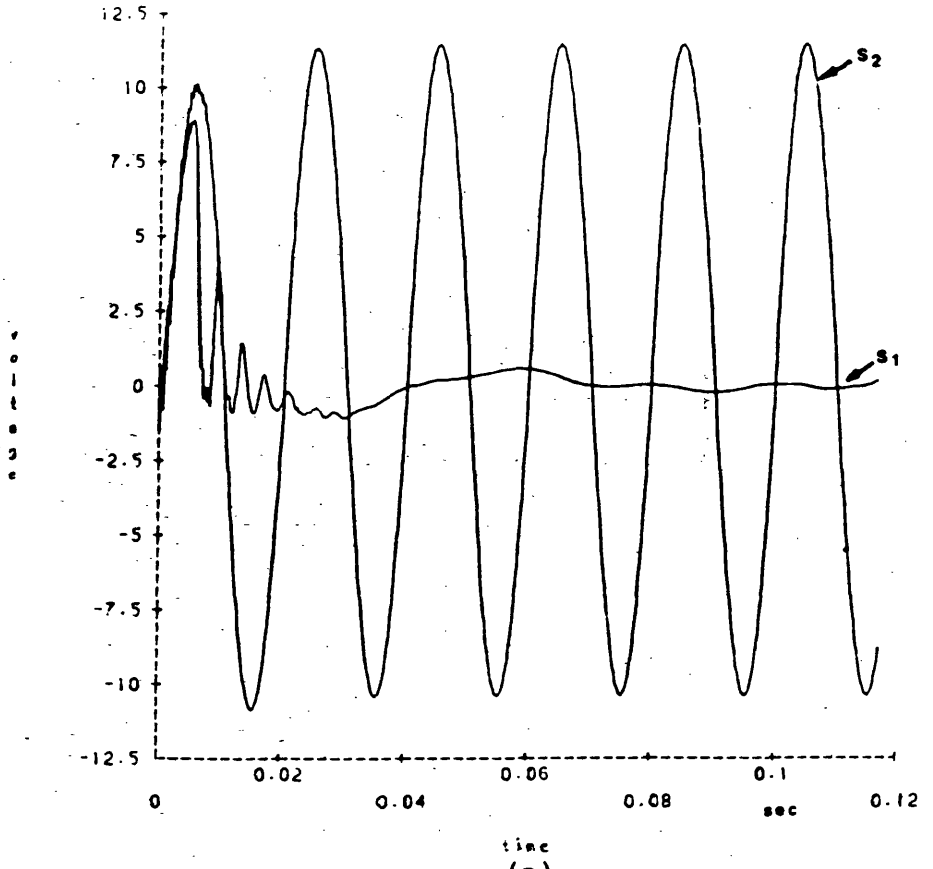


(a)

1 - Upcount
2 - Downcount

| Time | Count |
|---|---|
| 0.2500 E-03 | 2 |
| 0.5000 E-03 | 1 |
| 0.7500 E-03 | 2 |
| 0.2000 E-02 | 2 |
| 0.3250 E-02 | 1 |
| 0.5500 E-02 | 2 |
| 0.7750 E-02 | 1 |
| 0.9500 E-02 | 2 |
| 0.1050 E-01 | 2 |
| 0.1175 E-01 | 2 |
| 0.1275 E-01 | 1 |
| 0.2050 E-01 | 1 |
| 0.3050 E-01 | 2 |
| 0.3850 E-01 | 2 |
| 0.4050 E-01 | 2 |
| 0.5075 E-01 | 1 |
| 0.6050 E-01 | 2 |
| 0.6300 E-01 | 2 |
| 0.7075 E-01 | 2 |
| 0.8050 E-01 | 1 |
| 0.9075 E-01 | 2 |
| 0.1005 E+00 | 1 |
| 0.1107 E+00 | 2 |
| 0.1118 E+00 | 2 |

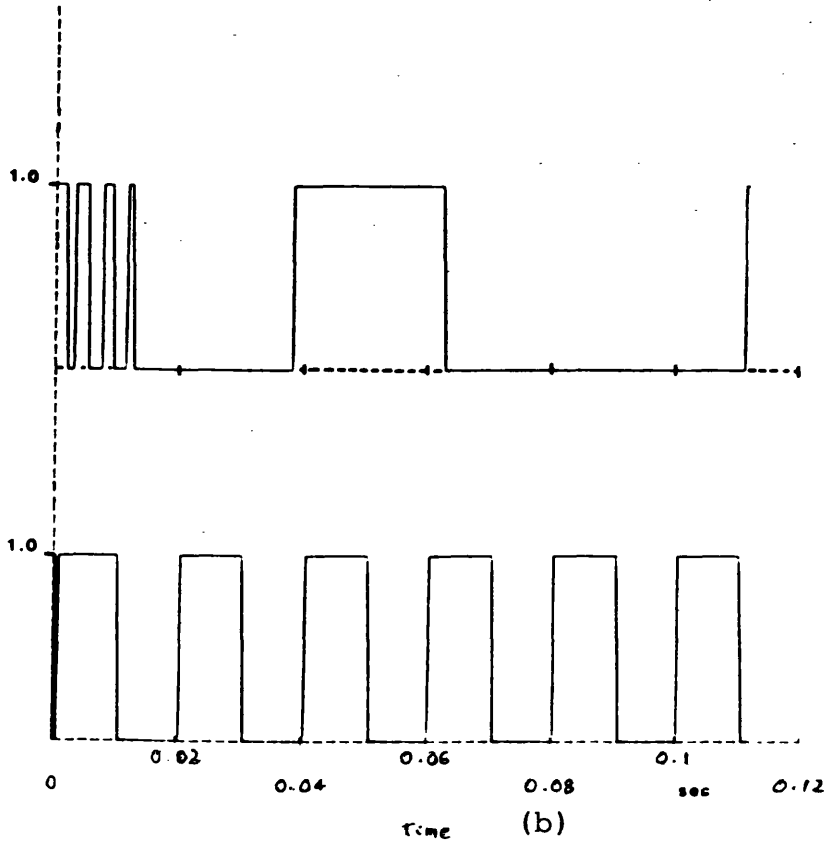


(b)

Figure 8.16 S.E. S/C responses for conditions similar to Figure 8.15.

(a) relaying signals $S_1$ and $S_2$

(b) comparator output

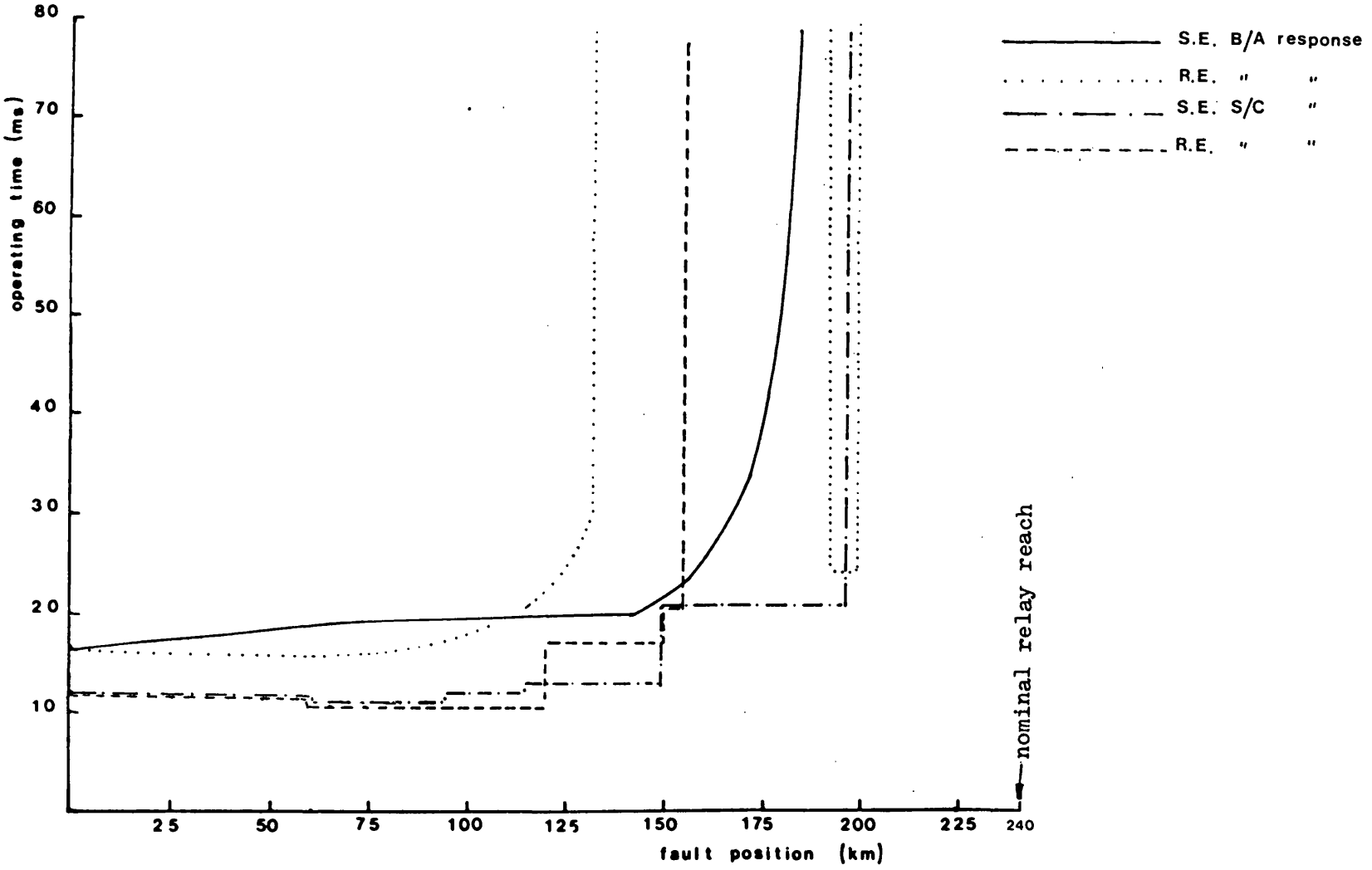


Figure 8.17 Operating characteristics of B/A and S/C relays (relay setting with capacitor in the circuit). Fault conditions are as shown in Table 8.3.

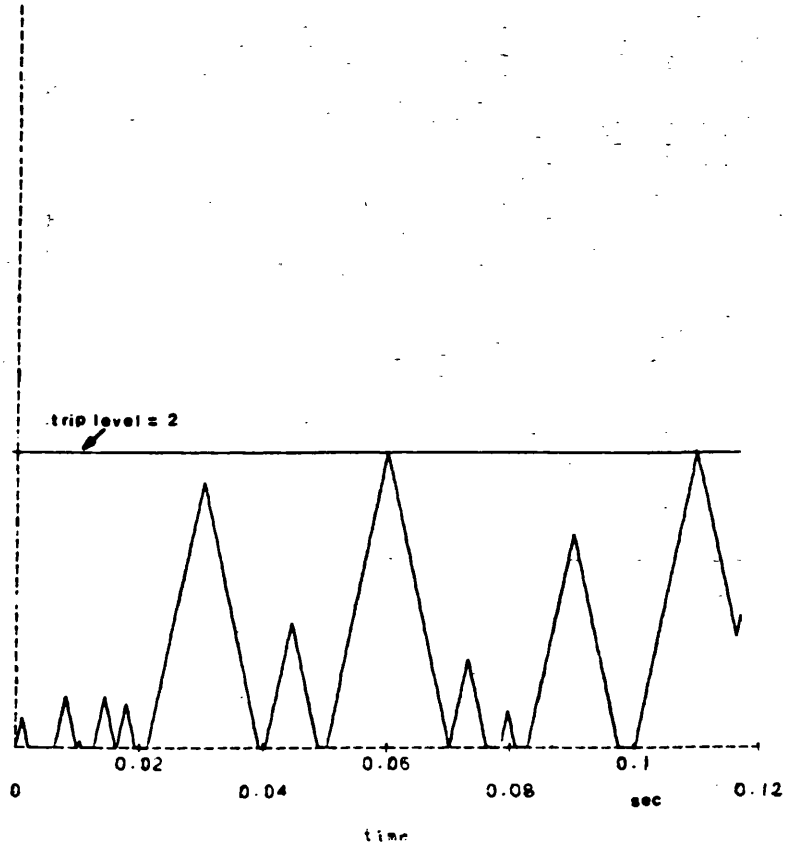


Figure 8.18 S.E. B/A output, using memory circuit for conditions similar to Figure 8.15.

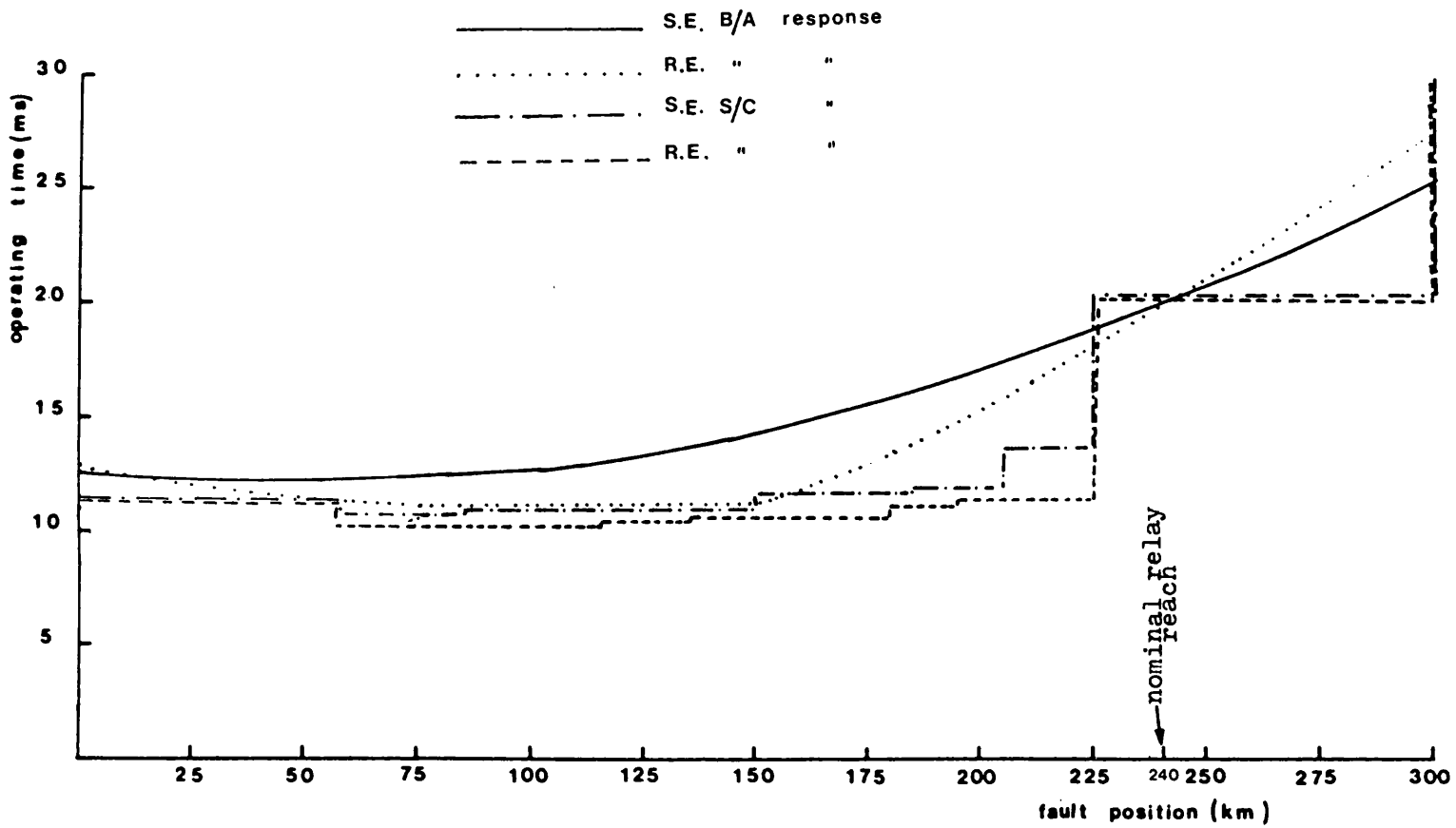


Figure 8.19 Operating characteristics of B/A and S/C relays (relay setting with no capacitor in the circuit). Fault conditions are as shown in Table 8.4.

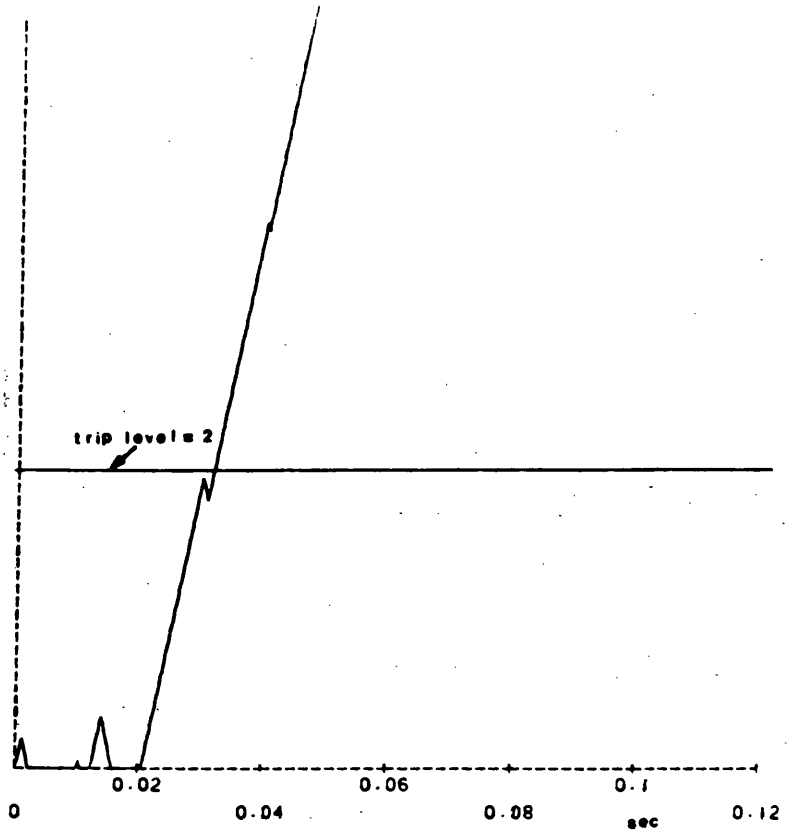


(a)

1 - Upcount
2 - Downcount

| Time | Count |
|---|---|
| 0.2500 E-03 | 2 |
| 0.5000 E-03 | 1 |
| 0.7500 E-03 | 2 |
| 0.5500 E-02 | 2 |
| 0.1050 E-01 | 2 |
| 0.2000 E-01 | 2 |
| 0.2050 E-01 | 1 |
| 0.2850 E-01 | 1 |
| 0.3050 E-01 | 1 |
| 0.3350 E-01 | 1 |
| 0.4050 E-01 | 1 |
| 0.4775 E-01 | 1 |
| 0.5075 E-01 | 1 |
| 0.5425 E-01 | 1 |
| 0.6050 E-01 | 1 |
| 0.6750 E-01 | 1 |
| 0.7075 E-01 | 1 |
| 0.7450 E-01 | 1 |
| 0.8050 E-01 | 1 |
| 0.8725 E-01 | 1 |
| 0.9075 E-01 | 1 |
| 0.9475 E-01 | 1 |
| 0.1005 E+00 | 1 |
| 0.1073 E+00 | 1 |
| 0.1107 E+00 | 1 |
| 0.1145 E+00 | 1 |

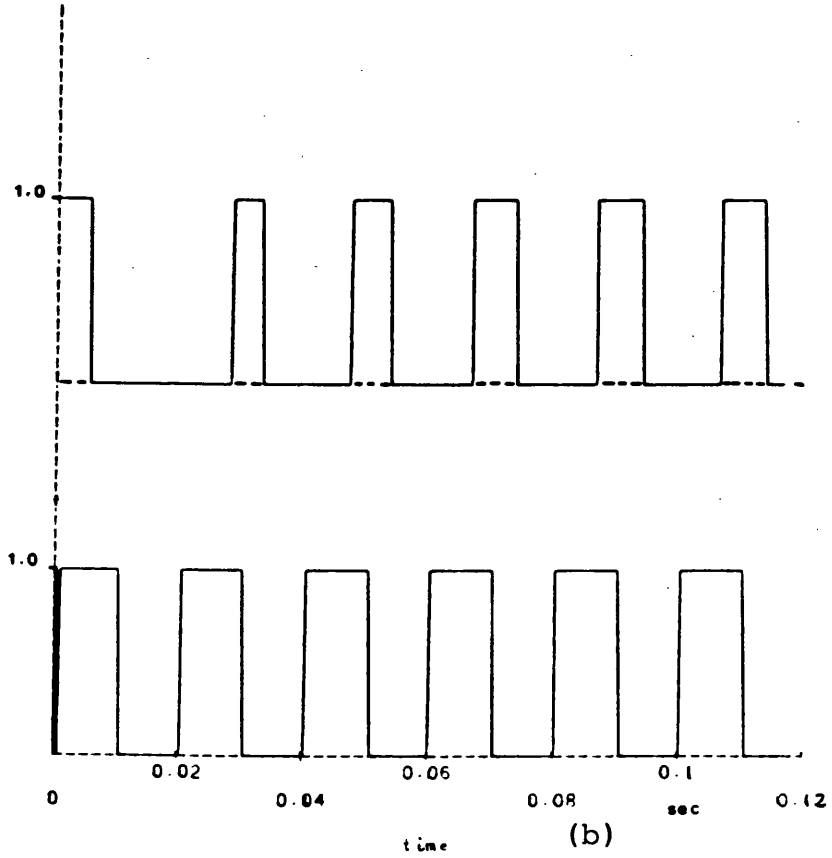


(b)

Figure 8.20 S.E. relay (set with cap. F/O) responses for a voltage minimum fault at 165km from the S.E. (multi-section feeder).

(a) block average ; (b) sequence comparator

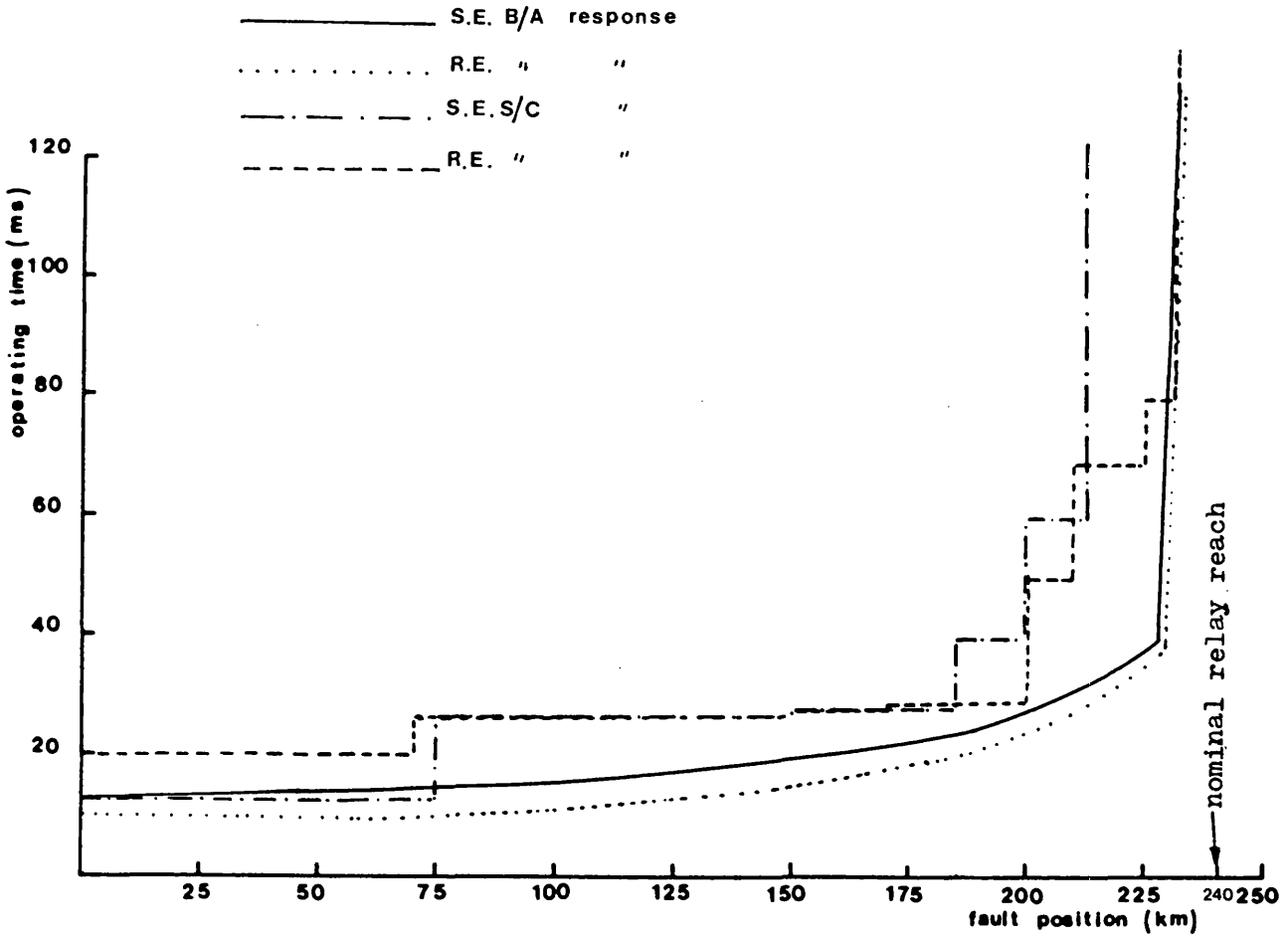


Figure 8.21 Operating characteristics of B/A and S/C relays (relay setting with no capacitor in the circuit). Voltage minimum faults.

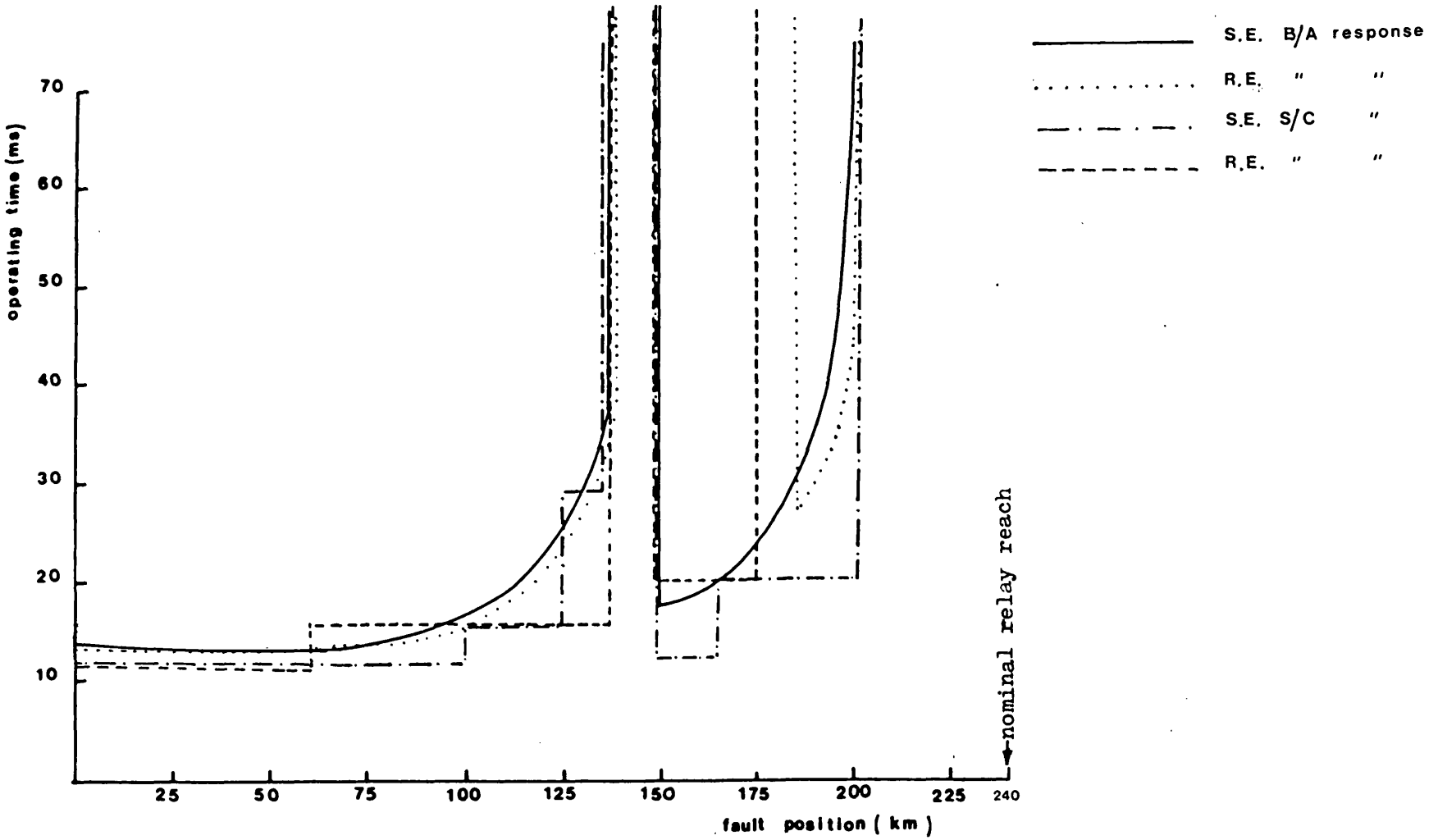


Figure 8.22 Operating characteristics of B/A and S/C relays (relay setting with capacitor in the circuit). Fault conditions are as shown in Table 8.6.

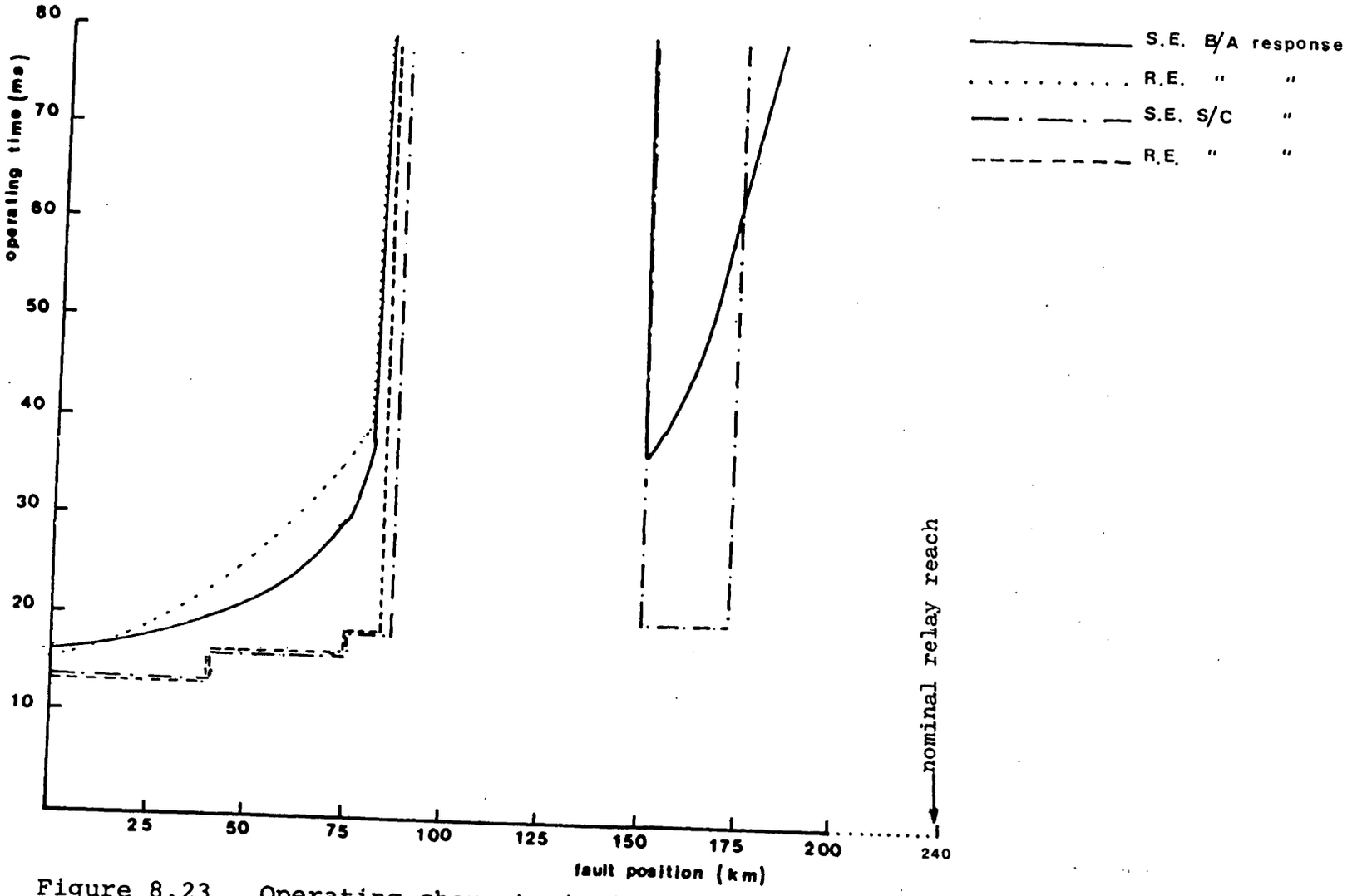


Figure 8.23 Operating characteristics of B/A and S/C relays (relay setting with capacitor in the circuit). Fault conditions are as shown in Table 8.7.

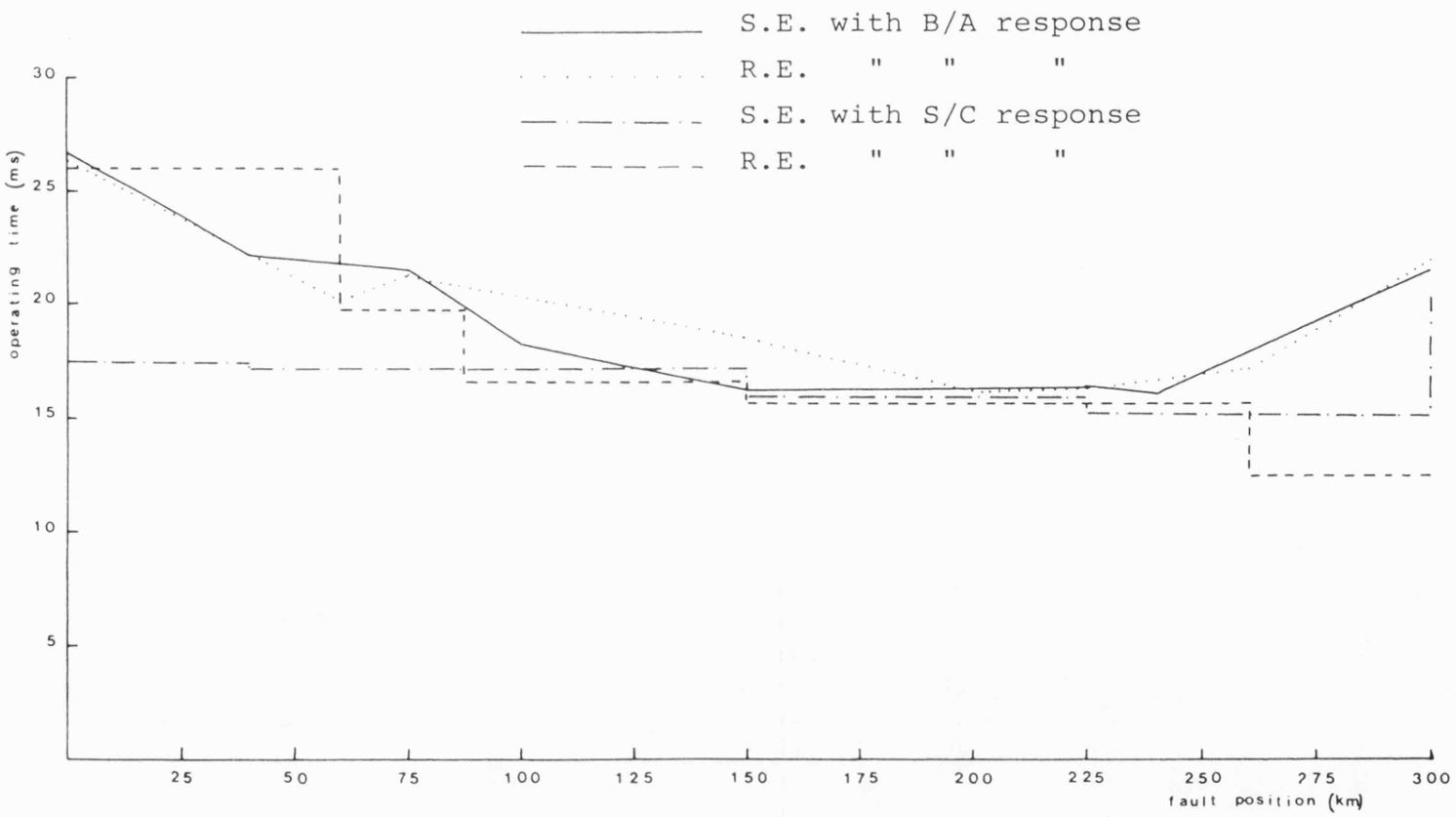


Figure 8.24 Operating characteristics of B/A and S/C relays utilising permissive overreach scheme. Fault conditions are as shown in Table 8.8

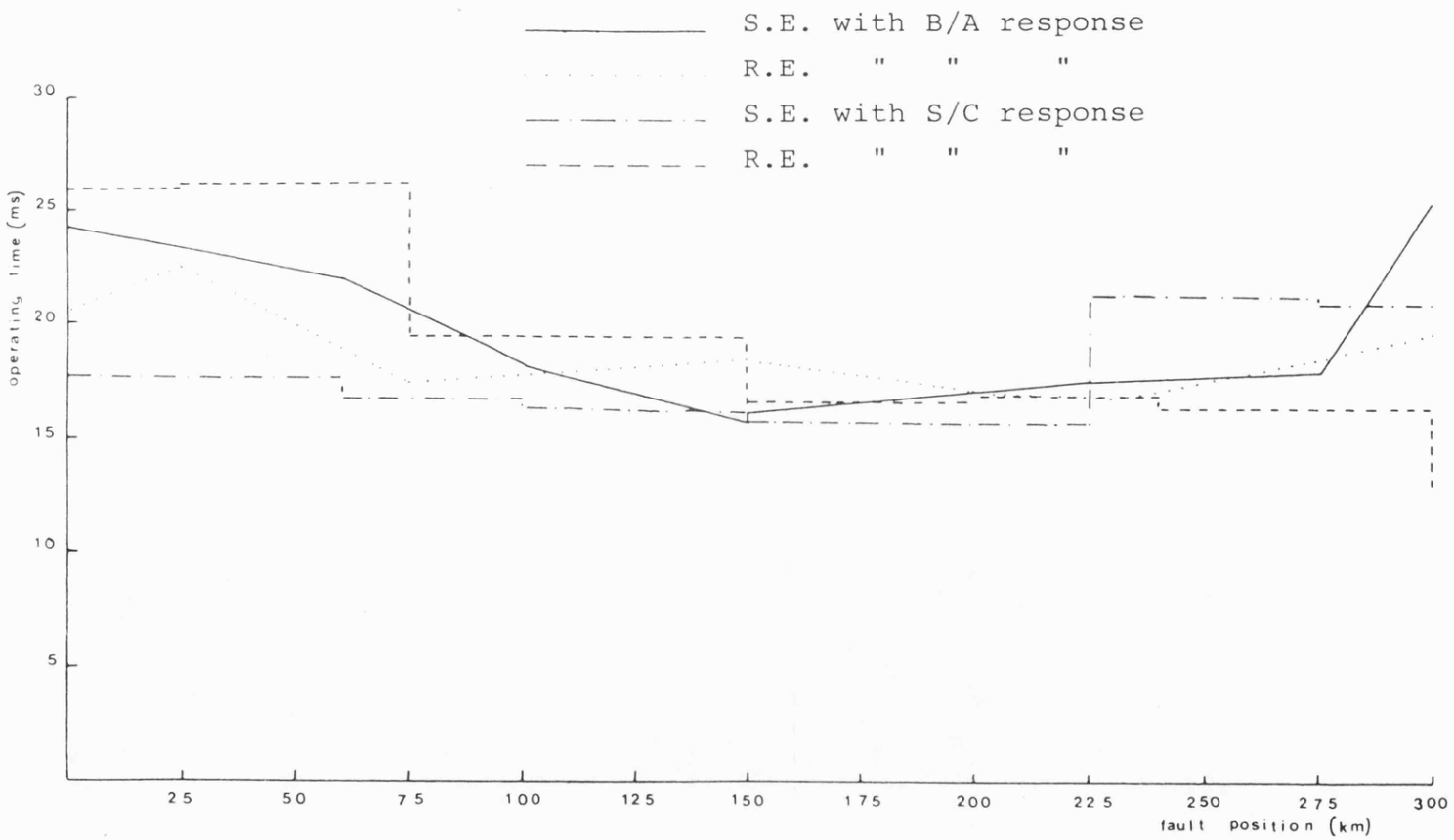


Figure 8.25 Operating characteristics of B/A and S/C relays utilising permissive overreach scheme. Fault conditions are as shown in Table 8.9

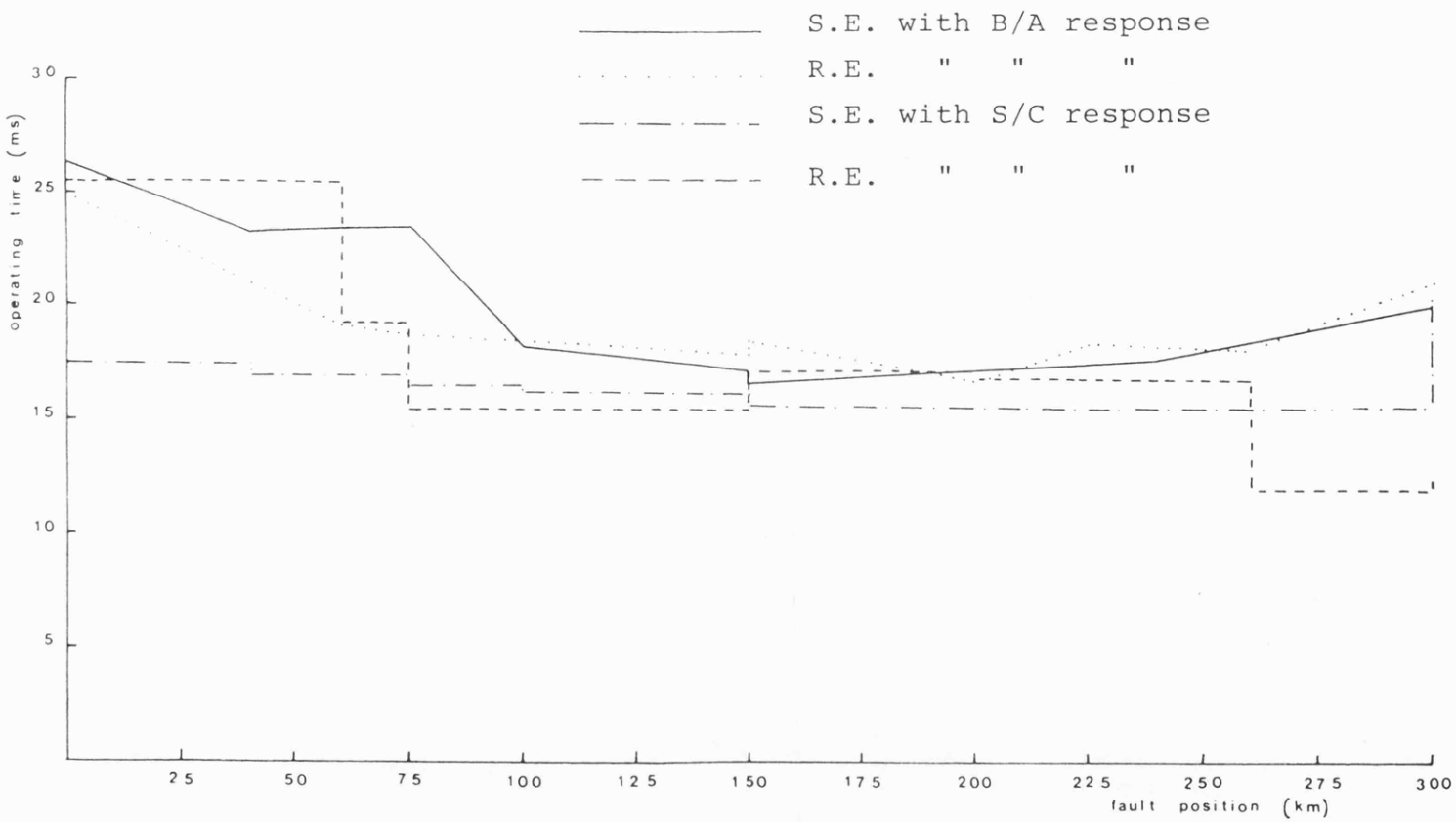


Figure 8.26 Operating characteristics of B/A and S/C relays utilising permissive overreach scheme. Fault conditions are as shown in Table 8.10

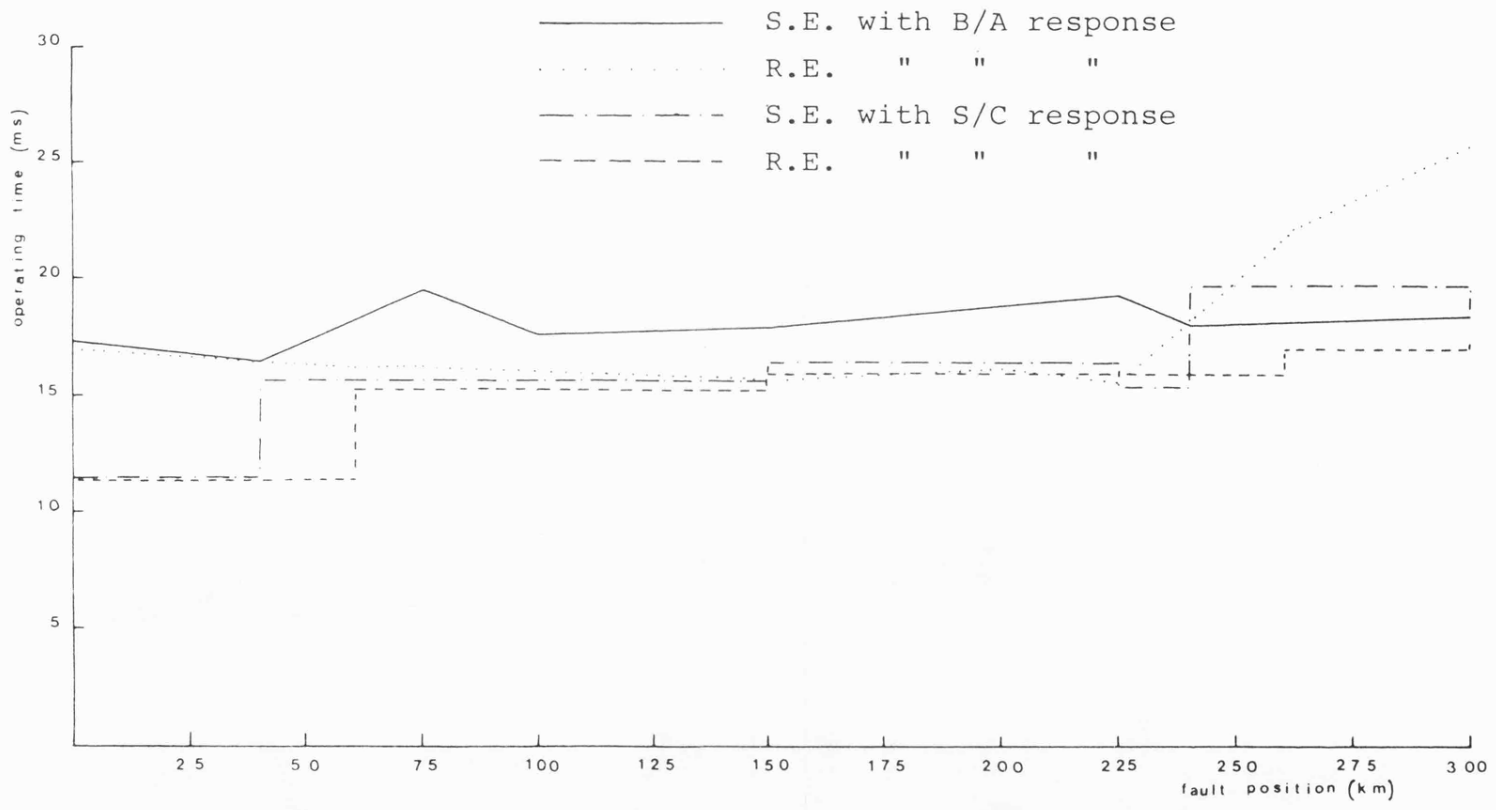


Figure 8.27 Operating characteristics of B/A and S/C relays utilising blocking scheme. Fault conditions are as shown in Table 8.11

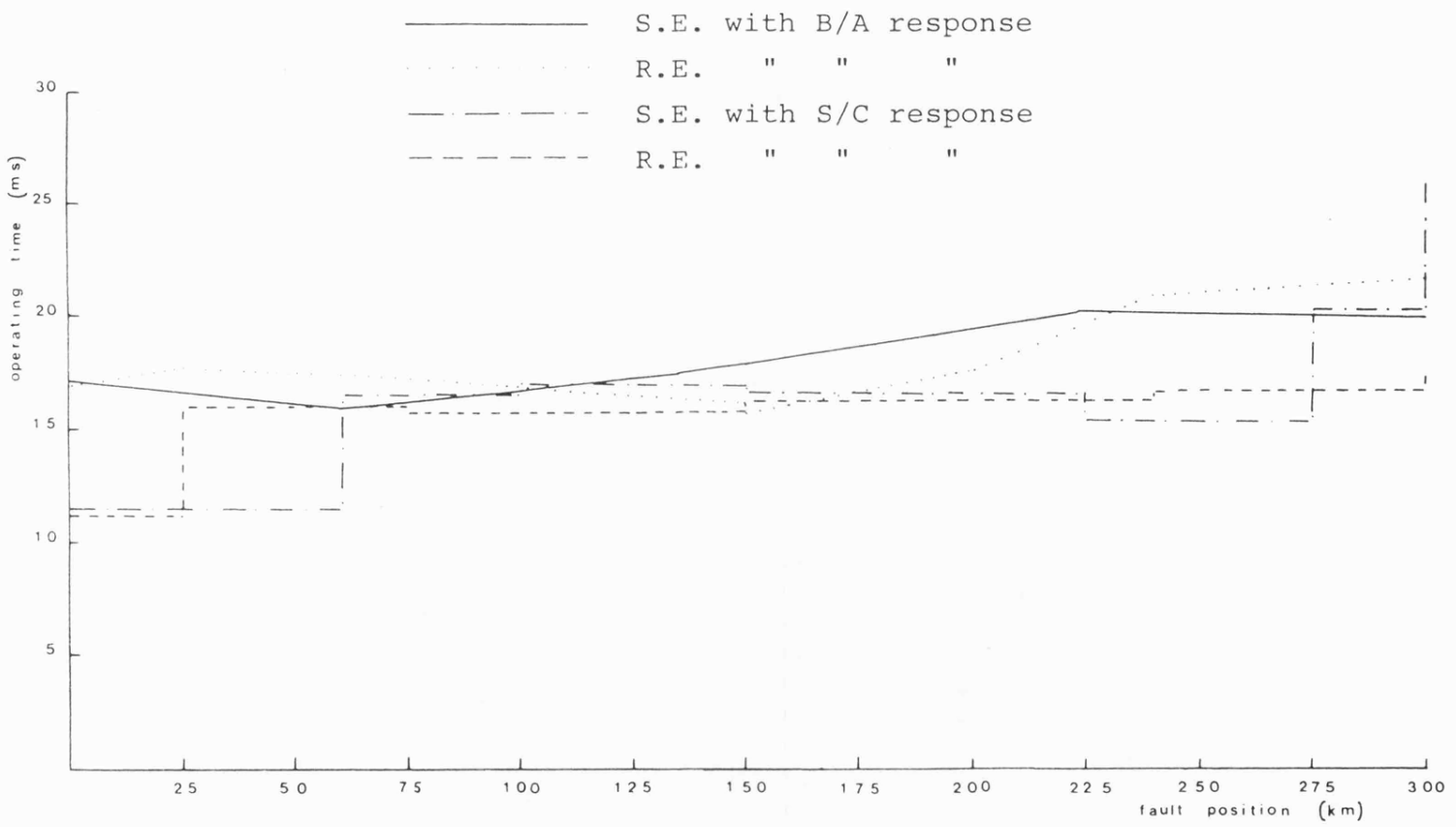


Figure 8.28 Operating characteristics of B/A and S/C relays utilising blocking schemes. Fault conditions are as shown in Table 8.12

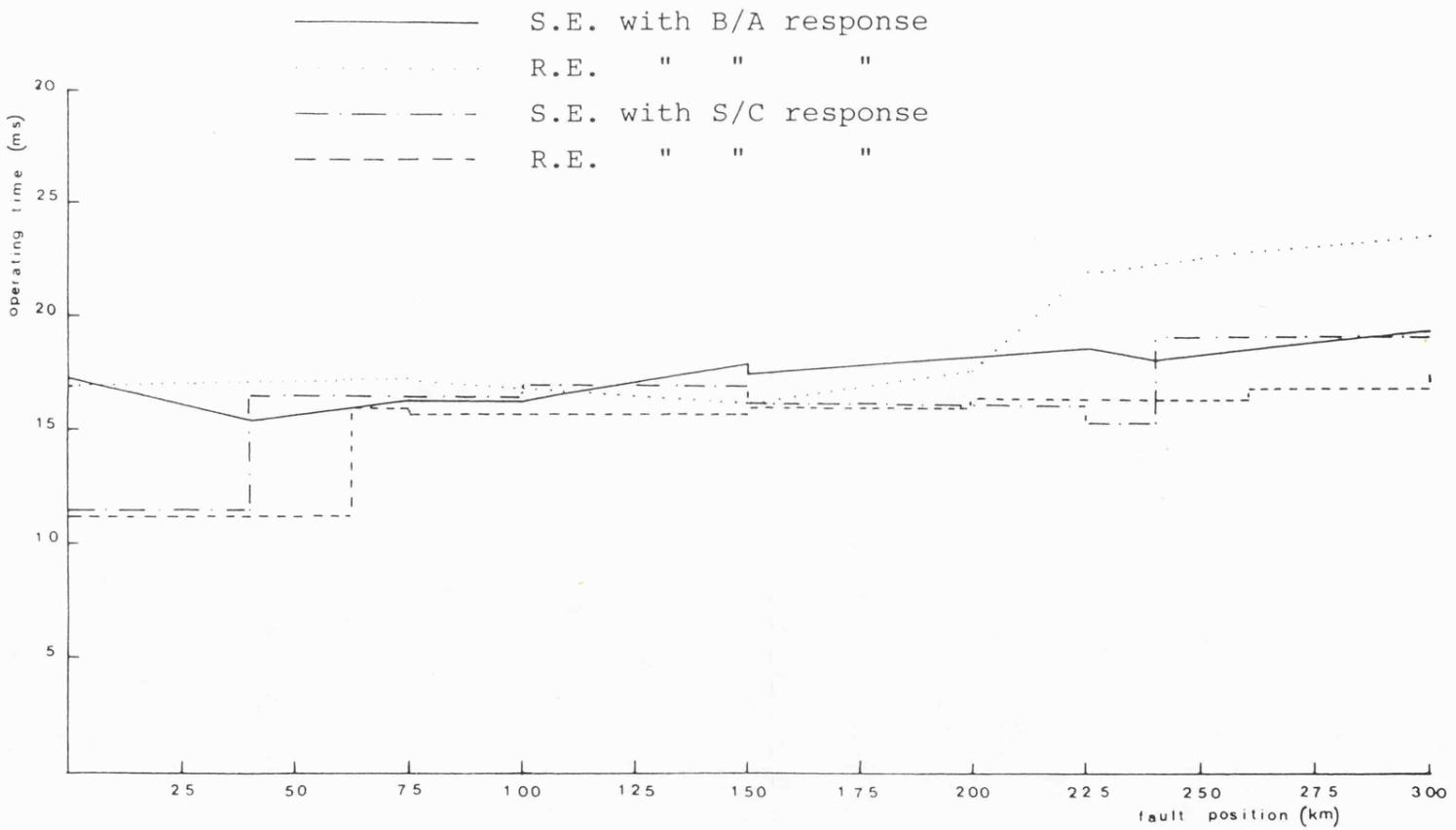


Figure 8.29 Operating characteristic of B/A and S/C relays utilising blocking scheme. Fault conditions are as shown in Table 8.13

# CHAPTER 9 GENERAL CONCLUSION AND SUGGESTIONS FOR FUTURE WORK

## 9.1 Conclusion

In this thesis, frequency domain techniques have been developed for realistically modelling a series capacitor compensated system with shunt reactor at each end of the line model. Such realistic and detailed modelling techniques are extremely useful for a number of things, such as: ascertaining the performance of the various existing protective schemes as applied to series compensated line and also for the future development of any other protection schemes associated with such lines,for determining the minimum capacitor gap settings and also the system insulation levels.

As mentioned in the previous Chapters, in the case of series compensated systems, protective gaps across the capacitors are arranged to sparkover whenever the voltage across a capacitor reaches a certain preset threshold value. Due to the non-linear and random nature in which the various capacitors get shorted out under fault conditions, the simulation methods can be quite complex. Furthermore, the complexity of the whole simulation process is accentuated when applying single pole autoreclosure sequences. In this work,

frequency domain techniques have been extended to solve such non-linearities, this being done by means of a standard matrix array which relates conditions at all points of possible non-linearities within the network. This makes the simulation techniques very efficient computationally, as the standard matrix can be computed and stored at the outset, right at the beginning of a fault simulation cycle and used over and over again for simulating the various sequences. The steps involved in the complete simulation process (as detailed in Chapters 2 and 3) can be summarised as follows:

(a) Calculation of the per unit length parameters of a line having series compensation with shunt reactors.

(b) Discrete transposition of the line.

(c) Calculation of the prefault steady state values of currents and voltages at different points along the line, eg the relaying point and the point of fault.

(d) Simulation of the source side networks which includes the multi-section feeder, the latter being for a more realistic source representation.

(e) Formulation of the standard matrix array,

which is then used for the following steps:

(1) Calculation of the post-fault current and voltage waveforms at different points along the line, eg the relaying point.

(2) Evaluating the voltage waveforms across capacitors to determine the time at which these voltages reach the preset threshold value.

(3) Simulating the shorting out of any capacitors and recalculating the new current and voltage waveforms at all points of interest.

(4) In the case of single pole autoreclosure studies:

    (i) Determining the pole opening times following breaker contact separation time (at the first zero current crossing) then simulating the opening of the breakers and re-evaluating the currents and voltages.

(ii) Simulating fault break-off, capacitor reinsertion and line reclosures respectively and recalculating the new current and voltage waveforms again at all points of interest.

The circuit configuration is shown in Chapter 4, which also includes the various power frequency system parameters such as the line, series capacitor bank (including the threshold voltage for various capacitor locations), shunt reactor bank and the parameter for the various protection schemes used.

The simulation methods developed in Chapters 2 and 3, together with the system parameters in Chapter 4 have been used to study the following:

(1) Effect of series compensation on the relaying point primary system responses for both single and multi-section feeders (both having shunt compensation).

(2) Overvoltage phenomena across the capacitors and at the relaying point during various fault conditions.

(3) Predicting the transient behaviour of series compensated lines, with spark gap in operation, when subjected to single pole switching.

(4) Examining the performance of the cross-polarised mho relays, as applied to a series compensated line with single spark gap scheme, both in the independent and dependent modes of operation using the well-known block average principle[69] and comparing its performance with a relatively new distance scheme based on the sequence comparator principle[84].

The computational results presented in Chapters 5-8 cover the aforementioned effects and the conclusions are as given below.

The effect of series compensation on primary system responses is examined in Chapter 5 and the following general conclusions can be drawn from it.

(1) In a series compensated system, high frequency reflection components pass through the capacitors virtually unchanged, whereas low frequency components, predominantly at power frequency, are reflected. As such

the voltage and current waveforms are identical in shape to the system without series compensation, except for the actual magnitudes of the faulted phase voltages and currents. The faulted phase voltages are reduced in magnitude and the corresponding phase currents increased with an increase in the degree of series compensation.

(2) Studies associated with faults on series compensated systems for both single and multi-section feeders show that the travelling wave distortion in voltage and current waveforms is significantly affected by the source side networks. For example, in the case of simple and multi-feeder models, a large sending end source capacity results into much smoother waveforms, voltages in particular, than the ones from the smaller sending end sources, the latter having considerable waveform distortion. Faults which occur near voltage zero in the faulted phase do not cause a sudden change in voltage level, and travelling waves are therefore much less pronounced. In the case of phase faults, the much lower

attenuation of the aerial modes of propagation gives rise to waveforms which remain noisy for a considerable time after fault inception. These findings are very much in line with the reported results for an uncompensated and shunt compensated system[34,37,70].

(3) For identical fault conditions, the results associated with multi-section feeder are significantly different from the single section arrangement, especially the current waveforms which are apparently more distorted in the former case. This is so because the travelling waves of currents set up on fault inception propagate through different line sections towards the terminating networks and are partially reflected by the latter back to the fault point to produce very significant current distortion. In this particular case, because of the lower frequency distortion, the waveforms are not only affected in magnitude, but also the actual profiles are slightly different from the corresponding case for a system without series compensation.

(4) Varying the amount of compensation and location of capacitors does not significantly affect the profile of the primary system waveforms, however the magnitude of the faulted phase current waveforms increases with an increase in the degree of series compensation.

(5) The effects of the aforementioned factors are also applicable to system responses at any other point of observation.

The overvoltage phenomena across the capacitor banks and the possible overvoltages due to fault inception at the relaying point are digitally evaluated in Chapter 6. The results presented in this Chapter show that:

(1) Depending on the system configuration and fault conditions, there can be a wide variation in the actual magnitudes of the overvoltages across the capacitors.

(2) On a single section feeder with simple sources on each side, irrespective of fault position, the amount of compensation and capacitor location, the capacitor protective gaps operate for a majority of

fault conditions. However, in the case of the multi-section feeder, the behaviour of the capacitor protective gaps is very random in nature and depends on fault position, capacitor location, amount of compensation, gap setting, etc. Also, for both the feeder arrangements, when a capacitor (or capacitors) flashes over it does so only on the faulted phase and within a time interval of one cycle after fault inception, in the majority of cases. A point to note is that in the case of a system employing two capacitors per phase both the faulted phase capacitors flash over in the case of a single section feeder, whereas in the multi-section arrangement it can be either one or none. The voltages detected across the healthy phase capacitors, on fault inception, are up to a maximum of 0.5 p.u. for the fault conditions studied.

(3) In the two systems considered, the maximum overvoltage observed at the relaying point is about 1.41 p.u., which is for the phase-to-phase fault, this being for a single section feeder with a single capacitor located at the mid-point. The overvoltage

here is significantly less than that produced for the corresponding case without series compensation[70]. Whereas the single-phase-to-earth fault produced a maximum overvoltage of about 1.3 p.u. These findings are in agreement with the fault induced overvoltage predicted by other authors[79,92], as applied to series compensated lines.

Evaluation of the primary system waveforms associated with single pole autoreclosure sequences is presented in Chapter 7. Again, the two different system configurations have been considered. As there are no field test results available, especially for the realistic multi-section model, the results for the single section feeder arrangement have been used as a basis for comparison. The digital computer results presented in this Chapter reveal the following:

(1) On fault inception the ringing effects, particularly in the faulted phase relaying point current waveforms due to the resonance between the line inductance and the capacitor banks, are clearly observed in both the single and multi-section feeder systems.

(2) In the single section feeder arrangement the shorting out of the faulted phase capacitor/capacitors produces a slight distortion in the faulted phase relaying point voltage waveforms, whereas the reinsertion of capacitor/capacitors does not produce significant changes in the relaying point voltages and currents. Also, for such a feeder system, the sound-phase currents remain small in magnitude on opening the line breaker poles, which also results in high frequency transients being set up particularly on the faulted phase voltage and these gradually ring down to almost zero until fault break-off. Thereafter a near power frequency voltage is induced in the faulted phase due to the capacitive and inductive coupling with the healthy phases. It has been found that for the fault conditions studied, in the majority of cases the magnitude of this induced voltage remains below the restrike voltage of 70 kV peak. Again, line reclosures produce significant amount of high frequency reclosing transients and normal steady state voltage across all capacitors are observed.

(3) In the case of the multi-section feeder, again the random nature of the capacitor flashover has clearly emerged. For the fault conditions studied and with a capacitor at each end, only the receiving end faulted phase capacitor flashes over, whereas for capacitor at mid-point none of them do so. The shorting out of the receiving end capacitor produces a slight distortion on the receiving end relaying point voltage waveforms, whereas the reinsertion of the capacitors does not significantly affect the waveforms. Also, for such feeder system , on current interruption the faulted phase voltages ring down until fault break-off. In the case of a capacitor at each end and fault at mid-point, the sending end voltage rings down to almost a steady d.c. level, whereas the receiving end voltage rings down to almost zero level. As in the simple source case, the fault break-off again causes a near sine wave voltage to be induced in the faulted phase. A point to note here is that in the multi-section feeder for certain fault conditions, especially for a fault at the receiving end, the faulted phase

receiving end relaying point voltage, which is also the fault point voltage, reaches a peak value of about 145 kV which is well above the permissive restrike voltage. Again, line reclosures produce normal steady state voltages across the healthy phase capacitors, whereas the faulted phase capacitor/capacitors are considerably distorted, in particular when the capacitor is located at the mid-point - the voltage across it rises to about 2.0 p.u.

It is worth mentioning here that when single pole autoreclosure techniques are applied to a series compensated line with shunt reactors for secondary arc extinction, the presence of the series capacitor has a detuning effect and therefore hinders the suppression of the secondary arc to a certain extent. This is particularly so if the capacitor spark gaps fail to operate for certain fault conditions. Such a difficulty was encountered during the course of this work. One way of overcoming this problem is to set the capacitor spark gaps sufficiently low in order to ensure that the capacitor, particularly on the faulted phase, does flashover on fault inception.

The detailed performance of the cross-polarised

mho relays with different polarising quantities as applied to series compensated line with single spark gap scheme, both in the independent and dependent modes of operation, using the well-known block average principle[69] and comparing its performance with a relatively new distance scheme based on the sequence comparator principle[84] is digitally evaluated in Chapter 8. The computational results presented in this Chapter examine the performance of the two types of distance protection relay as applied to both single and multi-section feeders. The results presented are for two schemes, one employing two capacitors per phase (one at each end) and the other in which there is a single capacitor in the middle, the former having a fixed compensation of 70% and the latter for 30% and 50% compensation. Relay performance in terms of measurement accuracy and speed of operation under different fault conditions is described. The following conclusions can be drawn from these studies:

(1) In the case of the single-section feeder and a capacitor at each end, both the block average and sequence comparator relays, with relay setting assuming capacitor is in the circuit, underreach considerably (about 50 and 60% respectively) for voltage maximum faults due to the capacitor spark gap

operation. Whereas, for identical fault conditions and with relay set without the capacitors in the circuit, the underreaching effects are considerably reduced (about 10% underreach for block average arrangement and the sequence comparator relay overreaches by about 2%). However, when the capacitor is located at the mid-point and 30% compensation is used, there is an underreaching of about 40% (relay setting assumes capacitor is in the circuit) for both the block average and sequence comparator arrangements. Also, when the relays are set without the capacitors in the circuit the underreaching is reduced to about 3% for the two cases. In both cases, the sequence comparator has a better performance in terms of operating times and relay reach than the block average arrangement. As regards the voltage minimum faults, again results have shown that faulted phase capacitors flashover for a majority of fault positions and this means that if the relays are set with the capacitor in the circuit, then like the corresponding case for voltage maximum faults, a considerable amount of underreaching is produced, for both types of relays. However, when the relays are set

without the capacitors in the circuit, then unlike the case of voltage maximum faults the block average has a slightly better performance in terms of speed and relay reach, than the sequence comparator relays.

(2) In the case of the multi-section feeder when a capacitor is located at each end and for voltage maximum faults (relay set with capacitor in the circuit), both the relays at end S shown an underreach of about 25%. As regards the block average relay at end R, it operates for faults up to about 44% of the line, restrains for faults up to about 65% of the line and then operates again for a very narrow region of about 5 km. However, in the case of the sequence comparator at end R, the relay operates for faults up to about 52% and unlike the block average relay, does not show the narrow band of operation. When the relay setting is changed assuming no capacitors in the circuit, both the relays overreach substantially.

For voltage minimum faults, with relay setting assuming capacitor is in the circuit,

substantial amount of underreaching is again observed, whereas with relay setting assuming no capacitors in the circuit, underreaching is about 4% and 12% for block average and sequence comparator relay respectively. Again, like the corresponding case for the simple source model, the block average has an overall better performance than the sequence comparator.

Again with a single capacitor at mid-point and 30% compensation the block average and sequence comparator relays, for voltage maximum faults, assuming capacitor is in the circuit, operates up to about 45% of the line, restrains for a narrow band of about 8 km, and then operates again for faults up to about 67% of the line. However, the responses of both relays at end R are different. In this case, the block average relay operates up to about 47% of the line, restrains for faults up to about 62% of the line and then operates again for a narrow band of 15 km. Whereas, the sequence comparator operates up to about 47% of the line, restrains for a narrow band of about 8 km and then operates up to about 58% of the

line. When the degree of compensation is increased to 50%, the band of no-operation increases considerably. Whereas when the relays are set without the capacitors in the circuit, both relays tend to overreach.

(3) When choosing the dependent mode of operation, the permissive overreach scheme gives 100% coverage. In this type of scheme the two relays at line ends are interdependent, hence the responses, particularly the scheme employing the block average relay vary a lot from one fault position to the other. The scheme employing sequence comparator relay has an operating time of about 1 cycle for the majority of fault positions, except for faults close to the remote end where the operating times are quite different. However, for a capacitor at the mid-point and 30% series compensation the operating times of the scheme employing both the block average and the sequence comparator relays vary a lot from one fault position to the other, especially for faults close to the two busbars. Changing the amount of compensation to 50%, the response of the relays are similar to those for the case where a capacitor is

located at each end with 70% compensation.

In general it can be said that using such a scheme the location of the capacitor and degree of compensation do not seriously affect relay responses. However, faults close to the line ends, especially for the end R scheme, have longer operating times due to the faulted phase capacitor/capacitors not flashing over.

(4) The blocking scheme has a superior response than the permissive overreach scheme, in terms of operating times. Also, both the sending and receiving end relays have similar operating times.

In general it can be said that the blocking scheme (for both block average and sequence comparator relays) is less affected by the spark gap operation and not only a faster response, but also more uniformity as compared to the permissive overreach scheme is attained.

In general, it can be said that, for the independent mode of operation, the sequence comparator relay has a better performance in terms of both operating times and relay reach than the block average relay, particularly

for voltage maximum faults. For the single section feeder, terminating in simple sources, satisfactory relay coverage is obtained by setting the relays, assuming no capacitors in the circuit. Whereas, when considering the more practical source side networks, ie the multi-section feeder, the situation is quite different in that both types of relays tend to overreach considerably, when they are set without the capacitors in the circuit. On the other hand, when they are set with the capacitors in the circuit, the opposite is observed, ie they tend to underreach considerably. However, the results quite clearly indicate that purely from a protection point of view it is desirable to have a single capacitor with a lower degree of compensation, but the economics of doing so are questionable. It should also be mentioned here that in all the results produced, the 10 per cent level of polarisation used in relay signal $S_2$ gives satisfactory coverage for all faults close to the busbar.

When considering the dependent mode of operation, blocking scheme has a much superior response than the permissive overreach scheme,

this being so for both the types of series compensated schemes considered, ie one utilising two capacitors per phase and the other with a single capacitor in the middle. Again, in this mode of operation the one utilising the sequence comparator arrangement has an overall better performance in terms of operating times than the block average relay.

Finally, from the studies carried out so far, it can be said that the sequence comparator relay has only a slight overall advantage over the block average relay, when applied to a series compensated line, especially when considering a more practical system configuration, this being so in spite of the faster operating times associated with the former. This is so because in the majority of cases, especially when considering the independent mode of operation, the sequence comparator relay fails to operate before the capacitor spark gap

operation, and therefore loses some of the advantages over the block average relay.

## 9.2 Future Work

The work presented in this thesis forms the basis for future investigation of series compensated e.h.v. and u.h.v. transmission systems for the purposes of further developing autoreclosure techniques and the present protective schemes if they prove inadequate for such applications.

Future work may therefore be carried out along the following lines:

(1) The universal admittance 'A' matrix described in Chapter 3 may be used as a reference to other future work in a similar field.

(2) In the multi-section feeder system fault inception has been carried out only on the second section feeder containing reactors and capacitors, whereas the same can be carried out on other line sections.

(3) In the present work, a single circuit three phase system has been considered. The present fault simulation techniques presented

can be easily extended for studying the behaviour of a double circuit system.

(4) Overvoltages can occur on unfaulted lines in series compensated systems, following fault inception on other lines and subsequent bypassing of the series capacitor. Hence, this should be considered especially on systems involving double circuit lines.

(5) A single-line-to-ground-fault may lead to fault on other phases and hence the simulation of simultaneous fault could be considered.

(6) Only results for phase-to-earth and double phase faults have been shown in this thesis, the majority of which are for voltage maximum faults and a limited study for the voltage minimum faults. However, the digital program is very general and hence any other type of fault at voltage maximum or minimum can be considered.

(7) A time invariant arc resistance has been assumed throughout this work. However, for more realistic studies the non-linear nature of the arc resistance can be simulated.

(8) In this study the simple gap scheme is simulated. However, the dual gap scheme

with lower gap setting as described in Chapter 2 is a future possibility. Moreover, repetitive flashing over of a particular capacitor has not been observed which could again be simulated,if such a case is found.

(9) The capacitors can be located anywhere on the line and between substations and various other levels of compensation can be considered. In this thesis as regards the multi-section feeder, the capacitor and reactor have been located in the second section feeder. The same can be placed in any other line sections and similar studies undertaken.

(10) Single pole autoreclosure studies have been confined to a total operating time of about 6 cycles as opposed to a more practical time of about 30 cycles. In future such practical time should be used in order to reveal more accurate prediction of the system.

(11) In this thesis, single pole autoreclosure techniques have been utilised; similar studies in the future could involve three-pole autoreclosure techniques.

(12) One of the most satisfactory alternatives for reducing the secondary arc current, is to use a reactor with suitable characteristics connected in parallel with the capacitor. Series capacitor banks are often provided with such a reactor across the terminal of the series capacitors to discharge the capacitor trapped charge when the capacitor is removed from the circuit. It is practical to select the characteristic of this reactor so that a considerable portion of the low frequency current resulting from the trapped charge will flow on the capacitor. So, in future, such types of studies should be undertaken so as to further reduce the secondary arc current.

(13) In this thesis distance protection when applied to series compensated lines has been considered. The subject is far wider and hence it is strongly suggested to study every compensated system, especially before decisions are taken on the type and performance of the relay.

(14) It is not uncommon to find series compensated lines utilising the phase comparison relays instead of distance protection, so to assess

the performance of the former, similar studies can be undertaken.

(15) When the capacitors are located at either end of the line, it might be better to locate the relays on the line side of the capacitor, so as to exclude the series capacitor from the protected zone and make the relay independent of capacitor flashover. Further studies in this connection would be very useful.

(16) The spark gap operation under fault conditions has a profound effect on the protection performance. However, there is a clear indication that some of the Zone 1 protection problems described in Chapter 8 can be overcome by replacing the conventional relays by the modern ultra high speed protective relays[97], with operating time of about 2 to 4 ms.

## APPENDIX (A1) EVALUATION OF THE UNIVERSAL MATRIX

### A1.1 Single-phase-to-earth fault

With reference to Figure 3.6 it can be seen that the voltage components $[\bar{V}_{BASk}]$ and $[\bar{V}_{BSk}]$ on either side of the sending end breaker are given by equation A1.1.

$$\bar{V}_{BSk} + \bar{E}_{BSk} = \bar{V}_{BASk} = -\bar{Z}_S \bar{I}_{BSk} + \bar{E}_{BSk} \quad \ldots \text{(A1.1)}$$

Also, the transform of voltage on either side of the receiving end breaker is given by equation A1.2.

$$\bar{V}_{BRk} - \bar{E}_{BRk} = \bar{V}_{BARk} = Z_R \bar{I}_{BRk} - \bar{E}_{BRk} \quad \ldots \text{(A1.2)}$$

Similarly, $\bar{I}_{SSka}$ is the frequency spectrum of current source which arises due to the injection of voltage $\bar{E}_{Ska}$, which is equal to $\int_{t_2}^{TOB} e_{sk} \exp(-j\omega t)dt$. The transforms of the current and voltage components ($\bar{I}_{Sk}$ , $\bar{V}_{Sk}$ , and $\bar{I}_{Rk}$ , $\bar{V}_{Rk}$ ) are known from equations A1.3 to A1.6.

$$\bar{I}_{Sk} = \bar{I}_{SSk} - Z_{cap}^{-1} \bar{E}_{Sk} \quad \ldots \text{(A1.3)}$$

$$\bar{I}_{Rk} = \bar{I}_{RRk} - Z_{cap}^{-1} \bar{E}_{Rk} \quad \ldots \text{(A1.4)}$$

$$\bar{V}_{Sk} = \bar{E}_{SSk} + \bar{E}_{Sk} \quad \ldots \text{(A1.5)}$$

$$\bar{E}_{RRk} = \bar{V}_{Rk} + \bar{E}_{Rk} \quad \ldots \text{(A1.6)}$$

The variation of the voltages and currents before the capacitors to that of the sending and receiving end of the line side busbars is defined by the canonical form of the two port or transfer matrix function in equations A1.7 and A1.13.

$$\begin{bmatrix} \bar{E}_{SSk} \\ -\bar{I}_{Sk} \end{bmatrix} = \begin{bmatrix} A_1 & B_1 \\ C_1 & D_1 \end{bmatrix} \begin{bmatrix} \bar{V}_{BASk} \\ -\bar{I}_{BSk} \end{bmatrix} \quad \ldots \text{(A1.7)}$$

Therefore:

$$\bar{E}_{SSk} = A_1 \bar{V}_{BASk} - B_1 \bar{I}_{BSk}$$

Substituting $\bar{V}_{BASk}$ from equation A1.1 :

$$\bar{E}_{SSk} = -(A_1 Z_S + B_1) \bar{I}_{BSk} + A_1 \bar{E}_{BSk}$$

$$= -U \bar{I}_{BSk} + A_1 \bar{E}_{BSk} \quad \ldots \text{(A1.8)}$$

where $U = A_1 Z_S + B_1$

and $\bar{I}_{Sk} = -C_1 \bar{V}_{BASk} + D_1 \bar{I}_{BSk}$

$$= (C_1 Z_S + D_1) \bar{I}_{BSk} - C_1 \bar{E}_{BSk}$$

$$= T \bar{I}_{BSk} - C_1 \bar{E}_{BSk} \quad \ldots \text{(A1.9)}$$

where $T = C_1 Z_S + D_1$

From equations A1.8 and A1.9 it can be seen that

$$\bar{E}_{SSk} = -UT^{-1} \bar{I}_{Sk} - (UT^{-1} C_1 - A_1) \bar{E}_{BSk} \quad \ldots \text{(A1.10)}$$

On substituting the value of $\bar{E}_{SSk}$ from equation A1.10 in equation A1.5, and the value of $\bar{I}_{Sk}$ from equation A1.3:

$$\bar{V}_{Sk} = -UT^{-1}\bar{I}_{Sk} - (UT^{-1}C_1 - A_1)\,\bar{E}_{BSk} + \bar{E}_{Sk} \quad \ldots \text{(A1.11)}$$

$$= -UT^{-1}(\bar{I}_{SSk} - Z_{cap}^{-1}\,\bar{E}_{Sk}) - (UT^{-1}C_1 - A_1)\bar{E}_{BSk} + \bar{E}_{Sk}$$

$$= -UT^{-1}\bar{I}_{SSk} + (UT^{-1}Z_{cap}^{-1} + 1)\bar{E}_{Sk} - (UT^{-1}C_1 - A_1)\bar{E}_{BSk}$$

$$\ldots \text{(A1.12)}$$

Again,

$$\begin{bmatrix} \bar{E}_{RRk} \\ \bar{I}_{Rk} \end{bmatrix} = \begin{bmatrix} A_6 & B_6 \\ C_6 & D_6 \end{bmatrix} \begin{bmatrix} \bar{V}_{BARk} \\ \bar{I}_{BRk} \end{bmatrix} \quad \ldots \text{(A1.13)}$$

Therefore

$$\bar{E}_{RRk} = A_6\bar{V}_{BARk} + B_6\bar{I}_{BRk}$$

Substituting $\bar{V}_{BARk}$ from equation A1.2

$$\bar{E}_{RRk} = (A_6 Z_R + B_6)\,\bar{I}_{BRk} - A_6\,\bar{E}_{BRk}$$

$$= Y\,\bar{I}_{BRk} - A_6\,\bar{E}_{BRk} \quad \ldots \text{(A1.14)}$$

and similarly $\bar{I}_{Rk} = C_6\,\bar{V}_{BARk} + D_6\,\bar{I}_{BRk}$

$$= (C_6 Z_R + D_6)\bar{I}_{BRk} - C_6\bar{E}_{BRk}$$

$$= X\,\bar{I}_{BRk} - C_6\,\bar{E}_{BRk} \quad \ldots \text{(A1.15)}$$

where $Y = A_6\,Z_R + B_6$ and $X = C_6\,Z_R + D_6$.

From equations A1.14 and A1.15 it can be seen that

$$\bar{E}_{RRk} = YX^{-1}(\bar{I}_{Rk} + C_6\bar{E}_{BRk}) - A_6\bar{E}_{BRk} \quad \ldots \text{(A1.16)}$$

On substituting the values of $\bar{E}_{RRk}$ from equation A1.16 in equation A1.6 and the value of $\bar{I}_{Rk}$ from equation A1.4

$$\bar{V}_{Rk} = YX^{-1}\bar{I}_{RRk} - (YX^{-1}Z_{cap}^{-1} + 1)\,\bar{E}_{Rk} + (YX^{-1}C_6 - A_6)\bar{E}_{BRk} \quad \ldots \text{(A1.17)}$$

Now the voltage and current variation at the fault point are related to beyond the receiving and sending end capacitor quantities by the transfer matrices, equations A1.18 and A1.22

$$\begin{bmatrix} \bar{V}_{FFk} \\ \bar{I}_{FRk} \end{bmatrix} = \begin{bmatrix} A_4 & B_4 \\ C_4 & D_4 \end{bmatrix}\begin{bmatrix} A_5 & B_5 \\ C_5 & D_5 \end{bmatrix}\begin{bmatrix} \bar{V}_{Rk} \\ \bar{I}_{Rk} \end{bmatrix}$$

$$= \begin{bmatrix} A_{45} & B_{45} \\ C_{45} & D_{45} \end{bmatrix}\begin{bmatrix} \bar{V}_{Rk} \\ \bar{I}_{Rk} \end{bmatrix} \quad \ldots \text{(A1.18)}$$

where $\begin{bmatrix} A_{45} & B_{45} \\ C_{45} & D_{45} \end{bmatrix} = \begin{bmatrix} A_4 & B_4 \\ C_4 & D_4 \end{bmatrix}\begin{bmatrix} A_5 & B_5 \\ C_5 & D_5 \end{bmatrix}$

Substituting the value of $\bar{I}_{Rk}$ from equation A1.4 in equation A1.18 and the value of $\bar{I}_{RRk}$ from equation A1.17.

$$\bar{V}_{FFk} = A_{45}\,\bar{V}_{Rk} + B_{45}\,\bar{I}_{Rk}$$

$$= A_{45}\,\bar{V}_{Rk} + B_{45}\,(\bar{I}_{RRk} - Z_{cap}^{-1}\,\bar{E}_{Rk})$$

$$= (A_{45} + B_{45}\,XY^{-1})\,\bar{V}_{Rk} + B_{45}\,XY^{-1}\,\bar{E}_{Rk}$$

$$- B_{45}\,(C_6 - XY^{-1}\,A_6)\,\bar{E}_{BRk}$$

$$= W\bar{V}_{Rk} + B_{45}\,XY^{-1}\,\bar{E}_{Rk} - B_{45}(C_6 - XY^{-1}A_6)\bar{E}_{BRk}$$

. . . (A1.19)

Similarly, $\bar{I}_{FRk} = C_{45}\,\bar{V}_{Rk} + D_{45}\,\bar{I}_{Rk}$

$$= (C_{45} + D_{45}\,XY^{-1})\bar{V}_{Rk} + D_{45}XY^{-1}\,\bar{E}_{Rk}$$

$$- D_{45}(C_6 - XY^{-1}A_6)\,\bar{E}_{BRk}$$

$$= V\,\bar{V}_{Rk} + D_{45}\,XY^{-1}\,\bar{E}_{Rk}$$

$$- D_{45}\,(C_6 - XY^{-1}A_6)\,\bar{E}_{BRk}$$

. . . (A1.20)

where $W = A_{45} + B_{45}XY^{-1}$ and $V = C_{45} + D_{45}XY^{-1}$.

From equations A1.19 and A1.20:

$$\bar{V}_{FFk} = WV^{-1}\bar{I}_{FRk} - (WV^{-1}D_{45} - B_{45})XY^{-1}\bar{E}_{Rk}$$

$$+ (WV^{-1}D_{45} - B_{45})(C_6 - XY^{-1}A_6)\bar{E}_{BRk}$$

. . . (A1.21)

$$\text{and} \begin{bmatrix} \bar{V}_{FFk} \\ -\bar{I}_{FSk} \end{bmatrix} = \begin{bmatrix} A_3 & B_3 \\ C_3 & D_3 \end{bmatrix} \begin{bmatrix} A_2 & B_2 \\ C_2 & D_2 \end{bmatrix} \begin{bmatrix} \bar{V}_{Sk} \\ -\bar{I}_{Sk} \end{bmatrix}$$

$$= \begin{bmatrix} A_{32} & B_{32} \\ C_{32} & D_{32} \end{bmatrix} \begin{bmatrix} V_{Sk} \\ -I_{Sk} \end{bmatrix} \qquad \ldots \text{(A1.22)}$$

where

$$\begin{bmatrix} A_{32} & B_{32} \\ C_{32} & D_{32} \end{bmatrix} = \begin{bmatrix} A_3 & B_3 \\ C_3 & D_3 \end{bmatrix} \begin{bmatrix} A_2 & B_2 \\ C_2 & D_2 \end{bmatrix}$$

Again substituting the value of $\bar{I}_{Sk}$ from equation A1.3 in equation A1.22 and the value of $\bar{I}_{SSk}$ from equation A1.12

$$\bar{V}_{FFk} = A_{32}\,\bar{V}_{Sk} - B_{32}\,\bar{I}_{Sk}$$

$$= A_{32}\,\bar{V}_{Sk} - B_{32}\,(\bar{I}_{SSk} - Z_{cap}^{-1}\,\bar{E}_{Sk})$$

$$= (A_{32} + B_{32}\,TU^{-1})\,\bar{V}_{Sk} - B_{32}TU^{-1}\,\bar{E}_{Sk}$$

$$+ B_{32}\,(C_1 - TU^{-1}A_1)\,\bar{E}_{BSk}$$

$$= S\,\bar{V}_{Sk} - B_{32}TU^{-1}\bar{E}_{Sk} + B_{32}(C_1 - TU^{-1}A_1)\bar{E}_{BSk}$$

$$\ldots \text{(A1.23)}$$

$$\text{and} \quad \bar{I}_{FSk} = -C_{32}\,\bar{V}_{Sk} + D_{32}\,\bar{I}_{Sk}$$

$$= -(C_{32} + D_{32}TU^{-1})\bar{V}_{Sk} + D_{32}TU^{-1}\bar{E}_{Sk}$$

$$- D_{32}(C_1 - TU^{-1}A_1)\,\bar{E}_{BSk}$$

$$= -R\bar{V}_{Sk} + D_{32}TU^{-1}\bar{E}_{Sk} - D_{32}(C_1 - TU^{-1}A_1)\bar{E}_{BSk}$$

$$\ldots \text{(A1.24)}$$

where $S = A_{32} + B_{32}\,TU^{-1}$ and $R = C_{32} + D_{32}\,TU^{-1}$.

From equations A1.23 and A1.24:

$$\bar{V}_{FFk} = -SR^{-1}\bar{I}_{FSk} + (SR^{-1}D_{32} - B_{32})TU^{-1}\bar{E}_{Sk} - (SR^{-1}D_{32} - B_{32})(C_1 - TU^{-1}A_1)\bar{E}_{BSk} \quad \ldots \text{(A1.25)}$$

For a general earth fault

$$\bar{V}_{FFk} = \bar{E}_{FFk} + R_F\bar{I}_{FSRk} \quad \ldots \text{(A1.26)}$$

From equations A1.21 and A1.25 a relationship with $\bar{I}_{FSRk}$ (which is equal to $\bar{I}_{FSk} - \bar{I}_{FRk}$) can be obtained and further with equation A1.26, a relationship in the form of equation A1.27 is known.

$$\begin{aligned}\bar{I}_{FSRk} &= -(RS^{-1} + VW^{-1})\bar{V}_{FFk} + (D_{32} - RS^{-1}B_{32})TU^{-1}\bar{E}_{Sk} \\ &\quad -(D_{45} - VW^{-1}B_{45})XY^{-1}\bar{E}_{Rk} - (D_{32} - RSB_{32}) * \\ &\quad (C_1 - TU^{-1}A_1)\bar{E}_{BSk} + (D_{45} - VW^{-1}B_{45})(C_6 - XY^{-1}A_6) * \\ &\quad \bar{E}_{BRk} \\ &= -[1 + (RS^{-1} + VW^{-1})R_F]^{-1}[(RS^{-1} + VW^{-1})\bar{E}_{FFk} \\ &\quad -(D_{32} - RS^{-1}B_{32})TU^{-1}\bar{E}_{Sk} + (D_{45} - VW^{-1}B_{45}) * \\ &\quad XY^{-1}\bar{E}_{Rk} + (D_{32} - RS^{-1}B_{32})(C_1 - TU^{-1}A_1)\bar{E}_{BSk} \\ &\quad -(D_{45} - VW^{-1}B_{45})(C_6 - XY^{-1}A_6)\bar{E}_{BRk}] \quad \ldots \text{(A1.27)}\end{aligned}$$

Moreover, the voltage and current variations beyond the receiving and sending end capacitors to that of the fault point quantities are given by equations A1.28 and A1.30.

$$\begin{bmatrix} \bar{V}_{Rk} \\ -\bar{I}_{Rk} \end{bmatrix} = \begin{bmatrix} A_5 & B_5 \\ C_5 & D_5 \end{bmatrix} \begin{bmatrix} A_4 & B_4 \\ C_4 & D_4 \end{bmatrix} \begin{bmatrix} \bar{V}_{FFk} \\ -\bar{I}_{RFk} \end{bmatrix}$$

$$= \begin{bmatrix} A_{54} & B_{54} \\ C_{54} & D_{54} \end{bmatrix} \begin{bmatrix} \bar{V}_{FFk} \\ -\bar{I}_{FRk} \end{bmatrix} \qquad \ldots \text{(A1.28)}$$

where

$$\begin{bmatrix} A_{54} & B_{54} \\ C_{54} & D_{54} \end{bmatrix} = \begin{bmatrix} A_5 & B_5 \\ C_5 & D_5 \end{bmatrix} \begin{bmatrix} A_4 & B_4 \\ C_4 & D_4 \end{bmatrix}$$

Substituting the values of $\bar{I}_{Rk}$ from equation A1.4 in equation A1.28 and substituting the values of $\bar{I}_{FRk}$, $\bar{V}_{FFk}$ and $\bar{I}_{FSRk}$ from equations A1.21, A1.26 and A1.27 respectively, to obtain equation A1.29.

$$\bar{I}_{Rk} = -C_{54}\bar{V}_{FFk} + D_{54}\bar{I}_{FRk}$$

$$\bar{I}_{RRk} = -C_{54}\bar{V}_{FFk} + D_{54}VW^{-1}\,[\bar{V}_{FFk} + (WV^{-1}D_{45} - B_{45}) * XY^{-1}\bar{E}_{Rk} - (WV^{-1}D_{45} - B_{45})(C_6 - XY^{-1}A_6)\bar{E}_{BRk}\,] + Z_{cap}^{-1}\,\bar{E}_{Rk}$$

$$= -(C_{54} - D_{54}VW^{-1})(\bar{E}_{FFk} + R_F\bar{I}_{FSRk})$$

$$+ D_{54}(D_{45} - VW^{-1}B_{45})XY^{-1}\bar{E}_{Rk} + Z_{cap}^{-1}\bar{E}_{Rk}$$

$$- D_{54}(D_{45} - VW^{-1}B_{45})(C_6 - XY^{-1}A_6)\bar{E}_{BRk}$$

$$= -(C_{54} - D_{54}VW^{-1})\ [1 - R_F\{1 + (RS^{-1} + VW^{-1})R_F\}^{-1} *$$

$$(RS^{-1} + VW^{-1})]\ \bar{E}_{FFk} - (C_{54} - D_{54}VW^{-1}) *$$

$$R_F\{1 + (RS^{-1} + VW^{-1})R_F\}^{-1}(D_{32} - RS^{-1}B_{32})TU^{-1}\bar{E}_{Sk}$$

$$+ [(C_{54} - D_{54}VW^{-1})R_F\{1 + (RS^{-1} + VW^{-1})R_F\}^{-1} *$$

$$(D_{45} - VW^{-1}B_{45})XY^{-1} + D_{54}\ (D_{45} - VW^{-1}B_{45})XY^{-1}$$

$$+ Z_{cap}^{-1}\ ]\ \bar{E}_{Rk} + (C_{54} - D_{54}VW^{-1})R_F\{1 + (RS^{-1} + VW^{-1}) *$$

$$R_F\}^{-1}(D_{32} - RS^{-1}B_{32})(C_1 - TU^{-1}A_1)\bar{E}_{BSk}$$

$$- [(C_{54} - D_{54}VW^{-1})R_F\{1 + (RS^{-1} + VW^{-1})R_F\}^{-1} + D_{54}] *$$

$$(D_{45} - VW^{-1}B_{45})(C_6 - XY^{-1}A_6)\bar{E}_{BRk}$$

. . . (A1.29)

and

$$\begin{bmatrix} \bar{V}_{Sk} \\ \bar{I}_{Sk} \end{bmatrix} = \begin{bmatrix} A_2 & B_2 \\ C_2 & D_2 \end{bmatrix} \begin{bmatrix} A_3 & B_3 \\ C_3 & D_3 \end{bmatrix} \begin{bmatrix} \bar{V}_{FFk} \\ \bar{I}_{FSk} \end{bmatrix}$$

$$= \begin{bmatrix} A_{23} & B_{23} \\ C_{23} & D_{23} \end{bmatrix} \begin{bmatrix} \bar{V}_{FFk} \\ \bar{I}_{FSk} \end{bmatrix} \qquad \text{. . . (A1.30)}$$

where $\begin{bmatrix} A_{23} & B_{23} \\ C_{23} & D_{23} \end{bmatrix} = \begin{bmatrix} A_2 & B_2 \\ C_2 & D_2 \end{bmatrix} \begin{bmatrix} A_3 & B_3 \\ C_3 & D_3 \end{bmatrix}$

Substituting the values of $\bar{I}_{Sk}$ from equation A1.3 in equation A1.30 and subsequently substituting $\bar{I}_{FSk}$, $\bar{V}_{FFk}$ and $\bar{I}_{FSRk}$ from equation A1.25, A1.26 and A1.27 respectively to obtain equation A1.31.

$$\bar{I}_{Sk} = C_{23}\bar{V}_{FFk} + D_{23}\bar{I}_{FSk}$$

Therefore

$$\begin{aligned}
\bar{I}_{SSk} &= C_{23}\bar{V}_{FFk} - D_{23}RS^{-1}\,[\bar{V}_{FFk} - (SR^{-1}D_{32} - B_{32})TU^{-1}\bar{E}_{Sk} \\
&\quad + (SR^{-1}D_{32} - B_{32})(C_1 - TU^{-1}A_1)\bar{E}_{BSk}] \\
&\quad + Z_{cap}^{-1}\,\bar{E}_{Sk} \\
&= (C_{23} - D_{23}RS^{-1})(\bar{E}_{FFk} + R_F\,\bar{I}_{FSRk}) \\
&\quad + D_{23}(D_{32} - RS^{-1}B_{32})TU^{-1}\bar{E}_{Sk} + Z_{cap}^{-1}\,\bar{E}_{Sk} \\
&\quad - D_{23}(B_{32} - RS^{-1}B_{32})(C_1 - TU^{-1}A_1)\bar{E}_{BSk} \\
&= (C_{23} - D_{23}RS^{-1})\,[1 - R_F\{1 + (RS^{-1} + VW^{-1})R_F\}^{-1} * \\
&\quad (RS^{-1} + VW^{-1})]\bar{E}_{FFk} + [(C_{23} - D_{23}RS^{-1})R_F\{1 + (RS^{-1} \\
&\quad + VW^{-1})R_F\}^{-1}(D_{32} - RS^{-1}B_{32})TU^{-1} \\
&\quad + D_{23}(D_{32} - RS^{-1}B_{32})TU^{-1} + Z_{cap}^{-1}]\bar{E}_{Sk} \\
&\quad - (C_{23} - D_{23}RS^{-1})R_F\,[1 + (RS^{-1} + VW^{-1})R_F]^{-1} *
\end{aligned}$$

$$(D_{45} - VW^{-1}B_{45})XY^{-1}\bar{E}_{Rk} - [(C_{23} - D_{23}RS^{-1}) *$$

$$R_F\{1 + (RS^{-1} + VW^{-1})R_F\}^{-1} + D_{23}] *$$

$$(D_{32} - RS^{-1}B_{32})(C_1 - TU^{-1}A_1)\bar{E}_{BSk}$$

$$+ (C_{23} - D_{23}RS^{-1})R_F\{1 + (RS^{-1} + VW^{-1})R_F\}^{-1} *$$

$$(D_{45} - VW^{-1}B_{45})(C_6 - XY^{-1}A_6)\bar{E}_{BRk}$$

. . . (A1.31)

Substituting the value of $\bar{I}_{Sk}$ from equation A1.3 in equation A1.9 and subsequently the value of $\bar{I}_{SSk}$ from equation A1.31, to obtain equation A1.32.

$$\bar{I}_{BSk} = T^{-1}(\bar{I}_{SSk} - Z_{cap}^{-1}\bar{E}_{Sk} + C_1\bar{E}_{BSk})$$

$$= T^{-1}(C_{23} - D_{23}RS^{-1})[1 - R_F\{1 + (RS^{-1} + VW^{-1})R_F\}^{-1} *$$

$$(RS^{-1} + VW^{-1})]\bar{E}_{FFk} + T^{-1}[(C_{23} - D_{23}RS^{-1}) *$$

$$R_F\{1 + (RS^{-1} + VW^{-1})R_F\}^{-1}(D_{32} - RS^{-1}B_{32})\,TU^{-1}$$

$$+ D_{23}(D_{32} - RS^{-1}B_{32})TU^{-1}]\bar{E}_{Sk} - T^{-1}(C_{23} - D_{23}RS^{-1}) *$$

$$R_F[1 + (RS^{-1} + VW^{-1})R_F]^{-1}(D_{45} - VW^{-1}B_{45})X_Y^{-1} *$$

$$\bar{E}_{Rk} - T^{-1}\Big[[(C_{23} - D_{23}RS^{-1})R_F\{1 + (RS^{-1} + VW^{-1}) *$$

$$R_F\}^{-1} + D_{23}](D_{32} - RS^{-1}B_{32})(C_1 - TU^{-1}A_1) - C_1\Big] *$$

$$\bar{E}_{BSk} + T^{-1}(C_{23} - D_{23}RS^{-1})R_F\{1 + (RS^{-1} + VW^{-1})R_F\}^{-1} *$$

$$(D_{45} - VW^{-1}B_{45})(C_6 - XY^{-1}A_6)\bar{E}_{BRk} \quad . . . (A1.32)$$

Substituting the value of $\bar{I}_{Rk}$ from equation A1.4 in equation A1.15 and subsequently the value of $\bar{I}_{RRk}$ from equation A1.29, to obtain equation A1.33.

$$\bar{I}_{Rk} = X\bar{I}_{BRk} - C_6\bar{E}_{BRk}$$

Therefore

$$\begin{aligned}\bar{I}_{BRk} = {} & -X^{-1}(C_{54} - D_{54}VW^{-1})[1 - R_F\{1 + (RS^{-1} + VW^{-1})R_F\}^{-1} * \\ & (RS^{-1} + VW^{-1})]\bar{E}_{FFk} - X^{-1}(C_{54} - D_{54}VW^{-1})R_F\{1 + (RS^{-1} \\ & + VW^{-1})R_F\}^{-1}(D_{32} - RS^{-1}B_{32})TU^{-1}\bar{E}_{Sk} + X^{-1}[(C_{54} \\ & - D_{54}VW^{-1})R_F\{1 + (RS^{-1} + VW^{-1})R_F\}^{-1}(D_{45} - VW^{-1}B_{45}) * \\ & XY^{-1} + D_{54}(D_{45} - VW^{-1}B_{45})XY^{-1}]\bar{E}_{Rk} + X^{-1}(C_{54} \\ & - D_{54}VW^{-1})R_F\{1 + (RS^{-1} + VW^{-1})R_F\}^{-1}(D_{32} - RS^{-1}B_{32}) * \\ & (C_1 - TU^{-1}A_1)\bar{E}_{BSk} - X^{-1}\Big[[(C_{54} - D_{54}VW^{-1}) * \\ & R_F\{1 + (RS^{-1} + VW^{-1})R_F\}^{-1} + D_{54}](D_{45} - VW^{-1}B_{45}) * \\ & (C_6 - XY^{-1}A_6) - C_6\Big]\bar{E}_{BRk}\end{aligned} \qquad \ldots \text{(A1.33)}$$

Hence, from equations A1.27, A1.31, A1.29, A1.32 and A1.33, the universal [A] (15 x 15) admittance matrix as shown in equation A1.34 is obtained. Depending upon whether in a superimposed circuit the injected quantity is a current or a voltage source, an impedance matrix relation as shown in equation A1.35 is also made use of, the impedance matrix being the inverse of the admittance matrix [A].

$$
\begin{bmatrix}
\bar{I}_{FSRka} \\ \bar{I}_{FSRkb} \\ \bar{I}_{FSRkc} \\ \bar{I}_{SSka} \\ \bar{I}_{SSkb} \\ \bar{I}_{SSkc} \\ \bar{I}_{RRka} \\ \bar{I}_{RRkb} \\ \bar{I}_{RRkc} \\ \bar{I}_{BSka} \\ \bar{I}_{BSkb} \\ \bar{I}_{BSkc} \\ \bar{I}_{BRka} \\ \bar{I}_{BRkb} \\ \bar{I}_{BRkc}
\end{bmatrix}
=
\begin{bmatrix}
A_{1,1} & A_{1,2} & A_{1,3} & A_{1,4} & A_{1,5} & A_{1,6} & A_{1,7} & A_{1,8} & A_{1,9} & A_{1,10} & A_{1,11} & A_{1,12} & A_{1,13} & A_{1,14} & A_{1,15} \\
A_{2,1} & A_{2,2} & A_{2,3} & A_{2,4} & A_{2,5} & A_{2,6} & A_{2,7} & A_{2,8} & A_{2,9} & A_{2,10} & A_{2,11} & A_{2,12} & A_{2,13} & A_{2,14} & A_{2,15} \\
A_{3,1} & A_{3,2} & A_{3,3} & A_{3,4} & A_{3,5} & A_{3,6} & A_{3,7} & A_{3,8} & A_{3,9} & A_{3,10} & A_{3,11} & A_{3,12} & A_{3,13} & A_{3,14} & A_{3,15} \\
A_{4,1} & A_{4,2} & A_{4,3} & A_{4,4} & A_{4,5} & A_{4,6} & A_{4,7} & A_{4,8} & A_{4,9} & A_{4,10} & A_{4,11} & A_{4,12} & A_{4,13} & A_{4,14} & A_{4,15} \\
A_{5,1} & A_{5,2} & A_{5,3} & A_{5,4} & A_{5,5} & A_{5,6} & A_{5,7} & A_{5,8} & A_{5,9} & A_{5,10} & A_{5,11} & A_{5,12} & A_{5,13} & A_{5,14} & A_{5,15} \\
A_{6,1} & A_{6,2} & A_{6,3} & A_{6,4} & A_{6,5} & A_{6,6} & A_{6,7} & A_{6,8} & A_{6,9} & A_{6,10} & A_{6,11} & A_{6,12} & A_{6,13} & A_{6,14} & A_{6,15} \\
A_{7,1} & A_{7,2} & A_{7,3} & A_{7,4} & A_{7,5} & A_{7,6} & A_{7,7} & A_{7,8} & A_{7,9} & A_{7,10} & A_{7,11} & A_{7,12} & A_{7,13} & A_{7,14} & A_{7,15} \\
A_{8,1} & A_{8,2} & A_{8,3} & A_{8,4} & A_{8,5} & A_{8,6} & A_{8,7} & A_{8,8} & A_{8,9} & A_{8,10} & A_{8,11} & A_{8,12} & A_{8,13} & A_{8,14} & A_{8,15} \\
A_{9,1} & A_{9,2} & A_{9,3} & A_{9,4} & A_{9,5} & A_{9,6} & A_{9,7} & A_{9,8} & A_{9,9} & A_{9,10} & A_{9,11} & A_{9,12} & A_{9,13} & A_{9,14} & A_{9,15} \\
A_{10,1} & A_{10,2} & A_{10,3} & A_{10,4} & A_{10,5} & A_{10,6} & A_{10,7} & A_{10,8} & A_{10,9} & A_{10,10} & A_{10,11} & A_{10,12} & A_{10,13} & A_{10,14} & A_{10,15} \\
A_{11,1} & A_{11,2} & A_{11,3} & A_{11,4} & A_{11,5} & A_{11,6} & A_{11,7} & A_{11,8} & A_{11,9} & A_{11,10} & A_{11,11} & A_{11,12} & A_{11,13} & A_{11,14} & A_{11,15} \\
A_{12,1} & A_{12,2} & A_{12,3} & A_{12,4} & A_{12,5} & A_{12,6} & A_{12,7} & A_{12,8} & A_{12,9} & A_{12,10} & A_{12,11} & A_{12,12} & A_{12,13} & A_{12,14} & A_{12,15} \\
A_{13,1} & A_{13,2} & A_{13,3} & A_{13,4} & A_{13,5} & A_{13,6} & A_{13,7} & A_{13,8} & A_{13,9} & A_{13,10} & A_{13,11} & A_{13,12} & A_{13,13} & A_{13,14} & A_{13,15} \\
A_{14,1} & A_{14,2} & A_{14,3} & A_{14,4} & A_{14,5} & A_{14,6} & A_{14,7} & A_{14,8} & A_{14,9} & A_{14,10} & A_{14,11} & A_{14,12} & A_{14,13} & A_{14,14} & A_{14,15} \\
A_{15,1} & A_{15,2} & A_{15,3} & A_{15,4} & A_{15,5} & A_{15,6} & A_{15,7} & A_{15,8} & A_{15,9} & A_{15,10} & A_{15,11} & A_{15,12} & A_{15,13} & A_{15,14} & A_{15,15}
\end{bmatrix}
\begin{bmatrix}
\bar{E}_{FFka} \\ \bar{E}_{FFkb} \\ \bar{E}_{FFkc} \\ \bar{E}_{Ska} \\ \bar{E}_{Skb} \\ \bar{E}_{Skc} \\ \bar{E}_{Rka} \\ \bar{E}_{Rkb} \\ \bar{E}_{Rkc} \\ \bar{E}_{BSka} \\ \bar{E}_{BSkb} \\ \bar{E}_{BSkc} \\ \bar{E}_{BRka} \\ \bar{E}_{BRkb} \\ \bar{E}_{BRkc}
\end{bmatrix}
$$

where 'A' is of the order 15 x 15 and is the universal admittance matrix

. . . (A1.34)

$$\begin{bmatrix} \bar{E}_{FFka} \\ \bar{E}_{FFkb} \\ \bar{E}_{FFkc} \\ \bar{E}_{SKa} \\ \bar{E}_{Skb} \\ \bar{E}_{Skc} \\ \bar{E}_{Rka} \\ \bar{E}_{Rkb} \\ \bar{E}_{Rkc} \\ \bar{E}_{BSka} \\ \bar{E}_{BSkb} \\ \bar{E}_{BSkc} \\ \bar{E}_{BRka} \\ \bar{E}_{BRkb} \\ \bar{E}_{BRkc} \end{bmatrix} = \begin{bmatrix} a_{1,1} & a_{1,2} & a_{1,3} & a_{1,4} & a_{1,5} & a_{1,6} & a_{1,7} & a_{1,8} & a_{1,9} & a_{1,10} & a_{1,11} & a_{1,12} & a_{1,13} & a_{1,14} & a_{1,15} \\ a_{2,1} & a_{2,2} & a_{2,3} & a_{2,4} & a_{2,5} & a_{2,6} & a_{2,7} & a_{2,8} & a_{2,9} & a_{2,10} & a_{2,11} & a_{2,12} & a_{2,13} & a_{2,14} & a_{2,15} \\ a_{3,1} & a_{3,2} & a_{3,3} & a_{3,4} & a_{3,5} & a_{3,6} & a_{3,7} & a_{3,8} & a_{3,9} & a_{3,10} & a_{3,11} & a_{3,12} & a_{3,13} & a_{3,14} & a_{3,15} \\ a_{4,1} & a_{4,2} & a_{4,3} & a_{4,4} & a_{4,5} & a_{4,6} & a_{4,7} & a_{4,8} & a_{4,9} & a_{4,10} & a_{4,11} & a_{4,12} & a_{4,13} & a_{4,14} & a_{4,15} \\ a_{5,1} & a_{5,2} & a_{5,3} & a_{5,4} & a_{5,5} & a_{5,6} & a_{5,7} & a_{5,8} & a_{5,9} & a_{5,10} & a_{5,11} & a_{5,12} & a_{5,13} & a_{5,14} & a_{5,15} \\ a_{6,1} & a_{6,2} & a_{6,3} & a_{6,4} & a_{6,5} & a_{6,6} & a_{6,7} & a_{6,8} & a_{6,9} & a_{6,10} & a_{6,11} & a_{6,12} & a_{6,13} & a_{6,14} & a_{6,15} \\ a_{7,1} & a_{7,2} & a_{7,3} & a_{7,4} & a_{7,5} & a_{7,6} & a_{7,7} & a_{7,8} & a_{7,9} & a_{7,10} & a_{7,11} & a_{7,12} & a_{7,13} & a_{7,14} & a_{7,15} \\ a_{8,1} & a_{8,2} & a_{8,3} & a_{8,4} & a_{8,5} & a_{8,6} & a_{8,7} & a_{8,8} & a_{8,9} & a_{8,10} & a_{8,11} & a_{8,12} & a_{8,13} & a_{8,14} & a_{8,15} \\ a_{9,1} & a_{9,2} & a_{9,3} & a_{9,4} & a_{9,5} & a_{9,6} & a_{9,7} & a_{9,8} & a_{9,9} & a_{9,10} & a_{9,11} & a_{9,12} & a_{9,13} & a_{9,14} & a_{9,15} \\ a_{10,1} & a_{10,2} & a_{10,3} & a_{10,4} & a_{10,5} & a_{10,6} & a_{10,7} & a_{10,8} & a_{10,9} & a_{10,10} & a_{10,11} & a_{10,12} & a_{10,13} & a_{10,14} & a_{10,15} \\ a_{11,1} & a_{11,2} & a_{11,3} & a_{11,4} & a_{11,5} & a_{11,6} & a_{11,7} & a_{11,8} & a_{11,9} & a_{11,10} & a_{11,11} & a_{11,12} & a_{11,13} & a_{11,14} & a_{11,15} \\ a_{12,1} & a_{12,2} & a_{12,3} & a_{12,4} & a_{12,5} & a_{12,6} & a_{12,7} & a_{12,8} & a_{12,9} & a_{12,10} & a_{12,11} & a_{12,12} & a_{12,13} & a_{12,14} & a_{12,15} \\ a_{13,1} & a_{13,2} & a_{13,3} & a_{13,4} & a_{13,5} & a_{13,6} & a_{13,7} & a_{13,8} & a_{13,9} & a_{13,10} & a_{13,11} & a_{13,12} & a_{13,13} & a_{13,14} & a_{13,15} \\ a_{14,1} & a_{14,2} & a_{14,3} & a_{14,4} & a_{14,5} & a_{14,6} & a_{14,7} & a_{14,8} & a_{14,9} & a_{14,10} & a_{14,11} & a_{14,12} & a_{14,13} & a_{14,14} & a_{14,15} \\ a_{15,1} & a_{15,2} & a_{15,3} & a_{15,4} & a_{15,5} & a_{15,6} & a_{15,7} & a_{15,8} & a_{15,9} & a_{15,10} & a_{15,11} & a_{15,12} & a_{15,13} & a_{15,14} & a_{15,15} \end{bmatrix} \begin{bmatrix} \bar{I}_{FSRka} \\ \bar{I}_{FSRkb} \\ \bar{I}_{FSRkc} \\ \bar{I}_{SSka} \\ \bar{I}_{SSkb} \\ \bar{I}_{SSkc} \\ \bar{I}_{RRka} \\ \bar{I}_{RRkb} \\ \bar{I}_{RRkc} \\ \bar{I}_{BSka} \\ \bar{I}_{BSkb} \\ \bar{I}_{BSkc} \\ \bar{I}_{BRka} \\ \bar{I}_{BRkb} \\ \bar{I}_{BRkc} \end{bmatrix}$$

where 'a' is the inverse of 'A' matrix, order 15 x 15 and is the universal impedance matrix . . . (A1.35)

A1.2 Phase-to-phase fault

The techniques described in the previous section about the single-phase-to-earth fault can be employed in the analysis of other types of faults, viz, double-phase-to-earth faults and three-phase-to-earth faults. But the interphase faults not involving earth are best dealt with by considering the superimposed voltages between phases. Hence, with reference to Figure 3.7, it can be seen that:

$$\bar{I}_{FSka} - \bar{I}_{FRka} = \bar{I}_{FSRka} = \bar{I}_{Fkab} - \bar{I}_{Fkca}$$

$$\bar{I}_{FSkb} - \bar{I}_{FRkb} = \bar{I}_{FSRkb} = \bar{I}_{Fkbc} - \bar{I}_{Fkab}$$

$$\bar{I}_{FSkc} - \bar{I}_{FRkc} = \bar{I}_{FSRkc} = \bar{I}_{Fkca} - \bar{I}_{Fkbc} \quad \ldots \text{(A1.36)}$$

and

$$\bar{E}_{FFka} = \bar{V}_{FFka} - R_F \bar{I}_{FSRka}$$

$$\bar{E}_{FFkb} = \bar{V}_{FFkb} - R_F \bar{I}_{FSRkb}$$

$$\bar{E}_{FFkc} = \bar{V}_{FFkc} - R_F \bar{I}_{FSRkc} \quad \ldots \text{(A1.37)}$$

When $R_F = 0.0$, equation A1.37 becomes

$$\bar{E}_{FFka} = \bar{V}_{FFka} \; ; \; \bar{E}_{FFkb} = \bar{V}_{FFkb} \; ; \; \bar{E}_{FFkc} = \bar{V}_{FFkc} \quad \ldots \text{(A1.38)}$$

On substituting equations A1.36 and A1.38 in equation A1.35, a new matrix relationship in the form of equation A1.39 develops.

$$
\begin{bmatrix} \bar{V}_{FFka} \\ \bar{V}_{FFkb} \\ \bar{V}_{FFkc} \\ \bar{E}_{Ska} \\ \bar{E}_{Skb} \\ \bar{E}_{Skc} \\ \bar{E}_{Rka} \\ \bar{E}_{Rkb} \\ \bar{E}_{Rkc} \\ \bar{E}_{BSka} \\ \bar{E}_{BSkb} \\ \bar{E}_{BSkc} \\ \bar{E}_{BRka} \\ \bar{E}_{BRkb} \\ \bar{E}_{BRkc} \end{bmatrix} = \begin{bmatrix} n_{1,1} & n_{1,2} & n_{1,3} & n_{1,4} & n_{1,5} & n_{1,6} & n_{1,7} & n_{1,8} & n_{1,9} & n_{1,10} & n_{1,11} & n_{1,12} & n_{1,13} & n_{1,14} & n_{1,15} \\ n_{2,1} & n_{2,2} & n_{2,3} & n_{2,4} & n_{2,5} & n_{2,6} & n_{2,7} & n_{2,8} & n_{2,9} & n_{2,10} & n_{2,11} & n_{2,12} & n_{2,13} & n_{2,14} & n_{2,15} \\ n_{3,1} & n_{3,2} & n_{3,3} & n_{3,4} & n_{3,5} & n_{3,6} & n_{3,7} & n_{3,8} & n_{3,9} & n_{3,10} & n_{3,11} & n_{3,12} & n_{3,13} & n_{3,14} & n_{3,15} \\ n_{4,1} & n_{4,2} & n_{4,3} & n_{4,4} & n_{4,5} & n_{4,6} & n_{4,7} & n_{4,8} & n_{4,9} & n_{4,10} & n_{4,11} & n_{4,12} & n_{4,13} & n_{4,14} & n_{4,15} \\ n_{5,1} & n_{5,2} & n_{5,3} & n_{5,4} & n_{5,5} & n_{5,6} & n_{5,7} & n_{5,8} & n_{5,9} & n_{5,10} & n_{5,11} & n_{5,12} & n_{5,13} & n_{5,14} & n_{5,15} \\ n_{6,1} & n_{6,2} & n_{6,3} & n_{6,4} & n_{6,5} & n_{6,6} & n_{6,7} & n_{6,8} & n_{6,9} & n_{6,10} & n_{6,11} & n_{6,12} & n_{6,13} & n_{6,14} & n_{6,15} \\ n_{7,1} & n_{7,2} & n_{7,3} & n_{7,4} & n_{7,5} & n_{7,6} & n_{7,7} & n_{7,8} & n_{7,9} & n_{7,10} & n_{7,11} & n_{7,12} & n_{7,13} & n_{7,14} & n_{7,15} \\ n_{8,1} & n_{8,2} & n_{8,3} & n_{8,4} & n_{8,5} & n_{8,6} & n_{8,7} & n_{8,8} & n_{8,9} & n_{8,10} & n_{8,11} & n_{8,12} & n_{8,13} & n_{8,14} & n_{8,15} \\ n_{9,1} & n_{9,2} & n_{9,3} & n_{9,4} & n_{9,5} & n_{9,6} & n_{9,7} & n_{9,8} & n_{9,9} & n_{9,10} & n_{9,11} & n_{9,12} & n_{9,13} & n_{9,14} & n_{9,15} \\ n_{10,1} & n_{10,2} & n_{10,3} & n_{10,4} & n_{10,5} & n_{10,6} & n_{10,7} & n_{10,8} & n_{10,9} & n_{10,10} & n_{10,11} & n_{10,12} & n_{10,13} & n_{10,14} & n_{10,15} \\ n_{11,1} & n_{11,2} & n_{11,3} & n_{11,4} & n_{11,5} & n_{11,6} & n_{11,7} & n_{11,8} & n_{11,9} & n_{11,10} & n_{11,11} & n_{11,12} & n_{11,13} & n_{11,14} & n_{11,15} \\ n_{12,1} & n_{12,2} & n_{12,3} & n_{12,4} & n_{12,5} & n_{12,6} & n_{12,7} & n_{12,8} & n_{12,9} & n_{12,10} & n_{12,11} & n_{12,12} & n_{12,13} & n_{12,14} & n_{12,15} \\ n_{13,1} & n_{13,2} & n_{13,3} & n_{13,4} & n_{13,5} & n_{13,6} & n_{13,7} & n_{13,8} & n_{13,9} & n_{13,10} & n_{13,11} & n_{13,12} & n_{13,13} & n_{13,14} & n_{13,15} \\ n_{14,1} & n_{14,2} & n_{14,3} & n_{14,4} & n_{14,5} & n_{14,6} & n_{14,7} & n_{14,8} & n_{14,9} & n_{14,10} & n_{14,11} & n_{14,12} & n_{14,13} & n_{14,14} & n_{14,15} \\ n_{15,1} & n_{15,2} & n_{15,3} & n_{15,4} & n_{15,5} & n_{15,6} & n_{15,7} & n_{15,8} & n_{15,9} & n_{15,10} & n_{15,11} & n_{15,12} & n_{15,13} & n_{15,14} & n_{15,15} \end{bmatrix} \begin{bmatrix} \bar{I}_{FSRka} \\ \bar{I}_{FSRkb} \\ \bar{I}_{FSRkc} \\ \bar{I}_{SSka} \\ \bar{I}_{SSkb} \\ \bar{I}_{SSkc} \\ \bar{I}_{RRka} \\ \bar{I}_{RRkb} \\ \bar{I}_{RRkc} \\ \bar{I}_{BSka} \\ \bar{I}_{BSkb} \\ \bar{I}_{BSkc} \\ \bar{I}_{BRka} \\ \bar{I}_{BRkb} \\ \bar{I}_{BRkc} \end{bmatrix}
$$

where [n] matrix is similar to [a] matrix of equation A1.35, but with $R_F = 0.0$

. . . (A1.39)

Again with reference to Figure 3.7, it can be seen that:

$$\bar{V}_{FFka} - \bar{V}_{FFkb} = \bar{V}_{FFkab}$$

$$\bar{V}_{FFkb} - \bar{V}_{FFkc} = \bar{V}_{FFkbc}$$

$$\bar{V}_{FFkc} - \bar{V}_{FFka} = \bar{V}_{FFkca} \quad \ldots \text{(A1.40)}$$

and

$$\bar{E}_{FFkab} = \bar{V}_{FFkab} - R_F \bar{I}_{Fkab}$$

$$\bar{E}_{FFkbc} = \bar{V}_{FFkbc} - R_F \bar{I}_{Fkbc}$$

$$\bar{E}_{FFkca} = \bar{V}_{FFkca} - R_F \bar{I}_{Fkca} \quad \ldots \text{(A1.41)}$$

Using equation A1.40 in equation A1.39 and from the knowledge of equation A1.36, the relationship of equation A1.42 is given.

$$
\begin{bmatrix}
\bar{V}_{FFkab} \\ \bar{V}_{FFkbc} \\ \bar{V}_{FFkca} \\ \bar{E}_{Ska} \\ \bar{E}_{Skb} \\ \bar{E}_{Skc} \\ \bar{E}_{Rka} \\ \bar{E}_{Rkb} \\ \bar{E}_{Rkc} \\ \bar{E}_{BSka} \\ \bar{E}_{BSkb} \\ \bar{E}_{BSkc} \\ \bar{E}_{BRka} \\ \bar{E}_{BRkb} \\ \bar{E}_{BRkc}
\end{bmatrix}
=
\begin{bmatrix}
p_{1,1} & p_{1,2} & p_{1,3} & p_{1,4} & p_{1,5} & p_{1,6} & p_{1,7} & p_{1,8} & p_{1,9} & p_{1,10} & p_{1,11} & p_{1,12} & p_{1,13} & p_{1,14} & p_{1,15} \\
p_{2,1} & p_{2,2} & p_{2,3} & p_{2,4} & p_{2,5} & p_{2,6} & p_{2,7} & p_{2,8} & p_{2,9} & p_{2,10} & p_{2,11} & p_{2,12} & p_{2,13} & p_{2,14} & p_{2,15} \\
p_{3,1} & p_{3,2} & p_{3,3} & p_{3,4} & p_{3,5} & p_{3,6} & p_{3,7} & p_{3,8} & p_{3,9} & p_{3,10} & p_{3,11} & p_{3,12} & p_{3,13} & p_{3,14} & p_{3,15} \\
n_{4,1} & n_{4,2} & n_{4,3} & n_{4,4} & n_{4,5} & n_{4,6} & n_{4,7} & n_{4,8} & n_{4,9} & n_{4,10} & n_{4,11} & n_{4,12} & n_{4,13} & n_{4,14} & n_{4,15} \\
n_{5,1} & n_{5,2} & n_{5,3} & n_{5,4} & n_{5,5} & n_{5,6} & n_{5,7} & n_{5,8} & n_{5,9} & n_{5,10} & n_{5,11} & n_{5,12} & n_{5,13} & n_{5,14} & n_{5,15} \\
n_{6,1} & n_{6,2} & n_{6,3} & n_{6,4} & n_{6,5} & n_{6,6} & n_{6,7} & n_{6,8} & n_{6,9} & n_{6,10} & n_{6,11} & n_{6,12} & n_{6,13} & n_{6,14} & n_{6,15} \\
n_{7,1} & n_{7,2} & n_{7,3} & n_{7,4} & n_{7,5} & n_{7,6} & n_{7,7} & n_{7,8} & n_{7,9} & n_{7,10} & n_{7,11} & n_{7,12} & n_{7,13} & n_{7,14} & n_{7,15} \\
n_{8,1} & n_{8,2} & n_{8,3} & n_{8,4} & n_{8,5} & n_{8,6} & n_{8,7} & n_{8,8} & n_{8,9} & n_{8,10} & n_{8,11} & n_{8,12} & n_{8,13} & n_{8,14} & n_{8,15} \\
n_{9,1} & n_{9,2} & n_{9,3} & n_{9,4} & n_{9,5} & n_{9,6} & n_{9,7} & n_{9,8} & n_{9,9} & n_{9,10} & n_{9,11} & n_{9,12} & n_{9,13} & n_{9,14} & n_{9,15} \\
n_{10,1} & n_{10,2} & n_{10,3} & n_{10,4} & n_{10,5} & n_{10,6} & n_{10,7} & n_{10,8} & n_{10,9} & n_{10,10} & n_{10,11} & n_{10,12} & n_{10,13} & n_{10,14} & n_{10,15} \\
n_{11,1} & n_{11,2} & n_{11,3} & n_{11,4} & n_{11,5} & n_{11,6} & n_{11,7} & n_{11,8} & n_{11,9} & n_{11,10} & n_{11,11} & n_{11,12} & n_{11,13} & n_{11,14} & n_{11,15} \\
n_{12,1} & n_{12,2} & n_{12,3} & n_{12,4} & n_{12,5} & n_{12,6} & n_{12,7} & n_{12,8} & n_{12,9} & n_{12,10} & n_{12,11} & n_{12,12} & n_{12,13} & n_{12,14} & n_{12,15} \\
n_{13,1} & n_{13,2} & n_{13,3} & n_{13,4} & n_{13,5} & n_{13,6} & n_{13,7} & n_{13,8} & n_{13,9} & n_{13,10} & n_{13,11} & n_{13,12} & n_{13,13} & n_{13,14} & n_{13,15} \\
n_{14,1} & n_{14,2} & n_{14,3} & n_{14,4} & n_{14,5} & n_{14,6} & n_{14,7} & n_{14,8} & n_{14,9} & n_{14,10} & n_{14,11} & n_{14,12} & n_{14,13} & n_{14,14} & n_{14,15} \\
n_{15,1} & n_{15,2} & n_{15,3} & n_{15,4} & n_{15,5} & n_{15,6} & n_{15,7} & n_{15,8} & n_{15,9} & n_{15,10} & n_{15,11} & n_{15,12} & n_{15,13} & n_{15,14} & n_{15,15}
\end{bmatrix}
\begin{bmatrix}
\bar{I}_{Fkab} - \bar{I}_{Fkca} \\ \bar{I}_{Fkbc} - \bar{I}_{Fkab} \\ \bar{I}_{Fkca} - \bar{I}_{Fkbc} \\ \bar{I}_{SSka} \\ \bar{I}_{SSkb} \\ \bar{I}_{SSkc} \\ \bar{I}_{RRka} \\ \bar{I}_{RRkb} \\ \bar{I}_{RRkc} \\ \bar{I}_{BSka} \\ \bar{I}_{BSkb} \\ \bar{I}_{BSkc} \\ \bar{I}_{BRka} \\ \bar{I}_{BRkb} \\ \bar{I}_{BRkc}
\end{bmatrix}
$$

where $p_{i,j} = n_{i,j} - n_{k,j}$ for $i = 1, 3$ and $j = 1, 15$

$k = i+1$ if $k \leq 3$

$k = i-2$ if $k > 3$ . . . (A1.42)

Let the impedance matrix of equation A1.42 be [Q]. Hence, equation A1.42 can be simplified as shown in equation A1.43, and rearranged to equation A1.44.

$$\begin{bmatrix} \bar{V}_{FFkab} \\ \bar{V}_{FFkbc} \\ \bar{V}_{FFkca} \\ \bar{E}_{Ska} \\ \bar{E}_{Skb} \\ \bar{E}_{Skc} \\ \bar{E}_{Rka} \\ \bar{E}_{Rkb} \\ \bar{E}_{Rkc} \\ \bar{E}_{BSka} \\ \bar{E}_{BSkb} \\ \bar{E}_{BSkc} \\ \bar{E}_{BRka} \\ \bar{E}_{BRkb} \\ \bar{E}_{BRkc} \end{bmatrix} = [Q] \begin{bmatrix} \bar{I}_{Fkab} \\ \bar{I}_{Fkbc} \\ \bar{I}_{Fkca} \\ \bar{I}_{SSka} \\ \bar{I}_{SSkb} \\ \bar{I}_{SSkc} \\ \bar{I}_{RRka} \\ \bar{I}_{RRkb} \\ \bar{I}_{RRkc} \\ \bar{I}_{BSka} \\ \bar{I}_{BSkb} \\ \bar{I}_{BSkc} \\ \bar{I}_{BRka} \\ \bar{I}_{BRkb} \\ \bar{I}_{BRkc} \end{bmatrix} - \begin{bmatrix} p_{1,1} & p_{1,2} & p_{1,3} \\ p_{2,1} & p_{2,2} & p_{2,3} \\ p_{3,1} & p_{3,2} & p_{3,3} \\ n_{4,1} & n_{4,2} & n_{4,3} \\ n_{5,1} & n_{5,2} & n_{5,3} \\ n_{6,1} & n_{6,2} & n_{6,3} \\ n_{7,1} & n_{7,2} & n_{7,3} \\ n_{8,1} & n_{8,2} & n_{8,3} \\ n_{9,1} & n_{9,2} & n_{9,3} \\ n_{10,1} & n_{10,2} & n_{10,3} \\ n_{11,1} & n_{11,2} & n_{11,3} \\ n_{12,1} & n_{12,2} & n_{12,3} \\ n_{13,1} & n_{13,2} & n_{13,3} \\ n_{14,1} & n_{14,2} & n_{14,3} \\ n_{15,1} & n_{15,2} & n_{15,3} \end{bmatrix} \begin{bmatrix} \bar{I}_{Fkca} \\ \bar{I}_{Fkab} \\ \bar{I}_{Fkbc} \end{bmatrix} \quad \ldots \text{(A1.43)}$$

$$[Q]\begin{bmatrix}\bar{I}_{Fkab}\\ \bar{I}_{Fkbc}\\ \bar{I}_{Fkca}\\ \bar{I}_{SSka}\\ \bar{I}_{SSkb}\\ \bar{I}_{SSkc}\\ \bar{I}_{RRka}\\ \bar{I}_{RRkb}\\ \bar{I}_{RRkc}\\ \bar{I}_{BSka}\\ \bar{I}_{BSkb}\\ \bar{I}_{BSkc}\\ \bar{I}_{BRka}\\ \bar{I}_{BRkb}\\ \bar{I}_{BRkc}\end{bmatrix} = \begin{bmatrix}\bar{I}_{Fkab}\\ \bar{I}_{Fkbc}\\ \bar{I}_{Fkca}\end{bmatrix} - \begin{bmatrix} p_{1,2} & p_{1,3} & p_{1,1}\\ p_{2,2} & p_{2,3} & p_{2,1}\\ p_{3,2} & p_{3,3} & p_{3,1}\\ n_{4,2} & n_{4,3} & n_{4,1}\\ n_{5,2} & n_{5,3} & n_{5,1}\\ n_{6,2} & n_{6,3} & n_{6,1}\\ n_{7,2} & n_{7,3} & n_{7,1}\\ n_{8,2} & n_{8,3} & n_{8,1}\\ n_{9,2} & n_{9,3} & n_{9,1}\\ n_{10,2} & n_{10,3} & n_{10,1}\\ n_{11,2} & n_{11,3} & n_{11,1}\\ n_{12,2} & n_{12,3} & n_{12,1}\\ n_{13,2} & n_{13,3} & n_{13,1}\\ n_{14,2} & n_{14,3} & n_{14,1}\\ n_{15,2} & n_{15,3} & n_{15,1}\end{bmatrix} \quad \ldots \text{(A1.44)}$$

Equation A1.41 is substituted in equation A1.44 to give equation A1.45.

$$
\begin{bmatrix}
\bar{E}_{FFkab} \\ \bar{E}_{FFkbc} \\ \bar{E}_{FFkca} \\ \bar{E}_{Ska} \\ \bar{E}_{Skb} \\ \bar{E}_{Skc} \\ \bar{E}_{Rka} \\ \bar{E}_{Rkb} \\ \bar{E}_{Rkc} \\ \bar{E}_{BSka} \\ \bar{E}_{BSkb} \\ \bar{E}_{BSkc} \\ \bar{E}_{BRka} \\ \bar{E}_{BRkb} \\ \bar{E}_{BRkc}
\end{bmatrix}
=
\begin{bmatrix}
N_{1,1} & N_{1,2} & N_{1,3} & p_{1,4} & p_{1,5} & p_{1,6} & p_{1,7} & p_{1,8} & p_{1,9} & p_{1,10} & p_{1,11} & p_{1,12} & p_{1,13} & p_{1,14} & p_{1,15} \\
N_{2,1} & N_{2,2} & N_{2,3} & p_{2,4} & p_{2,5} & p_{2,6} & p_{2,7} & p_{2,8} & p_{2,9} & p_{2,10} & p_{2,11} & p_{2,12} & p_{2,13} & p_{2,14} & p_{2,15} \\
N_{3,1} & N_{3,2} & N_{3,3} & p_{3,4} & p_{3,5} & p_{3,6} & p_{3,7} & p_{3,8} & p_{3,9} & p_{3,10} & p_{3,11} & p_{3,12} & p_{3,13} & p_{3,14} & p_{3,15} \\
N_{4,1} & N_{4,2} & N_{4,3} & n_{4,4} & n_{4,5} & n_{4,6} & n_{4,7} & n_{4,8} & n_{4,9} & n_{4,10} & n_{4,11} & n_{4,12} & n_{4,13} & n_{4,14} & n_{4,15} \\
N_{5,1} & N_{5,2} & N_{5,3} & n_{5,4} & n_{5,5} & n_{5,6} & n_{5,7} & n_{5,8} & n_{5,9} & n_{5,10} & n_{5,11} & n_{5,12} & n_{5,13} & n_{5,14} & n_{5,15} \\
N_{6,1} & N_{6,2} & N_{6,3} & n_{6,4} & n_{6,5} & n_{6,6} & n_{6,7} & n_{6,8} & n_{6,9} & n_{6,10} & n_{6,11} & n_{6,12} & n_{6,13} & n_{6,14} & n_{6,15} \\
N_{7,1} & N_{7,2} & N_{7,3} & n_{7,4} & n_{7,5} & n_{7,6} & n_{7,7} & n_{7,8} & n_{7,9} & n_{7,10} & n_{7,11} & n_{7,12} & n_{7,13} & n_{7,14} & n_{7,15} \\
N_{8,1} & N_{8,2} & N_{8,3} & n_{8,4} & n_{8,5} & n_{8,6} & n_{8,7} & n_{8,8} & n_{8,9} & n_{8,10} & n_{8,11} & n_{8,12} & n_{8,13} & n_{8,14} & n_{8,15} \\
N_{9,1} & N_{9,2} & N_{9,3} & n_{9,4} & n_{9,5} & n_{9,6} & n_{9,7} & n_{9,8} & n_{9,9} & n_{9,10} & n_{9,11} & n_{9,12} & n_{9,13} & n_{9,14} & n_{9,15} \\
N_{10,1} & N_{10,2} & N_{10,3} & n_{10,4} & n_{10,5} & n_{10,6} & n_{10,7} & n_{10,8} & n_{10,9} & n_{10,10} & n_{10,11} & n_{10,12} & n_{10,13} & n_{10,14} & n_{10,15} \\
N_{11,1} & N_{11,2} & N_{11,3} & n_{11,4} & n_{11,5} & n_{11,6} & n_{11,7} & n_{11,8} & n_{11,9} & n_{11,10} & n_{11,11} & n_{11,12} & n_{11,13} & n_{11,14} & n_{11,15} \\
N_{12,1} & N_{12,2} & N_{12,3} & n_{12,4} & n_{12,5} & n_{12,6} & n_{12,7} & n_{12,8} & n_{12,9} & n_{12,10} & n_{12,11} & n_{12,12} & n_{12,13} & n_{12,14} & n_{12,15} \\
N_{13,1} & N_{13,2} & N_{13,3} & n_{13,4} & n_{13,5} & n_{13,6} & n_{13,7} & n_{13,8} & n_{13,9} & n_{13,10} & n_{13,11} & n_{13,12} & n_{13,13} & n_{13,14} & n_{13,15} \\
N_{14,1} & N_{14,2} & N_{14,3} & n_{14,4} & n_{14,5} & n_{14,6} & n_{14,7} & n_{14,8} & n_{14,9} & n_{14,10} & n_{14,11} & n_{14,12} & n_{14,13} & n_{14,14} & n_{14,15} \\
N_{15,1} & N_{15,2} & N_{15,3} & n_{15,4} & n_{15,5} & n_{15,6} & n_{15,7} & n_{15,8} & n_{15,9} & n_{15,10} & n_{15,11} & n_{15,12} & n_{15,13} & n_{15,14} & n_{15,15}
\end{bmatrix}
\begin{bmatrix}
\bar{I}_{Fkab} \\ \bar{I}_{Fkbc} \\ \bar{I}_{Fkca} \\ \bar{I}_{SSka} \\ \bar{I}_{SSkb} \\ \bar{I}_{SSkc} \\ \bar{I}_{RRka} \\ \bar{I}_{RRkb} \\ \bar{I}_{RRkc} \\ \bar{I}_{BSka} \\ \bar{I}_{BSkb} \\ \bar{I}_{BSkc} \\ \bar{I}_{BRka} \\ \bar{I}_{BRkb} \\ \bar{I}_{BRkc}
\end{bmatrix}
$$

where [N] is defined as follows: $N_{i,j} = p_{i,j} - p_{i,k} - R_F$, $R_F = 0.0$ for off diagonal terms

For i = 1,3 and j = 1,3; k = j+1 if k $\leq$ 3; k = j-1 if k > 3. $N_{i,j} = n_{i,j} - n_{i,k}$,

For i = 4,15 and j = 1,3; k = j+1 if k $\leq$ 3; k = j-1 if k > 3.

. . . (A1.45)

## APPENDIX (A2) ANALYTICAL SOLUTION OF THE PRIMARY SYSTEM RELAYING POINT QUANTITIES

### A2.1

In order to verify the results of the primary system relaying point voltage and current obtained digitally in Chapter 5, the following approximate analytical solution is shown.

With reference to Figure A2.1(a) associated with a solid mid-point earth fault without series compensation, the fault loop impedance comprises of the self terms of the source and line impedances (ignoring the mutual effects).

$$Z_F = Z_{S1} + Z_{L1}$$

$$= j25 + 150\ (0.05430925 + j0.4269558)$$

$$= 8.14638 + j\ 89.04337\ \Omega$$

Therefore $|I_F| = 4.56$ kA.

The relaying point voltage is

$$|V_F| = 408 - 4.56\ (25)$$

$$= 294.0\ \text{kV}$$

For identical fault condition and a series capacitor located at each end, the fault loop impedance is (with reference to Figure A2.1(b)):

$$Z_F = j\ 25 + 150\ (0.05430925 + j\ 0.4269558) - j32.2$$

$$= 8.14638 + j\ 56.84337\ \Omega$$

Therefore $|I_F| = 7.105$ kA.

Similarly, the relaying point voltage is

$$|V_F| = 408 - 7.105\ (25)$$

$$= 230.38\ \text{kV}.$$

The Laplace method can also be used to get the relaying point current. Hence, with reference to Figure A2.1(b), for a fault at voltage maximum

$$\hat{E}\ \cos\omega t = \bar{I}_F\ (j\omega L + \frac{1}{j\omega C})$$

or $$\hat{E}\ \frac{s}{s^2 + \omega^2} = \bar{I}_F\ (sL + \frac{1}{sC})$$

or approximately $$\frac{\hat{E}}{s} = \bar{I}_F\ (sL + \frac{1}{sC})$$

Therefore

$$\bar{I}_F = \frac{\hat{E}}{(s^2L + \frac{1}{C})}$$

$$= \frac{408 \times 10^3}{s^2(0.08 + 0.2033) + \frac{1}{98.854} \times 10^{-6}}$$

$$= \frac{408 \times 10^3}{0.2833s^2 + 10.116 \times 10^3}$$

$$= \frac{1440.169 \times 10^3}{s^2 + 357.077 \times 10^2}$$

$$= \frac{1440.169 \times 10^3}{s^2 + (188.965)^2}$$

Therefore $i_F$ = 7.621 sin 188.965 t

= 6.176 kA (corresponding to fault time at 5.0 ms)

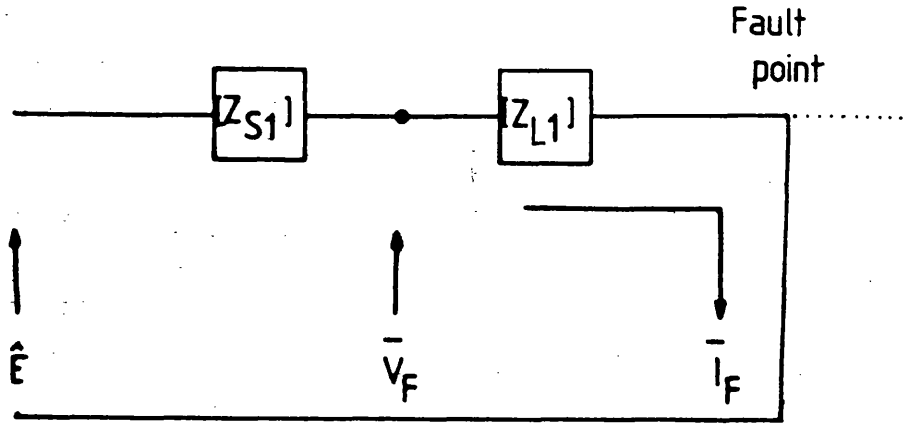


(a)

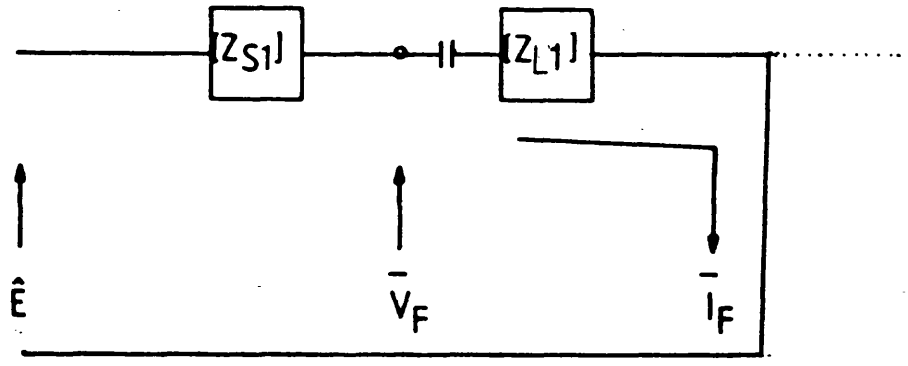


(b)

Figure A2.1 Circuit for a mid-point solid earth fault

(a) without compensation

(b) with capacitor located near the terminating busbar

## APPENDIX (A3) RELAYING PARAMETERS EVALUATION

### A3.1 Current (c.t.) and voltage (v.t.) transformer responses

In practice the primary system voltage and current signals are transduced before going into the mixing or comparator circuits. Because of the non-linearities associated with the c.ts and v.ts, the transient responses of such devices must be known. However, the burden of modern high-speed static comparators is such that non-linearities due to saturation, etc, can be avoided. The strategy adopted as regards the transducer simulation in assessing relay performance here is the same as that discussed in Reference 69, and which adequately serves the purpose.

### A3.2 Replica impedance arrangements

It is common practice to place replica impedances in the secondary of the current transformers in order to generate the relaying signal $S_1$ as given by equations 8.1 and 8.2. Two different types of arrangement have been used in this study:

(i) the transactor;

(ii) the transphasor.

A3.2.1 The transactor

The transactor which is basically a transformer with a core having air gaps and is extensively used in protection equipment using the block average comparator arrangement and has a circuit as shown in Figure A3.1(a). $R_b$ is a burden resistance so that neglecting the secondary winding reactance (which is relatively low because of the air gap) yields the equivalent circuit of Figure A3.1(b) referred to the primary. In a series compensated line, there are a number of variations on the relay settings depending on, for example, whether it is set with or without the capacitor/capacitors in the circuit under fault conditions, etc, and this means that the replica impedance needs to be frequently varied. With reference to Figure A3.1(b) it can be shown that the magnitude of the $Z_r$, the replica impedance referred to the primary of the transactor, is given by equation A3.1.

$$|Z_r| = \left| \frac{V_o'}{I} \right| = \frac{X_m}{\sqrt{1 + \cot^2 \phi_T}} \qquad \ldots \text{(A3.1)}$$

where $\phi_T = \tan^{-1}(R_b/n_t^2 X_m)$.

The relaying signal produced by the transactor (eg for an 'a'-earth fault) is therefore $S_1 = I Z_r - V_a$ or in the transduced form, it can be shown that:

$$S_1' = n_t^2 \frac{n_c}{n_v} \cdot Z_r I' - V_a'$$

where $n_c$, $n_v$ are the turns ratio of the c.t. and v.t. respectively, which are typically 1200/1 and 500/0.11 (for a 500 kV system) respectively. $n_t$ is normally taken as 1/1.

It can thus be seen that the $Z_r'$ replica impedance referred to the secondary is given by equation A3.2.

$$Z_r' = \frac{n_v}{n_c} Z_r \qquad \ldots \text{(A3.2)}$$

Due to the aperiodic nature of the c.t. secondary current, in order to simulate the voltages developed by the transformer-reactor replica impedance circuits, a step-by-step method of analysis is employed. The output voltage in terms of the c.t. secondary circuit is as derived in Reference 69 and is used here.

A3.2.2 The transphasor

In the studies relating to the relay performance based on the sequence comparator arrangement, a relatively new form of electromagnetic device known as the 'transphasor' is employed. This device is based on the simulation of two magnetic fluxes - one fixed in both phase and amplitude, whilst the other varying both in phase and magnitude. The arrangement is shown in Figure A3.2(a).

The transphasor arrangement has several distinct advantages over the conventional transformer-reactor circuit of Figure A3.1(a). These are:

(1) It has a constant amplitude phase shifting circuit, which allows the relay angle to be varied without changing the relay setting.

(2) A range of angles from about 85° to as low as -30° can easily be obtained.

(3) It has a much shorter time constant than a transformer circuit.

A3.2.2.1 Transphasor analysis

The transphasor arrangement shown in Figure A3.2(a) can be approximated to the two equivalent circuits shown in Figures A3.2(b,c) which are the two circuits referred to the primary side of cores $C_2$ and $C_1$ respectively. The extra turns link $R_b\ n_2^2$, $L_{m1}$, etc, are small and hence ignored in Figure A3.2(c).

The turns ratio as shown in Figure A3.2(a) is described as follows:

$$\frac{N_1}{N_2} = n_1 \ , \quad \frac{N_3}{N_4} = n_2 \quad \text{and} \quad \frac{N_5}{N_4} = n_3$$

With reference to Figure A3.2(c) it can be seen that

$$\frac{i_1}{n_1} = \frac{j\omega L_m}{Rn_1^2 + j\omega L_m} \; i$$

$$= \frac{jQ}{1 + jQ} \; i$$

where $Q = \frac{\omega L_m}{Rn_1^2}$

Therefore

$$i_1 = \frac{jQ}{1 + jQ} \; n_1 i \qquad \ldots \text{(A3.3)}$$

From the transphasor equivalent circuit of Figure A3.2(b) it can be observed that

$$v_o \; n_2 = \frac{i_x \; j\omega L_{m1} \; R_b n_2^2}{j\omega L_{m1} + R_b n_2^2}$$

$$= \frac{i_x \; j\omega L_{m1}}{1 + jQ'} \qquad \ldots \text{(A3.4)}$$

where $Q' = \frac{\omega L_{m1}}{R_b n_2^2}$

Now, $i_x = i_1 - i \left( \frac{N_5}{N_3} \right)$

$$= i_1 - i \left( \frac{N_5}{N_4} \Big/ \frac{N_3}{N_4} \right)$$

$$= i_1 - i \left( \frac{n_3}{n_2} \right) \qquad \ldots \text{(A3.5)}$$

Substituting the values of $i_1$ from equation A3.3 in equation A3.5:

$$i_x = \left[ \frac{jQ}{1+jQ} \quad n_1 - \frac{n_3}{n_2} \right] i \qquad \ldots \text{(A3.6)}$$

Substituting $i_x$ from equation A3.6 in equation A3.4 to obtain equations A3.7 and A3.8.

$$n_2 v_o = \frac{j\omega L_{m1}}{1+jQ'} \left[ \frac{jQ}{1+jQ} n_1 - \frac{n_3}{n_2} \right] i$$

or

$$\frac{v_o}{i} = \frac{j\omega L_{m1}}{(1+jQ')n_2} \left[ \frac{jQn_1}{1+jQ} - \frac{n_3}{n_2} \right]$$

$$= \frac{j\omega L_{m1}}{(1+jQ')n_2} \left[ \frac{jQn_1n_2 - n_3 - jn_3Q}{n_2(1+jQ)} \right]$$

$$= \frac{j\omega L_{m1}}{(1+jQ')n_2^2} \left[ \frac{-n_3 - jQ(n_3 - n_1n_2)}{1+jQ} \right] \qquad \ldots \text{(A3.7)}$$

$$= \frac{\omega L_{m1}}{(1+jQ')n_2^2} \left[ \frac{Q(n_3 - n_1n_2) - jn_3}{1+jQ} \right]$$

$$= \frac{\omega L_{m1}}{n_2^2\sqrt{1+Q'^2}} \sqrt{\frac{1 + Q^2(n_3 - n_1n_2)^2/n_3^2}{1 + Q^2}} \angle\theta \qquad \ldots \text{(A3.8)}$$

From equation A3.8 it can be seen that for $\left| \frac{v_o}{i} \right|$ to be independent of R and Q, the equation of A3.9 must be satisfied.

$$\left( \frac{n_3 - n_1n_2}{n_3} \right)^2 = 1$$

or $$\frac{n_3 - n_1n_2}{n_3} = -1 \quad \text{(ignoring positive sign)}$$

or $$n_1n_2 = 2n_3 \qquad \ldots \text{(A3.9)}$$

In common practice, however, it is required that the amplitude remains a constant whilst allowing the relay to be varied, without having to change the relay setting. Hence, substituting equation A3.9 in equation A3.7 gives equations A3.10 and A3.11.

$$\frac{v_o}{i} = \frac{j\omega L_{m1}}{(1+jQ')n_2^2}\left(\frac{-n_3 - jQ(-n_3)}{1+jQ}\right)$$

$$= \frac{j\omega L_{m1} n_3}{(1+jQ')n_2^2}\left(\frac{-1+jQ}{1+jQ}\right) \qquad \ldots \text{(A3.10)}$$

Thus, $\left|\frac{v_o}{i}\right| = \frac{\omega L_{m1} n_3}{\sqrt{1+Q'^2}\, n_2^2}$

and $\angle\theta = \angle\frac{v_o}{i} = 90° - \tan^{-1}\frac{Q'}{1} + \tan^{-1}\frac{Q}{-1} - \tan^{-1}\frac{Q}{1}$

$$\ldots \text{(A3.11)}$$

From equations A3.3 and A3.5 it can be seen that

$$i_x = \left(\frac{j\omega L_m n_1}{Rn_1^2 + j\omega L_m} - \frac{n_3}{n_2}\right) i \qquad \ldots \text{(A3.12)}$$

Substituting equation A3.12 in A3.4 it can be seen that

$$n_2 v_o = \frac{j\omega L_{m1} R_b n_2^2}{j\omega L_{m1} + R_b n_2^2}\left(\frac{j\omega L_m n_1}{Rn_1^2 + j\omega L_m} - \frac{n_3}{n_2}\right) i$$

$$v_o = \frac{j\omega L_{m1} R_b}{j\omega L_{m1} + R_b n_2^2}\left(\frac{j\omega L_{m1} n_1 n_2 - n_3 Rn_1^2 - j\omega L_m n_3}{Rn_1^2 + j\omega L_m}\right) i$$

$$\text{or } v_o \quad [(j\omega L_{m1} + R_b n_2^2)(Rn_1^2 + j\omega L_m)]$$

$$= j\omega L_{m1} R_b (j\omega L_m n_1 n_2 - n_3 Rn_1^2 - j\omega L_m n_3)\, i$$

$$\text{or } v_o \quad [j\omega L_{m1} Rn_1^2 + j^2\omega^2 L_{m1} L_m + R_b n_2^2 Rn_1^2 + j\omega L_m R_b n_2^2]$$

$$= [j^2\omega^2 L_{m1} L_m R_b n_1 n_2 - j\omega L_{m1} R_b Rn_1^2 n_3 - j^2\omega^2 L_{m1} L_m R_b n_3]\, i$$

$$\text{or } v_o \quad [L_{m1} Rn_1^2 + j\omega L_{m1} L_m + \frac{1}{j\omega} R_b n_2^2 Rn_1^2 + L_m R_b n_2^2]$$

$$= [j\omega L_{m1} L_m R_b n_1 n_2 - L_{m1} R_b Rn_1^2 n_3 - j\omega L_{m1} L_m R_b n_3]\, i$$

. . . (A3.13)

As $\frac{d}{dt} = j\omega$ and $\int dt = \frac{1}{j\omega}$ equation A3.13 yields

$$L_{m1} Rn_1^2 v_o(t) + L_{m1} L_m \frac{dv_o(t)}{dt} + R_b n_2^2 Rn_1^2 \int v_o(t)dt$$

$$+ L_m R_b n_2^2 v_o(t) = L_{m1} L_m R_b n_1 n_2 \frac{di(t)}{dt} - L_{m1} R_b Rn_1^2 n_3 i(t)$$

$$- L_{m1} L_m R_b n_3 \frac{di(t)}{dt} \qquad \text{. . . (A3.14)}$$

Again, since $n_1 = n_2 = 1/20$ and from equation A3.9

$$n_3 = \frac{n_1 n_2}{2} = \frac{1}{800}$$

Substituting the values of $n_1$, $n_2$ and $n_3$ equation A3.14 yields

$$\frac{L_{m1}R}{400}\ v_o(t) + L_{m1}L_m\ \frac{dv_o(t)}{dt} + \frac{R_bR}{16\ x\ 10^4} \int v_o(t)\ dt$$

$$+ \frac{L_mR_b}{400}\ v_o(t) = \frac{L_{m1}L_m}{400}\ R_b\ \frac{di(t)}{dt} - \frac{L_{m1}R_bR}{32x10^4}\ i(t)$$

$$- \frac{L_{m1}L_mR_b}{800}\ \frac{di(t)}{dt} \qquad \ldots \text{(A3.15)}$$

Equation A3.15 is again evaluated using piecewise linearisation techniques, in which the compensated current input is sampled at a rate of $1/\Delta T$. In terms of sampled values taken at times $t_n = n\Delta T$ and $t_{n-1} = (n-1)\Delta T$ after the process is commenced, the output voltage and input current at time $t = (n - \frac{1}{2})\Delta T$ may be written as

$$\frac{dv_o(t)}{dt} = [v_o(t_n) - v_o(t_{n-1})] \ / \ \Delta T$$

$$v_o(t) = [v_o(t_n) + v_o(t_{n-1})] \ / \ 2$$

$$\int v_o dt = [v_o(t_n) + v_o(t_{n-1})]\ \Delta T/2$$

$$i(t) = [i(t_n) + i(t_{n-1})] \ /2$$

$$\frac{di(t)}{dt} = [i(t_n) - i(t_{n-1})] \ /\Delta T$$

$$\ldots \text{(A3.16)}$$

Substituting equation A3.16 in equation A3.15 the output voltage of the transphasor at a time '$t_n$' is given by:

$$\frac{A_1}{2}\left[v_o(t_n) + v_o(t_{n-1})\right] + \frac{A_2}{\Delta T}\left[v_o(t_n) - v_o(t_{n-1})\right]$$

$$+ \frac{A_3\Delta T}{2}\left[v_o(t_n) + v_o(t_{n-1})\right] + \frac{A_4}{2}\left[v_o(t_n) + v_o(t_{n-1})\right]$$

$$= \frac{B_1}{\Delta T}\left[i(t_n) - i(t_{n-1})\right] - \frac{B_2}{2}\left[i(t_n) + i(t_{n-1})\right]$$

$$- \frac{B_3}{\Delta T}\left[i(t_n) - i(t_{n-1})\right]$$

$$\text{or} \quad v_o(t_n)\left(\frac{A_1}{2} + \frac{A_2}{\Delta T} + \frac{A_3\Delta T}{2} + \frac{A_4}{2}\right)$$

$$+ v_o(t_{n-1})\left(\frac{A_1}{2} - \frac{A_2}{\Delta T} + \frac{A_3\Delta T}{2} + \frac{A_4}{2}\right)$$

$$= i(t_n)\left(\frac{B_1}{\Delta T} - \frac{B_2}{2} - \frac{B_3}{\Delta T}\right) - i(t_{n-1})\left(\frac{B_1}{\Delta T} + \frac{B_2}{2} - \frac{B_3}{\Delta T}\right)$$

Therefore:

$$v_o(t_n) = \left\{\left(\frac{B_1}{\Delta T} - \frac{B_2}{2} - \frac{B_3}{\Delta T}\right) i(t_n)\right.$$

$$- \left(\frac{B_1}{\Delta T} + \frac{B_2}{2} - \frac{B_3}{\Delta T}\right) i(t_{n-1})$$

$$\left. - \left(\frac{A_1}{2} - \frac{A_2}{\Delta T} + \frac{A_3\Delta T}{2} + \frac{A_4}{2}\right) v_o(t_{n-1})\right\} \Big/$$

$$\left(\frac{A_1}{2} + \frac{A_2}{\Delta T} + \frac{A_3\Delta T}{2} + \frac{A_4}{2}\right)$$

. . . (A3.17)

where $A_1 = \frac{L_{m1}R}{400}$, $A_2 = L_{m1}L_m$, $A_3 = \frac{R_bR}{16 \times 10^4}$,

$A_4 = \frac{L_m R_b}{400}$, $B_1 = \frac{L_{m1}L_mR_b}{400}$, $B_2 = \frac{L_{m1}R_bR}{32 \times 10^4}$, $B_3 = \frac{L_{m1}L_mR_b}{800}$

## A3.3 Polarising circuits

There are essentially two types of polarising voltage components in the comparator signal $S_2$ used in this study. These are:

(1) The sound-phase polarising component (eg $k_p V_{bc}$ for an 'a'-earth fault) which needs to be shifted by ±90° and is used in both the block average and sequence comparator arrangements.

(2) The synchronous polarising component (eg $k_s E_a$ for an 'a'-earth fault) which is used in the sequence comparator arrangement only.

### A3.3.1 Phase shift circuit

The polarising voltage phase-shift circuit similated is as shown in Figure A3.3. This arrangement provides the necessary 90° phase-shift at power frequency if the component values are such that $R_p = \frac{1}{\omega_0 C_p}$.

Again, piecewise linearisation techniques are used and the relationship between the sound-phase voltage derived component and the output voltage is as given in Reference 69.

A3.3.2 Synchronous polarising component

In practice, this component (eg $k_s E_a$ for an 'a'-earth fault) is a square wave derived from the prefault synchronous polarising signal which is a power frequency sinusoidal voltage stored in a memory circuit. This is illustrated in Figure A3.4. The value of $k_s$ is such that the height of the square wave is +10 volts.

## A3.4 Pre-filters used in power system protective relaying

A low-pass filter is a device which passes signals of low frequencies and suppresses or attenuates those of high frequencies. Its performance may be illustrated by its amplitude response, which is a plot of the amplitude $|H(j\omega)|$ of its transfer function H(s) versus frequency $\omega$, where $\omega = 2\pi f$. In all case $H = \frac{V_o}{V_i}$ where $V_o$ and $V_i$ are the output and input voltages.

It is common practice to prefilter the signals $S_1$ and $S_2$ in a second order filter before going to a comparator, as shown in Figure A3.5. A second order approximation to an ideal low pass filter is achieved by the transfer function:

$$\frac{v_o}{v_i} = \frac{K_1}{p^2 + ap + b} \quad \ldots \text{(A3.18)}$$

where 'a' and 'b' are properly chosen constants and $K_1$ is a constant. The term 'second order' refers to the degree of the denominator polynomial. The gain of the low pass filter is the value of its transfer function at p=0 and is given in the case of equation A 3.18 by gain = $K_1/b$. The determination of constants $K_1$, 'a' and 'b' is shown in Section A3.4.2.

There are a number of ways of obtaining low pass filters using active devices instead of inductors. The method used is that of Sallen and Key, in which the active device is an operational amplifier (op-amp)[96]. A Sallen and Key second order low pass filter is shown in Figure A3.6(a), where the resistors and capacitors are properly chosen to realise given values of 'a' and 'b' in equation A3.18. The op-amp, together with the resistors $R_3$ and $R_4$, constitutes a voltage-controlled voltage source (VCVS) and hence the Sallen and Key network is of the VCVS type.

Analysis of FiguresA3.6 (a,b) as given later on in this Section, shows that:

$$K_1 = \frac{\mu \times 10^6}{R_1 R_2 C_1 C_f}$$

$$a = \frac{1}{R_2 C_1}(1 - \mu) + \frac{1}{R_1 C_f} + \frac{1}{R_2 C_f}$$

$$b = \frac{1}{R_1 R_2 C_f C_1} \qquad \ldots \text{(A3.19)}$$

The quantity $\mu = 1 + \frac{R_4}{R_3}$ is the gain of the VCVS and is also the gain of the filter since $\frac{K_1}{b} = \mu$ .

There are many types of low pass filter, but the two most commonly used are the Butterworth and Chebyshev types. In the course of this work only the Butterworth filter is used. The standard values for $R_1$, $R_2$, $R_3$, $R_4$, $C_1$, $C_f$ of the Butterworth type of filter are given in Section 4.8.

A3.4.1 Low pass Butterworth Filter[96]

Low pass Butterworth filter approximates the ideal low-pass filter with a relatively flat passband characteristic. Its amplitude response is given by equation A3.20.

$$|H(j\omega)| = \frac{K_1}{\sqrt{1 + (\frac{\omega}{\omega_c})^{2n}}} \qquad \ldots \text{(A3.20)}$$

where n is the order of the filter.

The Butterworth filter has the advantage of a so-called nominally flat, monotonic response in the passband.

A3.4.2 Simulation of filters

Equation A3.18 can be considered in integral form as follows.

$$K_1 \int v_i(t)dt = pv_o(t) + av_o(t) + b \int v_o(t)dt + k \qquad \ldots \text{(A3.21)}$$

On considering the samples on voltage output waveform as shown by Figure A3.7 and on evaluation of equation A3.21 at times $t_x$, $t_y$, where

$$t_x = (n-\tfrac{1}{2})\Delta T \quad \text{and} \quad t_y = (n+\tfrac{1}{2})\Delta T$$

Therefore:

$$K_1 \int_{t_x}^{t_y} v_i(t)dt = pv_o(t_y) - pv_o(t_x) + av_o(t_y) - av_o(t_x) + b \int_{t_x}^{t_y} v_o(t)dt \qquad \ldots \text{(A3.22)}$$

Also, from Figure 3.7 it can be seen that[69]:

$$pv_o(t_y) = \frac{v_o(t_{n+1}) - v_o(t_n)}{\Delta T}$$

$$pv_o(t_x) = \frac{v_o(t_n) - v_o(t_{n-1})}{\Delta T}$$

$$v_o(t_y) = \frac{v_o(t_{n+1}) + v_o(t_n)}{2}$$

$$v_o(t_x) = \frac{v_o(t_n) + v_o(t_{n-1})}{2}$$

$$\int_{t_x}^{t_y} v_o(t)dt = \left( \frac{v_o(t_{n-1})}{2} + 3v_o(t_n) + \frac{v_o(t_{n+1})}{2} \right) \frac{\Delta T}{4}$$

$$\int_{t_x}^{t_y} v_i(t)dt = \left( \frac{v_i(t_{n-1})}{2} + 3v_i(t_n) + \frac{v_i(t_{n+1})}{2} \right) \frac{\Delta T}{4}$$

Substituting the above values in equation A3.22

$$K_1 \left( \frac{v_i(t_{n-1})}{2} + 3v_i(t_n) + \frac{v_i(t_{n+1})}{2} \right) \frac{\Delta T}{4}$$

$$= [v_o(t_{n+1}) - v_o(t_n) - v_o(t_n) + v_o(t_{n-1})] / \Delta T$$

$$+ \frac{a}{2} [v_o(t_{n+1}) + v_o(t_n) - v_o(t_n) - v_o(t_{n-1})]$$

$$+ b \left( \frac{v_o(t_{n-1})}{2} + 3v_o(t_n) + \frac{v_o(t_{n+1})}{2} \right) \Delta T/4$$

$$= \left( \frac{1}{\Delta T} + \frac{a}{2} + \frac{b\Delta T}{8} \right) v_o(t_{n+1}) + \left( -\frac{2}{\Delta T} + \frac{3b\Delta T}{4} \right) v_o(t_n)$$

$$+ \left( \frac{1}{\Delta T} - \frac{a}{2} + \frac{b\Delta T}{8} \right) v_o(t_{n-1})$$

Therefore:

$$K_1 [v_i(t_{n-1}) + 6v_i(t_n) + v_i(t_{n+1})] \frac{\Delta T}{8}$$

$$= \frac{\Delta T}{8} \left( \frac{8}{\Delta T^2} + \frac{4a}{\Delta T} + b \right) v_o(t_{n+1}) + \frac{\Delta T}{8} \left( -\frac{16}{\Delta T^2} + 6b \right) v_o(t_n)$$

$$+ \frac{\Delta T}{8} \left( \frac{8}{\Delta T^2} - \frac{4a}{\Delta T} + b \right) v_o(t_{n-1})$$

Therefore:

$$K_1\,[v_i(t_{n-1}) + 6v_i(t_n) + v_i(t_{n+1})]$$

$$= \left(\frac{8}{\Delta T^2} + \frac{4a}{\Delta T} + b\right) v_o(t_{n+1}) + \left(6b - \frac{16}{\Delta T^2}\right) v_o(t_n)$$

$$+ \left(\frac{8}{\Delta T^2} - \frac{4a}{\Delta T} + b\right) v_o(t_{n-1})$$

Therefore:

$$v_o(t_{n+1}) = K_1 \frac{[v_i(t_{n-1}) + 6v_i(t_n) + v_i(t_{n+1})]}{} - \frac{\left(6b - \frac{16}{\Delta T^2}\right) v_o(t_n) - \left(\frac{8}{\Delta T^2} - \frac{4a}{\Delta T} + b\right) v_o(t_{n-1})}{\left(\frac{8}{\Delta T^2} + \frac{4a}{\Delta T} + b\right)}$$

$$= K_1 \Delta T^2 \frac{[v_i(t_{n-1}) + 6v_i(t_n) + v_i(t_{n+1})] - (6b\Delta T^2 - 16) v_o(t_n)}{} - \frac{(8 - 4a\Delta T + b\Delta T^2) v_o(t_{n-1})}{(8 + 4a\Delta T + b\Delta T^2)} \qquad \ldots \text{(A3.23)}$$

The constants $K_1$, a, b cannot be arbitrarily chosen because only certain values can be realised in a practical filter. A very common method of realisation is a VCVS active arrangement, as given by Sallen and Key.

With reference to Figure A3.6 and noting that no current flows in the input of the amplifier, the voltage at the inverting input terminal is:

$$v'(t) = v(t) = v_o(t) \frac{R_4}{R_3+R_4}$$

$$\text{or } \frac{v_o(t)}{v(t)} = \frac{R_3 + R_4}{R_4} = 1 + \frac{R_3}{R_4} = \mu \quad \ldots \text{(A3.24)}$$

The equations governing this filter are:

$$v_o(t) = \mu v(t)$$

$$i_2(t) = C_f p v_c(t)$$

$$i_1(t) = C_1 p v(t)$$

$$v_i(t) = R_1[i_1(t) + i_2(t)] + v_c(t) + v_o(t)$$

$$= R_1[i_1(t) + i_2(t)] + R_2\, i_1(t) + v(t)$$

It follows that

$$v_c(t) + v_o(t) = R_2 i_1(t) + v(t)$$

$$= R_2 C_1\, pv(t) + v(t)$$

$$= (R_2 C_1\, p + 1)\, v(t)$$

$$= (R_2 C_1\, p + 1)\, \frac{v_o(t)}{\mu}$$

$$\text{Therefore } v_c(t) = \frac{v_o(t)[1-\mu]}{\mu} + \frac{R_2 C_1 p\, v_o(t)}{\mu}$$

Also, knowing that:

$$i_1(t) + i_2(t) = C_f p v_c(t) + C_1 p v(t)$$

therefore:

$$[i_1(t) + i_2(t)] = \frac{C_f}{\mu} [\{1-\mu\} pv_o(t) + R_2C_1p^2v_o(t)]$$

$$+ \frac{C_1pv_o(t)}{\mu}$$

Now, $v_i(t) = R_1[i_1(t) + i_2(t)] + R_2C_1pv(t) + v(t)$

$$= \frac{R_1}{\mu} [C_f\{1-\mu\}pv_o(t) + R_2C_fC_1p^2v_o(t)+C_1pv_o(t)]$$

$$+ \frac{1}{\mu} [v_o(t)R_2C_1p + v_o(t)]$$

$$= \frac{R_1R_2C_1C_f}{\mu} \left( p^2v_o(t) + \left\{ \frac{R_1C_f(1-\mu)pv_o(t)}{R_1R_2C_1C_f} \right.\right.$$

$$\left.\left. + \frac{R_1C_1pv_o(t) + R_2C_1pv_o(t)}{R_1R_2C_1C_f} \right\} + \frac{v_o(t)}{R_1R_2C_1C_f} \right)$$

$$= \frac{R_1R_2C_1C_f}{\mu} \left( p^2v_o(t) + \frac{\left\{R_1C_f(1-\mu)+R_1C_1+R_2C_1\right\} pv_o(t)}{R_1R_2C_1C_f} \right.$$

$$\left. + \frac{v_o(t)}{R_1R_2C_1C_f} \right) \qquad \ldots \text{(A3.25)}$$

Now comparing equation A3.25 with equation A3.18 gives

$$K_1 = \frac{\mu}{R_1R_2C_1C_f}$$

$$a = \frac{R_1C_f(1-\mu) + R_1C_1 + R_2C_1}{R_1R_2C_1C_f}$$

$$b = \frac{1}{R_1R_2C_1C_f} \qquad \ldots \text{(A3.26)}$$

There are some standard design tables as presented in Section 4.8, from which the values of $R_1$, $R_2$, $R_3$, $R_4$, $C_1$, $C_f$ can be determined for the Butterworth filter.

At power frequency, the relationship between output and input is

$$\frac{v_o}{v_i} = \frac{K_1}{-\omega_o^2 + j\omega_o a + b}$$

$$= \frac{K_1}{\sqrt{(b - \omega_o^2)^2 + \omega_o^2 a^2}} \angle - \tan^{-1} \frac{\omega_o a}{b - \omega_o^2}$$

$$= H \angle - \theta \qquad \ldots \text{(A3.27)}$$

Thus, if in the steady state the input voltage to the filter is described in the time domain by $\bar{V}_1 \sin \omega_o t$, then

$$v_o(t) = H \bar{V}_1 \sin (\omega_o t - \theta)$$

where $v_i(t) = \bar{V}_1 \sin \omega_o t$

Therefore $$v_o(t) = \frac{H v_i(t) \sin(\omega_o t - \theta)}{\sin \omega_o t}$$

$$= H v_i(t) \frac{\sin\omega_o t \cos\theta - \cos\omega_o t \cos\theta}{\sin \omega_o t}$$

$$= H v_i(t) [\cos\theta - \cot\omega_o t \sin\theta]$$

$$\ldots \text{(A3.28)}$$

This could be used as a basis for starting the piecewise linear filter simulation. As the value of $|\theta|$ at power frequency is less than 10° for all low pass filters likely to be simulated, this means that it is enough to write the expression of equation A3.29 as $v_o(t) = Hv_i(t)$ to start the simulation.

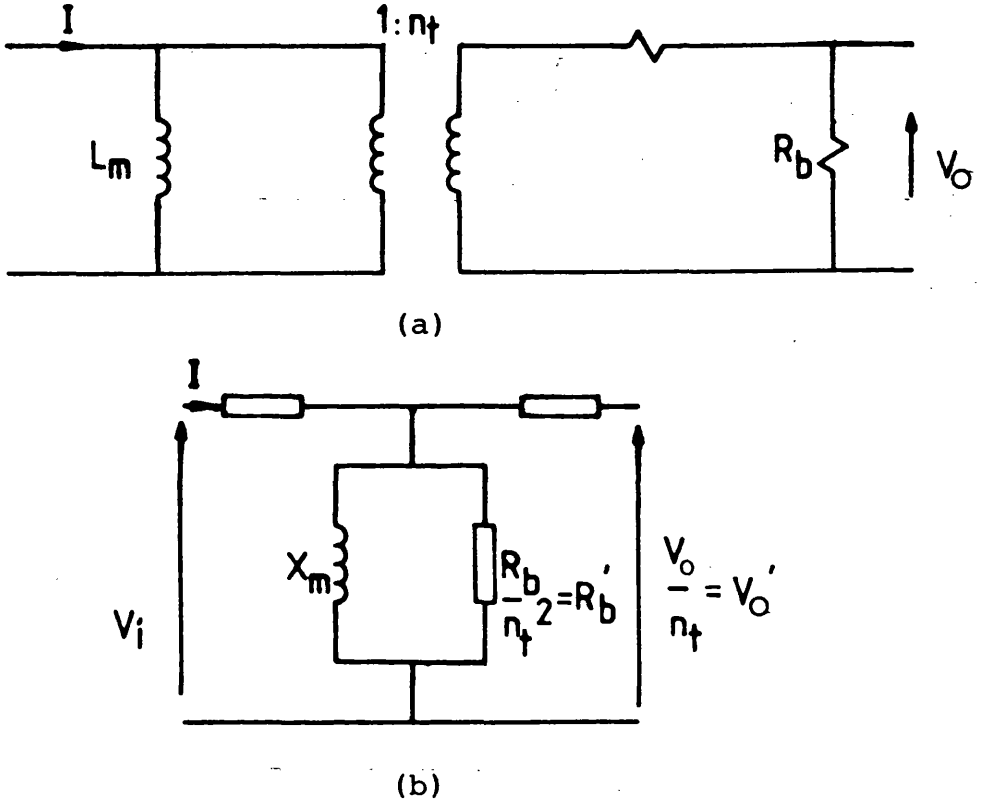


Figure A3.1 Transformer-reactor arrangement

(a) actual circuit

(b) equivalent circuit referred to the primary

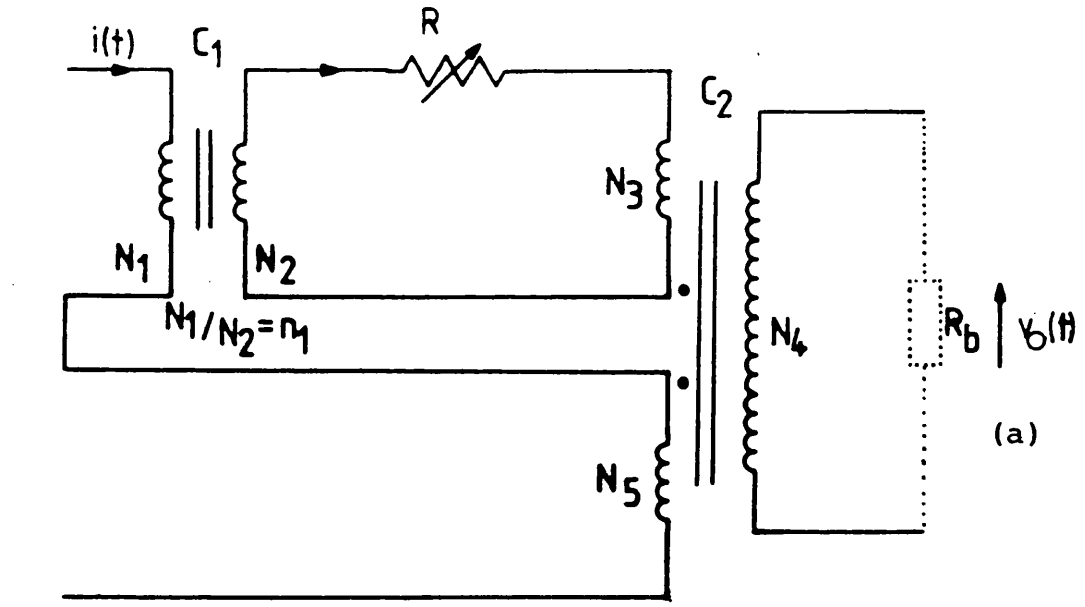


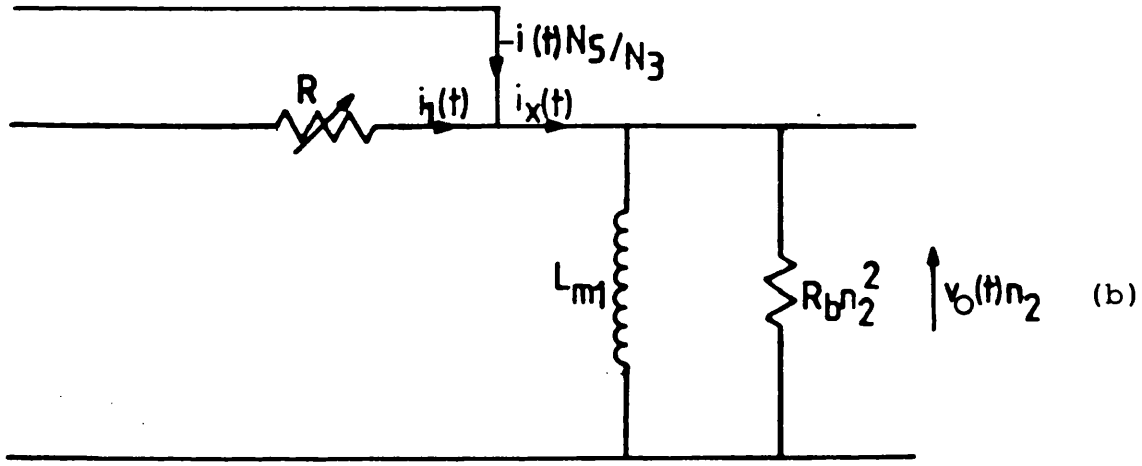


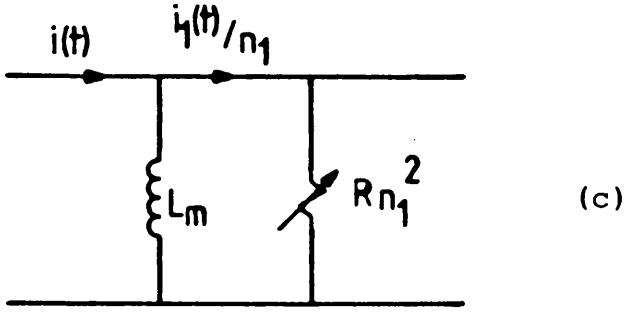


Figure A3.2 Basic transphasor arrangement

(a) original circuit

(b) equivalent circuit referred to the primary of core $C_2$

(c) equivalent circuit referred to the primary of core $C_1$

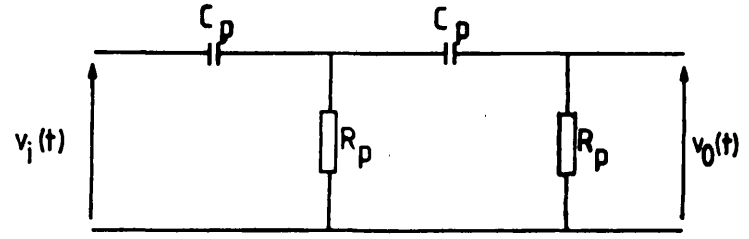


Figure A3.3 Polarising phase shift circuit

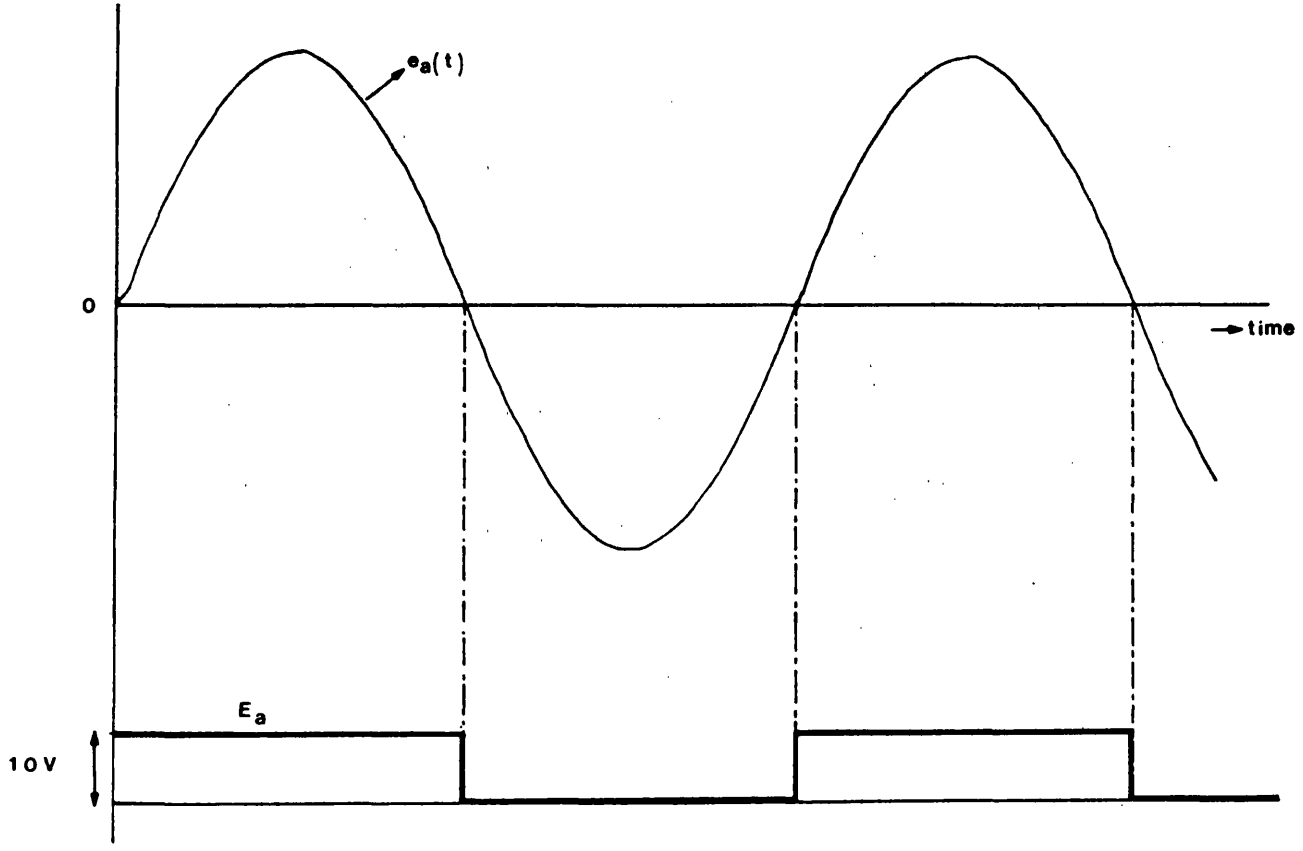


Figure A3.4 Steady state voltage (memory)

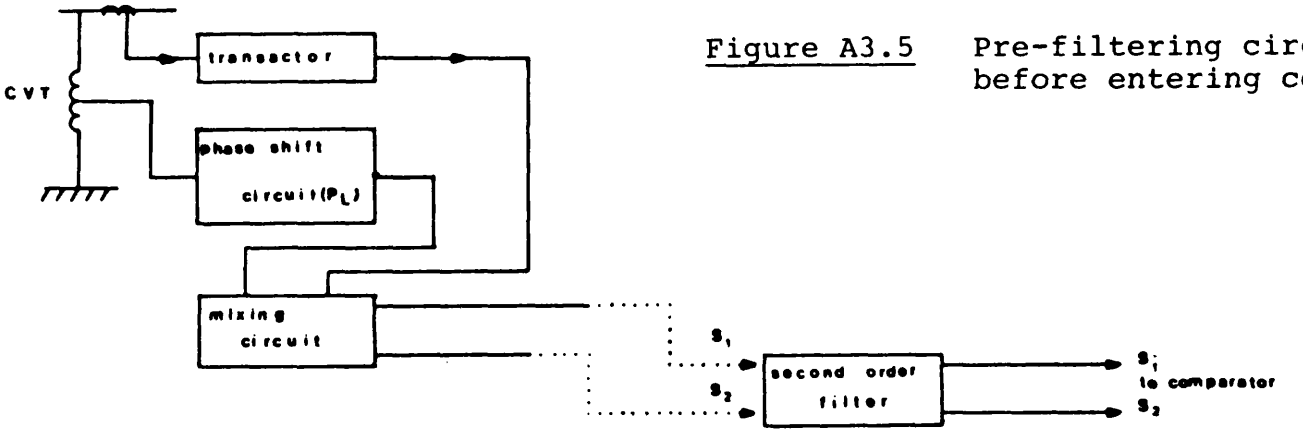


Figure A3.5 Pre-filtering circuits used before entering comparator

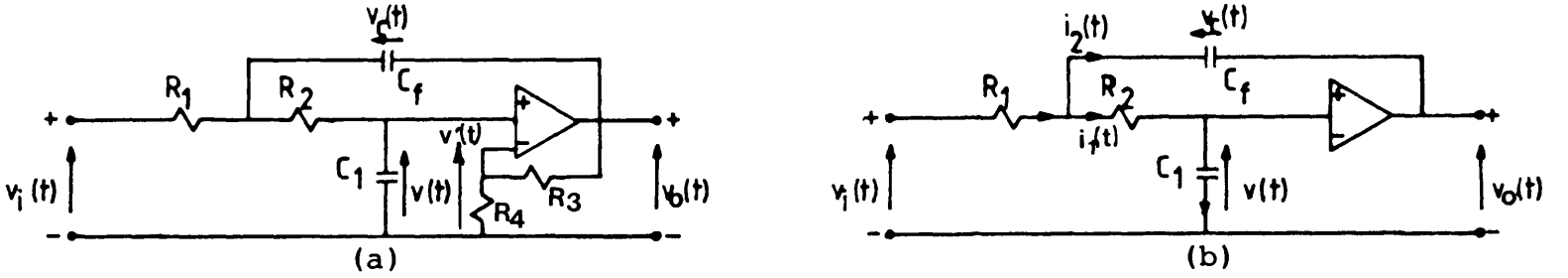


Figure A3.6 Sallen and Key second order low-pass filter

(a) actual circuitry

(b) equivalent circuit

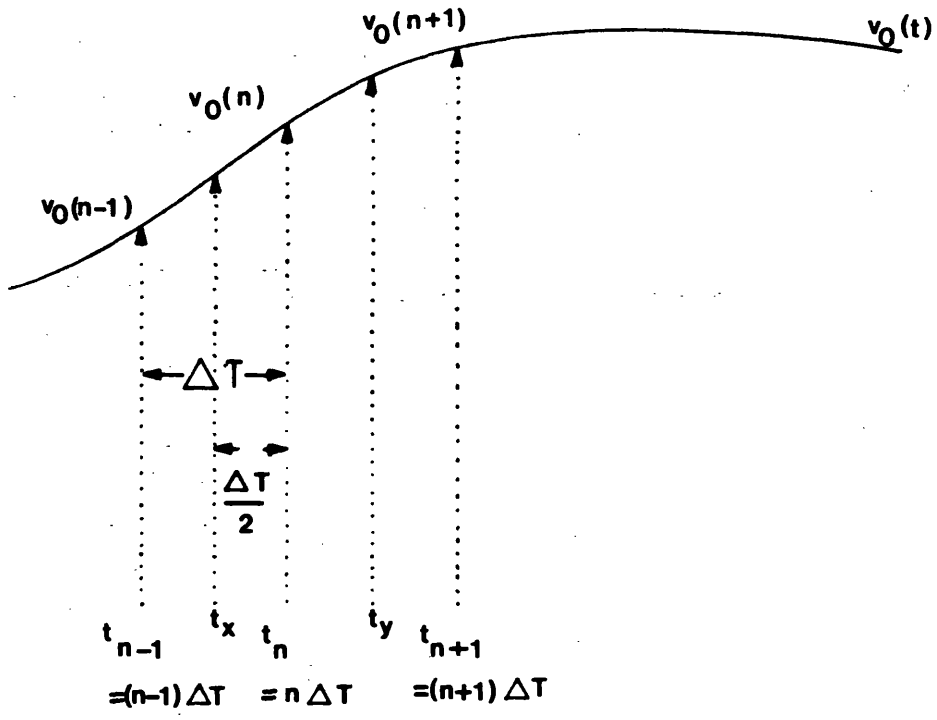


Figure A3.7 Samples on a typical waveform

## APPENDIX (A4) PUBLISHED WORK

Some of the work developed in this thesis has been published and is presented in this Appendix.

# DIGITAL SIMULATION OF FAULT TRANSIENTS IN EHV SERIES COMPENSATED TRANSMISSION LINES

A. Kalam, R.K. Aggarwal, A.T. Johns, University of Bath.

## 1. Introduction

The use of capacitors as a means of increasing the power transfer capabilities of long distance transmission lines is well known. There are however problems encountered in the protection of such lines and these essentially arise because, under faulted conditions, the primary system parameters are often subject to rapid changes due largely to capacitor protective gap operation. In order to be able to successfully develop new protection techniques for such compensated lines in the longer term, an accurate knowledge of their fault transient responses is very important.

This paper outlines the basis of new digital simulation techniques developed at Bath for realistically simulating the transient responses of series compensated systems. In particular, it highlights some of the problems of simulating the essentially random nature of series capacitor gap flashover and outlines the basis of the techniques developed to overcome them. The results of some interesting studies of the responses of a typical 500 kV long distance line are illustrated and the paper concludes with a brief discussion of the implications of such responses as regards future prospects for overcoming present day protection problems.

## 2. Basic Series Compensated System Model

Figure 1 shows a typical 500 kV quad conductor, compensated single section feeder with a series capacitor and a three reactor bank at either end of the line. The line is 300 km long and is of horizontal construction. The phase conductors are Al Alloy and the earthwires are Alumoweld. Frequency variance of all line and earth parameters has been included and the line section has the usual discrete transpositions at intervals of 1/3 of the total line length. There are various factors which determine the degree of series compensation [1] $S_c$. In terms of the p.p.s. line reactance $L_1$, the parameter of a series capacitor (assuming a capacitor bank C at either end of the line) compensating a line section of length $l$ is given by equation 1.

$$S_C = 2/(\omega_0^2 L_1 C l) \qquad (1)$$

The capacitor impedance can be determined from equation 2.

$$X_C = -2j/(S_C \omega_0^2 L_1 l)\omega \qquad (2)$$

Combination of the capacitor bank with the various line sections is conveniently achieved by using the relationship of equation 3.

$$\begin{bmatrix} \bar{V}_1 \\ \bar{I}_1 \end{bmatrix} = \begin{bmatrix} U & Z_C \\ 0 & U \end{bmatrix} \begin{bmatrix} \bar{V}_2 \\ \bar{I}_2 \end{bmatrix} \qquad (3)$$

where

$$[Z_C] = \begin{bmatrix} X_C & 0 & 0 \\ 0 & X_C & 0 \\ 0 & 0 & X_C \end{bmatrix}$$

Figure 2 shows an equivalent fault transient model derived from an actual system model of figure 1b. With reference to figure 2, it is thus possible to describe the matrix relationship between the sending end and the fault point using the two port polyphase relationship of equation 4 [2].

$$\begin{bmatrix} \bar{V}_{S2} \\ \bar{I}_{S2} \end{bmatrix} = \begin{bmatrix} U & 0 \\ Y_S & U \end{bmatrix} \begin{bmatrix} U & Z_C \\ 0 & U \end{bmatrix} \begin{bmatrix} A_{L1} & B_{L1} \\ C_{L1} & D_{L1} \end{bmatrix} \begin{bmatrix} \bar{V}_{f2} \\ \bar{I}_{fS2} \end{bmatrix} \qquad (4)$$

The sub-matrix $[Y_S]$ used to represent the reactor bank is as described in reference 3 and the method of obtaining the transient responses due to fault inception using Frequency Domain based digital techniques are given in reference 2. On fault inception, the magnitudes of the voltages across all the six capacitor banks are compared with the capacitor gap settings necessary for spark gap operation. The first capacitor to attain this value is shorted out and this process is simulated by injecting a voltage, equal and opposite to the voltage across it. This part of the simulation can best be explained with reference to figure 3 which shows the system model for an "a"-phase-earth fault. If the time after fault at which say the sending-end "a"-phase capacitor voltage reaches the threshold value first, is $T_{C1}$, then the frequency spectrum $\bar{E}_{S3a}$ of the injected voltage to simulate gap flashover is given by:-

$$\bar{E}_{S3a} = \int_{T_{C1}}^{T_{O_b}} (e_{S3a}) e^{-j\omega t}\, dt \qquad (5)$$

where $T_{O_b}$ = observation time,

$e_{S3a}$ = total instantaneous voltage across the capacitor.

$\bar{I}_{SS3a}$ is the frequency spectrum of a current which arises due to capacitor flashover. The variation of the sending-end relaying point quantities as a result of this voltage injection can then be derived from equations (6) and (7).

$$\begin{bmatrix} \bar{I}_{SC3} \end{bmatrix} = \begin{bmatrix} \bar{I}_{SS3} \end{bmatrix} - \begin{bmatrix} Z_C \end{bmatrix}^{-1} \begin{bmatrix} E_{S3} \end{bmatrix}$$
$$\begin{bmatrix} V_{SS3} \end{bmatrix} = \begin{bmatrix} \bar{E}_{SS3} \end{bmatrix} + \begin{bmatrix} \bar{E}_{S3} \end{bmatrix} \qquad (6)$$

$$\begin{bmatrix} \bar{V}_{S3} \\ \bar{I}_{S3} \end{bmatrix} = \begin{bmatrix} U & 0 \\ Y_S & U \end{bmatrix} \begin{bmatrix} \bar{E}_{SS3} \\ \bar{I}_{SC3} \end{bmatrix} \qquad (7)$$

The total time domain response of say the sending-end relaying point "a"-phase voltage at this stage would be:-

$$v_{Sa}(t) = v_{S1a}(t) + v_{S2a}(t - T_f) + v_{S3a}(t - T_{C1})$$

where $t = 0 \rightarrow T_{O_b}$, $T_f$ = fault occurs, $T_{C_1}$ = capacitor flashes over.

Similar relationships enable the receiving-end quantities to be determined.

## 3. Transient Fault Studies

The fault studies apply to a system with a total series compensation of 70%. The short circuit capacity levels of the two busbars are 10 GVA and an X:R ratio of 30 for the sources has been assumed. The results presented are for an "a"-phase-earth fault and are related to the sending-end relaying point.

3.1 Effect of capacitor gap setting variation:- From figure 4, it can be seen that a gap setting of 2.7 p.u. results in the faulted phase capacitors flashing over in about 15.5 msec after fault, whereas a setting of 5 p.u. does not produce spark gap operation. Comparing the waveforms in the two cases, it can be clearly seen that both the voltage and current waveforms (particularly in the faulted phase) are significantly different, especially in their relative magnitudes, subsequent to capacitor flashover.

3.2 Variation of fault position:- A fault at 25% of the line from the sending end results in much higher frequency transients (especially in the voltage waveforms) than the corresponding case for a midpoint fault (figures 4 and 5). As expected, the relative magnitudes of the faulted phase currents are significantly different both in the pre- and post spark gap operation periods. One interesting point to note is that with the same gap setting of 2.7 p.u., for a fault closer to the relaying point, the faulted phase capacitors flashover in a much shorter time of about 5 msec after fault as compared to 15.5 msec for the latter case. This can be clearly seen from figure 6 which shows the voltage waveforms across the capacitors.

3.3 Implications on protection performance:- Figure 7 shows the results of a typical study for the well known block-average zone one relay. The relay setting assumes that none of the capacitors flashover. Response (1), which is for a midpoint fault and with a gap setting of 2.7 p.u., shows the device output builds up gradually but fails to reach the set level due to the sudden change of system parameters. The latter results from capacitor spark gap operation and causes considerable under-reaching. On the other hand, the corresponding case with a higher gap setting (response 2) and in which there is no sparkover, results in relay operation in about 23 msec after fault. It is significant to note that in the former case, the capacitors do not flashover until about 15 msec after fault and the studies have indicated that in the majority of cases, for faults close to and beyond the midpoint, there is always a time lapse of about 10 msec from time of fault to spark gap operation. This clearly indicates that a faster protective scheme with an operating time of less than about $\frac{1}{2}$ cycle can be used to advantage in such systems.

## 4. Conclusions

The results clearly show that the relaying point waveforms are significantly affected by the capacitor spark gap operations under fault conditions and this in turn can have a profound effect on the present protection relay performance. However, there is a clear indication that some of the present day protection problems associated with series compensated long distance AC transmission can be overcome by high speed protective relays with operating times of less than about $\frac{1}{2}$ cycle.

## 5. References


1 Illiento F., et al: 'Transient voltages and currents in series compensated ehv lines', Proc. IEE, Vol. 123, No. 6, August 1976.

2 Johns A.T., Aggarwal R.K.: 'Digital simulation of faulted ehv transmission lines with particular reference to very-high speed protection', Ibid, Vol. 123, No. 4, April 1976.

3 Johns A.T., El-Nour M., Aggarwal R.K.: 'Performance of distance protection of ehv feeders utilising shunt-reactor arrangements for arc suppression and voltage control', Ibid, Vol. 123, No. 5, Part C.

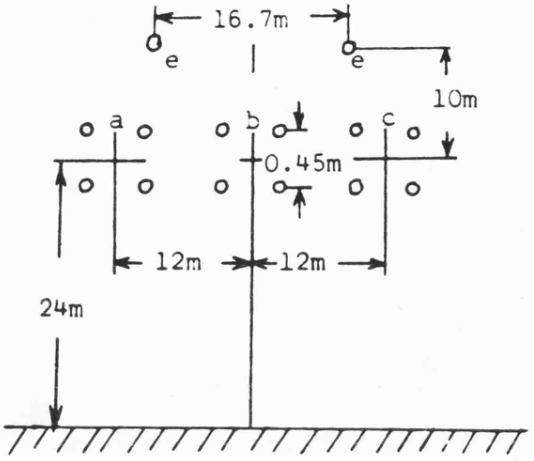


Figure 1a 500 kV line construction simulated

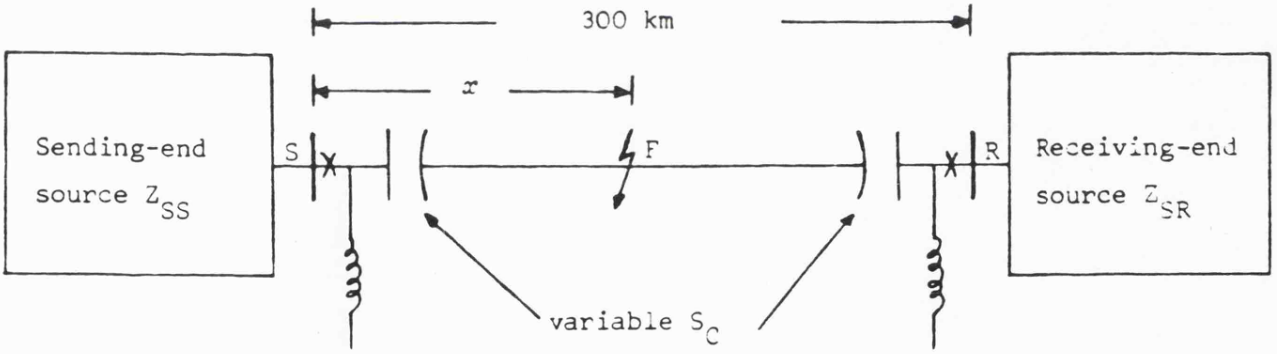


Figure 1b Basic series compensated system arrangement

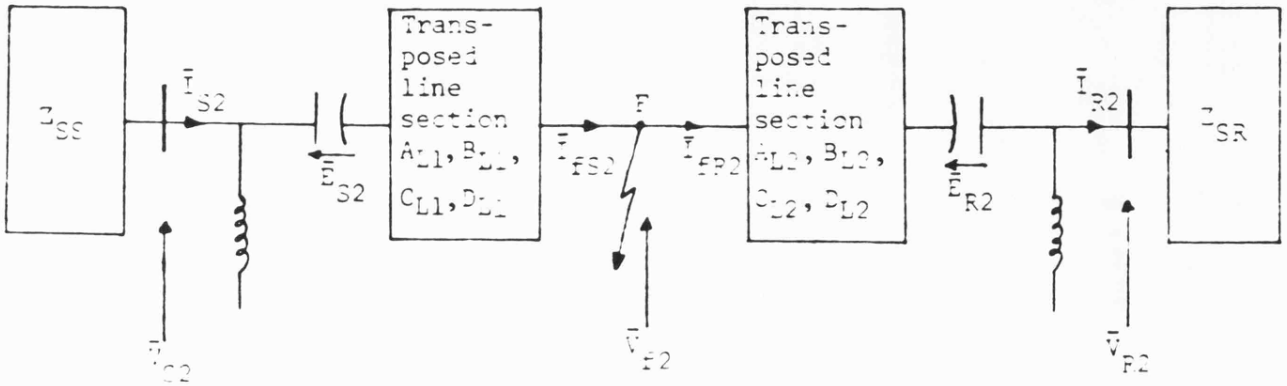


Figure 2 An equivalent fault transient model

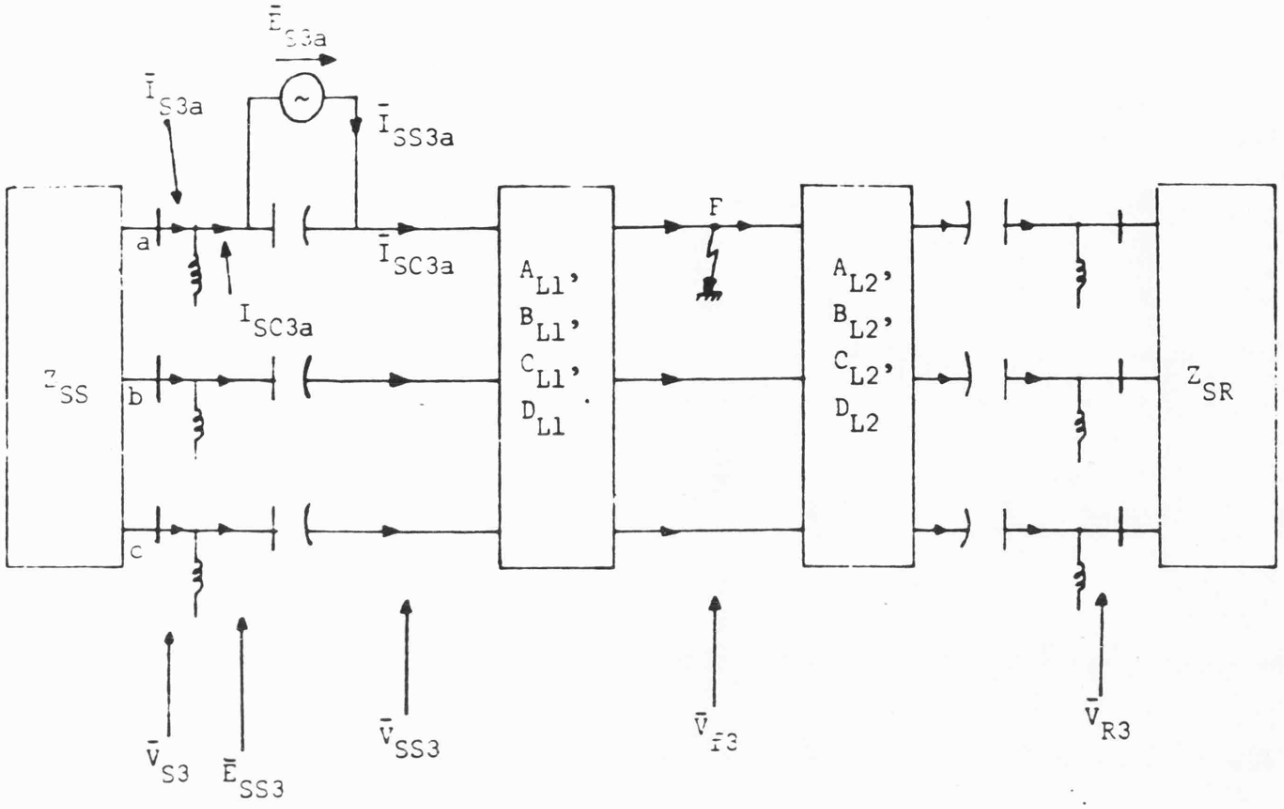


Figure 3 Sending-end a-phase capacitor flashover simulation

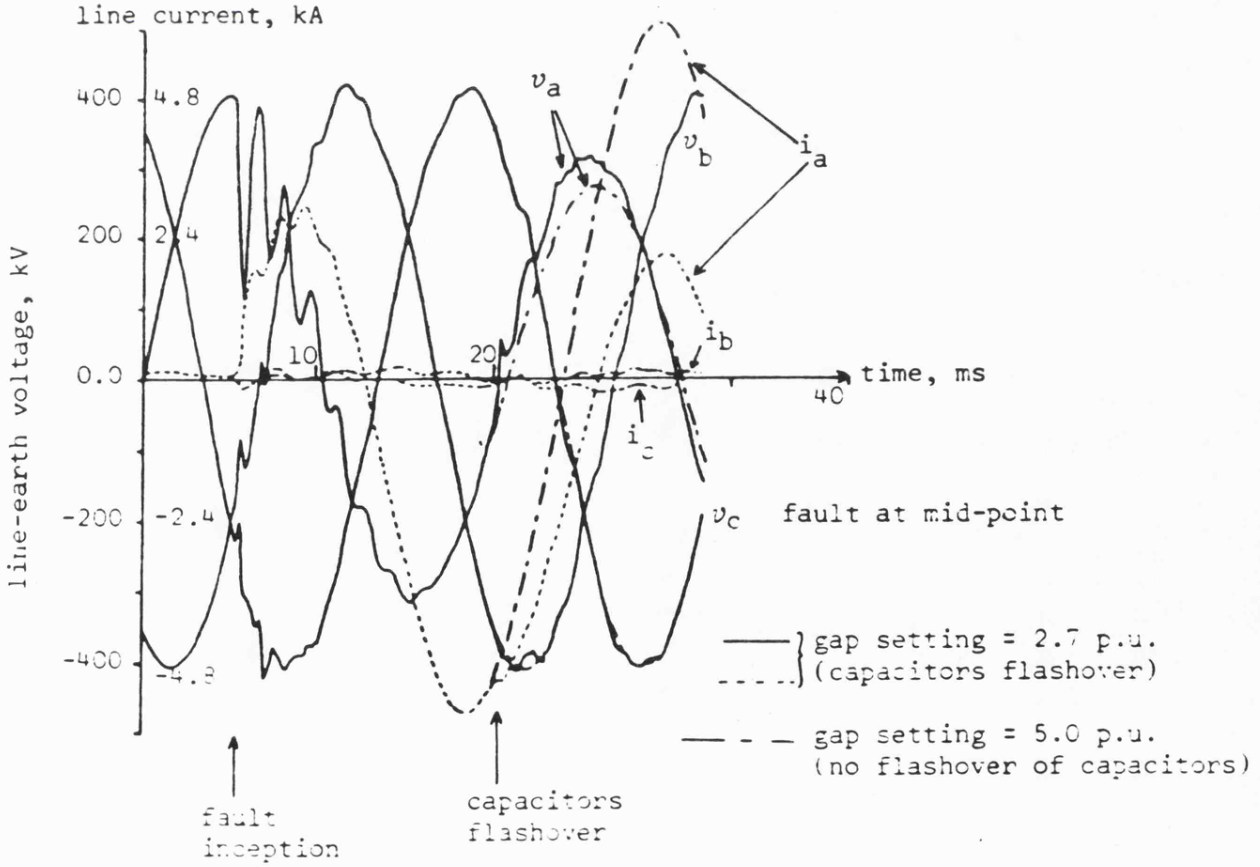


Figure 4 Relaying pt. waveforms for different gap settings

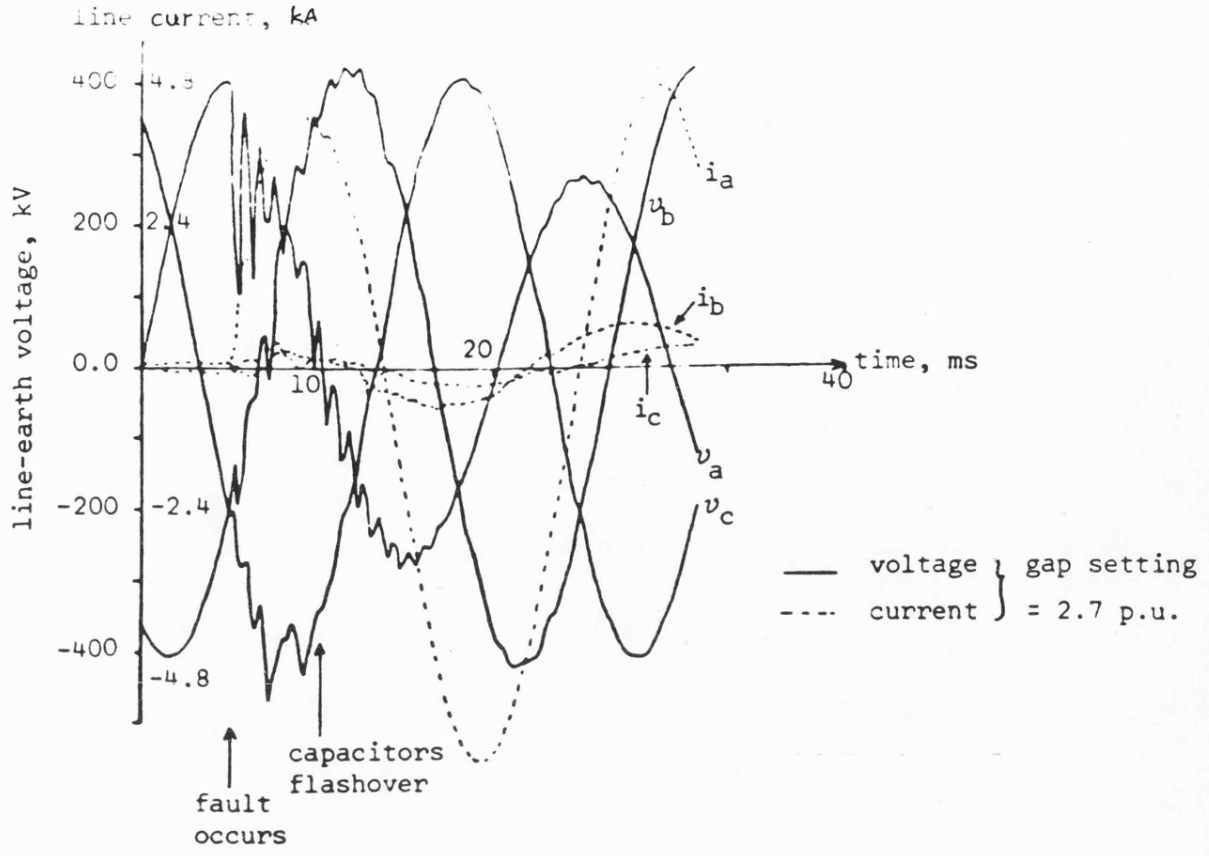


Figure 5 Waveforms for fault at 25% of the line from S. End

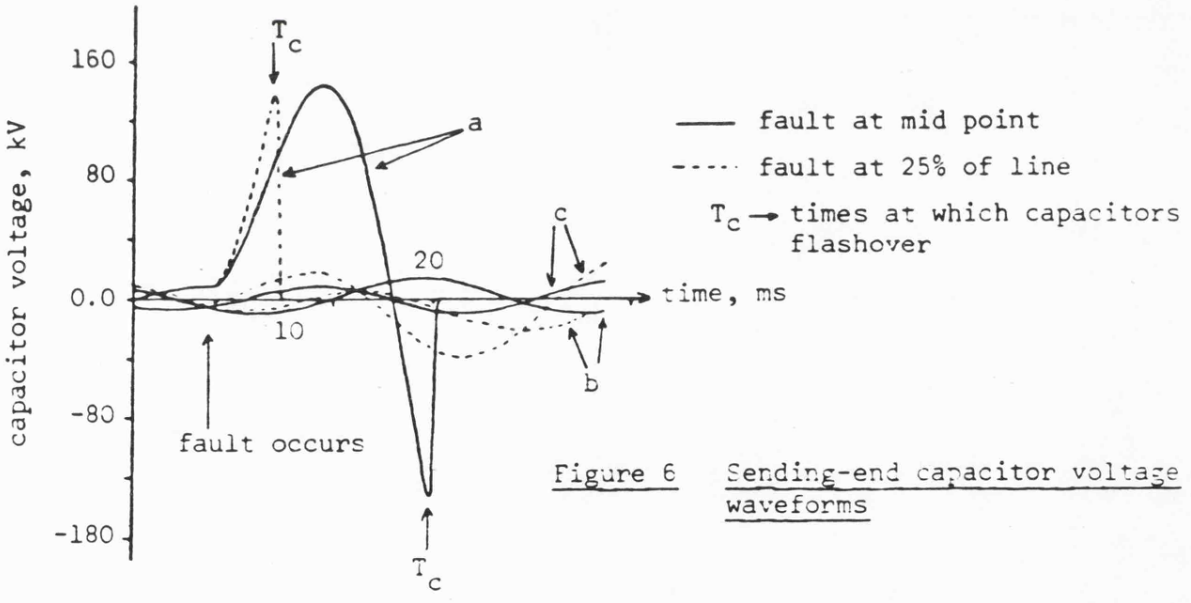


Figure 6 Sending-end capacitor voltage waveforms

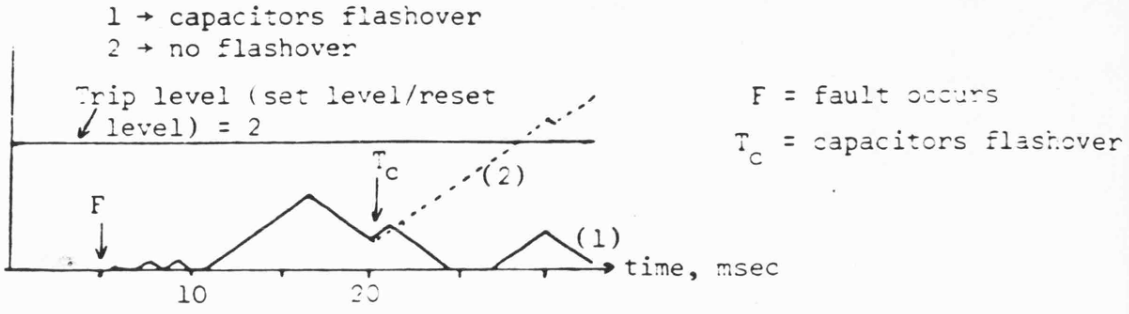


Figure 7 Integrator output of Block-Average relay

BIBLIOGRAPHY

1. CONCORDIA, C. et al: "Subsynchronous torques on generating units feeding series capacitor compensated lines", Proc. of the Power Conference, Chicago, USA, Vol.35, May 1973.

2. KILGORE, L.A.: "Longer transmission interties are within reach", Electrical World, Nov.1978.

3. ELLIOT, L.C. and CUTTINO, W.H.: "Series Capacitor Application and Experience", 1970 Electric Utility Eng. Conf., March 1970.

4. JANCKE, G.: "Series capacitors in power systems", IEEE Trans., Vol.PAS-94, No.3, May/June 1975.

5. FAHLEN, N.T.: "Series capacitors in power transmission - design and experience", International Conference on high voltage D.C. and/or A.C. Power Transmission, London, Nov.1973.

6. MAGOWAN, J.M.: "Voltage performance of series capacitors in transmission and distribution lines", Proc. IEE, 104(Pt.A), January 1977.

7. JANCKE, G. et al: "15 years development and experience

with series capacitors in transmission systems", CIGRE, Report 316, 1966.

8. GILLES, D.A. et al: "High voltage series capacitor experiences and planning", CIGRE, Report 118, 1966.

9. CUTTINO, W.H. et al: "Series capacitors for e.h.v. transmission lines", Westinghouse Engineer, Vol.27, No.1, January 1967.

10. BUTLER, J.W. et al: "Steady state and transient stability analysis of series capacitors in long transmission lines", AIEE Trans., Vol.62, February 1943.

11. AHLGREN, L.and GRUNDMARK, B.: "Self-extinguishing gaps in large series capacitor stations", CIGRE Report 317, 1956.

12. STARR, E.C. and EVANS, R.D.: "Series capacitors for transmission circuits", AIEE Trans., Vol. 61, 1942.

13. LA LANDER, S and NORLIN, L.: "The use of series capacitors in high voltage transmission systems", CIGRE, Report 330, June 1959.

14. BODINE, R.B. et al: "Self-excited oscillations of

capacitor-compensated long-distance transmission systems", AIEE Trans., Vol.62, January 1943.

15. CRARY, S.B. et al: Report on the work of the study committee no 13: 'System stability and voltage-load frequency control', CIGRE, Report 318, 1956.

16. CRARY, S.B. and SALINE, L.F.: "Location of series capacitors in high voltage transmission systems", Trans. AIEE, Vol.72, December 1953.

17. BRUER, G.D. et al: "The use of series capacitors to obtain maximum e.h.v. transmission capability", IEEE Winter Power Meeting, February 1964.

18. BLACK, L.H.: "The economics of transmission line voltage regulation by means of series capacitors", CIGRE, Report 312, 1956.

19. ALLEN, E.J. and CANTWELL, J.L.: "The effect of series capacitors upon steady state stability of power systems", General Electric Review, 1930.

20. JANCKE, G and AKERSTROM, K.F.: "The series capacitor in Sweden", Electrical Engg., March 1952.

21. HERLITZ, I.: "Economic potentialities of the series capacitors", ASEA Journal, Vol.23, 1950.

22. KNUDSEN, N.: "Technical problems arising from the use of series capacitors", ASEA Journal, Vol.23, 1950.

23. ZETTERSTEDT, B and VORTS, S.: "A 220 kV series capacitor", ASEA Journal, Vol.123, 1950.

24. ALIMNASKY, M.I.: "The application and performance of series capacitors", General Electric Review, Vol.33, Part II, 1930.

25. JOHNSON, A.A. et al: "Fundamental effect of series capacitors in high-voltage transmission lines", AIEE trans., Vol.70, 1951.

26. SALZMANN, A.: "Series capacitors in power transmission systems", Electrical Times, August 1955.

27. CLARK, L. and WALKER, H.: "Series Capacitors", Electrical Energy, September 1957.

28. MARBURY, R.E.: "The series capacitor and the high voltage line", Westinghouse Engineer, 1951.

29. AIEE Committee Report: "Guides for short-time 60-cycle overvoltage operation of power capacitors", AIEE Trans., Vol.71, January 1952.

30. O'NEIL, J.E. and BANKOSKE, J.W.: "EHV series capacitor economics", Transmission and Distribution, November 1966.

31. ANDERL, H.W. and MERRY, S.M.: "Lowering e.h.v. transmission costs with series capacitors", Indian J. Power and River Val. Dev., January 1975.

32. ILICATO, F. et al: "Transient voltages and currents in series compensated e.h.v. lines", Proc.IEE, Vol.123, No.8, August 1976.

33. WEDEPOHL, L.M.: "Application of matrix methods to solution of travelling wave phenomena in polyphase systems", Proc.IEE, Vol.110, No.12, December 1963.

34. JOHNS et al: "Performance of distance protection of e.h.v. feeders utilising shunt reactor arrangements for arc suppression and voltage control", Proc.IEE, Vol.127, No.5, September 1980.

35. MADZAREVIC, V.et al: "Overvoltages on e.h.v. transmission lines due to faults and subsequent

bypassing of series capacitors", IEEE Trans., Vol.PAS-96, No.6, November/December 1977.

36. DE BENNETOT, C.: "The choice of series capacitor bank and problems arising from its installation in a transformer station with particular reference to the operation of distance relays", CIGRE, Paper 303, 1960.

37. JOHNS, A.T. and AGGARWAL, R.K.: "Digital simulation of faulted e.h.v. transmission lines with particular reference to very-high-speed-protection", Proc.IEE, Vol.123, No.4, April 1976.

38. YERMOLENKO, V.M. and PETROV, S.J.: "The effect of series capacitor compensation on relay operation", CIGRE, Paper 323, 1956.

39. HARDER, E.L. et al: "Series capacitors during faults and reclosing", AIEE Trans., Vol.70, 1951.

40. ANDERL, H.W. and MERRY, S.M.: "Series capacitor increase e.h.v. capacity", Electrical World, May 1974.

41. GALLOWAY, R.H. et al: "Calculation of electrical parameters for short and long polyphase transmission lines", Proc.IEE, Vol.111, No.12, December 1964.

42. WEDEPOHL, L.M. and MOHAMMED, S.E.T.: "Multi-conductor transmission lines", Proc.IEE, Vol.116, No.9, September 1969.

43. DOMMEL, H.W.: "Digital computer solution of electro-magnetic transients in single and multi-phase networks", IEEE Trans., April 1969.

44. BEWLEY, L.V.: "Travelling waves on transmission systems", New York, Wiley, 1951.

45. AMETANI, A.: "The application of the fast Fourier transform to electrical transient phenomena", Int. J. Elec. Eng. Educ., Vol.10, 1973.

46. ROBERGE, R.M.: "Effect of unbalanced series compensation on open end of line voltage", IEEE, PES Winter Meeting, February 1978.

47. KERSTING, W.H. and DAVIET, L.L.: "A computer aided transmission line design problem", Southwest IEEE Conference Record, April 1970.

48. KERSTING, W.H.: "The application of series capacitor in high-voltage transmission lines", 21st Annual South Western IEEE Conference and Exhibition, April 1977.

49. JOHNS, A.T. et al: "Performance of high speed distance protection applied to 4-reactor static shunt compensated systems", Proc. 15th U.P.E.C., Leicester, 1980.

50. FRIEDLANDER, E. and JONES, K.M.: "Saturated reactors for long distance bulk power lines", Electrical Review, June 1969.

51. GUPTA, S.R. and SETH, JP.P: "Shunt compensation of e.h.v. long lines", J. Inst. Eng. (India), Elect. Eng. Div., Vol.53, June 1973.

52. KIMBARK, E.W.: "Suppression of ground-fault arcs on single-pole-switched e.h.v. lines by shunt reactors", IEEE Trans., Vol.83, March 1964.

53. EATON, J.R. and KOZAK, E.: "Single-pole switching on reactor compensated lines optimum operating conditions", IEEE PES Winter Meeting, February 1974.

54. KIMBARK, E.W.: "Selective-pole switching of long double circuit e.h.v. lines", IEEE Trans., Vol.PAS-95, No.1, January/February 1976.

55. STEVENSON, W.D.: "Elements of Power System Analysis", New York, McGraw Hill, 1975.

56. ILICETO, F. and CINIERI, E.: "Comparative analysis of series and shunt compensation schemes for a.c. transmission systems", IEEE Trans., Vol.PAS-96, No.6, November/December 1977.

57. SETH, S.P. and GUPTA, S.R.: "Analysis of shunt compensation of series compensated e.h.v. long lines", J. Inst. Eng(India), Elect. Eng. Div., April 1976.

58. DE FRANCO, N. et al: "Feasibility study of the Itaipu transmission", CIGRE Report 32-04, 1976.

59. NAGAMARA, J.: "Abnormal phenomena of the series capacitor compensated system", Researches of the electrotechnical laboratory, No.603, May 1961.

60. WOLF, H.B.: "Application of series capacitor for voltage regulation, fault current limitation, and voltage flicker control", IEEE Trans., Vol.IGA-5, No.4, July/August 1969.

61. CUTTINO, W.H. and O'NEIL, J.E.: "Series capacitor design and application for e.h.v. systems", American Power Conference, April 1966.

62. O'NEIL, J.E.: "Application of EHV Series capacitors", Transmission and Distribution, Vol.18, No.8, August 1966.

63. PETERSON, H.H.: "A method for reducing dead time for single-phase reclosing in e.h.v. transmission", IEEE Trans., Vol.PAS-88, No.4, April 1969.

64. KIMBARK, E.W. and LEGATE, A.C.: "Fault surge versus switching surge - a study of transient over voltages caused by line-to-ground faults", IEEE Trans., Vol.PAS-87, September 1968.

65. AMSTUTZ, A.: "Residual currents and voltages with single-pole rapid reclosing", The Brown Boveri Review, July/August 1948.

66. EDWARDS, L. et al: "Single-pole switching on TVAs Paradise-Davidson 500 kV line design aspects and staged fault test results", IEEE Winter Power Meeting, January/February 1977.

67. AHLGREN, L. et al: "EHV series capacitor with dual

gaps and non-linear resistors provide technical and economic advantages", IEEE PES Winter Meeting, February 1979.

68. JOHNS, A.T. and AGGARWAL, R.K.: "Digital simulation of fault autoreclosure sequences with particular reference to the performance evaluation of protection for e.h.v. transmission lines", Proc. IEE, Vol.128, No.4, July 1981.

69. JOHNS, A.T. and AGGARWAL, R.K.: "Performance of high speed distance relays with particular reference to travelling wave effects", Proc.IEE, Vol.124, No.7, July 1977.

70. ELNOUR ABU, M.A.H.: "Fault transient simulation of shunt compensated power systems", PhD Thesis, University of Bath, 1980.

71. ASHOK KUMAR, B.S. et al: "Effectiveness of series capacitors in long distance transmission lines", IEEE Trans., PAS, May/June 1970.

72. KRISHNA PRASUD, M.T. and THAPAR, B.: "Best location and percentage series compensation of long transmission line for maximum power transfer", J. Inst. Eng. (India) Elec. Eng. Div., April 1975.

73. PYLE, A.B.: "Series capacitors boost e.h.v. system capability", Electrical World, December 1966.

74. CRAIG, C.R. et al: "Series capacitor provide an average of 70% compensation for Pacific Inertia", Transmission and Distribution, February/March 1968.

75. MANEATIS, J.A. et al: "500 kV series capacitor installations in California", IEEE Trans., Vol.PAS-90, No.3, May 1971.

76. CLERICI, A.: "Analog and digital simulation for transient overvoltage determinations", Electra, Vol.22, 1972.

77. ARLETT, P.L. and MURRAY-SHELLEY, R.: "The study of overvoltage transients in large systems", PSCC Stockholm, Report 5.6, July 1979.

78. THAUSAAOULIS, P. et al: "Overvoltages on a series compensated 750 kV system for the 10000 MW Itaipu project", IEEE Trans., Vol. PAS-94, March/April 1975.

79. CAPASSO, A. and ILICETO, F.: "On the voltage control and transient overvoltages of extra-long distance a.c. transmission lines", L'Energia Elettrica, Milan, March 1980.

80. AGGARWAL, R.K. and JOHNS, A.T.: "Simulation of electrical transient phenomena associated with single-pole autoreclosure of short e.h.v. transmission lines", Proc. 14th U.P.E.C., Loughborough, 1979.

81. WINICK, K.: "System protection considerations related to single pole tripping of high voltage transmission lines", Proc., American Power Engg. Conf., Vol.37, 1975.

82. ELKATEB, M.M. and CHEETHAM, W.J.: "Problems in the protection of series compensated lines", IEE, 2nd Inter. Conf. on 'Developments in Power System Protection', June 1980.

83. MATHEWS, C.A. and WILKINSON, S.B.: "Series compensated line protection with a directional comparison relay scheme", IEE, 2nd Inter. Conf. on 'Developments in Power System Protection', June 1980.

84. WELLER, G.C. et al: "New principles for distance protective relays", IEE, 2nd Int. Conf. on 'Developments in Power System Protection', June 1980.

85. NARAYAN, C.V.: "Distance protection of high-voltage lines containing series capacitors", The Brown Boveri

Review, Vol.55, No.7, 1968.

86. JOHNS, A.T. and AGGARWAL, R.K.: "New ultra-high speed directional blocking scheme for transmission line protection", 2nd Int. Conf. on 'Developments in Power System Protection', June 1980.

87. CHANNIA, M. and LIBERMAN, S.: "Ultra high speed relay for ehv/uhv transmission lines - development, design and application", IEEE Trans., Vol.PAS-97, May 1978.

88. MARBURY, R.E. and OWENS, J.B.: "New series capacitor protective device", AIEE Trans., Vol.65, March 1946.

89. POWELL, R.O.M.: "Series capacitors in transmission systems", Journal IEE, Vol.7, Dec.1971.

90. HAMLIN, J.L.: "Protection of transmission and distribution lines containing series capacitors", Journal IEE, Vol.7, May 1961.

91. TURELI, A. et al: "Comparison of protection schemes applied to series compensated long lines", IEE 2nd Int. Conf. on 'Developments in Power System Protection', June 1980.

92. BIRKES, R.C.: "Series capacitors for e.h.v. systems", Transm. and Distrib., USA, Feb.1967.

93. PESONEN, A.J.: "400 kV series capacitor at Kangasula", Sahko (Finland), February 1965.

94. NAG, G.K.: "Application of series capacitor to e.h.v. and u.h.v. transmission lines", Indian J. Power and River Val Dev., Dec.1976.

95. KIMBARK, E.W.: "Charts of three quantities associated with single-pole switching", IEEE Trans., Vol.PAS-94, Mar/Apr. 1975.

96. HILBURN, J.L. and JOHNSON, D.E.: "Manual of Active Filter Design", McGraw-Hill, 1973.

97. JOHNS, A.T.: "New ultra-high-speed directional comparison technique for the protection of e.h.v. transmission lines", Proc.IEE, Vol.127, No.4, July 1980.